Nature, origine et réactivité de la matière organique fossile dans les sols et sédiments : développements et applications de la photoionisation - spectrométrie de masse haute résolution (APPI-QTOF) et couplage avec la chromatograhie d'exclusion stérique (SEC)

Thierry Ghislain

THÈSE

Présentée pour l'obtention du titre de

DOCTEUR DE L'UNIVERSITÉ DE LORRAINE

NANCY-UNIVERSITÉ

Université Henri Poincaré – Nancy I

École Doctorale RP2E Ressources, Procédés, Produits, Environnement

Spécialité : Géosciences

par

Thierry GHISLAIN

Nature, origine et réactivité de la matière organique fossile dans les sols et sédiments : Développements et applications de la Photoionisation – Spectrométrie de Masse Haute Résolution (APPI-QTOF) et couplage avec la Chromatographie d'Exclusion Stérique (SEC)

Date de soutenance : 8 juillet 2011

Membres du jury :

M. Christian RUBY	Professeur, Nancy-Université	*Président du jury*
M. Jean-Claude TABET	Professeur, UPMC, Paris	*Rapporteur*
M. Patrick G. HATCHER	Professeur, Old Dominion University, USA	*Rapporteur*
M. Laurent GRASSET	Maître de Conférences, Université de Poitiers	*Examinateur*
M. Frédéric AUBRIET	Maître de Conférences HDR, UPV, Metz	*Examinateur*
M. Raymond MICHELS	Chargé de Recherche CNRS, Nancy-Université	*Directeur de thèse*
M. Pierre FAURE	Chargé de Recherche CNRS, Nancy Université	*Directeur de thèse*

THÈSE

Présentée pour l'obtention du titre de

DOCTEUR DE L'UNIVERSITÉ DE LORRAINE

NANCY-UNIVERSITÉ

Université Henri Poincaré – Nancy I

École Doctorale RP2E Ressources, Procédés, Produits, Environnement

Spécialité : Géosciences

par

Thierry GHISLAIN

Nature, origine et réactivité de la matière organique fossile dans les sols et sédiments : Développements et applications de la Photoionisation – Spectrométrie de Masse Haute Résolution (APPI-QTOF) et couplage avec la Chromatographie d'Exclusion Stérique (SEC)

Date de soutenance : 8 juillet 2011

Membres du jury :

M. Christian RUBY	Professeur, Nancy-Université	*Président du jury*
M. Jean-Claude TABET	Professeur, UPMC, Paris	*Rapporteur*
M. Patrick G. HATCHER	Professeur, Old Dominion University, USA	*Rapporteur*
M. Laurent GRASSET	Maître de Conférences, Université de Poitiers	*Examinateur*
M. Fréderic AUBRIET	Maître de Conférences HDR, UPV, Metz	*Examinateur*
M. Raymond MICHELS	Chargé de Recherche CNRS, Nancy-Université	*Directeur de thèse*
M. Pierre FAURE	Chargé de Recherche CNRS, Nancy Université	*Directeur de thèse*

A ma mère, Martine, partie trop tôt,

tu m'as permis d'arriver jusque là par ton amour inconditionnel et ton soutien. J'aurais tant aimé que tu puisses voir l'aboutissement de ce travail que tu suivais avec tant d'attention.

Je n'aurais jamais assez de mots pour te dire tout mon amour et ma reconnaissance.

Remerciements

Je tiens en priorité à commencer ces remerciements par mes deux directeurs de thèse, Raymond MICHELS et Pierre FAURE, qui m'ont fait confiance en me choisissant pour cette thèse. Ce fut un plaisir de travailler avec eux et un enrichissement tant personnel que professionnel. Ils ont toujours été présents et particulièrement patients. J'ai énormément appris à leur contact et je les en remercie chaleureusement.

Je remercie également Jacques PIRONON et Michel CATHELINEAU pour leur accueil au sein de l'U.M.R. 7566 G2R.

Je remercie la Région Lorraine ainsi que le CREGU pour le financement de ma thèse et la ZAM pour sa participation aux frais de fonctionnement.

Je tiens également à remercier, tout particulièrement Jean-Michel BILLMANN, ingénieur chez BRUKER DALTONICS, pour son aide et sa patience lors de nos heures passées à « bricoler » le Q-TOF. Merci pour tous tes conseils et ton aide. Merci également à Yann HEBERT et Alex VERDU pour leurs précieux conseils.

Une pensée toute particulière pour ma meilleure camarade de jeu, Coco qui a traversé comme moi des épreuves difficiles pendant la thèse, qui m'a toujours soutenu et écouté de manière inconditionnelle. Un grand merci à toi.

Et bien sûr une autre pensée particulière pour ma compatriote du sud Olivia (même si elle ne vient pas vraiment du sud) qui a souffert comme moi de l'expatriation.

Bien sûr, je n'oublie pas Aymeric même s'il a choisi de nous quitter, merci à toi pour avoir toujours été là. Vivement l'été prochain.

Un immense merci aussi à Laurence MANSUY-HUAULT pour son aide sur les ACP, et pour tout le reste…

Une pensée toute particulière pour Yueming, qui fut une amie extraordinaire, merci encore pour ton aide et ton soutien. Merci aussi à mon coloc de bureau le très jovial Van Phuc pour ta bonne humeur et nos conversations. Enfin comment ne pas vous remercier tous les deux de m'avoir accueilli dans vos pays respectifs et m'avoir fait découvert votre culture.

Et bien évidemment je n'oublierai pas toute l'équipe de géochimie organique, mes collègues de galère, Pascale, Fatima, mais aussi Sabrina, Yann et Seyed. Je pense également à Gilles, nos conversations et débats vont beaucoup me manquer. Je dissocie bien sûr Aurélien que je remercie de m'avoir laissé poser mon vélo dans son labo. Enfin, même si elle ne fait pas partie de l'équipe de géochimie organique, comment ne pas remercier Audrey Billerot, avec qui j'ai passé d'excellents moments notamment en randonnées mais aussi en soirées.

Je n'oublie pas Christine, merci à toi pour tous les services rendus qui m'ont bien facilité la tâche et l'estomac… Merci bien sûr à Laurence, Marie-Odile pour leur aide administrative et les conversions d'entre porte sans oublier Patoche, merci pour toute l'aide que tu m'as apportée.

Que ferions-nous également sans les informaticiens, Roland Mairet et Vincent Merlet. Je les en remercie vivement.

Merci également à François Dupire et Marie-Camille Caumon pour nos discussions concernant le Q-TOF.

Une pensée pour tous les personnels de l'U.M.R. G2R.

Merci à la SFSM et la région Nord Pas de Calais pour leur soutien financier pour la participation a des congrès.

Enfin je tiens à terminer mes remerciements par ma sœur Caroline, qui m'a soutenu et aidé et sans qui je n'aurais pas réussi à surmonter l'épreuve que nous avons dû traverser tous les deux, mais je n'oublie pas non plus mon neveu préféré Thomas et son papa Anh Tuan.

Sommaire

AC: Alternative Current

API: Atmospheric Pressure Ionization

APCI: Atmospheric Pressure Chemical Ionization

APPI: Atmospheric Pressure PhotoIonization

EA: Electron Affinity

ESI: Electrospray ionization

eV: electron volt

Da: Dalton (atomic mass unit)

DC: Direct Current

DOM: Dissolved Organic Matter

EPR: Electron Paramagnetic Resonance

GC-MS: Gas Chromatography-Mass Spectrometry

GPC: Gel Permeation Chromatography

HPLC: High Pressure (Performance) Liquid Chromatography

id: internal diameter

IE: Ionization Energy

MALDI: Matrix Assisted Laser Desorption Ionization

MS: Mass Spectrometry

NMR: Nuclear Magnetic Resonance

PAH: PolyAromatic Hydrocarbon

ppm: parts per million

Py-GC-MS: Pyrolysis - gaz chromatography – mass spectrometry

RID: Refractive Index Detector

SEC: Size Exclusion Chromatography

TOC: Total Organic Carbon

TOF: Time-Of-Flight

UV: Utra-Violet

VIS: Visible

Préface

Ce travail de thèse s'inscrit dans le cadre de la Zone Atelier Moselle (ZAM) qui regoupe 20 laboratoires de recherche lorrains travaillant sur le thème de la « sureté et de la sécurité de l'approvisionnement en eau des métropoles régionales » (http://www.ensic.inpl-nancy.fr/Zam) et du Groupement d'Intérêts Scientifiques sur les Friches Industrielles (GISFI) qui regroupe 12 laboratoires de recherche, aux compétences pluridisciplinaires dédiées à la requalification durable des sites dégradés et pollués par les activités industrielles passées (http://www.gisfi.fr).

Le financement de cette thèse a été assuré par la Région Lorraine et par le Centre de Recherches sur la Géologie des Matières Premières Minérales et Energétiques (CREGU). La Zone Atelier Moselle a contribué financièrement à cette thèse par le versement annuel d'une subvention de fonctionnement et le financement de la source APPI ; le GISFI a participé aux financement des équipements du laboratoire de géochimie organique (GC-MS, Agilent Technologies et extracteur haute pression ASE 350, Dionex) Par ailleurs, les équipements du laboratoire de spectrométrie de masse du G2R (source ESI, Q-TOF, CLHP) ont été financés dans le cadre du Contrat Plan Etat-Région (CPER) en associant également la contribution du CNRS, de Nancy-Université, de la Fédération de Recherche Eaux-Sols-Terre (FR EST), du Fond Européen de Développement économique régional (FEDER), de l'UMR 7566 G2R et du CREGU.

Introduction Générale

Les objectifs de ce travail de thèse ont été d'améliorer la caractérisation de la fraction macromoléculaire soluble de matière organique fossile en s'appuyant sur la spectrométrie de masse haute résolution (i.e. Q-TOF). Habituellement, les recherches sur la caractérisation de cette fraction se font par spectrométrie de masse ultrahaute résolution, i.e. FT-ICR, cependant lorsque ce type d'instrument n'est pas disponible, la spectrométrie de masse haute résolution Q-TOF offre une alternative très intéressante. En effet, ce type d'instrument hybride permet d'effectuer des mesures plus rapides qu'avec un spectromètre de masse FT-ICR et permet également une détermination précise de la distribution des masses et ce malgré une résolution inférieure (environ 20 000 pour un Q-TOF et jusqu'à plusieurs centaines de milliers pour un FT-ICR). Il s'agissait donc, dans un premier temps, de déterminer et d'évaluer les capacités d'un spectromètre de masse Q-TOF vis-à-vis des problématiques de la géochimie organique.

Dans un second temps, deux approches distinctes ont été développées afin de pouvoir analyser et interpréter des solutions complexes composées d'un grand nombre de molécules :

- la simplification pré-analytique, dont le principe est de simplifier les solutions complexes avant analyse par spectrométrie de masse et ce au moyen de la chromatographie d'exclusion stérique (SEC) qui permet de trier les molécules en fonction de leur taille moléculaire et ainsi d'éviter de favoriser une fonction chimique, un type de molécule…,
- le traitement post-processing, qui correspond à un modèle mathématique, a été développé afin d'interpréter la très grande quantité d'informations obtenues par les analyses de spectrométrie de masse.

Dans un premier temps, chaque approche a été mise au point sur des systèmes simples puis développée sur des systèmes beaucoup plus complexes.

Ce manuscrit regroupe ainsi un chapitre théorique ciblant les différents outils utilisés au cours de la thèse puis différents chapitres regroupant les développements et applications rassemblés sous la forme de 6 articles dont la présentation a été adaptée pour la rédaction de ce manuscrit de thèse.

La **première partie** de ce manuscrit correspond à une étude théorique de la chromatographie d'exclusion stérique (SEC), des sources d'ionisation à pression atmosphérique ainsi que de la technologie hybride Q-TOF afin mieux comprendre les principes théoriques de chaque outil analytique et les limitations inhérentes à ces technologies.

Dans une **deuxième partie**, le spectromètre de masse a été adapté à l'étude des matières organiques fossiles en évaluant en particulier l'efficacité d'ionisation des différentes sources d'ionisation atmosphérique généralement utilisées : ESI (SlectroSpray Ionisation), APCI (Atmospheric Pressure Chemical Ionisation) et APPI (Atmospheric Pressure Photoionisation). Les résultats sont présentés dans l'article 1 "**Detection and monitoring of PAH and oxy-PAHs by high resolution mass spectrometry: Comparison of ESI, APCI and APPI source detection".**

Ce travail a conduit à sélectionner la source APPI et à l'utiliser pour étudier les transformation d'un composé modèle lors de processus d'oxydation à l'air à basse température (simulant une atténuation naturelle à long terme) en présence de différentes phases minérales fréquemment rencontrées dans les sols et sédiments. Dans l'Article 2 "**Low-temperature, mineral-catalyzed air oxidation: A possible new pathway for PAH stabilization in sediments and soils."** Le rôle catalytique des phases minérales a été clairement démontré et a conduit à la formation d'un résidu carboné « stable ».

Cette partie, concernant le développement et l'application de l'APPI-QTOF en injection directe, a démontré les potentialités de ce système analytique. Toutefois, les échantillons utilisés étaient issus d'expérimentation sur un composé modèle. Vouloir poursuivre sur des fractions organiques naturelles (extraits organique ou aqueux de charbon, de sols contaminés, de pétroles) dans des conditions analytiques similaires nous a conduit à devoir « simplifier » le système à l'aide de la Chromatographie d'Exclusion Stérique (SEC).

La **troisième partie** de ce manuscrit décrit le couplage entre la chromatographie d'exclusion stérique (SEC) et la spectrométrie de masse APPI-QTOF. Ce couplage a pour

objectif de pouvoir préalablement séparer, en fonction de leurs tailles moléculaires, les mélanges complexes avant analyse. Ce couplage permet alors de coupler (i) un tri en fonction de l'organisation spatiale des complexes moléculaires (SEC) et (ii) de déterminer la distribution en masse de chacune des entités séparées (Q-TOF). Les résultats sont décrits dans l'article 3 – "**On-line SEC-APPI-QTOF: a new analytical tool for complex mixtures: Validation by aromatic compounds."**

Ce couplage a ensuite été appliqué pour étudier la structure des asphaltènes qui, pour le moment, n'avait jamais été abordé de cette façon (Article 4 "**Molecular distribution of Asphaltenes from different origins: Contribution of on-line SEC-APPI-QTOF."**)

La dernière partie a été de développer un outil mathématique pour traiter le grand nombre de données fournit par la détection par spectrométrie de masse haute résolution. Nous avons donc développé des méthodes d'analyse post-processing. Un algorithme basé sur une analyse numérique et statistique des spectres de masse appelé SNAMS (Statistical and Numerical Analysis of Mass Spectra) a été développé en ce sens et appliqué à la fraction asphalténique d'échantillons issus de différents environnements (pétroles et sols contaminés). Ce travail est décrit dans l'article 5 – "**An easy and fast way to determine the origin of asphaltenes from SNAMS model."** Il a été possible de réaliser des regroupements (i) en fonction des sources organiques et (ii) en fonction des degrés d'altération (oxydation).

Les résultats positifs de l'application du modèle SNAMS sur des fractions organiques complexes (asphaltènes) nous ont conduit à le tester en l'adaptant à la matière organique en phase aqueuse : Article 6 – "**Application of SNAMS model to APPI-QTOF mass spectra from dissolved organic matter."** Les résultats montrent que même en phase aqueuse, le traitement statistique de la distribution de masse peut fournir des informations en termes de source et de réactivité.

Un bilan de l'ensemble de ces travaux sera présenté en conclusion suivi de propositions de perspectives que ce travail suggère.

Introduction

1. Cycle du carbone

Le cycle du carbone organique, cycle fondamental pour la vie sur Terre, est généralement scindé en deux cycles comprenant le cycle biochimique superficiel et le cycle géochimique.

Le cycle biochimique débute avec la formation des composés organiques essentiellement par voie photosynthétique et se poursuit jusqu'à leur incorporation dans les sédiments avec de nombreuses étapes intermédiaires (transformation – dégradation – humification…) et de nombreux échanges entre réservoirs (atmosphère – biosphère – sols terrestres et sédiments marins). Ce cycle biogéochimique inclus des processus qui s'étalent sur des temps inférieurs aux siècles. Même si les échanges sont relativement importants, le réservoir concernant ce cycle court reste limité.

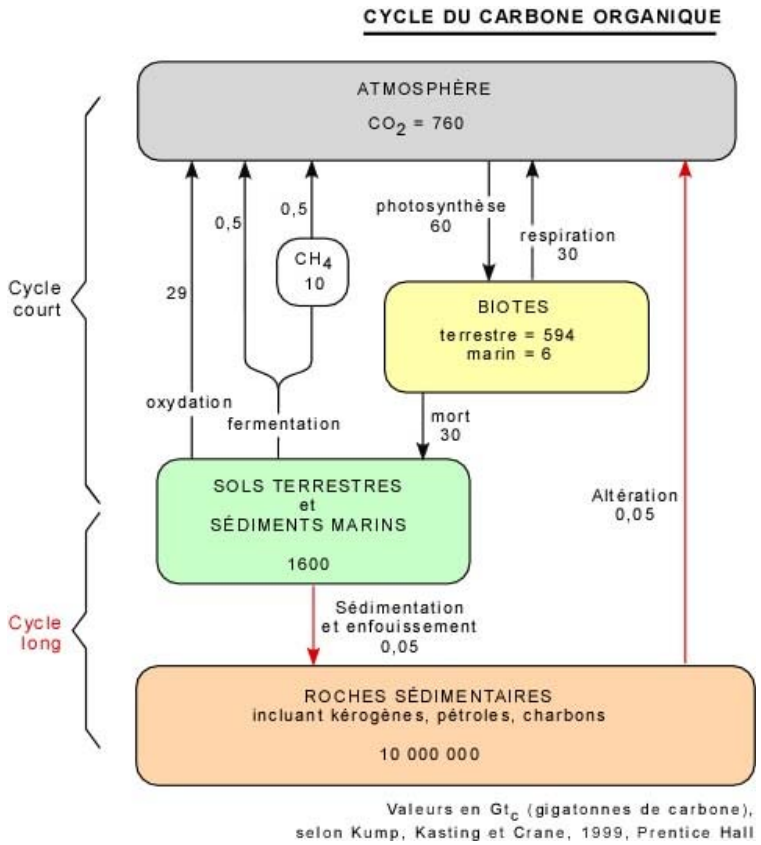

Figure 1: Cycle du carbone (en gigatonnes de C), d'après (Kump *et al.* 2010)

Le cycle **géochimique** concerne des échelles de temps beaucoup plus longues, car ce sont les processus de nature géologique qui contrôlent l'évolution des composés organiques sur des milliers voire des millions d'années. Ce cycle est contrôlé par des processus tels l'enfouissement des matières organiques dans les sédiments, leur transformation en composés fossiles et leur altération. Les flux de carbone reliés à ces processus sont faibles; en revanche, les réservoirs sont immenses (Figure 1) et le temps impliqué très long.

Toutefois, l'exploitation, l'extraction et la combustion des pétroles, gaz et charbons ont conduit à introduire en un temps très court des quantités significatives de carbone appartenant à ce cycle long dans le cycle superficiel. Cette introduction induit d'importantes perturbations du cycle biochimique avec notamment le rejet de CO_2 dans l'asmosphère pouvant contribuer à augmenter la température moyenne du globe, induisant des modifications climatiques. Cette production de CO_2 est associée à l'introduction de produits organiques fossiles dont la nature et les effets sur les différents compartiments superficiels (atmosphère, biosphère, hydrosphère, pédosphère…) ne sont que partiellement connus.

Ce travail cible plus précisement l'introduction de ces produits organiques dans l'environnement. Même si la dispertion de certains de ces produits est suivie, étudiée et

quantifiée de façon régulière (par exemple le dosage de composés ciblés comme les 16 HAP réglementaires), la majeur partie d'entre eux reste peu étudiée et mal connue en condition de sub-surface. En revanche, la géochimie organique focalise ces travaux sur cette matière organique fossile. Cette discipline est donc incourtournable pour servir de base à l'étude de la dissimination de produits fossiles dans l'environnement. En effet, comprendre la dissémination de produits fossiles implique tout d'abord de bien comprendre leur formation et leur réactivité.

2. Matière organique fossile

2.1. Formation et évolution de la matière organique fossile

La matière organique issue du cycle biochimique, une fois « piégée» dans le compartiment sédimentaire, va partiellement être décomposée (essentiellement par minéralisation) sous conditions anaérobies puis aérobies (diagénèse précoce). Une faible partie de cette matière organique va échapper à cette dégradation et être retirée progressivement du cycle biochimique pour être transférée dans le cycle géochimique. Après incorporation dans les sédiments, la matière organique peut subir, suivant les caractéristiques et l'évolution du bassin sédimentaire (enfouissement, gradient géothermique…) plusieurs étapes de transformations communément scindées en trois phases successives : la diagénèse, la catagénèse et la métagénèse (Figure 2).

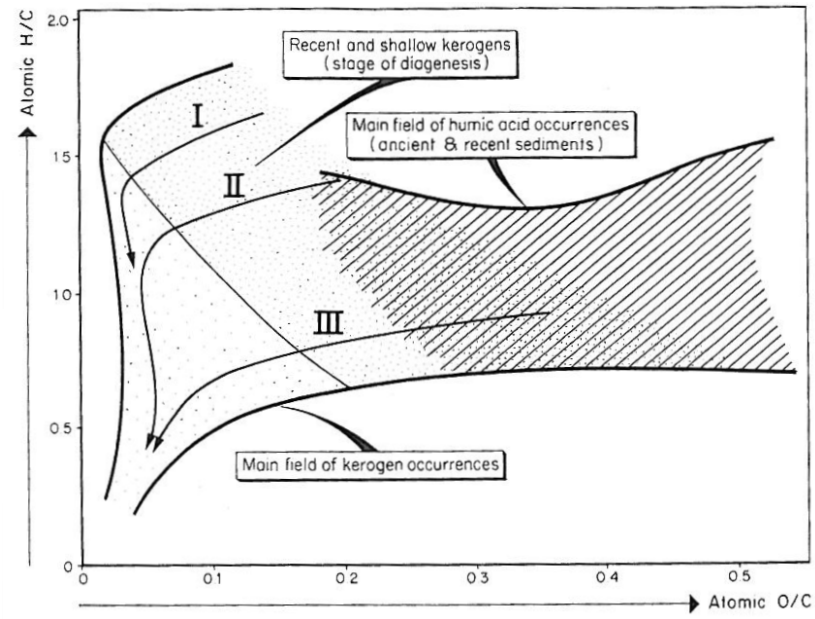

Figure 2: Diagramme de Van Krevelen indiquant la composition élémentaire des trois principaux types de kérogène au début de la diagenèse et leurs évolutions chimiques jusqu'au stade de métagenèse (d'après Tissot et Welte, 1984 (Tissot *et al.* 1984))

Diagénèse : Ce processus correspond aux premiers stades de la transformation de la matière organique. Les conditions de température et de pression, restant relativement limitées à ce stade, permettent une activité biologique. Cette activité va permettre la poursuite du dégagement de gaz (CH_4 et CO_2 principalement) et la matière organique résiduelle va se réorganiser et évoluer vers une structure carbonée tridimentionnelle de type kérogène (Figure 3). La nature de ce kérogène est essentiellement dépendante de l'origine des constituants organiques issus du cycle biochimique.

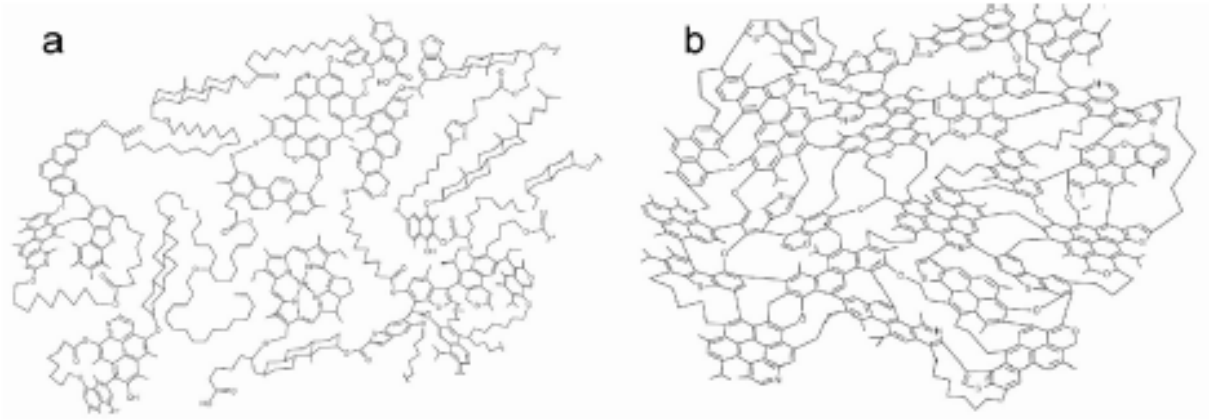

Figure 3: Modèle structural d'un kérogène de type II (origine marine) au début de la diagénèse (a) et à la fin de la catagenèse (b), d'après Béhar *et al.* (Béhar *et al.* 1987).

Catagénèse : Au fur et à mesure de l'enfouissement du kérogène, la température va augmenter (entre 60°C et 100°C) et ainsi limiter puis stoppper l'activité microbienne. Le kérogène subit une perte intense d'oxygène et d'hydrogène conduisant à la formation de pétrole (fenêtre à huile) et de gaz humides.

Métagénèse : Cette phase est caractérisée par la production de gaz sec (à CH_4 dominant ou exclusif) provenant de la rupture de liaisons plus stables au sein du kérogène et à la libération de groupements résiduels de plus petites tailles (e.g. alcanes ayant 1 à 4 carbones). Le solide résiduel s'aromatise fortement et tend à acquérir une structure graphitoïde.

2.2. De la matière organique fossile naturelle à anthropique

Même si la matière organique fossile correspond à de la matière organique naturelle (appartenant au cycle géologique), et que son introduction dans le cycle superficielle peut se faire de façon naturelle (érosion de formations géologiques, fuites de réservoirs pétroliers par exemple), son introduction intensive par l'homme depuis la révolution industrielle dans le cycle biochimique, en a fait une fraction organique anthropique. Cette introduction artificielle de produits fossiles dans l'environnement (dérivant essentiellement de produits pétroliers et de charbons) peut être regroupée en deux catégories :

- introduction des produits ou sous-produits directement issus de la matière organique fossile (pétroles bruts, charbons, produits de distillation…) sans processus de combustion préalable (pétrochimie – carbochimie). Ces introductions peuvent être accidentelles (marées noires, fuites de réservoirs, contamination de sols abritant ou ayant abrité des usines de traitements) ou intensionnelles (épandage de bitume routier, traitement du bois…),
- introduction de sous-produits hérités de la combustion incompléte de produits fossiles (notamment le kérosène, l'essence, le fuel, le fuel lourd), mais également issus de l'élimination des produits issus de la plasturgie (incinérateurs…). Parmi les sous produits de cette catégorie, les hydrocarbures aromatiques polycycliques sont les plus étudiés en terme de réactivité et de dissémination (Figure 4).

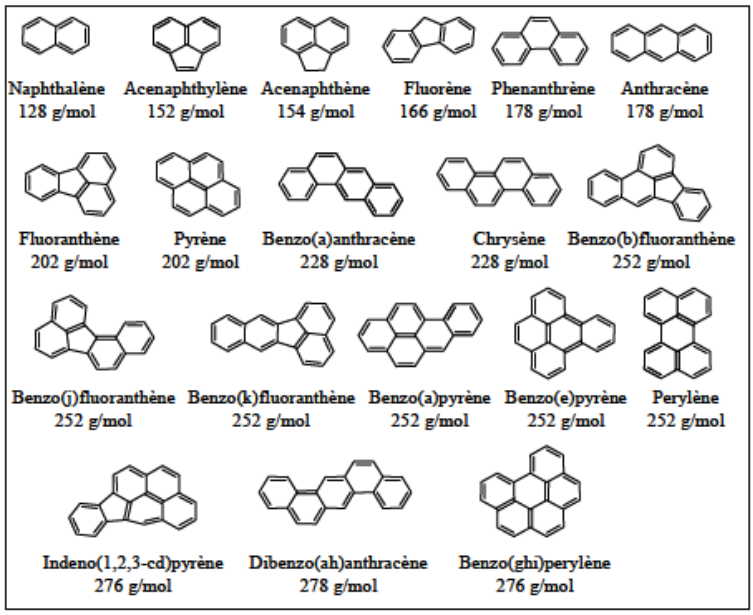

Figure 4: 16 HAP classés comme polluants prioritaires par l'US-EPA

Il est important de noter que l'essort des filières « vertes » permettant le développement d'agrocarburants ou de biomasse destiné à la production d'énergie peut conduire à la formation de sous-produits organiques relativement semblables même s'ils ne sont pas initialement issus de matière organique fossile.

2.3. Matière organique fossile hydrosoluble

La matière organique dissoute (MOD) correspond au plus grand réservoir de carbone des océans, dont la quantité (~700 Pg de C) est approximativement celle du carbone issu du CO_2 contenu dans l'air (~750 Pg C) (Hedges 2002). La compréhension de la composition de la matière organique dissoute d'origine marine est de première importante pour prédire le comportement des cycles géochimiques et des écosystèmes globaux dans un contexte de réchauffement climatique (Mopper *et al.* 2007).

La difficulté dans l'analyse de la matière organique dissoute réside dans sa structure qui correspond à un système polydispersé complexe composé d'une grande variété de molécules, de tailles, de fonctions chimiques et de polarités différentes. La principale difficulté pour caractériser la MOD réside à la fois dans les techniques d'extraction qui peuvent potentiellement altérer les échantillons ainsi que dans la détermination de sa composition moléculaire (Mopper *et al.* 2007).

Par ailleurs, la présence de matière organique fossile dans les sols et les sédiments conduit en partie à un transfert de cette matière dans les systèmes hydrauliques. En effet, dans les sols et les sédiments la matière organique fossile est dégradée en partie par les microorganismes ainsi que par les conditions physico-chimiques qui règnent dans ces systèmes. Il est donc important de caractériser cette matière organique dissoute en suivant sa réactivité afin de mieux comprendre son rôle et ses capacités de dispersion dans l'environnement.

2.4. Bilan de la caractérisation de la matière organique

Malgré les avancées technologiques dans le domaine analytique, plus de la moitié de la matière organique dans les sols, les sédiments et les eaux reste encore non caractérisée (Figure 5) au nivau moléculaire (Hedges *et al.* 2000). Wakeham *et al.* (1997) (Wakeham *et al.* 1997), dans une étude sur 100 acides aminés, sucres et lipides ont montré que plus de 75% des molécules organiques particulaires, i.e. en suspension dans les eaux, restent non identifiées. Un résultat similaire a été montré par Stevenson (1994) (Stevenson 1994) pour l'humus du sol.

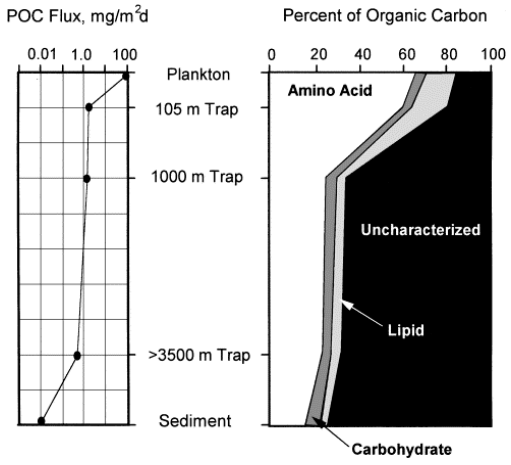

Figure 5: Carbone organique moléculaire non caractérisé dans le plancton, les trappes sédimentaires et les échantillons provenant des sédiments de la partie équatoriale de l'océan pacifique (d'après Wakeham *et al.*, 1997).

La matière organique subit donc un grand nombre de transformations complexes au cours de son évolution et change de propriétés physico-chimiques. Il est important de progresser dans notre compréhension des principaux stades de ces transformations, d'autant

plus que les activités industrielles ont commencé à impacter le cycle de subsurface de la matière organique.

3. Composition de la matière organique fossile

En géochimie organique des roches pétroligènes, la matière organique fossile est scindée en deux parties suivant la solubilité de ses composants dans les solvants organiques (généralement chloroforme ou toluène). La fraction organique correspond à l'**extrait organique** (bitumen en anglais) et la fraction insoluble correspond au **kérogène** (Figure 6).

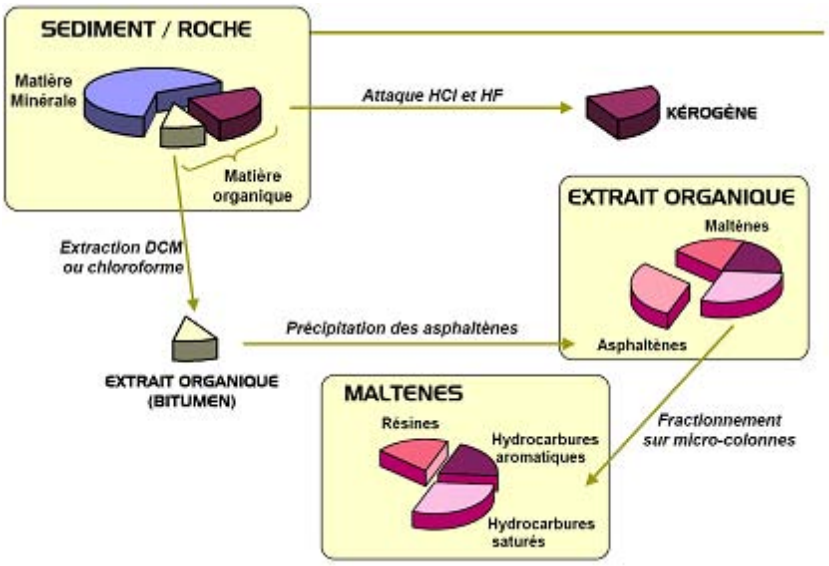

Figure 6: Schéma de synthèse des différentes parties composant la matière organique (d'après Faure *et al.*, 2000).

3.1. Le kérogène

Le kérogène est défini comme étant la fraction organique insoluble dans les solvants organiques usuels (Durand *et al.*, 1980). Etant intimement lié aux phases minérales, il est isolé par dissolution des minéraux carbonatés (acide chlorhydrique) et silicatés (acide fluorhydrique).

3.2. L'extrait organique

L'extrait organique est isolé par extraction à l'aide des solvants organiques usuels. Cet extrait organique est ensuite décomposé en 4 classes de composés obtenus par des étapes de précipitation et de fractionnement sur colonne. Cette séparation est appélé le fractionnement SARA (Saturés – Aromatiques – Résines – Asphaltènes).

3.2.1. Les asphaltènes

Les asphlatènes se différencient des autres fractions de l'extrait organique par leur insolubilité dans le *n*-pentane (ou *n*-heptane) (Speight 2004; Speight 2004). Ils sont donc généralement isolés par précipitation. Les asphaltènes sont constitués d'entités hydrocarbonées portant des fonctions aliphatiques et aromatiques, des hétéroatomes (N,S,O) et des métaux. Ils sont considérés comme un édifice supramoléculaire de hautes masses moléculaires (supérieures à 1000 Da) composés de noyaux aromatiques polycondensés substitués présentant une forte polarité.

3.2.2. les résines et les hydrocarbures

Les résines, les hydrocarbures saturés et aromatiques sont séparés par chromatographie liquide sur colonne d'alumine et de silice.

Les hydrocarbures saturés regroupent des molécules constituées uniquement de carbone et d'hydrogène à structure non aromatique : les *n*-alcanes, les iso et cyclo-alcanes et les alcènes.

Les hydrocarbures aromatiques sont caractérisés par la présence d'un ou de plusieurs noyaux aromatiques condensés.

Les résines correspondent à des molécules généralement polycycliques contenant des hétéroatomes (N, S et O principalement).

4. Les outils de caractérisation de la matière organique fossile

Aborder la caractérisation des produits organiques fossiles disséminés dans l'environnement superficiel implique bien évidemment l'utilisation des outils développés, entre autre, par la géochimie organique.

4.1. Méthodes globales

Parmi les méthodes globales classiquement utilisées, la teneur en carbone organique (TOC) et les analyses élémentaires (C,H,N,S,O) restent les caractérisations de base. Ces caractérisations permettent (i) d'évaluer la quantité de carbone organique présente dans l'échantillon et lorsque la mesure est faite sur le kérogène (avec préalablement élimination des fractions minérales et de l'extrait organique) (ii) de mesurer les rapports atomiques H/C et O/C pour placer l'échantillon dans un diagramme de Van Krevelen (Van Krevelen 1950) et déterminer son type et son degré de maturation.

En géochimie organique, ces analyses classiques sont généralement complétées ou remplacées par la méthode de pyrolyse Rock-Eval (Béhar *et al.* 2001). Cette technique analytique a été développée et principalement utilisée pour l'exploration pétrolière. La méthode consiste à pyrolyser un échantillon avec un gradient de température sous atmosphère inerte. Des gaz vont être libérés puis quantifiés. La quantité d'hydrocarbures libres est déterminée par le pic S1 (à 300°C); le pic S2 (entre 300°C et 650°C) détermine, quant à lui, le potentiel d'hydrocarbures après maturation. Un autre paramètre mesuré pendant la pyrolyse est la température au maximum du pic S2 ; le Tmax est un paramêtre standardisé qui permet d'évaluer de degré de maturité thermique de la matière organique fossile. De plus, la combinaison du pic S3 et du TOC permet d'obtenir l'indice d'oxygène (OI) qui permet de déterminer le degré de maturation des charbons et du kerogène.

Ces études globales permettent ainsi d'obtenir des informations de façon rapide et donc de traiter un grand nombre d'échantillons (notamment la pyrolyse Rock-Eval). Il est alors possible de sélectionner des échantillons d'intérêt pour réaliser des caractérisations plus poussées notamment à l'échelle moléculaire.

4.2. Caractérisations moléculaires

La **chromatographie en phase gazeuse couplée à la spectrométrie de masse** (GC-MS) est la technique analytique la plus utilisée en géochimie pétrolière pour l'étude des biomarqueurs moléculaires. Ces biomarqueurs moléculaires (Eglinton *et al.* 1964); Eglinton et Calvin, 1967) correspondent à des molécules organiques possédant des squelettes carbonés directement hérités de molécules synthétisées par des organismes vivants. Habituellement présents dans les huiles et les roches-mères, ces biomarqueurs sont couramment utilisés en géochimie organique afin d'appréhender l'origine de la matière organique et les conditions de dépôt sédimentaire. Ainsi, la GC-MS qui présente une qualité de séparation moléculaire très élevée permet d'identifier ces molécules d'intérêt.

En GC-MS, l'extrait organique ou bien une sous-fraction (hydrocarbures saturés, hydrocarbures aromatiques ou résines) est injecté via un injecteur chauffé à haute température (environ 300°C). Les molécules présentes vont être vaporisées puis entrainées par un gaz vecteur vers une colonne. Chauffés progressivement par programmation de température, ils vont être séparés par différence d'affinité avec la phase stationnaire de la colonne. A la sortie de celle-ci, les échantillons arrivent dans une source d'ionisation et vont subir un bombardement d'électrons (impact électronique) qui va les ioniser puis les fragmenter. Les rapports masse sur charge (m/z) des fragments obtenus vont être mesurés par un analyseur de masse (le plus souvent de type quadripolaire).

Du fait de l'utilisation de l'ionisation par impact électonique, dont les électrons (émis par un filament de tungstène ou de rhénium) vont être accélérés par une différence de potentiel qui va leur conférer une énergie cinétique de 70eV (accélération identique d'une source à l'autre), il va être possible de constituer des bibliothèques de spectres de fragmentation qui permettront ensuite une identification plus facile.

Cependant, du fait de son principe d'utilisation, seuls les composés vaporisables et thermostables à la température de l'injecteur pourront être analysés. Cette limitation est souvent corrélée à la masse des composés et il est ainsi couramment admis que les composés analysables en GC sont ceux dont la masse molaire n'excède pas 600 Da. De surcroît, l'analyse des substances polaires nécessite des modifications physico-chimiques préalables comme la dérivatisation obtenue, par exemple, avec le BSTFA (**bis-(Trimethylsilyl) trifluoroacetamide)**.

Pour améliorer les connaissances sur les fractions plus lourdes de la matière organique (notamment le kérogène et les asphaltènes), la Py-GC-MS (couplage de **pyrolyse**

flash - chromatographie en phase gazeuse - spectrométrie de masse) a été développée. Il s'agit d'une technique de pyrolyse (généralement de 600°C à 700°C) réalisée pendant un temps court environ 10 secondes). Les produits générés sont ensuite injectés « on-line » en GC-MS.

Cette technique permet l'analyse structurale des systèmes macromoléculaires. Sous l'effet de la température, les structures macromoléculaires vont se briser en plus petites entités qui seront analysables par GC-MS selon le même principe que décrit précédemment.

Toutefois, cette technique même si elle permet de déterminer les structures moléculaires des systèmes macromolécules, elle transforme de façon importante les molécules initiales. Par ailleurs, au cours de la pyrolyse, des réarrangements moléculaires peuvent se produire notamment en présence de minéraux (Faure *et al.* 2006; Faure *et al.* 2006). Cependant, la méthylation *in situ* (utilisation de l'hydroxyde de tétraméthyl ammonium – TMAH) semble limiter ces réorganisations.

Plus récemment, le développement de la GC-MS/MS a permis d'augmenter la sensibilité de cette technique, notamment dans le cadre de la quantification des composés cibles dans les matrices complexes.

La chromatographie liquide haute pression (HPLC) a pour but principal de séparer les molécules en fonction de leur affinité avec la phase stationnaire (chromatographie liquide d'adsorption, de partage, chirale…) ou de leur taille moléculaire (chromatographie d'exclusion stérique).

Cette technique, contraitement à la GC-MS, n'est pas limitée aux molécules de petites tailles (600 Da) car elle concerne tous les composés pouvant être mis en solution (en phase organique ou aqueuse).

Toutefois, la résolution chromatographique de la chromatographie en phase liquide est nettement plus limitée que la chromatographie en phase gaz. De plus les détecteurs généralement associés (réfractomètre, détection UV, barrette de diode…) ne permettent d'obtenir des informations précises que pour des mélanges de composés assez simples. Mais lors de l'analyse de mélanges naturels et donc complexes, les phénomènes de coélution associés à la détection, souvent spécifique à des groupements fonctionnels, ne permettent pas d'obtenir des informations spécifiques sur l'ensemble des molécules.

Cependant, avec l'introduction de différents couplages ente l'HPLC et la spectrométrie de masse (LC-MS et LC-MS/MS) et l'utilisation des sources à pression

atmosphérique (ESI, APCI et APPI), cette technique est devenue incontournable tant pour la caractérisation que pour la quantification de composés cibles.

4.3. Caractériations spectroscopiques

Différentes techniques spectroscopiques permettent de traiter des fractions organiques complexes notamment celles qui ne sont pas analysables par chromatographie, tels que les composés très polaires et aromatiques de hauts poids moléculaires.

La micro-spectroscopie infrarouge à transformée de Fourier permet, par exemple, d'évaluer l'aromaticité, l'aliphaticité et le degré de fonctionnalisation des macromolécules.

En revanche, la spectrométrie de Résonance Magnétique Nucléaire (RMN) en phase liquide permet la détermination de la structure des molécules par détermination des déplacements chimiques (RMN ^{1}H ^{13}C ^{15}N) qui peuvent ensuite être comparé à des bibliothèques de spectres existantes pour déterminer leur environnement.

Par ailleurs, lorsque l'échantillon ne peut être mis en solution dans les solvants classiques de RMN (ou pour les études sur les matériaux), la RMN du solide avec notamment la CPMAS (Cross Polarization Magical Angle Spinning) a permis d'analyser en routine la matière organique (Cardoza *et al.* 2004; Cook 2004). Plus récemment de nouvelles techniques de RMN comme la RMN à deux ou multidimensions ont permis d'améliorer la caractérisation de la matière organique naturelle (Mao *et al.* 2007; Mao *et al.* 2007; Deshmukh *et al.* 2007)).

Toutefois, ces méthodes spectroscopiques sont des méthodes analytiques spécifiques dans le cas d'un échantillon relativement simple. Dans le cas de solutions complexes, ces méthodes fournissent des informations structurales « grossières », et restent donc des méthodes de caractérisation globale.

4.4. Limitations des techniques analytiques : les asphaltènes

L'ensemble des techniques décrites précedemment, les plus fréquement utilisées en géochimie organique, permettent d'obtenir beaucoup d'informations sur la matière organique à la fois moléculaires et structurales. Cependant, elles ne sont pas adaptées à l'analyse de

fractions macromoléculaires, ces dernières présentant une forte polarité, une masse moléculaire élevée, une grande compléxité de composition et d'association…

Pourtant cette fraction macromoléculaire joue un rôle majeur : la composition chimique des asphaltènes est directement héritée des kérogènes dont elles sont issues. Les asphaltènes portent ainsi des informations géochimiques. Par ailleurs, les asphaltènes sont des entités très réactives qui sont transformées par les conditions diagénétiques. Elles forment aussi un milieu réactif privilégié dans le cadre des interactions chimiques avec les hydrocarbures (craquage) ou avec l'eau (Michels *et al.*, 1996).

Par ailleurs, cette fraction macromoléculaire est la source de différents problèmes relatifs à l'exploitation et à l'utilisation du pétrole. Lors de l'exploitation des réservoirs pétroliers ainsi que lors du transport du pétrole, les asphaltènes ont tendance à précipiter et à boucher les conduits provoquant des chutes de production. Il est donc important de comprendre leur stabilité et leurs propriétés physiques et chimiques (Cimino *et al.* 1995; Speight 1998) afin de maîtriser leur comportement. De plus, lors du raffinage, les aphaltènes ont un effet négatif sur l'efficacité sur le processus d'hydrodésulfurisation. Enfin, étant donné qu'ils agissent comme des précurseurs de coke, ils causent une désactivation des catalyseurs et conduisent à la formation de boues, ce qui diminue l'efficacité de la conversion du pétrole brut lors du processus de craquage hydraulique. (Oballa *et al.* 1994)

La composition en métaux est également importante à connaître. En effet, certains métaux jouent un rôle dans la génèse et le raffinage du pétrole. D'autres métaux permettent d'obtenir des informations sur l'origine la migration et la maturation du pétrole

D'un point de vue environnemental, les métaux posent également des problèmes, en plus d'être responsable partiellement de la corrosion des équipements et de l'empoisonnement des catalyseurs, au niveau de l'environnement (lors de fuites), surtout dans le cas des métaux lourds.

De plus, les métaux que renferment les asphaltènes permettent également de classer les pétroles. Thompson a proposé une classification des huiles et condensats par le rapport S/N puis Ni/(V+Ni). Le nickel et le vanadium sont présents dans les pétroles sous la forme de métalloporphyrines.

Plus récemment, les travaux de Selby et Creaser (Selby *et al.* 2005) ouvrent la voie à la création d'un géochronomètre basé sur la quantification de certains isotopes du rhénium et de l'osmium qui permettrait de dater les réservoirs pétroliers. L'importance de la

caractérisation des asphaltènes se retrouve particulièrement dans ce cas car ces deux métaux ont une affinité particulière pour les asphaltènes.

4.5. Avancées récentes dans la compréhension de la structure des asphaltènes

L'essor de la spectrométrie de masse depuis une dizaine d'années avec notamment le développement la spectrométrie de masse ultra haute résolution (i.e. FT-ICR) a permis des grandes avancées dans la caractérisation des sytèmes macromoléculaires. En revanche, malgré le développement de la spectrométrie de masse ultra haute résolution, i.e. FT-ICR (Marshall *et al.* 1998), la composition et la gamme de masses de la matière organique supramoléculaire soluble (e.g. asphaltènes de pétrole, acides « humiques » et « fulviques ») sont toujours sujet à débats. Certains ont rapporté des masses de 300 à 700 Da (Koch *et al.* 2005) d'autres de quelques centaines à plusieurs milliers de daltons pour la fraction colloïdale (Leenheer *et al.* 2003).

L'utilisation de la spectrométrie de masse FT-ICR équipée d'une source d'ionisation ESI (Electrospray Ionization) a été largement utilisée pour l'analyse de la matière organique dissoute (Kujawinski 2002; Kujawinski *et al.* 2002; Stenson *et al.* 2002; Kim *et al.* 2003; Kim *et al.* 2003; Stenson *et al.* 2003; Kim *et al.* 2006; Kujawinski *et al.* 2009).

Du fait de la présence de fonctions polaires et apolaires, D'Andrilli *et al.* (D'Andrilli *et al.* 2010) ont démontré l'importance de l'utilisation combinée des sources à pressions atmosphériques, l'ESI pour les composés polaires et l'APPI (Atmospheric Pressure PhotoIonization) ou l'APCI (Atmospheric Pressure Chemical Ionization) pour les composés apolaires ou peu polaires ainsi que la plupart des composés soufrés. Par ailleurs, les avantages de l'utilisation de la source APPI sont la faible sensibilité à la présence des sels, et la réduction des effets de suppression ionique (Robb *et al.* 2000; Hanold *et al.* 2004). Cependant, l'étude sur la matière organique fossile reste très peu décrite car la majorité des travaux se focalise sur l'utilisation de l'ESI pour l'analyse des composés polaires, majoritairement présents dans la matière organique (Sleighter *et al.* 2007). Cependant l'augmentation de la proportion de la matière organique fossile dans les sols et sédiments poussent à s'intéresser de plus en plus aux composés apolaires ou peu polaires.

Cependant, la spectrométrie de masse ne permet pas la comparaison directe des spectres de masse de différents échantillons entre eux du fait de la forte influence de divers

paramètres, comme les effets « matrices »; il n'est donc pas possible de constituer des bibliothèques de spectres, de même que pour les spectres de fragmentation puisqu'à l'exception de l'impact électronique, les règles de fragmentation existent mais sont assez générales. Par ailleurs, la spectrométrie de masse FT-ICR apporte beaucoup plus d'informations (plusieurs milliers de composés peuvent être détectés grâce à la très haute résolution) et cette très quantité d'informations inhérente à ce type d'analyseur de masse rend très difficile et très long l'interprétation des spectres de masse. Pour y remédier des recherches concernant le traitement numérique et statistique ont commencé à se développer, comme dans le cas de la spectrométrie de masse FT-ICR par l'utilisation des diagrammes de Van Krevelen (Van Krevelen 1950) ou de Kendrick (Kendrick 1963) qui permettent de réaliser une représentation graphique des données obtenues par spectrométrie de masse. D'autres travaux ont développé des analyses statistiques en utilisant par exemple l'Analyse en Composante Principale (ACP) (Sleighter *et al.* 2010) et semblent prometteurs.

Cependant, la spectrométrie de masse FT-ICR n'est pas la seule technique utilisée pour l'analyse de la matière organique dissoute. Des travaux ont montré que l'utilisation de la spectrométrie de masse Q-TOF permettait également d'obtenir des informations qualitatives lorsque des échantillons étaient comparés entre eux (Kujawinski *et al.* 2002) mais n'autorisait pas la détermination de la composition au niveau moléculaire du fait du manque de résolution, contrairement au FT-ICR.

5. Références

Béhar, F., Beaumont, V., and De B. Penteado, H.L., Technologie Rock-Eval 6 : performances et développements. *Oil & Gas Science and Technology - Rev. IFP*, **2001**. *56*(2): p. 111-134.

Béhar, F. and Vandenbroucke, M., Chemical modelling of kerogens. *Org. Geochem.*, **1987**. *11*(1): p. 15-24.

Cardoza, L.A., Korir, A.K., Otto, W.H., Wurrey, C.J., and Larive, C.K., Applications of NMR spectroscopy in environmental science. *Prog. Nucl. Magn. Reson. Spectrosc.*, **2004**. *45*(3-4): p. 209-238.

Cimino, R., Correra, S., Del, B.A., and Lockhart, T.P. Solubility and phase behavior of asphaltenes in hydrocarbon media. 1995. Plenum.

Cook, R.L., Coupling NMR to NOM. *Anal. Bioanal. Chem.*, **2004**. *378*(6): p. 1484-1503.

D'Andrilli, J., Dittmar, T., Koch, B.P., Purcell, J.M., Marshall, A.G., and Cooper, W.T., Comprehensive characterization of marine dissolved organic matter by fourier transform ion cyclotron resonance mass spectrometry with electrospray and atmospheric pressure photoionization. *Rapid Commun. Mass Spectrom.*, **2010**. *24*(5): p. 643-650.

Deshmukh, A.P., Pacheco, C., Hay, M.B., and Myneni, S.C.B., Structural environments of carboxyl groups in natural organic molecules from terrestrial systems. Part 2: 2D NMR spectroscopy. *Geochim. Cosmochim. Acta*, **2007**. *71*(14): p. 3533-3544.

Durand, B., Sedimentary organic matter and kerogen. Definition and quantitative importance of kerogen. *Kerogen: insoluble organic matter from sedimentary rocks*, **1980**: p. 13-34.

Durand, B. and Espitalie, J., Evolution of organic matter during embedding of sediments. *C. R. Acad. Sci., Ser. D*, **1973**. *276*(Copyright (C) 2011 American Chemical Society (ACS). All Rights Reserved.): p. 2253-6.

Eglinton, G., Scott, P.M., Belsky, T., Burlingame, A.L., and Calvin, M., Hydrocarbons of biological origin from a one-billion-year-old sediment. *Sci*, **1964**. *145*(3629): p. 263-264.

Faure, P., Jeanneau, L., and Lannuzel, F., Analysis of organic matter by flash pyrolysis-gas chromatography-mass spectrometry in the presence of Na-smectite: When clay minerals lead to identical molecular signature. *Org. Geochem.*, **2006**. *37*(12): p. 1900-1912.

Faure, P., Schlepp, L., Mansuy-Huault, L., Elie, M., Jardé, E., and Pelletier, M., Aromatization of organic matter induced by the presence of clays during flash pyrolysis-gas chromatography-mass spectrometry (PyGC-MS): A major analytical artifact. *J. Anal. Appl. Pyrolysis*, **2006**. *75*(1): p. 1-10.

Hanold, K.A., Fischer, S.M., Cormia, P.H., Miller, C.E., and Syage, J.A., Atmospheric pressure photoionization. 1. General properties for LC/MS. *Anal. Chem.*, **2004**. *76*(10): p. 2842-2851.

Hedges, J.I., Why Dissolved Organics Matter, in *Biogeochemistry of Marine Dissolved Organic Matter*, A.H. Dennis and A.C. Craig, Editors. 2002, Academic Press: San Diego. p. 1-33.

Hedges, J.I., Eglinton, G., Hatcher, P.G., Kirchman, D.L., Arnosti, C., Derenne, S., Evershed, R.P., Kogel-Knabner, I., De, L.J.W., Littke, R., Michaelis, W., and Rullkotter, J., The molecularly-uncharacterized component of nonliving organic matter in natural environments. *Org. Geochem.*, **2000**. *31*(Copyright (C) 2011 American Chemical Society (ACS). All Rights Reserved.): p. 945-958.

Kendrick, E., A mass scale based on CH2 = 14.0000 for high resolution mass spectrometry of organic compounds. *Anal. Chem.*, **1963**. *35*(13): p. 2146-2154.

Kim, S., Kaplan, L.A., and Hatcher, P.G., Biodegradable dissolved organic matter in a temperate and a tropical stream determined from ultra-high resolution mass spectrometry. *Limnol. Oceanogr.*, **2006**. *51*(2): p. 1054-1063.

Kim, S., Kramer, R.W., and Hatcher, P.G., Graphical Method for Analysis of Ultrahigh-Resolution Broadband Mass Spectra of Natural Organic Matter, the Van Krevelen Diagram. *Anal. Chem.*, **2003**. *75*(20): p. 5336-5344.

Kim, S., Simpson, A.J., Kujawinski, E.B., Freitas, M.A., and Hatcher, P.G., High resolution electrospray ionization mass spectrometry and 2D solution NMR for the analysis of DOM extracted by C18 solid phase disk. *Org. Geochem.*, **2003**. *34*(9): p. 1325-1335.

Koch, B.P., Witt, M., Engbrodt, R., Dittmar, T., and Kattner, G., Molecular formulae of marine and terrigenous dissolved organic matter detected by electrospray ionization

Fourier transform ion cyclotron resonance mass spectrometry. *Geochim. Cosmochim. Acta*, **2005**. *69*(13): p. 3299-3308.

Kujawinski, E.B., Electrospray ionization Fourier transform ion cyclotron resonance mass spectrometry (ESI FT-ICR MS): Characterization of complex environmental mixtures. *Environmental Forensics*, **2002**. *3*(3-4): p. 207-216.

Kujawinski, E.B., Freitas, M.A., Zang, X., Hatcher, P.G., Green-Church, K.B., and Jones, R.B., The application of electrospray ionization mass spectrometry (ESI MS) to the structural characterization of natural organic matter. *Org. Geochem.*, **2002**. *33*(3): p. 171-180.

Kujawinski, E.B., Hatcher, P.G., and Freitas, M.A., High-resolution fourier transform ion cyclotron resonance mass spectrometry of humic and fulvic acids: Improvements and comparisons. *Anal. Chem.*, **2002**. *74*(2): p. 413-419.

Kujawinski, E.B., Longnecker, K., Blough, N.V., Vecchio, R.D., Finlay, L., Kitner, J.B., and Giovannoni, S.J., Identification of possible source markers in marine dissolved organic matter using ultrahigh resolution mass spectrometry. *Geochim. Cosmochim. Acta*, **2009**. *73*(15): p. 4384-4399.

Kump, L.R., Kasting, J.F., and Crane, R.G., The Earth System, ed. P. Hall 2010: Pennsylvania State University. 432.

Leenheer, J.A. and Croué, J.P., Characterizing aquatic dissolved organic matter. *Environ. Sci. Technol.*, **2003**. *37*(1): p. 18A-26A.

Mao, J., Cory, R.M., McKnight, D.M., and Schmidt-Rohr, K., Characterization of a nitrogen-rich fulvic acid and its precursor algae from solid state NMR. *Org. Geochem.*, **2007**. *38*(8): p. 1277-1292.

Mao, J.D., Tremblay, L., Gagné, J.P., Kohl, S., Rice, J., and Schmidt-Rohr, K., Humic acids from particulate organic matter in the Saguenay Fjord and the St. Lawrence Estuary investigated by advanced solid-state NMR. *Geochim. Cosmochim. Acta*, **2007**. *71*(22): p. 5483-5499.

Marshall, A.G., Hendrickson, C.L., and Jackson, G.S., Fourier transform ion cyclotron resonance mass spectrometry: A primer. *Mass Spectrom. Rev.*, **1998**. *17*(1): p. 1-35.

Mopper, K., Stubbins, A., Ritchie, J.D., Bialk, H.M., and Hatcher, P.G., Advanced instrumental approaches for characterization of marine dissolved organic matter:

Extraction techniques, mass spectrometry, and nuclear magnetic resonance spectroscopy. *Chem. Rev.*, **2007**. *107*(2): p. 419-442.

Oballa, M.C., Shih, S.S., and Editors, Catalytic Hydroprocessing of Petroleum and Distillates. (Based on the Proceedings of the AIChE Spring National Meeting, Houston, Texas, March 28-April 1, 1993.) [In: Chem. Ind. (Dekker), 1994; 58] 1994: Dekker. 464 pp.

Robb, D.B., Covey, T.R., and Bruins, A.P., Atmospheric pressure photoionization: An ionization method for liquid chromatography-mass spectrometry. *Anal. Chem.*, **2000**. *72*(15): p. 3653-3659.

Selby, D. and Creaser, R.A., Geochemistry: Direct radiometric dating of hydrocarbon deposits using rhenium-osmium isotopes. *Sci*, **2005**. *308*(5726): p. 1293-1295.

Sleighter, R.L. and Hatcher, P.G., The application of electrospray ionization coupled to ultrahigh resolution mass spectrometry for the molecular characterization of natural organic matter. *J. Mass Spectrom.*, **2007**. *42*(5): p. 559-574.

Sleighter, R.L., Liu, Z., Xue, J., and Hatcher, P.G., Multivariate statistical approaches for the characterization of dissolved organic matter analyzed by ultrahigh resolution mass spectrometry. *Environ. Sci. Technol.*, **2010**. *44*(19): p. 7576-7582.

Speight, J.G., The Chemistry and Technology of Petroleum, Third Edition, Revised and Expanded. [In: Chem. Ind. (Dekker), 1998; 76] 1998: Dekker. 918 pp.

Speight, J.G., Petroleum asphaltenes - Part 1: Asphaltenes, resins and the structure of petroleum. *Oil and Gas Science and Technology*, **2004**. *59*(5): p. 467-477.

Speight, J.G., Petroleum asphaltenes - Part 2: The effect of asphaltenes and resin constituents on recovery and refining processes. *Oil and Gas Science and Technology*, **2004**. *59*(5): p. 479-488.

Stenson, A.C., Landing, W.M., Marshall, A.G., and Cooper, W.T., Ionization and fragmentation of humic substances in electrospray ionization Fourier transform-ion cyclotron resonance mass spectrometry. *Anal. Chem.*, **2002**. *74*(17): p. 4397-4409.

Stenson, A.C., Marshall, A.G., and Cooper, W.T., Exact masses and chemical formulas of individual Suwannee River fulvic acids from ultrahigh resolution electrospray ionization Fourier transform ion cyclotron resonance mass spectra. *Anal. Chem.*, **2003**. *75*(6): p. 1275-1284.

Stevenson, F.J., Humus chemistry : genesis, composition, reactions. 2nd ed 1994, New York: Wiley. xiii, 496 p.

Van Krevelen, D.W., Graphical-statistical method for the study of structure and reaction processes of coal. *Fuel*, **1950**. *29*(Copyright (C) 2011 American Chemical Society (ACS). All Rights Reserved.): p. 269-84.

Wakeham, S.G., Hedges, J.I., Lee, C., Peterson, M.L., and Hernes, P.J., Compositions and transport of lipid biomarkers through the water column and surficial sediments of the equatorial Pacific Ocean. *Deep-Sea Research Part II: Topical Studies in Oceanography*, **1997**. *44*(9-10): p. 2131-2162.

PART I: Principles of Size Exclusion Chromatography and Mass Spectrometry

Ce chapitre a pour but de fournir les éléments de base de la théorie des principaux outils analytiques utilisés afin de mieux comprendre leur principe de fonctionnement ainsi que les principales limitations. Ainsi, ce chapitre se décompose en trois parties :

- la première partie concerne la théorie de la chromatographie d'exclusion stérique (SEC),
- la seconde partie explore la théorie des différents éléments qui composent le spectromètre de masse utilisé, à savoir les sources d'ionisation : ESI (ElectroSpray Ionization), APCI (Atmospheric Pressure Chemical Ionisation) et APPI ainsi que les analyseurs de masse de type « quadripôle » (Q) et « temps de vol » (TOF),
- la dernière partie met en évidence la nécessité de coupler ces deux techniques ainsi que les principaux problèmes qui ont empéché jusqu'à présent le couplage de la SEC avec la spectrométrie de masse APPI-QTOF.

1. Size Exclusion Chromatography (SEC)

Size exclusion chromatography (SEC) is a separation technique; it is the given name to High Performance (Pressure) Liquid Chromatography (HPLC) which uses columns that distinguish molecules according to their molecular size. The early work is attributed to Porath and Flodin (Porath *et al.* 1959), who worked on the separation process of biomacromolecules. Then, the first gel column based chromatography was developed by Moore (Moore 1964) and was named at that time: Gel Permeation Chromatography (GPC).

Nowadays, SEC is the generic term for the technique whereas GPC is used for SEC based on column filled with gel. Thus, that technique gives a molecular mass distribution based on molecular size distribution. The linear dimension of a molecule is related to the molecular mass because a relationship exists between them in a freely jointed polymeric chain (random coil) as either the root-mean-square end-to-end distance or the radius of gyration is proportional (Wu *et al.* 1995).

1.1. Principle

During a SEC experiment, a mixture of different molecular mass compounds is injected at the top of the column in a mobile liquid phase with a fixed flow rate. These compounds will be differently retained by the stationary phase which is made of a porous material containing fixed size pores. As presented on a simplified scheme (Figure 1), the mixture is injected at the beginning of the column; the heavier molecular mass compounds will not be able to penetrate through the porous material and will go into the interstitial area outside of the porous materials. They will elute faster. On the contrary, smaller molecules will penetrate inside pores and they will be temporally retained; the pressure in the column and the constant flow rate will push them outside the column. After the column, a detector will detect every compound, giving a broadband chromatogram specific to this kind of experiments.

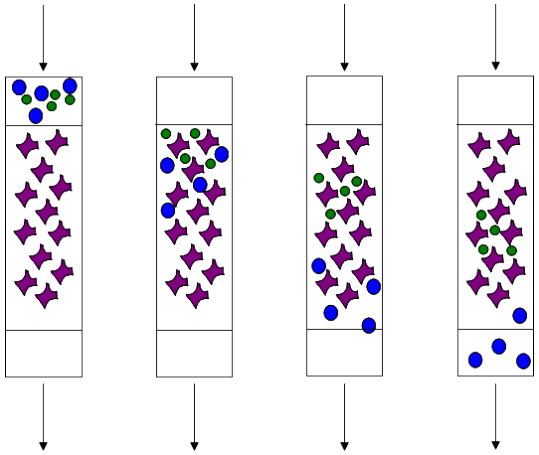

Figure 1: Principle scheme of SEC chromatography for 2 different molecules. After the sample injection the molecule will evaluate differently according to their molecular mass, the bigger ones will pass through the column faster than the small ones.

1.2. Separation process

Separation process (adapted from Nguyen) (Nguyen 1998) is based on the entropy decrease of a macromolecule when it is entering in a same size pore as its own dimensions (Figure 2). Allowed conformations are decreasing for a flexible polymer when it is getting closer to a solid limit. To avoid these regions, the polymer keeps distance between its gravity center and the solid/gel interface which is usually the same distance than the hydrodynamic radius (R_h) of the molecule. R_h is defined as the radius of a sphere which has equivalent thermodynamic properties of the macromolecule ($R_h \approx 0.7 R_g$; with Rg: gyration radius).

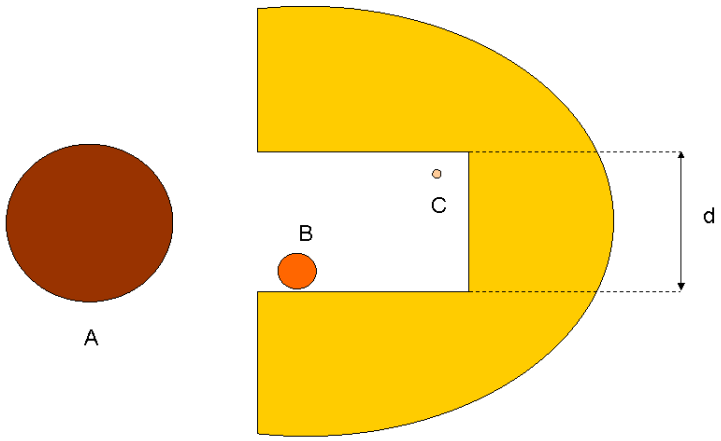

Figure 2 : Size exclusion mechanism, according to the ratio $2R_h/d$, there are 3 possibilities, a complete exclusion (A), a selective exclusion (B) or complete permeation (C) of the macromolecule.

According to that model, the accessible volume (V_{acc}) to the polymer in a cylindrical pore with a diameter d is equal to:

$$V_{acc} = (1 - 2R_h / d)^2 \times V_p \quad (1)$$

where (Vp) is the pore volume

and $2R_h \leq d$ (2)

A similar formula is obtained for cone-shaped pores with an aperture d:

$$V_{acc} = (1 - 2R_h / d)^3 \times V_p \quad (3)$$

and $2R_h \leq d$ (4)

As partition coefficient (K_{SEC}) is determined by the ratio between polymer concentration in mobile phase and in pores, it can be determined as following:

$$K_{SEC} = V_{acc} / V_p \quad (5)$$

From a thermodynamic point of view, partition coefficient at equilibrium (K_I) depends on the free energy variation of the specie (I) when it is moving from mobile phase to stationary phase:

$$K_i = \exp(-\Delta H^0{}_i / RT) \times \exp(\Delta S^0{}_i / R) \quad (6)$$

where ($\Delta H^0{}_i$) and ($\Delta S^0{}_i / R$) are respectively enthalpy and entropy at infinite dilution, at temperature and pressure in experimental conditions.

In ideal conditions of size exclusion, $\Delta H^0{}_i = 0$, i.e., partition of macromolecules between mobile phase and solvent inside pores is uniquely entropic.

In fact, it is difficult to completely eliminate enthalpy interactions, especially for strongly polar compounds as some additives, hydrosolubles or ionic polymers. Non-size effects can be minimized by the solvent judiciously chosen, which can to be a good solvent

for polymer solubilization, and have close solubility parameters from column packing material.

Solute holdup in SEC can be expressed as a function of three parameters:

- the partition coefficient (K_{SEC}),
- the mobile phase volume which is also equal to interstitial volume between particles (V_0),
- the pore volume (V_p).

From equation (5), elution volume (V_e) can be expressed as following:

$$V_e = V_0 + V_{acc} = V_0 + K_{SEC} x V_p \quad (7)$$

Partition coefficient depends on macromolecule relative size in regard to pore diameter (equation (1) or (3)), K_{SEC} is ranging from K_{SEC}=0 for big macromolecules to K_{SEC} =1 for the smaller ones. And so, molecules which cannot entered in pores are eluted first at V_0, whereas the ones which can entered in all pores are eluted with the solvent at ($V_0 + V_p$), In ideal conditions, SEC separation domain is ranging between these elution volume limits $V_0 < V_e < (V_0 + V_p)$. However some peaks can be observed out of these limits as impurities or compounds can induce enthalpic interactions, which lead to wrong retention times and thus, after calibration, to wrong molecular masses.

1.3. System overview

1.3.1. Experimental system

All experiments were performed on a Ultimate 3000 HPLC system (Dionex, Sunnyvale, CA, USA) composed of a degasser, an HPG (High-Pressure Gradient) pump (HPG-3200SD) which delivers a flow rate within 1µL.min^{-1} to 10mL.min^{-1}. A high accuracy autosampler (ACC 3000) carries 20µL of solution from a sample loop to a thermostated compartment (TCC-3000SD) which contains the analytical column(s). After separation, compounds are detected by an on-line detector system composed of a DAD (Diode Array Detector, Dionex DAD 3000) with a spectral range from 190 to 800 nm (Figure 3).

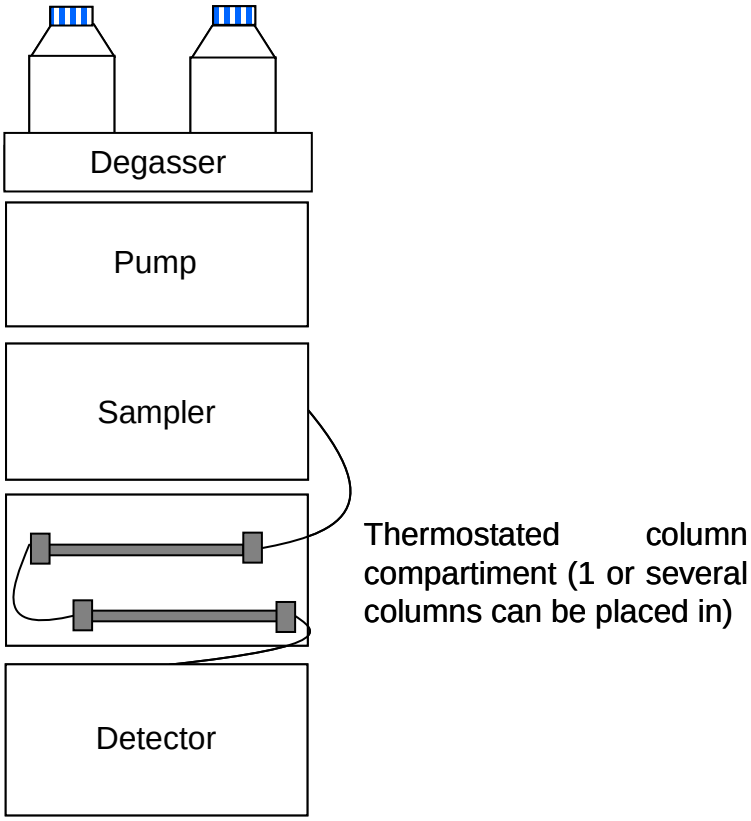

Figure 3 : Schematic representation of a classical SEC system.

1.3.2. Degasser and Pump

The degasser is an important part of the system as it removes gases from solvents through special polymer membranes which are permeable to gas but not liquid and thus permits to reduce pulsation in the pump. The HPG pump (High Pressure Gradient) is a serial dual-piston with electronic compressibility compensation and permits a zero-pulsation to avoid variations in detection such as RID (Refractive Index Detector), which are highly sensitive to pressure variations.

1.3.3. Sampler

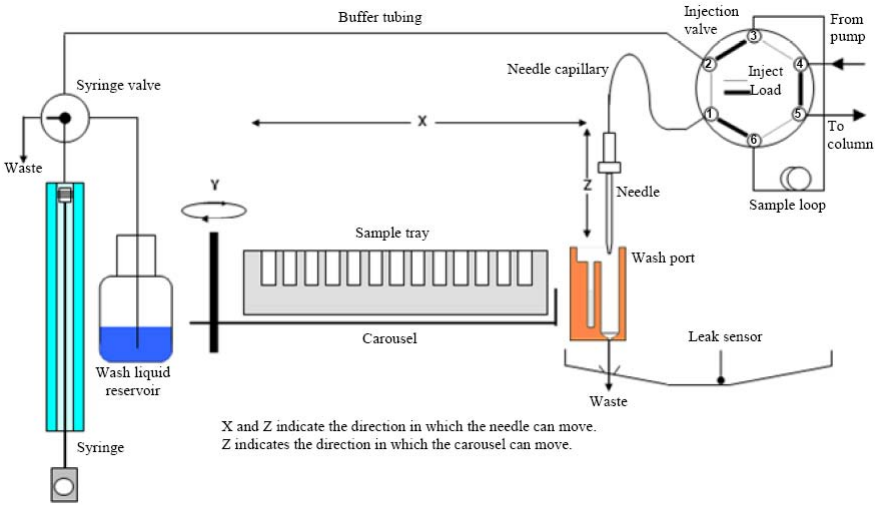

Figure 4: Schematic representation of the sampler (Dionex ACC300), reproduced form Dionex operating manual.

The sampler uses a 6 way valve with a 20 µL injection loop (Figure 4). While the injection valve is still in the inject position, the syringe aspirates the sample from a vial into the buffer tubing, thus filling the entire needle capillary with sample. Then, the injection valve is switched into the load position. The sample is drawn by the syringe through the needle and needle capillary and placed in the sample loop. Afterward, the injection valve is switched to the Inject position, directing the solvent flow from the sample loop through the high-pressure flow path to the column. The sample is transported into the column in back flush mode: In the Load position, the sample is drawn into the sample loop from the syringe. In the Inject position, the sample is drawn to the column by the solvent flow in the opposite direction (Figure 5).

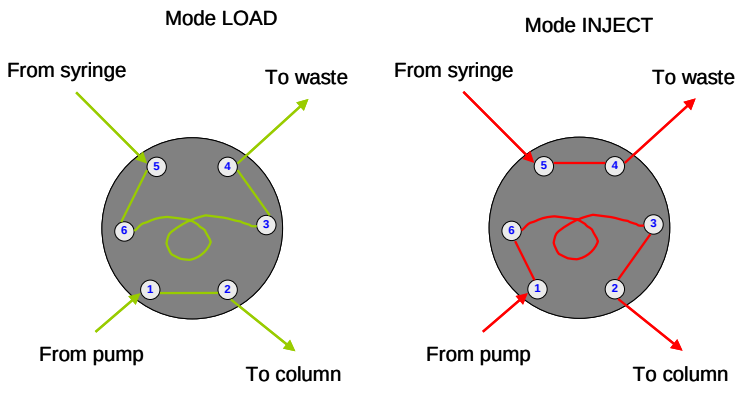

Figure 5: Representation of the 2 operating modes (load and inject) of the 6 way valve.

1.3.4. Columns and Oven

The optimum choice for a stationary phase should take in account several parameters. The packing material should not interact chemically with the solute, it must rendered completely wet by the mobile phase but should not suffer adverse swelling effects, it must be stable at the required operating temperature, and must have sufficient pore volume and an adequate range of pore sizes to resolve the sample's molecular mass distribution (Wu and Editor 1995).

All experiments were performed in organic phase and thus PLgel Organic GPC columns were chosen. Two different columns were tested according to their mass range limit. For both of them the packing material is composed of porous polystyrene divinyl benzene copolymers (PS/DVB) the monomer of which is presented on figure 6. This type of column is interesting for its wide availabilities of pore sizes and lack of adsorptive characteristics. Copolymers have excellent physical strength and are not easily subject to degradation by oxidation, hydrolysis or elevated temperature and can be used with a wide range of organic solvents.

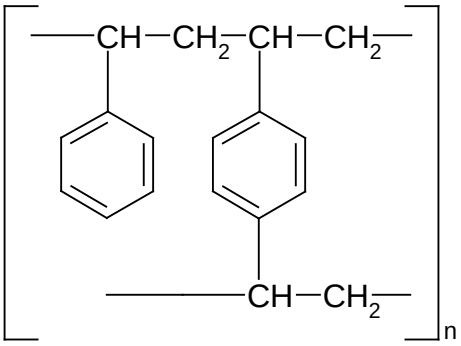

Figure 6: Structural formula of the styrene divinyl benzene monomer.

Column choice is often based on molecular mass range of the sample and the efficiency. The chosen columns are described in Table 1.

Column description	Linear mass range	Efficiency	Optimum flow rate	Maximum pressure	Maximum temperature
Plgel 5µm 100Å 250x4.6 mm ID	Up to 4 000 Da	>60 000 plates/m	1 mL/min	150 bar	150°C
Plgel Mixed E 3µm 300x7.5 mm ID	Up to 30 000 Da	>80 000 plates/m	1 mL/min	180 bar	110°C

Table 1: Specifications of the two GPC columns used.

1.3.5. UV-VIS detectors

Different types of UV detectors are commercialized, fixed wavelength UV detectors, multi-wavelength detectors, multi-wavelength disperse UV detectors, and Diode Array Detectors (DAD). In this part, only DAD will be described, especially because it often contains a visible lamp which completes the wavelength range of DAD with visible spectral domain (from 180 to 800 nm) which is more suitable for the detection of compounds containing aromatic rings and/or heteroatoms.

UV-VIS detectors respond to substances that absorb light in the range 180 to 800 nm. A great number of substances absorb light in this wavelength range when they possess a chromophore, i.e. structures composed of one or several double bonds and/or unshared electron groups (e.g. heteroatoms). DAD uses Deuterium (D) or Xenon (Xe) lamps generally coupled to a Tungsten (W) lamp for the visible light emission as strongly conjugated molecules (e.g. with polycondensed rings) have their maximum absorbance wavelength shifted to visible domain.

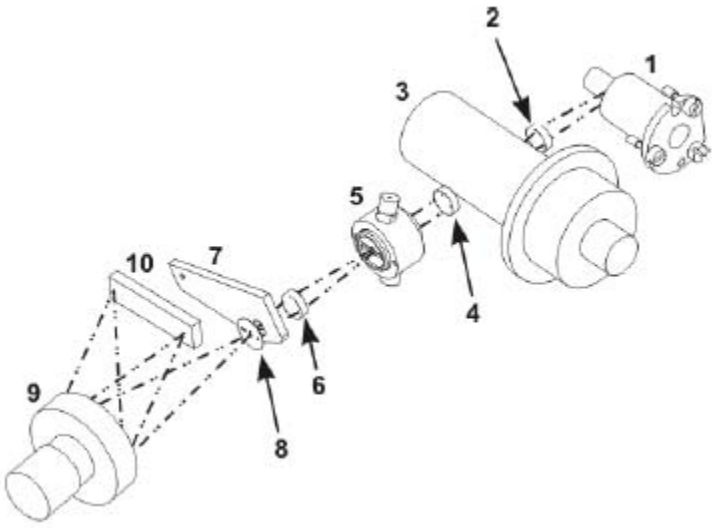

Figure 7: optical system for Dionex DAD3000, reproduced from Dionex user manual.

Figure 7 represents a schematic of the optical system Dionex DAD 3000. Incident light from the tungsten lamp (no. 1) is focused by a lens (no. 2) through an opening in the internal structure of the deuterium lamp (no. 3). Incident light from the tungsten and deuterium lamps is then focused by the achromat (no. 4) through the flow cell (no. 5). After exiting the cell, the light passes through a lens (no. 6) and is focused into the slit (no. 8).The light then goes through the slit to the grating (no. 9), where it is diffracted into the component wavelengths. Measurement of the light occurs at the photodiode array (no. 10). Each diode measures a narrow portion of the spectrum. A spectrum is obtained by measuring the light intensity of each diode and reporting the results over the selected wavelength range (principle adapted from Dionex user manual).

The principle of UV-VIS detection is based on the absorbance of a monochromatic wavelength by a molecule containing chromophore groups. The absorbance is given by the Beer-Lambert's law:

$$A = \varepsilon c l = \log\left(\frac{I_0}{I}\right) \tag{8}$$

where: (ε) is the molar excitation coefficient of the analyte ($L.mol^{-1}.cm^{-1}$), (c) is the concentration ($mol.L^{-1}$), (l) is the cell path (cm), (I_0) is the light intensity at the reference wavelength, (I) is the light intensity at the measured wavelength.

Thus this detection mode is particularly adapted to environmental samples especially because molecules which composed these samples have a high content of heteroatoms, aromatic rings polycondensed or not and high molecular mass compounds for which the conjugation of double bonds can shift the maximum absorbance wavelengths into the visible domain (Table 2). Considerations must also focus on the UV cutoff of solvents (Table 3).

Chromophore	Typical wavelength (nm)
$-C=C-$	180
$-C\equiv C-$	180 195 223
$>C=O$ (Ketone)	160 185 270-280
$-CHO$ (Aldehyde)	280-300
$-COOH$ (Carboxyl)	200-210
$-COOR$ (Ester)	208
$-O-$ (Ether)	185
$-C=C-C=C-$	217
$-C=C-C=O$	220 315
Benzene	184 204 255
Naphthalene	220 275 312
Anthracene	252 375

Table 2: UV absorbance wavelength for usual chromophores.

Solvent	UV cutoff (nm)
Acetone	330
Acetontrile	190
Acetic Acid	208
Benzene	280
Chloroform	245
Cyclohexane	210
n-Hexane	190
Methanol	205
Methylene chloride	233
THF	212
Toluene	285

Table 3: UV cutoffs of different usual solvents (below each value, corresponding solvent will fully absorb the incoming light).

1.4. Calibration

In SEC systems, the response given by detectors needs to be converted to obtain information on molecular masses. As SEC distinguishes molecules according to their hydrodynamic size and not to their molecular mass, it is very important to find a reliable method to convert chromatograms into molecular mass distribution diagrams. Three main methods are used.

1.4.1. Classical method

Polymer standards (usually polystyrenes), with small polydispersity and a perfectly known molecular masses, allow establishing a calibration curve ($\log M = f(V_e)$). As polymers have their own hydrodynamic size, the calibration curve will be specific to each polymer. An example of calibration curve is presented on (Figure 8), representing $\log(M)=f(t_r)$ as retention is proportional to elution volume when the flow rate remains constant.

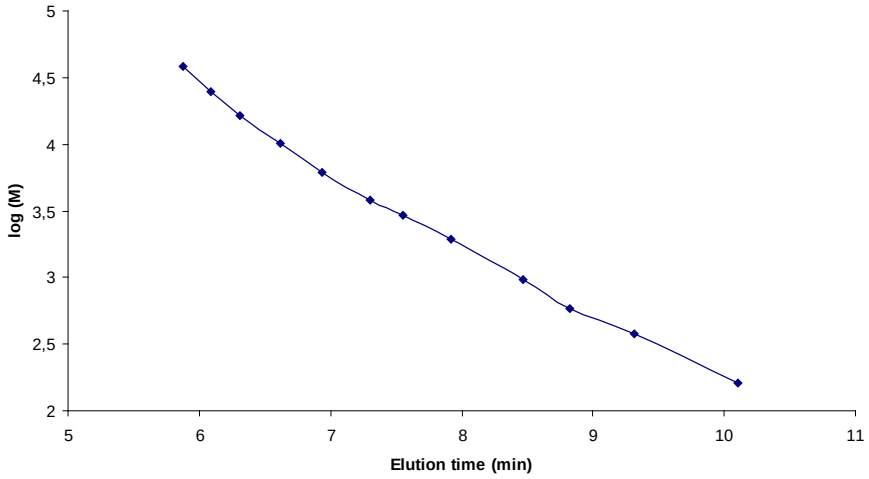

Figure 8: Example of classical calibration using polystyrenes as standards using THF as eluant at 25°C on Mixed E GPC column.

However, in standard practice, it is not easy to find standards for calibration, especially for complex mixtures such as environmental samples due to the large amount of different molecule classes and thus classical calibration would necessitate standards for each class of molecules.

1.4.2. Universal calibration

In SEC separation process, same hydrodynamic size molecules should elute at the same time, regardless of the chemical structure or ramifications. Based on that principle, Benoit *et al.* (Gallot-Grubisic *et al.* 1967) proposed to replace the term (M) by ($[\eta]xM$) as a universal calibration parameter where [η] is intrinsic viscosity. According to the Flory-Fox equation, molecular volume for flexible polymer chains in solution is linked to $[\eta]xM$:

$$[\eta]xM = \Phi\left\langle R^2\right\rangle^{3/2} \quad (9)$$

where $\left\langle R^2\right\rangle$ is mean quadratic distance from end to end of polymer chain, Φ is Flory constant which varies according to Ptitzyn-Einster, from 2.86×10^{23} mol^{-1} in Θ solvent (for which all interactions between polymer chains are neglected) to 1.7×10^{23} mol^{-1} in a good solvent.

The equation $\log([\eta]xM = f(V_e)$ is known under the name of universal calibration curve. Once it is established for a polymer it is still reliable for other polymers or copolymers only when size exclusion is the main phenomenon.

1.4.3. SEC in multidetection mode

SEC using simple concentration detection (RI, UV, IR, densitometry, evaporative light scattering) does not allow to determine the absolute molecular mass. However, the association of a molecular mass sensitive detector such as continuous viscometer or light scattering detector to a concentration detector allows resolving problems due to calibration.

Viscosimetric detector gives intrinsic viscosity distribution $[\eta]=f(V_e)$. The information is thus converted in molecular mass distribution through a universal calibration curve. Quality of the results depends on precision and reliability of the universal calibration.

Low-angle laser light scattering (LALLS) or multi-angle laser light scattering (MALLS) are the only techniques able to give absolute information on molecular mass distribution without calibration curves. With these techniques, results are independent of experimental error sources such as flow rate variations, column overflow, dispersion and non-size effects. The main problem remains the reliability on low molecular mass compounds.

2. Mass spectrometry

2.1. Introduction

Mass spectrometry is an analytical technique which determines mass to charge ratios (m/z) of ions and which may also gives structural information. The molecular mass determination is performed by mass analyzers which operate under strong electric or magnetic fields in order to separate the different ions. As a particle can only be deflected by an electric or magnetic field if it is charged itself, this is why, before mass analyzers, there is always an ionization source. Ions can be formed from gases, liquids or solids according to the ionization sources.

Mass spectrometry is characterized by its unequal analytical qualities such as sensibility, limits of detection and fast analysis. Recent developments in ionization sources

such as atmospheric pressure sources (APPI, APCI, APLI …) and also in mass analyzers (Orbitrap, hybrid instruments) has allowed to extend the mass spectrometry application field and also to simplify its use. Mass spectrometry is the instrument of choice in many applications such as proteomics, metabolomics, petroleomics, environmental analysis… Mass spectrometry is able to detect all kind of compounds, with various polarities and high molecular masses.

2.2. Mass spectrometry and molecular separation techniques

In organic geochemistry, samples are mostly complex mixtures which require high performance separations prior to the use of mass spectrometry. Usual techniques are GC-MS, HPLC and more precisely SEC in organic or aqueous phase in order to achieve compound separations. However, in the case of the high molecular mass compounds, both techniques (GC-MS and HPLC) present important inconveniences. Only thermostable compounds and compounds with a boiling temperature in the range of the injector temperature can be analyzed in GC-MS. And thus, compounds with high molecular masses, which usually have high boiling temperatures, cannot be analyzed (boiling temperature is often correlated to molecular mass). In the case of standard GC-MS experiments, the injector temperature is set to 300°C, and so it does not allow vaporization of compounds heavier than 600 Da.

GC-MS may be suited to analyze polar compounds but samples need pre-treatment and obviously aqueous solutions cannot be analyzed this way.

For SEC chromatography, the main inconvenience is the poor resolution. This chromatographic technique can analyze compounds up to 4 000 000 Da, but give average information on the molecular mass distribution especially in the case of complex mixtures.

Mass spectrometry, in our experiments, is considered as a technique of choice as it solves previously described inconveniences.

2.3. Principle

2.3.1. Overview

Mass spectrometry principle concerns the determination of the mass to charge ratio (m/z) of ions produced in the gas phase by an ionization source. This technique is composed

of three invariable elements regardless of the mass spectrometry instruments. The three invariable elements of a mass spectrometer (Figure 9) are:

- the ionization source which produces ions,
- the mass analyzer,
- the detector to convert information from mass analyzer (except for FT-ICR and orbitrap for which mass analyzer and detector are the same component) .

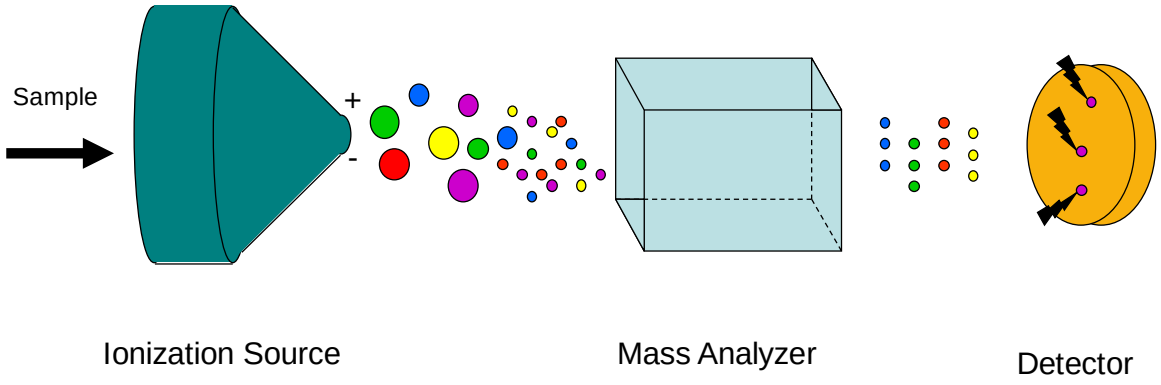

Figure 9 : Principal scheme of mass spectrometry instrumentation.

Ionization sources are fundamental elements in mass spectrometry as all mass analyzers work under electric or magnetic fields and a particle can only be deflected if it is charged itself.

Mass spectrometry is used to perform two different types of experiments: the MS experiments and MS/MS experiments

2.3.2. Simplified MS experiments at atmospheric pressure

In this configuration, the mixture to analyze (M_1 and M_2) is first ionized, then ions are distinguished according to their mass to charge ratio (m/z) (Figure 10).

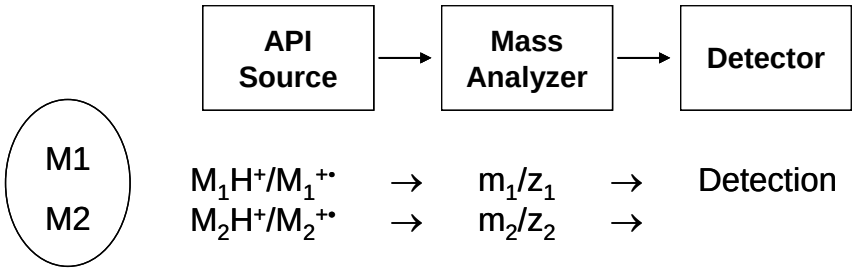

Figure 10: Simplified MS experiments.

As a result of the MS experiment, a mass spectrum is obtained.

2.3.3. Simplified MS/MS experiments at atmospheric pressure

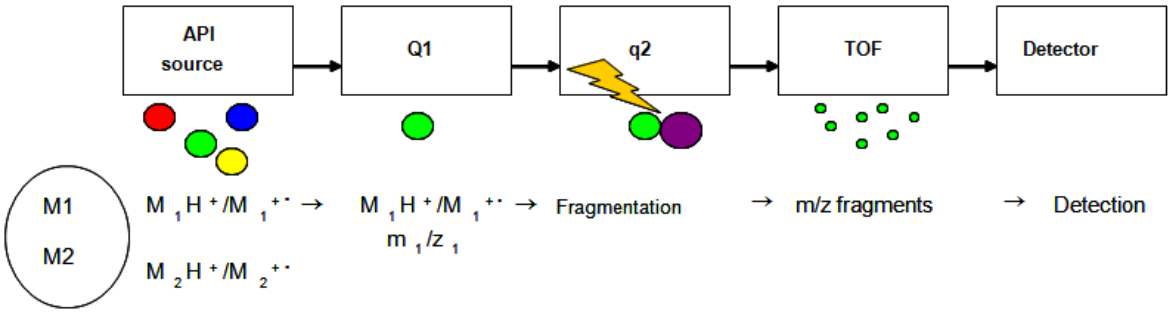

Figure 11: Simplified MS/MS experiments (case of Q-TOF mass analyzer).

As previously, the mixture to analyze is ionized, then formed ions enter in the first mass analyzer which is set to allow only ions with a specific mass to charge ratio to pass. Then, they enter into the second mass analyzer, which is commonly a quadrupole filled with gas atoms (ex: Argon) and called the collision cell, where ions collide with gas atoms. Gas atoms transfer energy to the ions and induce fragmentations. Ultimately, the last mass analyzer measures mass to charge ratios of the produced fragments.

2.4. Atmospheric Pressure Ionization (API) sources

There are three main API sources commonly used:

- ElectroSpray Ionization (ESI) source,
- Atmospheric Pressure Chemical Ionization (APCI) source,
- Atmospheric Pressure PhotoIonization (APPI) source.

There are called atmospheric pressure sources, because they are used at atmospheric pressure whereas mass analyzers work under a strong vacuum (in the case of TOF mass analyzers around 10^{-10} bar).

2.4.1. ElectroSpray Ionization (ESI)

The ESI source developments are due to the work of Fenn *et al.* (Wong *et al.* 1988; Fenn *et al.* 1989; Mann *et al.* 1989) which was awarded by the Chemistry Nobel Prize in 2002. The first use of ESI mainly concerns multicharged ions such as proteins. It is actually used for many applications, including coupling with HPLC. Indeed, ESI allows us to extend the mass spectrometry application field to the study of molecules with high molecular masses (up to 4 000 000 Da). This technique has been mainly applied to polar compounds that can stabilize an ionic charge state.

The ESI source (Kebarle *et al.* 1993; Ghislain *et al.* 2006) creates gas-phase ions from a solution under a strong electric field at atmospheric pressure (~ 10^6 V/m) (Hoffmann *et al.* 2007). However, solution should contain the analyte, a salt and a solvent to allow the ESI process.

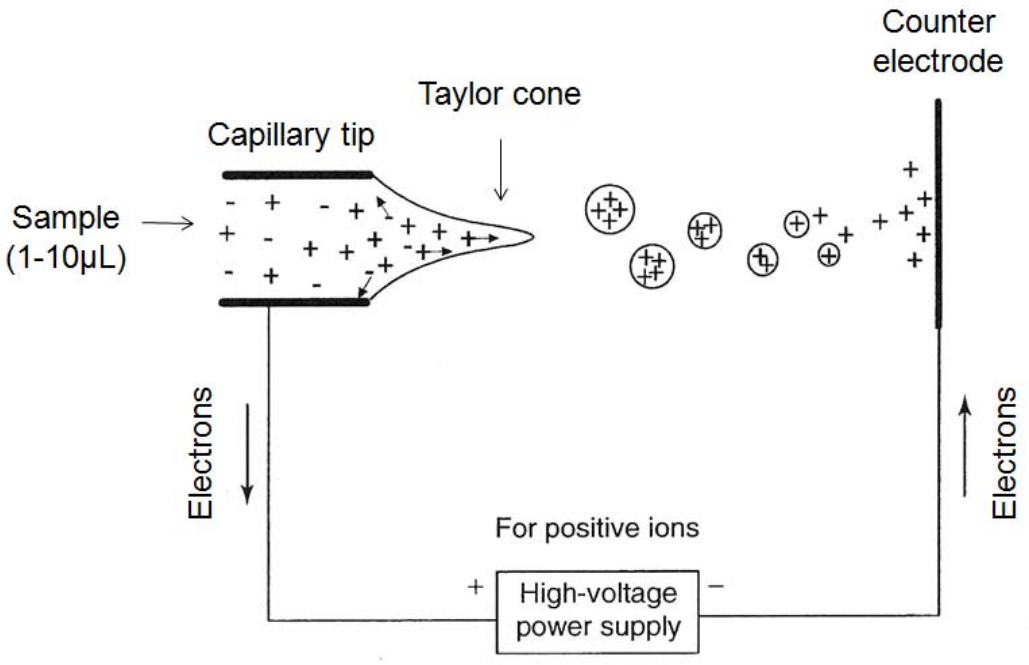

Figure 12: Principle scheme of an ESI source (modified from Hoffman *et al.*)

The principle can be divided into three parts:

- Charged droplet production (Figure 12):

The solution to analyze is introduced into a capillary. Between the other extremity of the capillary and a counter electrode, a strong electrical potential is applied (usually between 4-6 kV). Under a negative electric field, cations from the solution will be focused at the capillary tip inside the emerging liquid and anions will be discharged on the capillary shell. After a certain time, positive charges distort the liquid under a particular form called Taylor's cone. As cations continue to be accumulated the cone expanses and becomes very thin until it breaks. This phenomenon is usually pneumatically assisted by a coaxial gas (ex: heated nitrogen) to accelerate the process.

- Charged droplet core-crack (Figure 13):

Charged droplet core-crack is produced by solvent evaporation due to the heat of the ESI source and also induced by friction between droplets and air molecules.

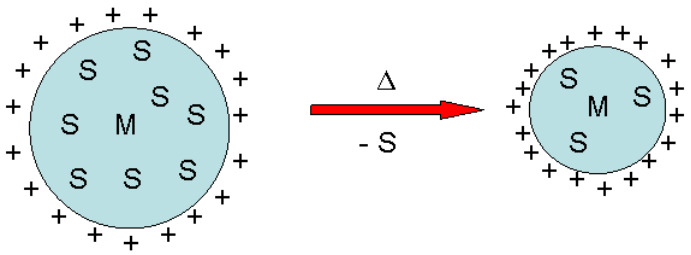

Figure 13: Evaporation scheme of the solvent from charged droplet (M is the analyte and S is the solvent)

The progressive evaporation of the solvent will lead to a diminution of the droplet size. At a certain point, the volume of the droplet is not big enough to allow all electric charges to coexist, i.e. electrostatic repulsions become greater than the surface cohesion forces (surface tension). At that point, Rayleigh's limit radius is reached, and the droplet will explode into several smaller droplets called columbic explosion. Rayleigh's limit radius is defined by equation (10):

$$Q^2 = 64\pi^2\varepsilon_0\gamma R_R^{\ 3} \qquad (10)$$

where (R_R, m) is Rayleigh's limit radius, (Q, C) is charge total quantity on the droplet, (ε_0, $C^2 \cdot N^{-1} \cdot m^{-2}$) the electric permittivity of the environment and (γ, $N.m^{-1}$) surface tension of the liquid.

- Gas-phase ion emission

The exact phenomenon can be explained by two different theories which are currently proposed to describe the gas-phase emission and depend on the type of compounds.

- Residual charge model (Dole *et al.* 1968)

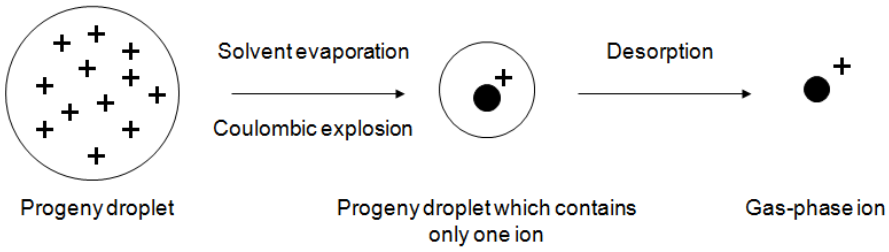

Figure 14: Residual charge model.

This model considers that after a certain droplet size, the Rayleigh's limit radius does not apply anymore. Continuous evaporation leads to gas-phase ions.

- Ion evaporation model (Thomson *et al.* 1979)

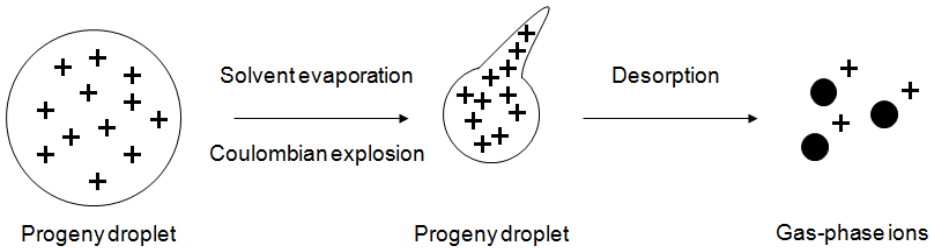

Figure 15: Ion evaporation model.

In contrast to the previous theory, gas-phase ions are created as soon as the diameter of the droplet is small enough.

Electrospray ionization is a soft ionization method which transfers a small quantity of energy leading to little fragmentation and the dominance of molecular ions.

2.4.2. Atmospheric Pressure Chemical Ionization (APCI)

Atmospheric Pressure Chemical Ionization (APCI) uses ion-molecule gas-phase reactions. Ion production is obtained through an electric discharge from the Corona needle (Corona discharge) on the solvent spray whose intensity represents few µA. APCI is used for molecular masses up to 1500 Da. This source extends the ESI application field to weakly polar compounds, but can also ionize polar compounds (Carroll *et al.* 1975; Hoffmann *et al.* 2007). It forms monocharged ions (i.e. $[M+H]^+$ or $M^{+\bullet}$).

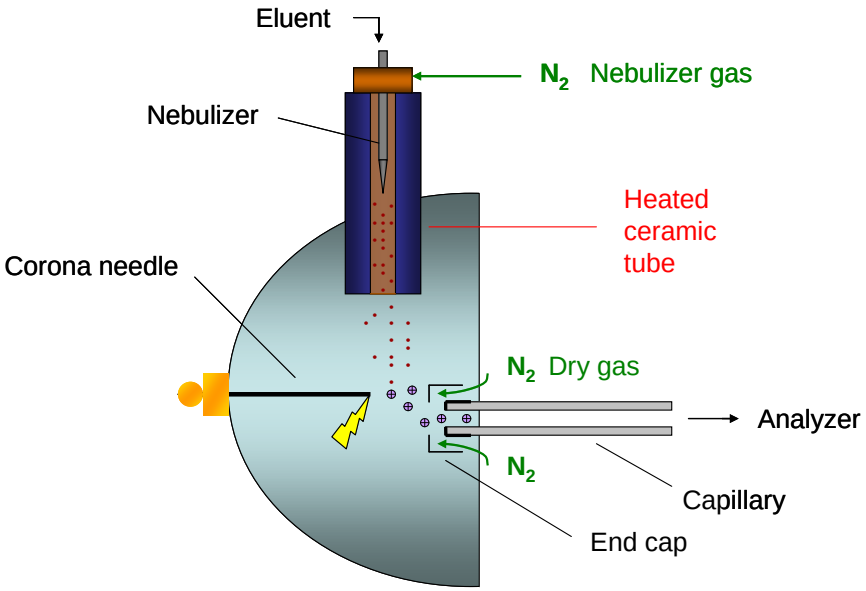

Figure 16 : Schematic of an APCI source.

2.4.2.1. Principle of the ionization process:

The analyte is directly introduced thought a pneumatic nebulizer inlet with a high speed nitrogen beam which converts the analyte/gas mixture into a thin spray (Figure 16). Droplets are carried by the gas flow to the heated ceramic tube where desolvatation/vaporization occurs (typical temperatures ranging from 250 to 450°C). The heat vaporizes the solvent and the sample. Due to rapid desolvatation and vaporization of the

droplets, thermal decomposition of the analyte is reduced, as a result little fragmentation occurs.

Then compounds are carried outside the nebulizer and are ionized by the corona discharge. The process can be split into five steps:

- gaz/eluent spray formation,
- mixture transport carried by the gas to the heated ceramic tube,
- evaporation/desolvatation of the solvent and the analyte,
- hot gas and compounds leave the chamber,
- ionization is then produced by the Corona discharge.

As the temperature of the heated ceramic tube is controlled, vaporization conditions are independent from nature of the solvent and the flow rate.

2.4.2.2. Ionization process in positive ionization

Several reactions were described to explain the formation of either molecular or protonated ions. The following reactions are considered to be most favored (Carroll *et al.* 1975, Herrera *et al.* 2008).

- Primary ion formation:

Corona discharge forms primary ions such as $N_2^{+\bullet}$ and $O_2^{+\bullet}$ which then collide with solvent molecules to form secondary reactant gas ions. However, gas-phase reaction in positive mode is rare with O_2 because of the large excess of N_2 used as nebulization and desolvatation gas

$$e^- + N_2 \rightarrow {N_2}^{+\bullet} + 2e^- \quad (11)$$

$${N_2}^{+\bullet} + N_2 \rightarrow {N_4}^{+\bullet} \quad (12)$$

An advantage of a system using Corona discharge remains in the relative insensitivity to the presence of corrosive and oxidizing gases.

The formation of primary ions from solvent molecules (S), such as water is also possible.

- Secondary ion formation:

$$N_2^{+\bullet} + S \rightarrow S^{+\bullet} + N_2 \quad (13)$$

$$N_4^{+\bullet} + S \rightarrow 2N_2 + S^{+\bullet} \quad (14)$$

It is also possible to obtain a reaction between the radical ion of the solvent and another molecule of solvent.

$$S^{+\bullet} + S \rightarrow SH^+ + [S-H]^\bullet \quad (15)$$

- Radical ion formation:

A charge exchange reaction can occur between the solvent and the analyte (M)

$$S^{+\bullet} + M \rightarrow S + M^{+\bullet} \quad (16)$$

- Cluster formation

In the case of cluster formation, two different reactions are considered, involving proton transfer.

$$(S+H)^+ + M \rightarrow S + (M+H)^+ \text{ if } \Delta H < 0 \quad (17)$$

and/or

$$S^{+\bullet} + M \rightarrow [M+H]^+ + [S-H]^\bullet \quad (18)$$

In fact, ionization by proton transfer or gas reactant ions depends on proton affinity of M.

2.4.2.3. Ionization process in negative ionization

Ionization in the negative mode can occur by direct ionization, charge transfer or proton transfer (Dzidic *et al.* 1974, Kostiainen *et al.* 2009)

- Direct ionization

This ionization depending on electron affinity (EA) occurs if EA(M)>0, i.e. if $E(M^{-\bullet})<E(M)$:

$$M + e^- \rightarrow M^{-\bullet} \quad (19)$$

- Charge transfer ionization

Since O_2 has a positive electron affinity (EA=0.48eV), it can act as a reactant gas.

$$O_2 + e^- \rightarrow O_2^{-\bullet} \quad (20)$$

$$O_2^{-\bullet} + M \rightarrow M^{-\bullet} + O_2 \quad (21)$$

- Cluster formation

This ionization mode involves gas-phase acidity between two compounds A and B.

$$HA + O_2^{-\bullet} \rightarrow A^- + HO_2^{\bullet} \text{ if } \Delta G_{acid}(HA) < \Delta G_{acid}(HO_2^{\bullet}) \quad (22)$$

$$A + [B-H]^- \rightarrow [A-H]^- + B \text{ if } \Delta G_{acid}(A) < \Delta G_{acid}(B) \quad (23)$$

- Rearrangement:

$$M + O_2^{-\bullet} \rightarrow [M - X + O]^- + OX^{\bullet} \quad (24)$$

$$O_2 + M^{-\bullet} \rightarrow [M - X + O]^- + OX^\bullet \quad (25)$$

where X can be: halogen, NO_2, or H

2.4.3. Atmospheric Pressure PhotoIonization (APPI)

The APPI source is one of the latest ionization sources commercialized. It was developed to complement the detection of non-polar compounds excluded from the application field of the ESI and APCI sources. Two commercialized sources are available, one based on the work of Robb (Robb *et al.* 2000) under the name of Photospray™ and the other one Photomate™ is based on the work of Syage (Syage *et al.* 2000). However the first description of photoionization detector was reported coupled to GC (Driscoll *et al.* 1976; Driscoll 1977) then with LC (Baim *et al.* 1983).

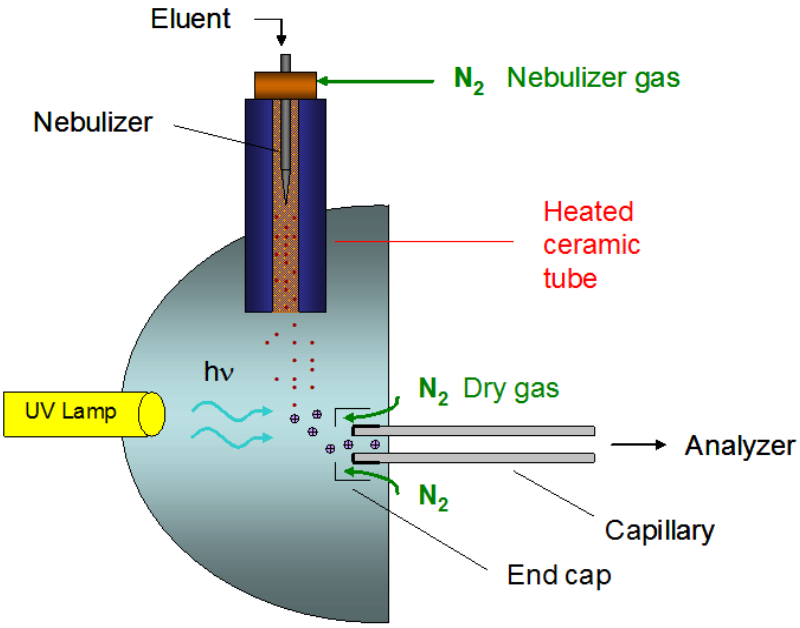

Figure 17 : Schematic of an APPI source

2.4.3.1. Principle of ionization

The principle is very similar to APCI, but instead of using Corona discharge, the ionization is performed by an UV-lamp (Figure 17). APPI is based on ionization energy of

the molecules and usually organic compounds have ionization energy below 10eV whereas organic solvents have ionization energies above this limit (Table 5).

2.4.3.1.1. Light sources

Several different gases can fill the lamp used in APPI process due to their excitation energy in gas-phase (Table 4).

Gas	Metastable state	Wavelength (nm)	Excitation Energy (eV)	Approximate population (%)
Xenon (Xe)	$^3P_0$	129.5	9.5	<7
	$^3P_2$	147.0	8.4	>93
Krypton (Kr)	$^3P_0$	116.5	10.6	<10
	$^3P_2$	123.6	10.0	>90
Argon (Ar)	$^3P_0$	106.7	11.8	14
	$^3P_2$	116.5	11.6	86

Table 4: Excitation energy available in gas-phase. (Tabet 2008)

Krypton as filling gas is widely used mainly because it can ionize most of organic compounds without ionized gases or most of organic solvents (Table 5).

Compound	IE (eV)	PA (kJ.mol^{-1})
Nitrogen	15.58	493.8
Water	12.62	691.0
Oxygen	12.07	421.0
Argon:11.6 and 11.8 eV		
Chloroform	11.37	n/a
Methylene chloride	11.33	n/a
Methanol	10.84	754.3
Krypton: 10.6 eV		
Isopropanol	10.17	793.0
n-Hexane	10.13	n/a
Krypton: 10.0eV		
Heptane	9.93	n/a
Acetone	9.70	812.0
Xenon: 9.5 eV		
Tetrahydrofuran	9.4	822.1
Pyridine	9.26	930.0
Benzene	9.24	750.4
Toluene	8.83	784.0
Xenon: 8.4 eV		
Anisole	8.20	839.6
Naphtalene	8.14	802.9
Anthracene	7.44	877.3
Phenanthrene	7.89	825.7
Fluoranthene	7.90	828.6
Pyrene	7.43	869.2

Table 5: Ionization energies and Proton affinities for some usual compounds (from http://webbook.nist.gov/chemistry/)

2.4.3.1.2. Dopants

The use of dopant is often preferable when using APPI. Indeed, when compounds have ionization energy above the photons' energy, the dopant may contribute to compound ionization. During the past years, dopants tested in the literature were: acetone, toluene, anisole, benzene, T.H.F., hexafluorobenzene. When the dopant is used as solvent, the phenomenon is called "self-doping effect".

2.4.3.1.2.1. Ionization process in positive mode

Ionization in positive mode can be described as was by Marchi *et al.* (Marchi *et al.* 2009) and Hoffman *et al.* (Hoffman *et al.* 2007). The absorption of a photon (E=hν) leads to an excited state of the molecule M,

$$M + h\nu \rightarrow M^{*} \quad (26)$$

if IE(M) <E(hν), the photon will be absorbed and M will be in an excited state. It follows the released of an electron to create an odd-electron ion.

$$M^{*} \rightarrow M^{+\bullet} + e^{-} \quad (27)$$

if IE(M)>E(hν), M^{*} may return to the ground state under several pathways, such as photodissociation (equation 28), photon emission (equation 29) or collisional quenching (equation 45) with a non-excited molecule (C) (equation 30),

$$M^{*} \rightarrow A + B \quad (28)$$

$$M^{*} \rightarrow M + h\nu \quad (29)$$

$$M^{*} + C \rightarrow M + C^{*} \quad (30)$$

However when IE(M)>E(hν), the use of a molecule which has a low ionization energy (dopant, D) can be used in order to favor ionization of M.

$$D + h\nu \rightarrow D^{*} \rightarrow D^{+\bullet} + e^{-} \quad (31)$$

According to Marchi (Marchi *et al.* 2009), the dopant must be added in large quantity compared to the analyte in order to act as an intermediate between photons and analytes. There are two different ionization mechanisms involving dopant: charge transfer based on ionization energy (IE) (equation 32) and proton transfer based on proton affinity (equation 33):

$$D^{+\bullet} + M \rightarrow D + M^{+\bullet}, \text{ if IE(D)>IE(M)} \quad (32)$$

$D^{+\bullet} + M \rightarrow [D-H]^{\bullet} + [M+H]^{+}$, if PA(M)>PA([D-H]$^{\bullet}$) (33)

The use of dopant has also to be considered when the analyte is dilute in a solvent with high IE and/or when the flow rate is high i.e., ~ 100 µL.min^{-1}), mainly because photons cannot reach the analyte.

2.4.3.1.2.2. Ionization process in negative mode

Ionization in negative mode (Kauppila *et al.* 2004; Marchi *et al.* 2009, Hoffman *et al.* 2007) mainly concerns compounds with high gas-phase acidities and/or positive electron affinities. The ionization can be performed by proton transfer (equations 38, 39 and 40), electron capture (equation 42), charge exchange (equation 43) and anion attachment (Song *et al.* 2007).

$D + h\nu \rightarrow D^{+\bullet} + e^{-}$, if IE(D) <E(hν) (34)

$S + e^{-} \rightarrow S^{-\bullet}$, if EA(S)>0eV, i.e. if E(S$^{-\bullet}$)<E(S) (35)

$S + e^{-} \rightarrow [S-F]^{\bullet} + F^{-}$ (36)

$O_2 + e^{-} \rightarrow O_2^{-\bullet}$ (37)

$M + O_2^{-\bullet} \rightarrow [M-H]^{-} + HO_2^{\bullet}$, if $\Delta G_{acid}(M) < \Delta G_{acid}(HO_2^{\bullet})$ (38)

$S + O_2^{-\bullet} \rightarrow [S-H]^{-} + HO_2^{\bullet}$, if $\Delta G_{acid}(S) < \Delta G_{acid}(HO_2^{\bullet})$ (39)

$M + [S-H]^{-} \rightarrow [M-H]^{-} + S$, if $\Delta G_{acid}(S) < \Delta G_{acid}(M)$ (40)

$M + e^{-} \rightarrow M^{-\bullet}$, if EA(M)>0eV, i.e. if E(M$^{-\bullet}$)<E(M) (41)

$M + O_2^{-\bullet} \rightarrow M^{-\bullet} + O_2$, if EA(M)>EA($O_2$)=0,451eV (42)

$M + O_2^{-\bullet} \rightarrow [M-X+O]^{-} + OX^{\bullet}$, X=H, Cl, NO_2 (43)

Equation 38 mainly concerns chloroform dissociation as noticed by Kauppila (Kauppila *et al.* 2004) when observing compounds containing chloride atoms.

2.4.4. Application field of the API sources

In atmospheric pressure ionization sources, it is commonly accepted that Electrospray Ionization (ESI) is mainly used for ionic species or easily ionizable compounds and compounds with labile hydrogen. Atmospheric Pressure Chemical ionization (APCI) and Atmospheric Pressure Photoionization (APPI) sources are more efficient in the case of non polar compounds, because the principle of the ionization is mainly based on compound ionization energy.

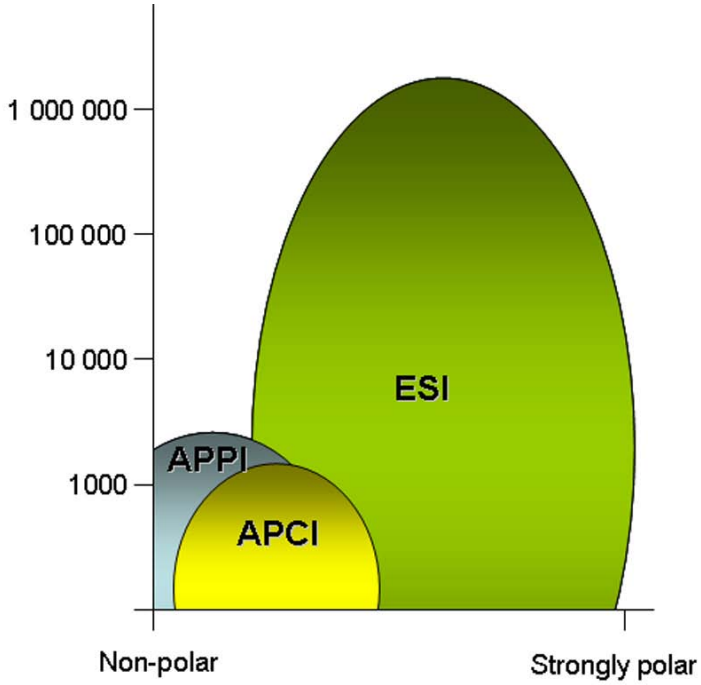

Figure 18: Comparative application field of the three API sources

Figure 18, based on previous descriptions of API sources, reveals the application field of ESI, APCI, and APPI sources by plotting the polarity versus the molecular masses. The ESI application field represents the largest part as it includes a wide range of molecules especially because ESI creates multi-charged ions, allowing increasing its application field towards very high molecular mass compounds. Concerning APCI and APPI sources, the main difference consists in the highest sensitivity of the APPI to aromatic compounds such as PAHs. Moreover, both sources are limited in terms of molecular masses due to their application principle which makes the analyte going through a high temperature ceramic (for the desolvatation process).

2.5. Mass Analyzers

2.5.1. Quadrupole analyzer

The role of mass analyzers is to distinguish ions according to their mass to charge ratio (m/z).

Quadrupole analyzers were first described in 1953 by Paul and Steinwegen (Paul *et al.* 1953). The principle is based on the stability of ion trajectories in oscillating electric fields (Hoffman *et al.* 2007).Quadrupole analyzer is composed of four hyperbolic section rods. A positive ion will enter into the space between rods and will be attracted by the rods on which the potential $-\phi_0$ is applied, when changing the potential from $-\phi_0$ to ϕ_0, the positive ion will change direction. Ions enter into the quadrupole along z-axis and will submitted to a quadrupolar alternative field due to the application of potential ϕ_0 and $-\phi_0$ on the rods. The potential ϕ_0 composed of a direct potential U and a "zero-to-peak" amplitude of the RF voltage V. The result is equipotential lines as represented (Figure 19). The potential ϕ_0 is given by the following equation:

$$\Phi_0 = U - V\cos(\omega t) \text{ and } -\Phi_0 = -U + V\cos(\omega t) \quad (44)$$

where (ω) is the angular frequency.

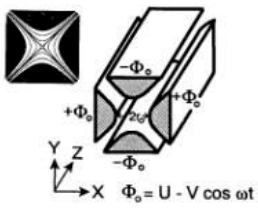

Figure 19 : Quadrupole with hyperbolic rods
(reproduced from Hoffman *et al.* (Hoffman *et al.* 2007))

To allow an ion to cross the quadrupole on z-axis, amplitude of its trajectory must be inferior to r_0 on x and y axis, ($2r_0$ is the distance between two opposite rods), if not, ion will be discharged on the rod and thus will not be detected.

Inside the quadrupole, in addition of their initial velocity along z-axis, ions are also submitted to electric field forces along x and y-axis, resulting forces can be described as follows:

$$F_x = ma = m\frac{d^2x}{dt^2} = -ze\frac{\delta\Phi}{\delta x} \quad (45)$$

$$F_y = ma = m\frac{d^2y}{dt^2} = -ze\frac{\delta\Phi}{\delta y} \quad (46)$$

where: (m) is ion mass, (ze) is ion charge, (a) is acceleration and (Φ) is a function of (Φ_0)

$$\Phi_{(x,y)} = \Phi_0(x^2 - y^2)/r_0^2 = (x^2 - y^2)(U - V\cos\omega t)/r_0^2 \quad (47)$$

After differentiating and rearranging the terms, equations of movement are given by Paul equations:

$$\frac{d^2x}{dt^2} + \frac{2ze}{mr_0^2}(U - V\cos\omega t)x = 0 \quad (48)$$

$$\frac{d^2y}{dt^2} + \frac{2ze}{mr_0^2}(U - V\cos\omega t)y = 0 \quad (49)$$

After integration of these equations, the following equation is established (first described by Mathieu in 1866)

$$\frac{d^2u}{d\xi^2} + (a_u - 2q_u\cos 2\xi)u = 0 \quad (50)$$

where u stands for x or y and with:

$$\xi = \omega t/2 \quad (51)$$

It leads to the following equations by changing and rearranging these terms:

$$a_u = a_x = -a_y \frac{8zeU}{m\omega^2 r_0^2} \text{ and } q_u = q_x = -q_y \frac{4zeV}{m\omega^2 r_0^2} \quad (52) \text{ and } (53)$$

Considering a given quadrupole, r_0 is a constant and ω is maintained constant. Only U, V, m and z are variables. Thus, for a given ion with a mass to charge ratio m/z, a superposition of stability diagram along x-axis (a_x, q_x diagram) and stability diagram along y-axis (a_y, q_y diagram) gives Mathieu's equation solutions, i.e. in these regions, the given ion will have a stable trajectory along x-axis and y-axis (Figure 20). After superposition, four areas correspond to ion stability upon x and y axis but for technological reasons only intersection area A will be used.

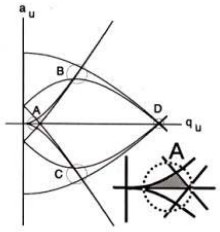

Figure 20: Stability diagram, $a_u=f(_u)$ for an ion with a specific mass m (reproduced from Hoffman *et al.* (Hoffman *et al.* 2007))

There will be as many stability diagrams as there are different ions with different m/z ratios (Figure 21).

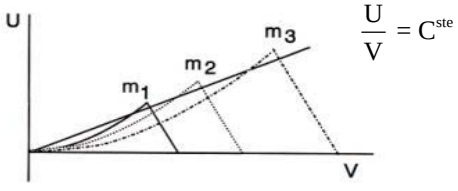

Figure 21: Stability area A (U=f(V) for different mass ions ($m_1<m_2<m_3$)) (reproduced from Hoffman *et al.* (Hoffman *et al.* 2007))

To allow ions to pass through the quadrupole, a straight operating line (U/V = constant) is used and thus ions will be observed successively. Mass spectrometer will scan

along this line; if the slope is high, resolution will be better but with less sensitivity. On the contrary, a low slope will give poor resolution but will allow all ions to be transmitted.

2.5.2. Time-Of-Flight (TOF) analyzer

TOF analyzers were first described by Stephens in 1946 (Stephens 1946).

2.5.2.1. Linear TOF

The TOF analyzer separates ions according to their velocity in a free-field region called flight tube, after initial acceleration by an electric field (Figure 22).

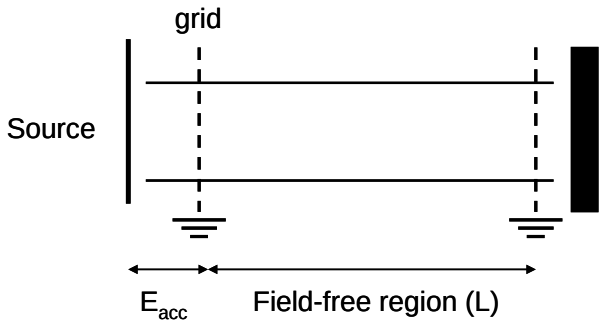

Figure 22: Principle of a linear TOF analyzer

Ions are expelled from the source with the application of a potential (Figure 22). Then, ions are accelerated toward the flight tube by a difference of potential applied between an electrode and the extraction grid. Theoretically, as ions will receive the same kinetic energy, they will be separated according to their velocity in the field-free region until they reach the detector.

Mass to charge ratios will be determined by measuring the time needed for ions to go from the grid to the detector. According to the Newton's second law of motion (also called translation dynamic fundamental principle):

$$\sum \vec{F} = m\vec{a} \tag{54}$$

where $\vec{F}$ are forces applied to the object and $\vec{a}$ the acceleration.

The force applied on a charge in an electric field is equal to:

$$\vec{F}_e = q\vec{E} \tag{55}$$

where (q) is the charge and $\vec{E}$ is the electric field strength. By combining equations (54) and (55):

$$\vec{a} = \frac{q}{m}\vec{E} \tag{56}$$

By considering the mass-velocity relationship and for constant energy ions regularly accelerated under strong vacuum, the electrostatic force applied on a charge and the Newton's second law of motion, the potential energy (E_p) is considered to be converted in kinetic energy (E_k) and so:

$$E_c = 1/2mv^2 = E_p = qV_S = zeV_S \tag{57}$$

where (v) is the ion velocity, (q) is the charge and (V_s) is the electrical potential.

The velocity of ions is thus:

$$v = \sqrt{\frac{2zeV_S}{m}} \tag{58}$$

After ions reach the field-free region, ion velocities remain constant and they travel in a straight line:

$$v = \frac{L}{t} \tag{59}$$

where (L) is the length of the flight tube and (t) the time needed for ions to travel from the grid to the detector. Combining equations (58) and (59) gives the classic TOF analyzer equation:

$$t^2 = \frac{m}{z}\left(\frac{L^2}{2eV_S}\right) \tag{60}$$

Equation (60) shows that m/z ratio is proportional to the ion travel time through the flight tube.

However several drawbacks concern TOF analyzers and especially its poor resolution. In TOF analyzers, resolution depends on flight tube length and flight time:

$$R = \frac{m}{\Delta m} = \frac{t}{2\Delta t} \approx \frac{L}{2\Delta x} \tag{61}$$

Based on TOF analyzer principle, all ions with the same m/z ratio must reach the detector at the same time to get a high resolution. However several problems occur in the source:

- ions are not created at the same time (time distribution),
- ions are not located at the same place in the source (space distribution),
- ions have velocities in different directions and even with the same initial kinetic energy, these ions will arrive at the detector at different times (kinetic energy distribution).

In practice, time and space distributions are difficult to correct but they are considered to have lesser important effects than kinetic energy distribution. Thus, two different systems were developed to increase the TOF analyzer resolution by reducing kinetic energy distribution):

- the delayed pulsed extraction: a time lag is introduced between ion formation and extraction. In the source (fied-free region), ions are allowed to separate according to their initial velocities. After the pulse, ions with less energies will

receive more kinetic energy as they remain a longer time in the source and will join those with higher energies and which will move further towards the detector.

- the reflectron.

2.5.2.2. Reflectrons

The reflectron is an electrostatic reflector first described in 1973 by Mamyrin (Mamyrin *et al.* 1973). Three different types of reflectrons were developed: the single-stage reflectron, the double-stage reflectron and the quadratic-field reflectron. Only the first-stage reflectron will be described as it is a part of the instrument used in this work.

A single-stage reflectron is composed of several electrostatic lenses which create an electric field and reflect incident ions from the source to the detector (Figure 23).

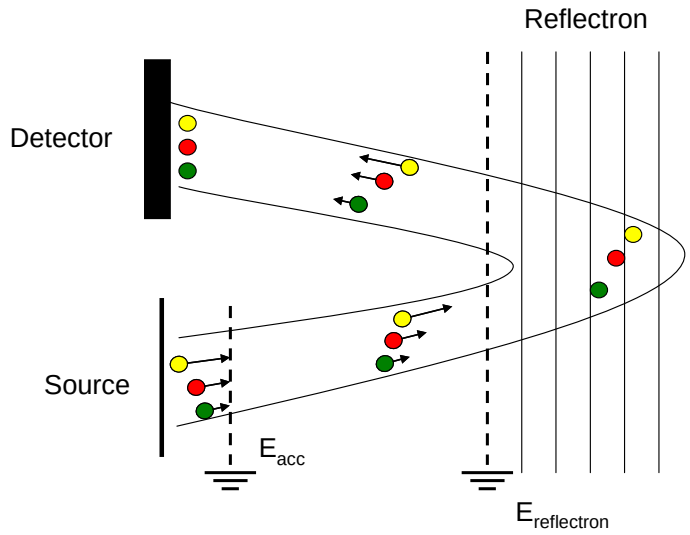

Figure 23: Principle of the use of reflectron in TOF analyzer

The aim, for same m/z ratio ions, is to reach the detector at the same time. On Figure 23, three same m/z ratio ions (yellow, green and red) are represented with different initial kinetic energies. Before entering the reflectron, the yellow ion has the highest kinetic energy and will go deeper in the reflectron. When going out of the reflectron, it will be delayed in regards to the green ions, but they will arrive at the same time.

2.5.2.3. Orthogonal injection TOF mass analyzer

Since the beginning of TOF analyzers, pulsed ionization sources, such as MALDI were manly used. But performances of TOF analyzers lead to develop methods using a continuous ion beam such as API sources. An off-axis TOF was described in the 1964 by O'Halloran (O'Halloran *et al.* 1964), but orthogonal acceleration TOF (oa-TOF) mass analyzers were described only several years after. The ion beam is placed orthogonally in regards to the flight tube. A small proportion of ions are maintained in field-free region. An orthogonal electrostatic impulse to the incident ion beam pushes ions into the flight tube. Orthogonal acceleration presents several advantages (Guilhaus *et al.* 1997; Guilhaus *et al.* 2000):

- high efficiency in storing ions from external continuous ion source,
- simultaneous correction for velocity and spatial dispersions,
- capability of mass resolving power,
- maximum duty factor at the high mass end of the mass spectrum,
- minimal temporal dispersion from gating method.

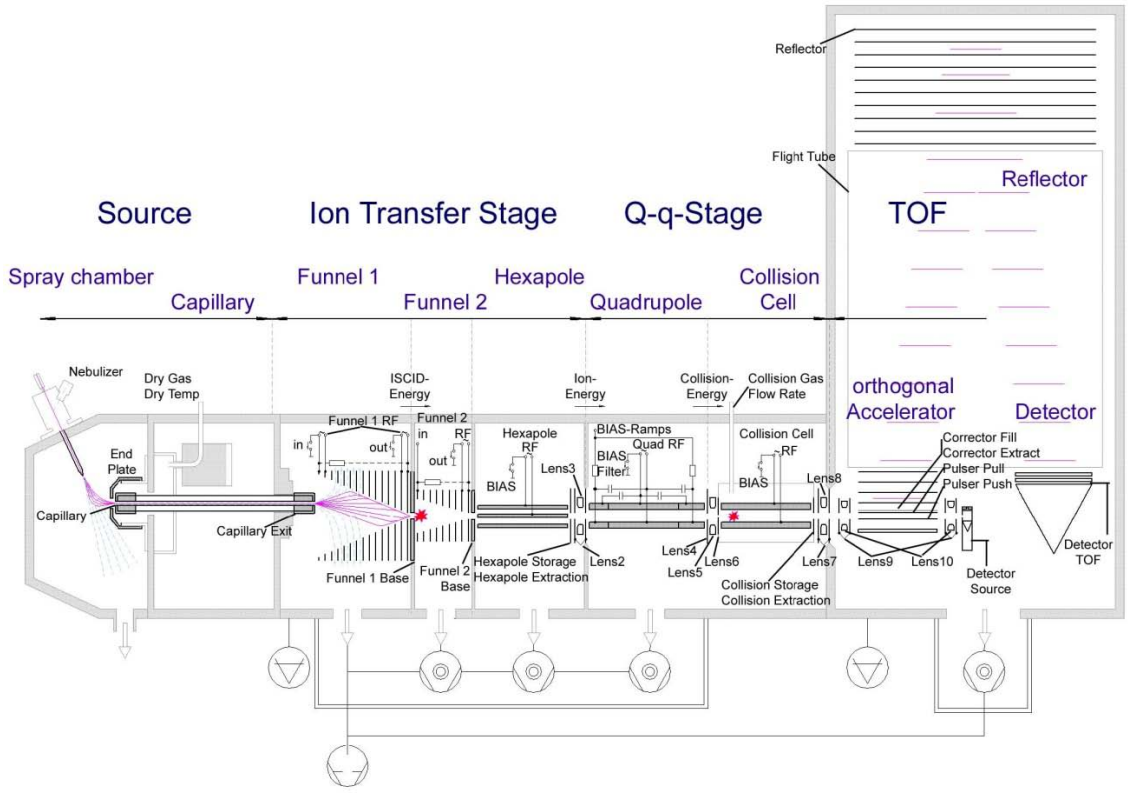

Figure 24: Schematic of orthogonal injection Q-TOF (reproduced from Bruker MicrOTOF$_Q$ user manual).

3. Coupling between SEC and Mass Spectrometry

3.1. State of art

Very recently, the need for performing separation techniques has increased as several samples need to be simplified to be characterized, i.e. humic substances, polymers, organic matter, asphaltenes… SEC represents a good alternative to classic HPLC to separate molecules in regards to their molecular mass. However, the calibration needed for result interpretation is often difficult to find. Few papers describe coupling between SEC and Mass spectrometry using ESI or APCI (Persson *et al.* 2000; Deery *et al.* 2001; Prokai 2001; These *et al.* 2003; Toy *et al.* 2004). However as presented previously, APPI source for environmental samples is of upmost interest but to our knowledge no work was published using SEC-APPI-MS.

3.2. Interface

The difficulty about coupling both techniques resides in their very different operating conditions, (i.e. flow rate, concentrations but also the choice of solvent) which must perform separation without interference with the ionization process. The set-up of the coupling will be fully described in part II of this manuscript.

The interface between the SEC and the MS which corresponds to the ionization source (APPI) must fill the following requirements:

- allowing the pressure decrease (SEC at atmospheric pressure and MS under strong vacuum),
- no chromatographic performance loss by the interface,
- high ionization efficiency,
- no physical or chemical modification,
- small background noise.

4. References

Baim, M.A., Eatherton, R.L., and Hill Jr, H.H., Ion mobility detector for gas chromatography with a direct photoionization source. *Anal. Chem.*, **1983**. *55*(11): p. 1761-1766.

Carroll, D.I., Dzidic, I., Stillwell, R.N., Haegele, K.D., and Horning, E.C., Atmospheric pressure ionization mass spectrometry. Corona discharge ion source for use in a liquid chromatograph-mass spectrometer-computer analytical system. *Anal. Chem.*, **1975**. *47*(14): p. 2369-2373.

Deery, M.J., Stimson, E., and Chappell, C.G., Size exclusion chromatography/mass spectrometry applied to the analysis of polysaccharides. *Rapid Commun. Mass Spectrom.*, **2001**. *15*(23): p. 2273-2283.

Dole, M., Mack, L.L., Hines, R.L., Chemistry, D.O., Mobley, R.C., Ferguson, L.D., and Alice, M.B., Molecular beams of macroions. *J. Chem. Phys.*, **1968**. *49*(5): p. 2240-2249.

Driscoll, J.N., Evaluation of a new photoionization detector for organic compounds. *J. Chromatogr. A*, **1977**. *134*(1): p. 49-55.

Driscoll, J.N. and Clarici, J.B., A new photoionization detector for gas chromatography. *Chromatographia*, **1976**. *9*(11): p. 567-570.

Fenn, J.B., Mann, M., Meng, C.K., Wong, S.F., and Whitehouse, C.M., Electrospray ionization for mass spectrometry of large biomolecules. *Sci*, **1989**. *246*(4926): p. 64-71.

Gallot-Grubisic, Z., Rempp, P., and Benoit, H., Universal calibration for gel permeation chromatography. *J. Polym. Sci., Polym. Lett. Ed.*, **1967**. *5*(Copyright (C) 2010 American Chemical Society (ACS). All Rights Reserved.): p. 753-9.

Ghislain, T. and Charles, L., Chiral analysis using the kinetic method by ESI/MS/MS: Influence of the mass analyzer, in *Chemistry Department*2006, University Aix-Marseille III: Marseille.

Guilhaus, M., Mlynski, V., and Selby, D., Perfect timing: time-of-flight mass spectrometry. *Rapid Commun. Mass Spectrom.*, **1997**. *11*(Copyright (C) 2010 American Chemical Society (ACS). All Rights Reserved.): p. 951-962.

Guilhaus, M., Selby, D., and Mlynski, V., Orthogonal acceleration time-of-flight mass spectrometry. *Mass Spectrom. Rev.*, **2000**. *19*(2): p. 65-107.

Herrera, L.C., Grossert, J.S., and Ramaley, L., Quantitative Aspects of and Ionization Mechanisms in Positive-Ion Atmospheric Pressure Chemical Ionization Mass Spectrometry. *J. Am. Soc. Mass. Spectrom.*, **2008**. *19*(12): p. 1926-1941.

Hoffmann, E.d. and Stroobant, V., Mass spectrometry principles and applications. 3rd ed 2007, Chichester: Wiley. 502.

Kauppila, T.J., Kotiaho, T., Kostiainen, R., and Bruins, A.P., Negative ion-atmospheric pressure photoionization-mass spectrometry. *J. Am. Soc. Mass. Spectrom.*, **2004**. *15*(2): p. 203-11.

Kebarle, P. and Tang, L., From ions in solution to ions in the gas phase - The mechanism of electrospray mass spectrometry. *Anal. Chem.*, **1993**. *65*(22): p. 972A-986A.

Kostiainen, R. and Kauppila, T.J., Effect of eluent on the ionization process in liquid chromatography-mass spectrometry. *J. Chromatogr. A*, **2009**. *1216*(4): p. 685-699.

Mamyrin, B.A., Karataev, V.I., Shmikk, D.V., and Zagulin, V.A., Mass reflectron. New nonmagnetic time-of-flight high-resolution mass spectrometer. *Zh. Eksp. Teor. Fiz.*, **1973**. *64*(Copyright (C) 2010 American Chemical Society (ACS). All Rights Reserved.): p. 82-9.

Mann, M., Meng, C.K., and Fenn, J.B., Interpreting mass spectra of multiply charged ions. *Anal. Chem.*, **1989**. *61*(15): p. 1702-1708.

Marchi, I., Rudaz, S., and Veuthey, J.-L., Atmospheric pressure photoionization for coupling liquid-chromatography to mass spectrometry: A review. *Talanta*, **2009**. *78*(1): p. 1-18.

Moore, J.C., Gel permeation chromatography. I. A new method for molecular weight distribution of high polymers. *J. Polym. Sci., Part A: Polym. Chem.*, **1964**. *2*(2): p. 835-843.

Nguyen, T., Q., Liquid chromatography of synthetic polymers: Principles and applications (in French). *Analusis*, **1998**. *26*(2): p. 35-41.

O'Halloran, G.J., Fluegge, R.A., J.F., B., and Everett, W.L., Technical Documentary Report n° ASD-TDR-62-644, 1964, The Bendix Corporation, research Laboratory Division: Southfield, MI.

Paul, W. and Steinwedel, H., A new mass spectrometer without magnetic field. *Z. Naturforsch.*, **1953**. *8a*(Copyright (C) 2010 American Chemical Society (ACS). All Rights Reserved.): p. 448-50.

Persson, L., Alsberg, T., Kiss, G., and Odham, G., On-line size-exclusion chromatography/electrospray ionisation mass spectrometry of aquatic humic and fulvic acids. *Rapid Commun. Mass Spectrom.*, **2000**. *14*(4): p. 286-292.

Porath, J. and Flodin, P., Gel Filtration: A method for desalting and group separation. *Nature*, **1959**. *183*(4676): p. 1657-1659.

Prokai, L., Characterization of Macromolecules by Electrospray Ionization Mass Spectrometry. *Int. J. Polym. Anal. Charact.*, **2001**. *6*(3-4): p. 379-391.

Robb, D.B., Covey, T.R., and Bruins, A.P., Atmospheric pressure photoionization: An ionization method for liquid chromatography-mass spectrometry. *Anal. Chem.*, **2000**. *72*(15): p. 3653-3659.

Song, L., Wellman, A.D., Yao, H., and Bartmess, J.E., Negative Ion-Atmospheric Pressure Photoionization: Electron Capture, Dissociative Electron Capture, Proton Transfer, and Anion Attachment. *J. Am. Soc. Mass. Spectrom.*, **2007**. *18*(10): p. 1789-1798.

Stephens, W.E., a pulsed mass spectrometer with time dispersion. *Phys. Rev.*, **1946**. *69*: p. 691.

Tabet, J.C. Coupling of unsual ionization sources with FTMS. in *Ecole Thématique CNRS*. 2008. Ambleuteuse, FRANCE.

These, A. and Reemtsma, T., Limitations of Electrospray Ionization of Fulvic and Humic Acids as Visible from Size Exclusion Chromatography with Organic Carbon and Mass Spectrometric Detection. *Anal. Chem.*, **2003**. *75*(22): p. 6275-6281.

Thomson, B.A. and Iribarne, J.V., Field-induced ion evaporation from liquid surfaces at atmospheric pressure. *J. Chem. Phys.*, **1979**. *71*(Copyright (C) 2010 American Chemical Society (ACS). All Rights Reserved.): p. 4451-63.

Toy, A.A., Vana, P., Davis, T.P., and Barner-Kowollik, C., Reversible Addition Fragmentation chain Transfer (RAFT) polymerization of methyl acrylate: Detailed structural investigation via coupled Size Exclusion Chromatography-Electrospray Ionization Mass Spectrometry (SEC-ESI-MS). *Macromolecules*, **2004**. *37*(3): p. 744-751.

Wong, S.F., Meng, C.K., and Fenn, J.B., Multiple charging in electrospray ionization of poly(ethylene glycols). *J. Phys. Chem.*, **1988**. *92*(2): p. 546-550.

Wu, C.-s. and Editor, Handbook of Size Exclusion Chromatography. [In: Chromatogr. Sci. Ser., 1995; 69] 1995: Dekker. 463 pp.

PART II: Optimization of ionization for PAHs; implications for a novel stabilization pathway in soils

La première étape de ce travail de thèse consistait à déterminer et mettre au point les conditions expérimentales pour la mesure des composés apolaires ou peu polaires de hautes masses moléculaires. L'étude a donc porté sur les trois sources à pression atmosphérique les plus couramment utilisées : l'ionisation electrospray (ESI), l'ionisation chimique à pression atmosphérique (APCI) et la photoionisation à pression atmosphérique (APPI). Ces trois sources ont été testées afin de mesurer leur efficacité à ioniser une solution composée d'un HAP (fluoranthène) et de ses dérivés de hautes masses moléculaires.

Dans cette étude, l'ESI n'a pas été capable de détecter les dérivés de hautes masses moléculaires. L'APCI et l'APPI ont démontré leur efficacité à ioniser l'ensemble des espèces présentes. Cependant, la compétition à l'ionisation s'est révélée plus importante pour l'APCI que pour l'APPI. Cette dernière a donc été retenue pour les expérimentations suivantes.

Le choix de la source d'ionisation fait, il a été possible de suivre la réactivité du fluoranthène (un des HAP les plus présents dans les sols pollués des friches industrielles de Lorraine) vis-à-vis des matrices minérales les plus présentes dans le sol (calcite, argile et sable) en contexte d'oxydation naturelle (i.e. oxydation à basse température pour simuler un effet à long terme). Les différentes expériences ont mis en évidence un phénomène de polycondensation qui s'est prolongé jusqu'à la formation d'un résidu carboné stable permettant ainsi de fixer les polluants de type HAP dans le sol, les excluant ainsi du cycle du carbone.

Detection and Monitoring of PAH and Oxy-PAHs by High Resolution Mass Spectrometry: Comparison of ESI, APCI and APPI source detection

Thierry Ghislain*, Pierre Faure, Raymond Michels

Accepted at Journal of the American Society for Mass Spectrometry,

G2R, Nancy-Université, CNRS, B.P. 239, 54506 Vandœuvre-lès-Nancy, France

* Corresponding author. Tel.: +33 3 83 68 47 41; fax: +33 3 83 68 47 01.

E-mail address: Thierry.Ghislain@g2r.uhp-nancy.fr

Abstract

The objective of this work was to compare direct infusion in Q-TOF mass spectrometer through three different atmospheric pressure sources, ElectroSpray Ionization (ESI), Atmospheric Pressure Chemical Ionization (APCI) and Atmospheric Pressure PhotoIonization (APPI) coupled to a high resolution Q-TOF mass spectrometry. A complex mixture of PAH and oxy-PAHs, obtained after the air oxidation of fluoranthene on mineral substrates, was used to compare the different ionization abilities of these sources. Here we propose analytical methods for the use of all sources. Final goal was to provide background to the choice of the most appropriate source in order to analyze complex organic mixtures as those encountered in polluted soils, water, sediments as well as in petroleum.

1. Introduction

Natural organic matter encountered in rocks, soils, sediments or water is a complex mixture of organic compounds. This complexity is inherited from the many steps implied in the fate of organic matter in the coupling of the subsurface and geological organic carbon cycles: biosynthesis (type of living organisms), bioproduction (quantities and proportions of organism types), degradation (organic decay), diagenetic processes (organic matter preservation, kerogen formation, burial at depth and heating under geothermal gradient) (Tissot *et al.* 1984; Killops 1993).

Organic matter composition thus ranges from mixtures typical of soils (free carbohydrates, lipids, organic acids, humic and fulvic acids…) to fossil organic matter (kerogen, coal) and its transformation products, (petroleum, gas). This complexity led to the development of a large variety of procedures and techniques as to gain chemical information, useful to understand the origins, reactivity and fate of organic matter in natural systems. Among them, mass spectrometry allowed significant progress over the last 50 years in the knowledge of organic geochemistry.

One of the latest challenge in the field of mass spectrometry is to be able to characterize and study the fate of the most polar and high molecular mass fractions. While the molecular composition of the lighter and non polar molecular mass fractions of solvent soluble compounds is commonly studied by GC-MS techniques, the most polar and high molecular mass fractions (humic and fulvic acids, petroleum asphaltenes for instance) cannot be investigated without significant pretreatment (i.e. derivatization, pyrolysis, stepwise chemical degradation). Coupling with spectroscopic studies were thus privileged (i.e. FTIR, NMR) and leads to a description of these high molecular mass entities. These compounds account for most of the solvent soluble organic matter extracted from samples and encountered in petroleum. Recent development in mass spectrometry focused on hyphenated methods combining low energy ionization with ultrahigh resolution mass spectrometry (Marshall *et al.* 2006). Low energy ionization sources (ESI, APCI and APPI) have the advantage to allow the ionization of high molecular mass organic compounds (several hundred thousand Daltons for ESI, and between 1500 and 2000 Da for APPI and APCI) with minimum sample treatment (i.e. direct infusion of aqueous or organic solutions). High resolution mass spectrometry allows separation and detection of a very large range of the produced ions as to determine mass distributions or to identify specific compounds.

In this very general context, we focused on the origin and fate of polyaromatic hydrocarbons (PAHs) in soils and sediments polluted by the input of coal processing plants. These compounds are known for their high toxicity and carcinogenic properties, and are thus on the priority list of US-EPA. From the perspective of estimating the capacity of natural systems to self-recover over time, our studies consider for the first time the possibility of a new reactive pathway in which PAHs undergo mineral catalyzed low temperature oxidation leading to their immobilization in sediments (Ghislain *et al.* 2010; Biache *et al.* 2011). Our capacity on analyzing and identifying the higher molecular mass reaction products by high resolution mass spectrometry was key in this investigation.

In atmospheric pressure ionization sources, it is commonly accepted that Electrospray Ionization (ESI) is mainly used for ionic species or for easily ionizable compounds (with a labile hydrogen for instance). Yet, ESI can also be used for the detection of non polar compounds when ionization is favored using additives like silver (Hand *et al.* 1989) or tropylium (Moriwaki *et al.* 2004; Lien *et al.* 2007). The original work using silver cationization was performed by Hand *et al.* in solid phase using Secondary Ion mass Spectrometry (SIMS). Then, electron transfer reactions using an oxidant in liquid phase (methylene chloride with trifluoacetic acid for instance) extended the application field of the ES ionization by allowing the detection of non polar compounds such as PAHs (Van Berkel *et al.* 1992; Van Berkel *et al.* 1994). More recently several works investigate the benefit of the use of silver mediated ionization for PAHs (Kwan Ming Ng 2003; Maziarz Iii *et al.* 2005), for its ability to provoke a Lewis acid-base reaction (Deng *et al.* 1998) and mainly create the radical cation $M^{+\bullet}$ or its binding form $[Ag+M]^{+}$.

Other ionization techniques, like Atmospheric Pressure Chemical ionization (APCI) and Atmospheric Pressure PhotoIonization (APPI) sources are more efficient in the case of non polar organic compounds, because the principle of the ionization is based on compound ionization energy. For instance, APCI is used for the detection of high molecular mass PAHs (Lafleur *et al.* 1996). Yet, it is preferentially used coupled to High Performance Liquid Chromatography (HPLC) for PAH quantification (Marvin *et al.* 1999; Grosse *et al.* 2007; Lien *et al.* 2007).

APPI is known to be more sensitive than APCI to non polar compounds and especially PAHs compared to APCI and ESI (Cai *et al.* 2009). Yet, better sensitivity is often obtained by the use of dopant.

Thus, different dopants, type of solvents and flow rates were investigated for the analysis of pure PAHs. (Kauppila *et al.* 2002; Kauppila *et al.* 2005; Short *et al.* 2007; Robb *et al.* 2008; Smith *et al.* 2009).

We are presenting comparative results on the use of ElectroSpray Ionization (ESI), Atmospheric Pressure Chemical Ionization (APCI) and Atmospheric Pressure PhotoIonization (APPI) in order to allow the best choice of an ionization source as to identify reaction products from low temperature mineral catalyzed oxidation experiments of pure PAHs (Ghislain *et al.* 2010).

2. Experimental section

2.1. Samples and Chemicals

The experiments were carried out on PAH oxidation experiments described elsewhere (Ghislain *et al.* 2010). They consist in the air oxidation at 100°C of fluoranthene mixed with various mineral matrices (quartz, clay, limestone) during 2, 4 and 6 months. A range of high molecular mass compounds were thus created. These compounds are based on fluoranthene units ($C_{16}H_{10}$, 202 g.mol^{-1}) on which the addition of fluoranthene reactional intermediates ($C_{16}H_8$, 200 g.mol^{-1} or $C_{16}H_8O$, 216 g.mol^{-1}) lead to higher molecular mass oxy-PAHs such as $C_{32}H_{16}O$, $C_{48}H_{24}O_2$ (respectively 418 and 632 g.mol^{-1}). In this work, Fluoranthene ($C_{16}H_{10}$) and its derivatives ($C_{32}H_{16}O$ and $C_{48}H_{24}O_2$) will be considered in order to compare the ionization procedures using different ionization sources

The concentration of the sample (77µmol.mL^{-1} based on fluoranthene quantification) was diluted 100 times in the appropriate solvent for analysis.

Pure fluoranthene (Fla) 99.9% and silver nitrate ($AgNO_3$) ≥99 .9% were purchased from Sigma-Aldrich Co. and was used with no further purification. *n*-Hexane, methanol, chloroform, toluene, (H.P.L.C. grade), were purchased from V.W.R. and used as received. Silver Nitrate for ESI experiments was diluted in methanol then stirred until complete dissolution. It was added to the sample solution to obtain a final concentration of 100nM prior to injection in the ionization sources.

2.2. Q-TOF Mass Spectrometry

Mass spectra were recorded on a hybrid Quadrupole – Time Of Flight mass spectrometer (Bruker Daltonics, Bremen, Germany) equipped with the different atmospheric pressure sources. All intensities are average of 60 mass spectra recorded for 1 minute after stabilization of the total ion current (TIC) at 1 spectrum/sec rate.

2.3. ESI, APCI, APPI Parameters

All sources were optimized for the $C_{48}H_{24}O_2$ ion (m/z 632) to perform the best characterization of the mixture and allow comparison of the ionization sources. For ESI source, the capillary voltage was set at 5kV and 167V for cone voltage. Nitrogen gas was maintained at 0.4bar for nebulisation and 4L.min^{-1} at 190°C for evaporation. APCI capillary voltage was set at -2500V with a corona discharge at 5µA. APPI (Syagen Technology Inc., Tustin, CA, USA), contains a Krypton lamp which produced a 10eV photon beam operating in positive mode. The source was set at capillary voltage -4500V.

Direct infusion of the sample solutions was performed using a syringe pump (Kd Scientific, USA). Flow rate was set at 3µL.min^{-1} for ESI and 100µL.min^{-1} for APCI and APPI.

2.4. Shared parameters for APCI and APPI

Nitrogen gas was maintained at 3bar for nebulisation and 7L.min^{-1} at 250°C for evaporation and 450°C for vaporizer temperature. In the case of APCI and APPI the flow rate was also tested and in both cases set at 100µL.min^{-1}.

3. Results

3.1. ESI source

Due to its base principle, ESI hardly ionizes non polar compounds (Kebarle *et al.* 1993; Kebarle 2000). Thus, the ESI source was used using silver ions as ionization mediator

(Figure 1), which allows an electrochemical reaction consisting in the transfer of an electron from aromatics to the silver ions according to equation (1) (Maziarz Iii *et al.* 2005).

$$PAH + Ag(I) \rightarrow PAH^{+\bullet} + Ag(0) \quad (1)$$

However, other reactions were proposed by Ng *et al.* (Ng *et al.*, 2003) when the silver complex $[Ag + PAH]^+$ is observed and this complex can undergo dissociation according to equations (2a), (2b) and (2c)

$$[2PAH + Ag]^+ \rightarrow PAH + [PAH + Ag]^+ \quad (2a)$$

$$[PAH + Ag]^+ \rightarrow PAH + Ag(I) \quad (2b)$$

$$\rightarrow PAH^{+\bullet} + Ag(0) \quad (2c)$$

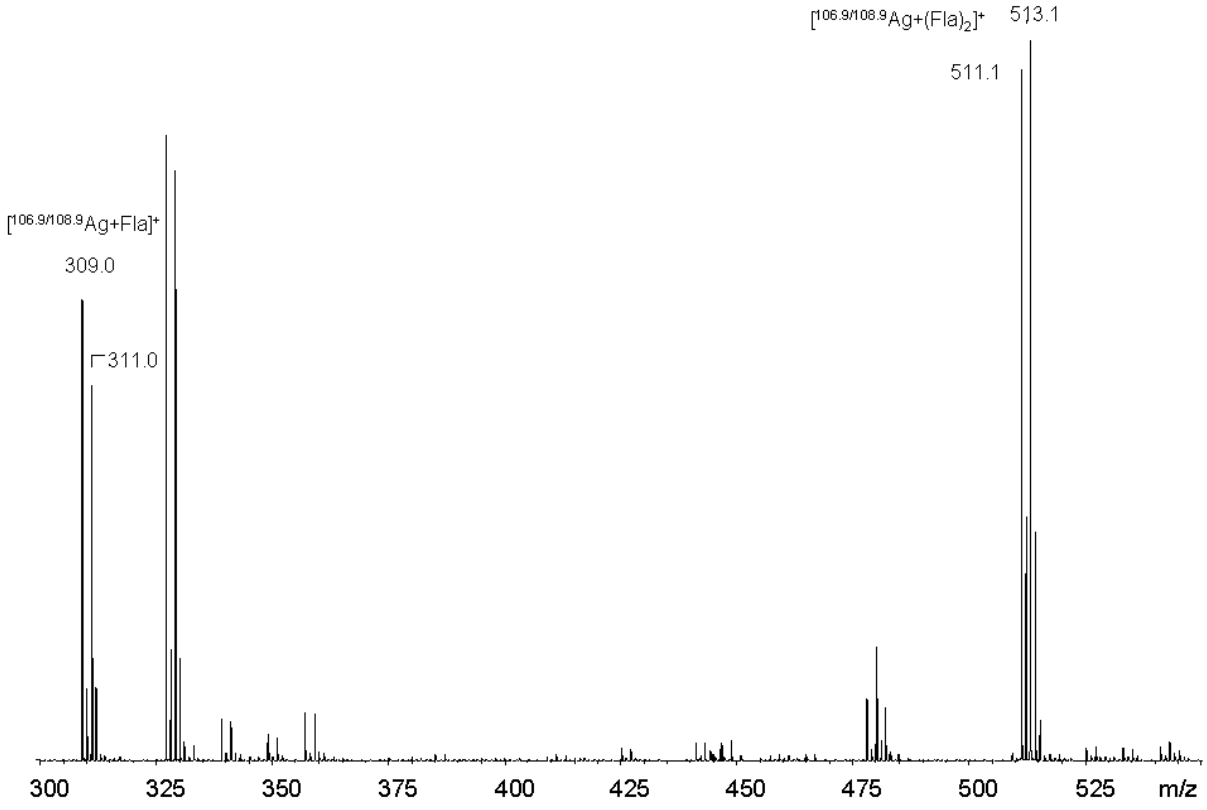

Figure 1: ESI+ mass spectrum of Ag(I) cationized mixture of PAHs and oxy-PAHS reaction products obtained after oxidation of fluoranthene on limestone at 100°C for 4 months

In general, the odd-electron radical is observed ($M^{+\bullet}$) when mixing PAHs with silver ions at a high cone voltage (Kwan Ming Ng 2003). This was observed when we tested pyrene ($C_{16}H_{10}$) in our system, a result consistent with Hager and Wallace (1988) (Hager *et al.* 1988).

In the case of fluoranthene, no odd-radical ions were observed, only clusters such as [Ag + Fla]$^+$ and [Ag + (Fla)$_2$]$^+$ at respectively m/z 309/311 and 509/511. Maziarz *et al.* (2005) (Maziarz Iii *et al.* 2005) related these phenomena to the ionization energy difference between Ag and PAHs. When the Ag ionization energy (7.57eV) (Shenstone 1940; Loock *et al.* 1999) is greater than that of the PAH, the radical PAH$^{+\bullet}$ is observed. This was the case in our experiments using pyrene (7.42eV) (Hager and Wallace 1988) but such radical was not observed using fluoranthene (7.9eV), in accordance with Ling and Lifshitz (1995) (Ling *et al.* 1995).

With the ESI source, the mass spectrum does not show any ion corresponding to $C_{32}H_{16}O$ or $C_{48}H_{24}O_2$ even when silver nitrate is used as cationization mediator.

3.2. APCI and APPI sources

3.2.1. APCI

As shown on Figure 2 and Figure 3, APCI was able to ionize the PAHs and oxy-PAHs present in the reference solution. All measurements are summarized in Table 1. The highest detection intensity for fluoranthene under its radical ion form (M$^{+\bullet}$) was obtained with chloroform as solvent. *n*-Hexane and methanol lead only to lower intensities. For the protonated form [M+H]$^+$, the highest intensity was reached using *n*-hexane. Intensity decreased from chloroform to methanol.

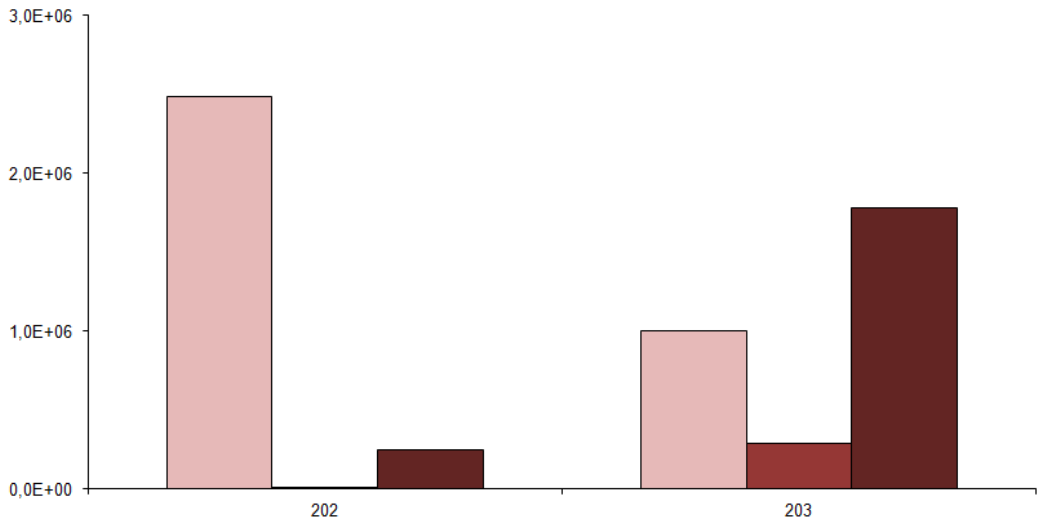

Figure 2: Absolute abundance of m/z 202 (M$^{+\bullet}$) and m/z 203 ([M+H]$^+$ ions using APCI operated with different solvents chloroform, methanol, *n*-hexane.

For higher molecular mass compounds, such as $C_{32}H_{16}O$, the highest intensity was found for the protonated form (m/z 417) using *n*-hexane, followed by methanol and chloroform. The highest intensity for the radical ion (m/z 416) was obtained with chloroform; methanol and *n*-hexane gave very low intensities. In the case of $C_{48}H_{24}O_2$ the highest detection intensity was reached using *n*-hexane while its adduct form was $[M+H]^+$. Intensity values, for ion m/z 633 were lower and decreased when chloroform and methanol were used for the protonated ion. Considering the radical form (m/z 632) intensities decrease as following $I_{chloroform}>I_{n\text{-}hexane}>I_{methanol}$.

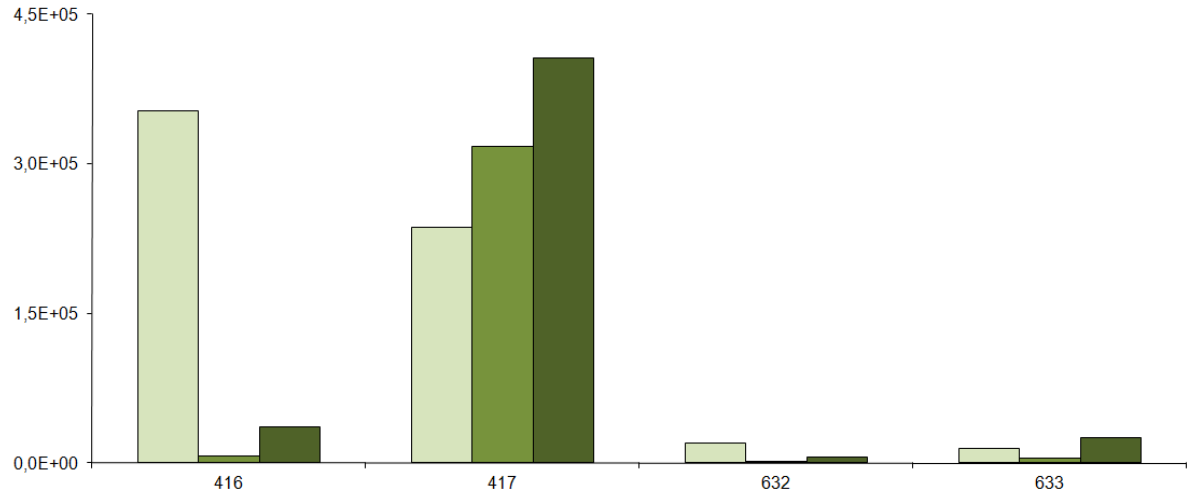

Figure 3: Absolute abundance at m/z 416 ($M^{+\bullet}$), m/z 417 ($[M+H]^+$), m/z 632 ($M^{+\bullet}$) and m/z 633 ($[M+H]^+$) ions using APCI for different solvents ⬚ chloroform, ■ methanol, ▨ *n*-hexane.

	$C_{16}H_{10}$	$C_{16}H_{11}$	$C_{32}H_{16}O$	$C_{32}H_{17}O$	$C_{48}H_{24}O_2$	$C_{48}H_{25}O_2$
m/z	202.078	203.086	416.120	417.127	632.177	633.185
Ion form	$M^{+\bullet}$	$[M+H]^+$	$M^{+\bullet}$	$[M+H]^+$	$M^{+\bullet}$	$[M+H]^+$
Chloroform	2488185	1000182	352750	236336	20272	14869
Methanol	12004	286349	6776	317623	1321	5132
***n*-Hexane**	249585	1782453	35768	406691	6011	25327

Table 1: Measured intensities determined by APCI-QTOF of different molecules according to the solvent used.

3.2.2. APPI

The experiments with APPI were run with and without toluene as dopant, using the same solvents as for APCI (*n*-hexane, chloroform and methanol). Results are presented on Figure 4 and Figure 5 and summarized in Table 2. Toluene was preferred because it has low ionization energy (8.83eV) and it is less harmful to health than benzene or its halogenated derivates. Toluene as dopant was successfully applied to naphthalenes (Kauppila *et al.* 2002). The highest intensities found for fluoranthene, under both ion forms was found using *n*-hexane. Chloroform, methanol and *n*-hexane, all with dopant gave similar results when chloroform and methanol gave lower signal more noticeable for methanol (Figure 4 and Table 2).

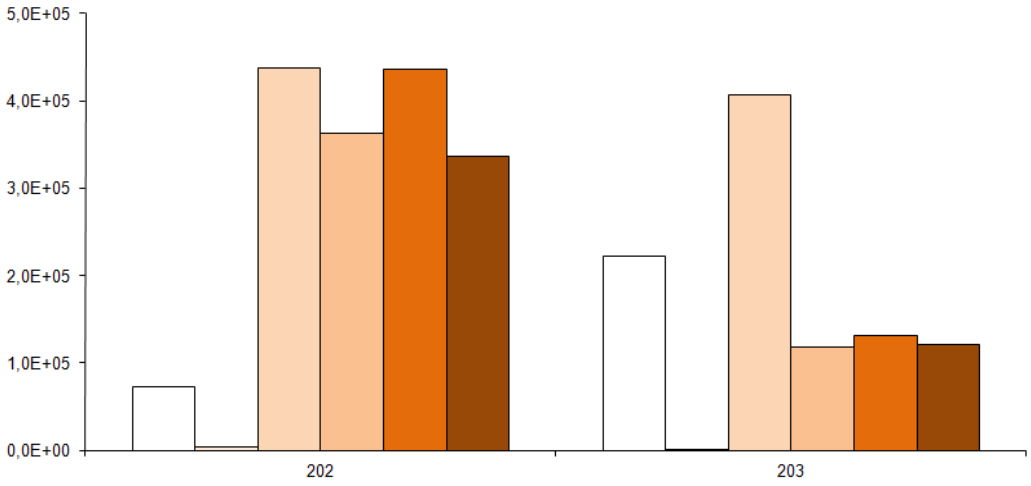

Figure 4: Absolute abundance of m/z 202 ($M^{+\bullet}$) and m/z 203 ($[M+H]^+$ ions using APPI for different solvents chloroform, methanol, *n*-hexane, chloroform+10% toluene, methanol+10% toluene, *n*-hexane+10% toluene.

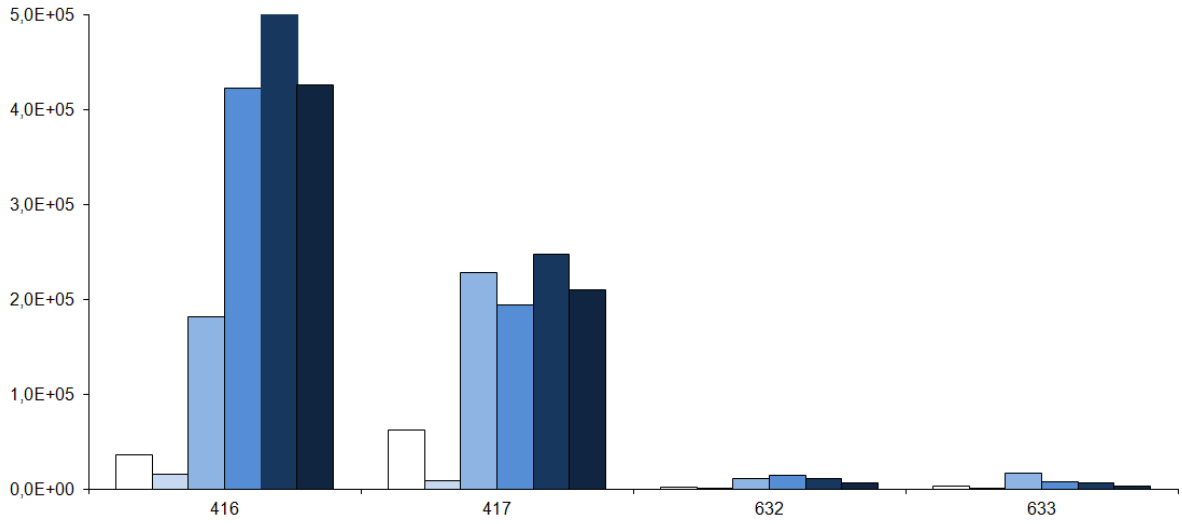

Figure 5: Absolute abundance of m/z 416 ($M^{+\bullet}$), m/z 417 ($[M+H]^+$), m/z 632 ($M^{+\bullet}$) and m/z 633 ($[M+H]^+$) ions using APPI for different solvents chloroform, methanol, *n*-hexane, chloroform+10% toluene, methanol+10% toluene, *n*-hexane+10% toluene.

	$C_{16}H_{10}$	$C_{16}H_{11}$	$C_{32}H_{16}O$	$C_{32}H_{17}O$	$C_{48}H_{24}O_2$	$C_{48}H_{25}O_2$
m/z	202.078	203.086	416.120	417.127	632.177	633.185
Ion form	$M^{+\bullet}$	$[M+H]^+$	$M^{+\bullet}$	$[M+H]^+$	$M^{+\bullet}$	$[M+H]^+$
Chloroform	72048	222808	35958	62199	1813	2291
Methanol	3131	714	15555	8395	893	570
***n*-Hexane**	438037	407450	181436	228023	10648	16940
Chloroform + toluene	362820	117704	421677	194047	14593	7044
Methanol + toluene	436436	130747	499798	246669	10274	6385
***n*-Hexane + toluene**	336042	121505	425090	209581	5743	3162

Table 2: Measured intensities determined by APPI-QTOF of different molecules according to the solvent and dopant used.

For higher molecular mass oxy-PAHs (Figure 5 and Table 2), i.e. C_{32} compounds, all solvents with dopant gave the highest intensity values. In the absence of dopant, *n*-hexane leads to intensities almost 50% lower than with dopant, while values for chloroform and methanol were 30 times lower. For the detection of its protonated form (m/z 417), *n*-hexane pure as well as all solvents with dopant gave similar results. Methanol and chloroform lead to the lowest values.

For $C_{48}H_{24}O_2$, the most oxygenated form (m/z 632), the results were in the same range, except for chloroform, methanol and *n*-hexane + toluene which gave very low intensities. For the protonated form, using *n*-hexane without dopant gave intensity more than twice that of the others solvents.

4. Discussion

Ghislain *et al.* (Ghislain *et al.* 2010) studied the air oxidation of fluoranthene catalyzed by minerals. Reactions were conducted at 100°C for several hours to months. The compounds in the reference solution of this paper were among the end-products obtained by these reactions. Testing different ionization sources allowed evaluating their incidence on the results, especially their ability in detecting higher molecular mass compounds, which are the major outcome of the reaction studied.

4.1. APCI vs. APPI vs. ESI

ESI was only able to detect pure PAH in the PAH + oxy-PAH mixture and lead to the use of silver ions as cationization mediator. The electrochemical reaction using silver ions was not successful for heavier oxy-PAH as we assume that their ionization energy might be too high for silver mediation.

When APCI is used for the PAH and oxy-PAH mixture studied, the radical ion forms were better detected using chloroform (Figure 2 and Figure 3). On the contrary best detection of the protonated forms was performed using *n*-hexane. Yet, these differences are reduced concerning the higher molecular mass compounds ($C_{48}H_{24}O_2$) (Figure 3).

In the case of APPI, without consideration of either radical or protonated ions, *n*-hexane gave the best results for fluoranthene and $C_{48}H_{24}O_2$ detection and acceptable results

for $C_{32}H_{16}O$ (Figure 4 and Figure 5). These results can be explained by the self-doping effects usually observed when using *n*-Hexane *(*Cai *et al*. 2007*)*.

The higher molecular mass compounds $C_{32}H_{16}O$ (m/z 416) and $C_{48}H_{24}O_2$ (m/z 632) which were not detected using ESI, are clearly identified using APCI and APPI.

4.2. APCI vs APPI

Q-TOF mass spectrometry is not a quantitative detection method. Thus, the evolution of the reaction products from the oxidation experiments as a function of time was followed up by using intensities ratios between each oxy-PAH (reaction products) and fluoranthene (reactant). APPI and APCI were compared, and ions under radical or protonated forms using *n*-hexane were considered, (Figure 6, Figure 7, Figure 8 and Figure 9). In these experiments, an additional compound was also considered, i.e. $C_{64}H_{32}O_3$ (m/z 848).

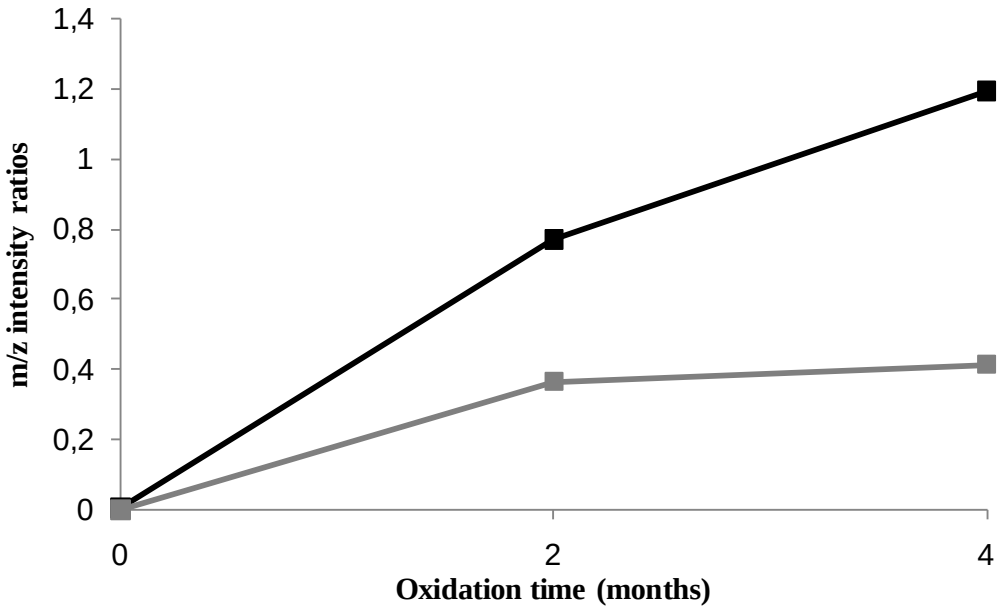

Figure 6: Relative contribution of oxygenated high molecular mass reaction products normalized to unreacted fluoranthene as determined by either APCI-QTOF (■ $I_{m/z\ 416}/I_{m/z\ 202}$) or APPI-QTOF (■ $I_{m/z\ 416}/I_{m/z\ 202}$). The measurements were performed on $CHCl_3$ extracts obtained after oxidation at 100°C as a function of time of a fluoranthene/limestone mixture. Oxidation leads to the formation of oxygenated products of molecular masses higher than the initial reactant.

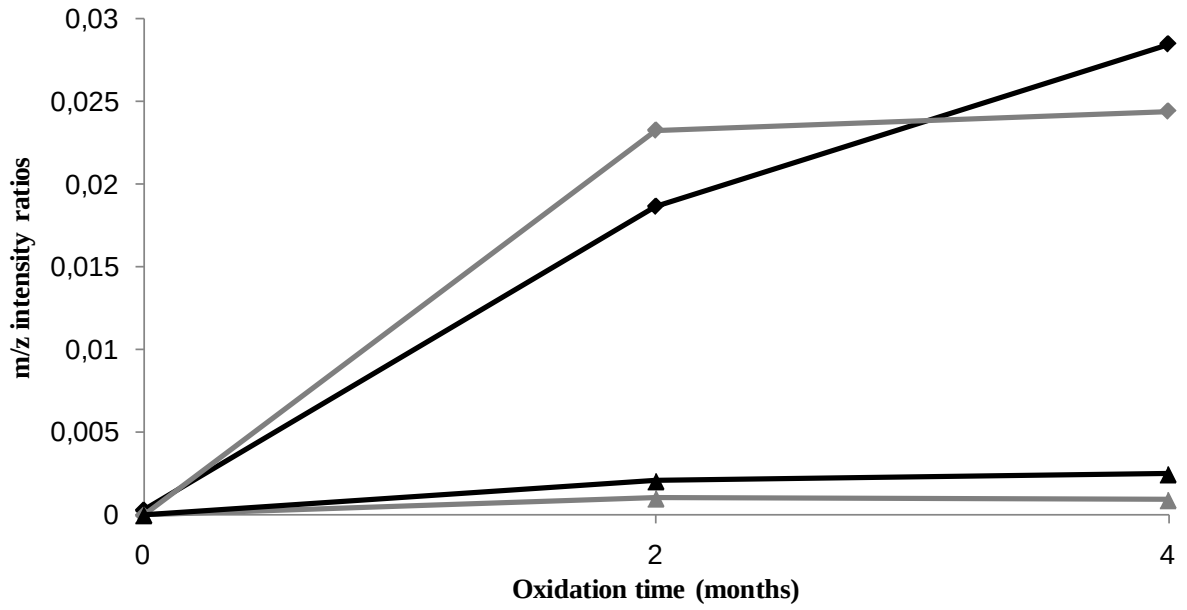

Figure 7: Relative contribution of oxygenated high molecular mass reaction products normalized to unreacted fluoranthene as determined by either APCI-QTOF(♦ $I_{m/z\ 632}/I_{m/z\ 202}$; ▲ $I_{m/z\ 848}/I_{m/z\ 202}$) or APPI-QTOF (♦ $I_{m/z\ 632}/I_{m/z\ 202}$; ▲ $I_{m/z\ 848}/I_{m/z\ 202}$). The measurements were performed on $CHCl_3$ extracts obtained after oxidation at 100°C as a function of time of a fluoranthene/limestone mixture. Oxidation leads to the formation of oxygenated products of molecular mass higher than the initial reactant.

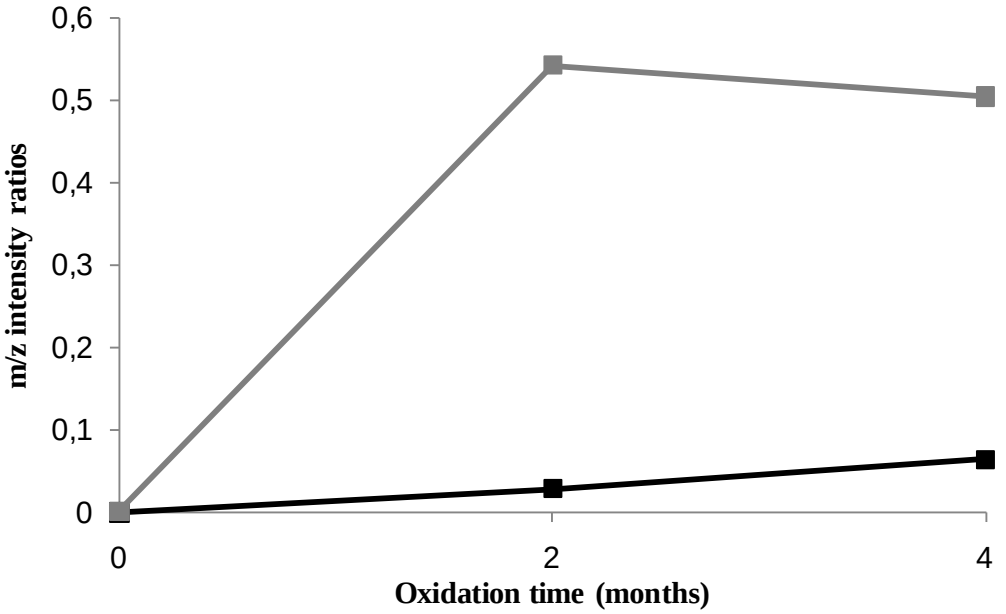

Figure 8: Relative contribution of oxygenated high molecular mass reaction products normalized to unreacted fluoranthene as determined by either APCI-QTOF (■ $I_{m/z\ 417}/I_{m/z\ 203}$) or APPI-QTOF (■ $I_{m/z\ 417}/I_{m/z\ 203}$). The measurements were performed on $CHCl_3$ extracts obtained after oxidation at 100°C as a function of time of a fluoranthene/limestone mixture. Oxidation leads to the formation of oxygenated products of molecular masses higher than the initial reactant.

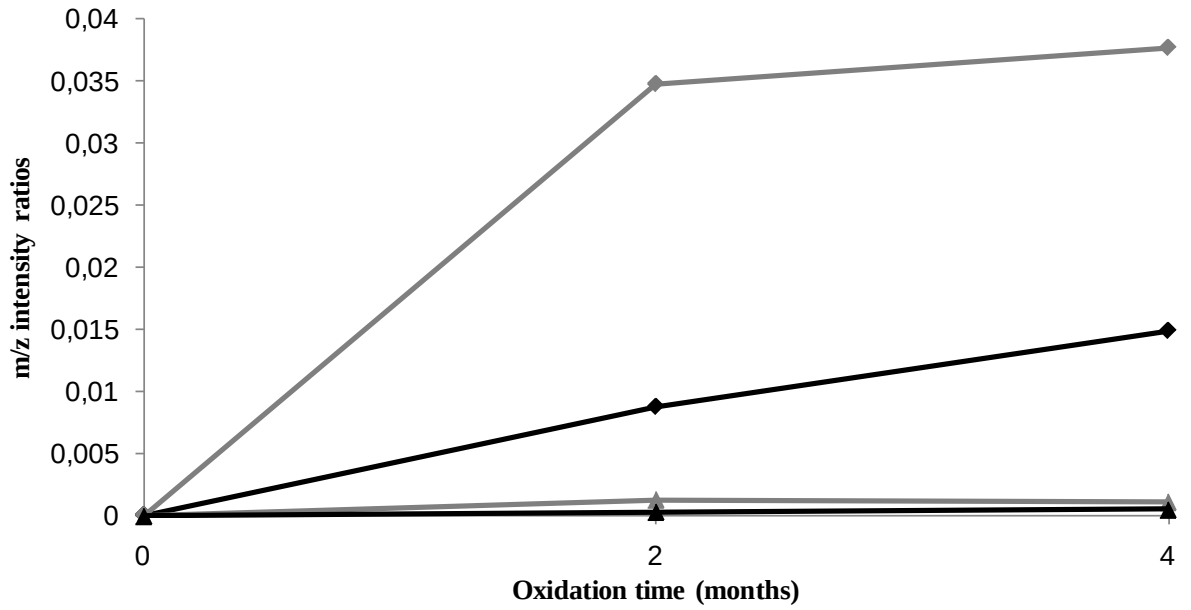

Figure 9: Relative contribution of oxygenated high molecular mass reaction products normalized to unreacted fluoranthene as determined by either APCI-QTOF (♦ $I_{m/z\ 633}/I_{m/z\ 203}$; ▲ $I_{m/z\ 849}/I_{m/z\ 203}$) or APPI-QTOF (♦ $I_{m/z\ 633}/I_{m/z\ 203}$; ▲ $I_{m/z\ 849}/I_{m/z\ 203}$). The measurements were performed on $CHCl_3$ extracts obtained after oxidation at 100°C as a function of time of a fluoranthene/limestone mixture. Oxidation leads to the formation of oxygenated products of molecular masses higher than the initial reactant.

When the molecular ions are considered (Figure 6 and Figure 7), a main difference appears in the ratio values nearly 2-3 times higher for APCI ($I_{m/z\ 416}/I_{m/z\ 202}$) than for APPI. However for the $I_{m/z\ 632}/I_{m/z\ 202;\ and}$ $I_{m/z\ 848}/I_{m/z\ 202}$, APPI and APCI gave similar results (Figure 7).

When using protonated ion ratios (Figure 8 and Figure 9), the main difference appears for the $I_{m/z\ 417}/I_{m/z\ 203}$ ratio values nearly 10 times higher for APPI than for APCI and 3 times higher in the case of $I_{m/z\ 633}/I_{m/z\ 203}$. This mainly implies a better detection of fluoranthene using APCI. Ion suppression between fluoranthene and the reaction products seems to be stronger when APCI is used.

On both spectra using APCI and APPI (Figure 10 and Figure 11), it can also be observed that regardless of fluoranthene, more compounds in the intermediate m/z 202 to 250 range are detected using APPI than APCI.

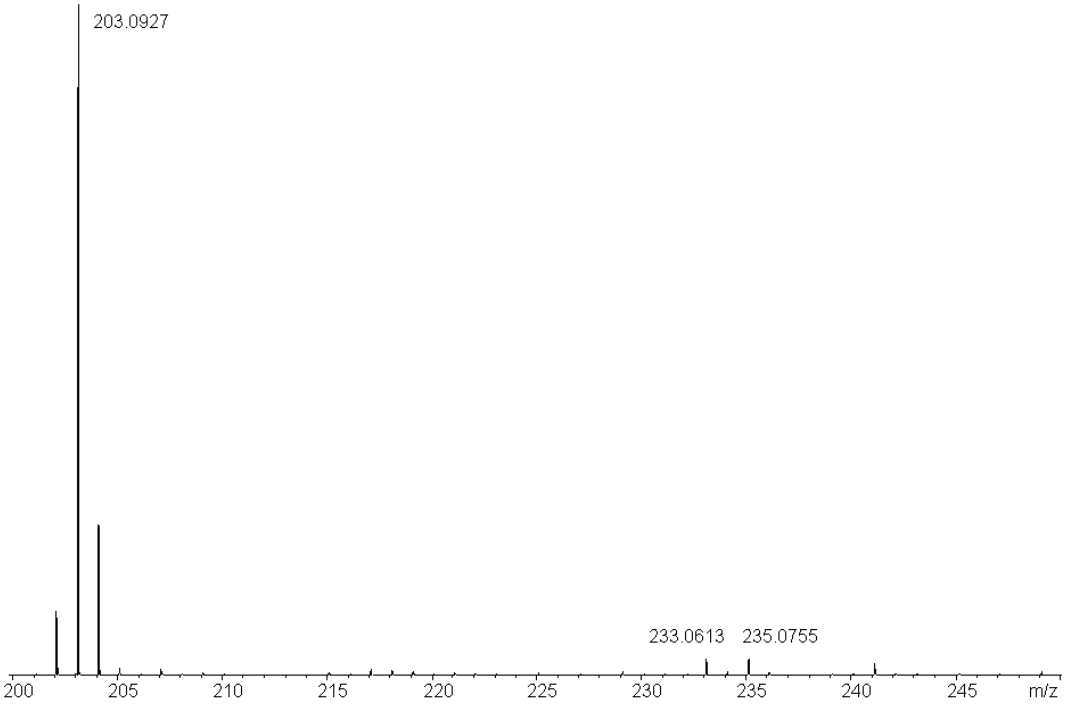

Figure 10: APCI+ mass spectrum within the range m/z 200 -250 using *n*-hexane

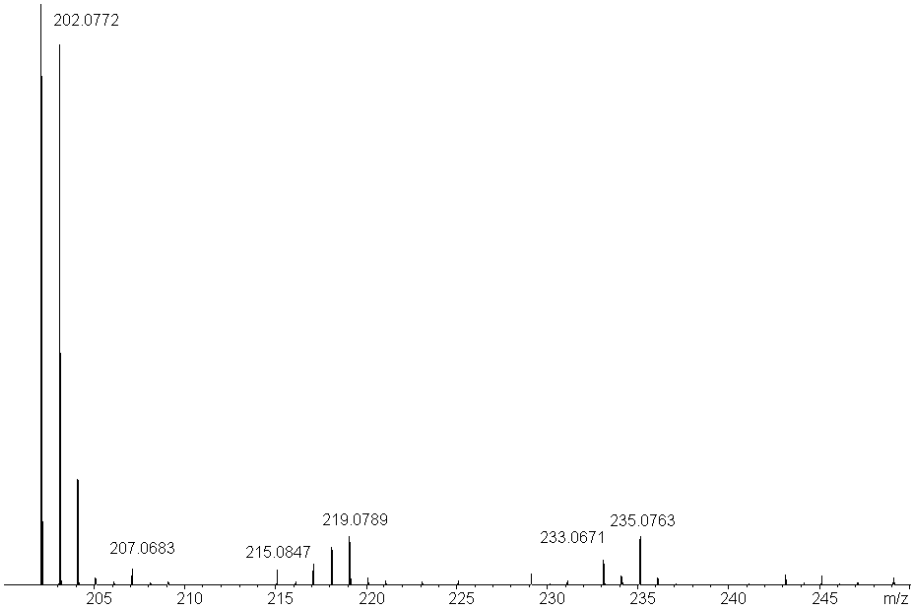

Figure 11: APPI+ mass spectrum within the range m/z 200-250 using *n*-hexane

APPI thus appears as the most suitable ionization source for the compounds studied because:

- it allows the detection of the higher molecular mass compounds ($C_{32}H_{16}O$ and $C_{48}H_{24}O_2$) not detected by ESI,
- it reduces the ionization competition between fluoranthene and the reaction products compared to APCI,

- it favors the ionization of the intermediate molecular mass reaction compounds (m/z 202 to 250) compared to APCI. These compounds may probably be weakly polar or have low proton affinity, thus not ionized by APCI.

All these characteristics lead to chose APPI as ionization source in order to characterize the full extent of reaction products, thus allowing to propose a condensation reaction mechanism during the low temperature oxidation of fluoranthene on mineral matrix (Ghislain *et al.* 2010).

5. Conclusion

In our experiments, ESI did not prove to be capable of analyzing the PAHs and oxy-PAHS mixture even with the use of silver ions as cationization mediator. On the contrary, APPI and APCI gave better results using *n*-hexane as solvent, especially in the detection of higher molecular mass compounds ($C_{32}H_{16}O$ and $C_{48}H_{24}O_{2)}$. APPI was preferentially used without dopant (as *n*-hexane presents self-doping effect).

Yet, concerning the study of our reaction products mixture, the APCI source favored the ionization of fluoranthene (the reactant) compared to the reaction products. This leads to ionization competition which lowered the relative detection of the higher molecular mass compounds in the following up of the reactions. Also, APCI was less efficient than APPI to detect the intermediate molecular mass range of products (probably weakly polar compounds not favorably ionized by APCI).

The APPI source finally appeared as the most suitable ionization source for e following up of our reaction products, because it allowed the detection of the full range of compounds from low to high molecular mass. Consequently, it permitted to identify full series of reaction products that were interpreted as being formed through a polycondensation mechanism (Ghislain *et al.* 2010).

Acknowledgements

The authors wish to thank François Dupire from the Mass Spectrometry Facility of the Nancy University for the APCI loan. The doctoral grant of Thierry Ghislain was provided by

the Regional Council of Lorraine (France) and CREGU. The Q-TOF instrument was funded by Regional Council of Lorraine and CNRS (CPER 2004).

6. References

Biache, C., Ghislain, T., Faure, P., and Mansuy-Huault, L., Low temperature oxidation of a coking plant soil organic matter and its major constituents: An experimental approach to simulate a long term evolution. *J. Hazard. Mater.*, 2011. *188*(1-3): p. 221-230.

Cai, S.-S., Syage, J.A., Hanold, K.A., and Balogh, M.P., Ultra Performance Liquid Chromatography−Atmospheric Pressure Photoionization-Tandem Mass Spectrometry for High-Sensitivity and High-Throughput Analysis of U.S. Environmental Protection Agency 16 Priority Pollutants Polynuclear Aromatic Hydrocarbons. *Anal. Chem.*, 2009. *81*(6): p. 2123-2128.

Cai, S.S., Hanold, K.A., and Syage, J.A., Comparison of atmospheric pressure photoionization and atmospheric pressure chemical ionization for normal-phase LC/MS chiral analysis of pharmaceuticals. *Anal. Chem.*, 2007. *79*(6): p. 2491-2498.

Deng, H. and Kebarle, P., Binding energies of silver ion-ligand, L, complexes AgL2 + determined from ligand-exchange equilibria in the gas phase. *J. Phys. Chem. A*, 1998. *102*(3): p. 571-579.

Ghislain, T., Faure, P., Biache, C., and Michels, R., Low-Temperature, Mineral-Catalyzed Air Oxidation: A Possible New Pathway for PAH Stabilization in Sediments and Soils. *Environ. Sci. Technol.*, 2010. *44*(22): p. 8547-8552.

Grosse, S. and Letzel, T., Liquid chromatography/atmospheric pressure ionization mass spectrometry with post-column liquid mixing for the efficient determination of partially oxidized polycyclic aromatic hydrocarbons. *J. Chromatogr. A*, 2007. *1139*(1): p. 75-83.

Hager, J.W. and Wallace, S.C., Two-Laser photoionization supersonic jet mass spectrometry of aromatic molecules. *Anal. Chem.*, 1988. *60*(1): p. 5-10.

Hand, O.W., Winger, B.E., and Cooks, R.G., Enhanced silver cationization of polycyclic aromatic hydrocarbons containing bay regions in molecular secondary ion mass spectrometry. *Biomedical and Environmental Mass Spectrometry*, 1989. *18*(1): p. 83-85.

Kauppila, T.J., Bruins, A.P., and Kostiainen, R., Effect of the solvent flow rate on the ionization efficiency in atmospheric pressure photoionization-mass spectrometry. *J. Am. Soc. Mass. Spectrom.*, 2005. *16*(8): p. 1399-1407.

Kauppila, T.J., Kuuranne, T., Meurer, E.C., Eberlin, M.N., Kotiaho, T., and Kostiainen, R., Atmospheric pressure photoionization mass spectrometry. Ionization mechanism and the effect of solvent on the ionization of naphthalenes. *Anal Chem*, 2002. *74*(21): p. 5470-9.

Kebarle, P., A brief overview of the present status of the mechanisms involved in electrospray mass spectrometry. *J. Mass Spectrom.*, 2000. *35*(7): p. 804-817.

Kebarle, P. and Tang, L., From ions in solution to ions in the gas phase - The mechanism of electrospray mass spectrometry. *Anal. Chem.*, 1993. *65*(22): p. 972A-986A.

Killops, S.D., An introduction to organic geochemistry / S.D. Killops, V.J. Killops. Geochemistry series, ed. V.J. Killops 1993, Harlow, Essex, England : New York :: Longman Scientific & Technical ; Wiley.

Kwan Ming Ng, N.L.M.C.W.T., Differentiation of isomeric polyaromatic hydrocarbons by electrospray Ag(I) cationization mass spectrometry. *Rapid Commun. Mass Spectrom.*, 2003. *17*(18): p. 2082-2088.

Lafleur, A.L., Taghizadeh, K., Howard, J.B., Anacleto, J.F., and Quilliam, M.A., Characterization of flame-generated c10 to c160 polycyclic aromatic hydrocarbons by atmospheric-pressure chemical ionization mass spectrometry with liquid introduction via heated nebulizer interface. *J. Am. Soc. Mass. Spectrom.*, 1996. *7*(3): p. 276-286.

Lien, G.W., Chen, C.Y., and Wu, C.F., Analysis of polycyclic aromatic hydrocarbons by liquid chromatography/tandem mass spectrometry using atmospheric pressure chemical ionization or electrospray ionization with tropylium post-column derivatization. *Rapid Commun Mass Spectrom*, 2007. *21*(22): p. 3694-700.

Ling, Y. and Lifshitz, C., Time-dependent mass spectra and breakdown graphs. 19. Fluoranthene. *J. Phys. Chem.*, 1995. *99*(28): p. 11074-11080.

Loock, H.P., Beaty, L.M., and Simard, B., Reassessment of the first ionization potentials of copper, silver, and gold. *Phys. Rev. A: At. Mol. Opt. Phys.*, 1999. *59*(1): p. 873-875.

Marshall, A.G., Kim, D.G., Klein, G.C., Stanford, L.A., Purcell, J.M., Schaub, T.M., Smith, D.F., Hendrickson, C.L., and Rodgers, R.P. Compositional characterization of petroleum by ultrahigh-resolution Fourier transform ion cyclotron resonance mass spectrometry with multiple ionization sources. 2006.

Marvin, C.H., Smith, R.W., Bryant, D.W., and McCarry, B.E., Analysis of high-molecular-mass polycyclic aromatic hydrocarbons in environmental samples using liquid

chromatography-atmospheric pressure chemical ionization mass spectrometry. *J Chromatogr A*, 1999. *863*(1): p. 13-24.

Maziarz Iii, E.P., Baker, G.A., and Wood, T.D., Electrospray ionization Fourier transform mass spectrometry of polycyclic aromatic hydrocarbons using silver(I)-mediated ionization. *Can. J. Chem.*, 2005. *83*(11): p. 1871-1877.

Moriwaki, H., Ishitake, M., Yoshikawa, S., Miyakoda, H., and Alary, J.F., Determination of polycyclic aromatic hydrocarbons in sediment by liquid chromatography-atmospheric pressure photoionization-mass spectrometry. *Anal Sci*, 2004. *20*(2): p. 375-7.

Robb, D.B., Smith, D.R., and Blades, M.W., Investigation of Substituted-Benzene Dopants for Charge Exchange Ionization of Nonpolar Compounds by Atmospheric Pressure Photoionization. *J. Am. Soc. Mass. Spectrom.*, 2008. *19*(7): p. 955-963.

Shenstone, A.G., The arc spectrum of silver. *PhRv*, 1940. *57*(10): p. 894-898.

Short, L.C., Cai, S.S., and Syage, J.A., APPI-MS: effects of mobile phases and VUV lamps on the detection of PAH compounds. *J Am Soc Mass Spectrom*, 2007. *18*(4): p. 589-99.

Smith, D.R., Robb, D.B., and Blades, M.W., Comparison of Dopants for Charge Exchange Ionization of Nonpolar Polycyclic Aromatic Hydrocarbons with Reversed-Phase LC-APPI-MS. *J. Am. Soc. Mass. Spectrom.*, 2009. *20*(1): p. 73-79.

Tissot, B.P. and Welte, D.H., Petroleum Formation and Occurrence. 2nd Ed. 1984: Springer Verlag. 699 pp.

Van Berkel, G.J., McLuckey, S.A., and Glish, G.L., Electrochemical origin of radical cations observed in electrospray ionization mass spectra. *Anal. Chem.*, 1992. *64*(14): p. 1586-1593.

Van Berkel, G.J. and Zhou, F., Chemical electron-transfer reactions in electrospray mass spectrometry: Effective oxidation potentials of electron-transfer reagents in methylene chloride. *Anal. Chem.*, 1994. *66*(20): p. 3408-3415.

Low temperature - mineral catalyzed air oxidation: A possible new pathway for PAHs stabilization in sediments and soils

Thierry Ghislain*, Pierre Faure, Coralie Biache, Raymond Michels

Environmental Science & Technology, 2010, 44(22),

UMR CNRS 7566 G2R, Nancy-Université, CNRS, B.P. 239, 54506 Vandœuvre-lès-Nancy, France

* Corresponding author. Tel.: +33 3 83 68 47 41; fax: +33 3 83 68 47 01.

E-mail address: Thierry.Ghislain@g2r.uhp-nancy.fr

Abstract.

Reactivity of polycyclic aromatic hydrocarbons (PAHs) in the subsurface is of importance to environmental assessment, as they constitute a highly toxic hazard. Understanding their reactivity in the long term in natural recovering systems is thus a key issue. This article describes an experimental investigation on the air oxidation of fluoranthene (a PAH abundant in natural systems polluted by industrial coal use) at 100 °C on different mineral substrates commonly found in soils and sediments (quartz sand, limestone, and clay). Results demonstrate that fluoranthene is readily oxidized in the presence of limestone and clay, leading to the formation of high molecular mass compounds and a carbonaceous residue as end product especially for clay experiments. As demonstrated elsewhere, the experimental conditions used permitted the reproduction of the geochemical pathway of organic matter observed under natural conditions. It is therefore suggested that low-temperature, mineral-catalyzed air oxidation is a mechanism relevant to the stabilization of PAHs in sediments and soils.

1. Introduction

The origin and fate of polycyclic aromatic hydrocarbons (PAHs) in the environment are of utmost interest to the environmental assessment of polluted sediments and soils. Most studies focus on the 16 PAHs on the US EPA list, the behavior of which are studied in terms of aqueous solubility, biodegradation, oxidation, and adsorption/complexation. In a context of polluted soil remediation, different solutions may be considered, such as invasive treatments through industrial reprocessing and cleaning of the sediments and soils. Among them, thermal desorption consists of heating at 500 °C the substrates previously excavated. This may lead to the removal of 90% of the initial PAH content in soils (Biache *et al.* 2008). It is believed that PAHs are either thermodesorbed or mainly converted into CO_2 (Merino *et al.* 2003). While, thermal desorption may drastically reduce PAH concentrations, the total organic carbon (TOC) of the soil does not change significantly (Biache *et al.* 2008). Instead, the initial PAHs are converted into a solid residue (Biache *et al*. 2008).

Complex chemical treatment of soils and sediments may be another possibility for polluted soil remediation. Strong oxidants (hydrogen peroxide, permanganate, persulfate, etc.) (Rivas 2006) have been considered (Fenton process and Fenton-like processes) to degrade pollutants; however, as for thermal treatments, soil sterility is a major consequence. Therefore, another option, which is less drastic, is to rely on the natural recovery of polluted sites. However, the fate of the pollutants in naturally recovering systems may be complex and needs long-term monitoring as well as deep understanding of natural reactivity mechanisms.

Natural soils and sediments are complex mixtures of organic and mineral constituents. In order to understand the influence of minerals on the organic compound reactivity in sediments, Faure *et al.* (Faure *et al.* 2000; Faure *et al.* 2006; Faure *et al.* 2006) studied the air oxidation of pure n-alkanes on Na-smectite and described the processes involved in the formation of oxygen-bearing compounds. It has also been demonstrated that air oxidation experiments conducted on sediments at low temperatures (60 to 130 °C) may reproduce geochemical features of organic matter transformations similar to those observed under natural conditions. Other works showed the potential of mineral matrixes such as silica (Dabestani *et al.* 1998; Granqvist *et al.* 2007) as well as binary mineral systems involving silica (such as SiO_2/Al_2O_3 and SiO_2/TiO_2) (Rooney *et al.* 1962) to create organic radicals (specially from PAHs) through Lewis acid-base reaction. Moreover, clays are also well-known for their Lewis acidity surface functions (Trombetta *et al.* 2000). The oxidative effects

of calcite have been investigated at various temperatures and indicate that calcium can act as a medium for molecular oxygen transfer to coal chars (Zhang *et al.* 1988; Zhang *et al.* 1989).Theoretical investigation of the molecular interactions between π-systems (as PAHs) and a Lewis acid-base considers electron transfer as the main mechanism of reaction (Kawahara *et al.* 2005).

Could low-temperature air oxidation catalyzed by minerals be a significant pathway for the transformation of PAHs in soils? If yes, would the reaction products lead to a higher molecular mass carbonaceous residue? In order to study the fate of PAHs in polluted soils during natural oxidation, air oxidation at 100 °C of fluoranthene was studied (a major pollutant found in polluted soils inherited from coal-using industries) in the presence of different mineral matrixes commonly found in soils and sediments (limestone, quartz sand, and clay). The objective was to establish the mass balance of reaction products and propose empirical formulas. To ensure a full characterization of high molecular mass compounds, GC-MS was complemented by high resolution quadrupole-time-of-flight mass spectrometry (Q-TOF) equipped with an APPI source, allowing the determination of the mass to charge ratio (m/z) up to 1500 Da.

2. Experimental Section

2.1. Samples and Chemicals

Pure fluoranthene 99.9% was purchased from Sigma-Aldrich Co. and was used with no further purification. *n*-Hexane, methanol, chloroform, and tetrahydrofuran (HPLC grade) were purchased from VWR and used as received.

The limestone ($CaCO_3$) was prepared from a mudstone of Triassic age (Muschelkalk formation of Heming, France). The Wyoming Clay sample was provided by the French Society of Bentonites (France) and consists of smectite with the formula $(Si_{3.92}Al_{0.08})(Al_{1.66}Fe_{0.17}Mg_{0.22})O_{10}(OH)_2Na_{0.17}Ca_{0.01}$. Quartz sand (Fontainebleau Sand, SiO_2) was provided by Prolabo. Mineral samples were powdered at 100 μm and Soxhlet-extracted two times with *n*-hexane and two times with methanol during 96 h.

Oxidation experiments were run with 200 mg of fluoranthene and 20 g of mineral matrix. Pure fluoranthene or mixtures with minerals were loaded into closed 150mL glass

bottles and placed into an oven at 100°C. Sampling was performed at 2, 4, and 6 months, and released CO_2 concentrations were measured at a rate of 5 days for the first month of experimentation and then every 15 days until the end of the oxidation time by infrared spectroscopy (λ=2325.6 cm^{-1}) using a Binos analyzer. After each measurement, the bottles were opened to renew the air and brought back to the oven at 100 °C.

2.2. Quantitative and qualitative analysis

C, H, O elemental analysis was performed on the organic extracts isolated from nonoxidized and oxidized samples using a Thermo Finnigan EA 1112 elementary analyzer. After experimentation, the samples were submitted to five cycles of $CHCl_3$ Soxhlet extractions for 24h each. The solvent volume was then reduced to 10 mL under a nitrogen flow, and then 1 mL of the solution was dried and weighed in order to determine the amount of organic matter.

GC-MS quantitation of reactant and products were performed by adding internal standards to the samples. An internal n-alkanes standard mix ($C_{16}D_{34}$, $C_{20}D_{42}$, $C_{24}D_{50}$, and $C_{30}D_{62}$) as well as an internal deuterated PAHs standard mix (naphthalene-*d*8, acenaphthene-*d*10, phenanthrene-*d*10, chrysene-*d*12, and perylene-*d*12, supplied by Cluzeau) were added. A 2 μL amount of solution was then injected into an Agilent 5973 gas chromatograph equipped with a DB 5-MS (length:60 m; diameter: 0.125 mm) capillary column coupled to an Agilent 5973 mass spectrometer operating in full scan mode. The temperature program was the following: 60 to 250 °C at 15 °C min-1, then 250 to 315 °C at 3 °C min-1, and 60 min hold at 315 °C. The carrier gas was helium at 1.5 mL min-1 constant flow.

Gel permeation chromatography was performed by injecting 50 μL of sample into an Agilent HPLC 1100 series chromatograph (Agilent, Waldbronn, Germany) equipped with a Varian PLgel Organic Mixed E column (300 × 7.5mm ID, 5 μmfor particle size) maintained at 25 °C. Detection was ensured by an Agilent diode array detector. Relative molecular mass distributions were calibrated by a polystyrene standard mix (Varian, Les Ulis, France). Tetrahydrofuran was used as mobile phase and maintained at 1 mL/min. Mass spectra of organic extracts were recorded on a hybrid quadrupole time-of-flight mass spectrometer (Bruker Daltonics, Bremen, Germany) equipped with an atmospheric pressure photoionization (APPI) manufactured by Syagen (Syagen Technology Inc., Tustin, CA),

containing a Krypton lamp which produces a 10.6 eV photon beam operating in positive mode. The sample was injected with a Hamilton syringe, and the flow rate was set at 100 μL/min with a syringe pump (Kd Scientific, Holliston, MA). The source parameters were optimized in order to obtain the best signal-to-noise ratio (i.e., capillary voltage -4500 V, end plate offset -500 V). Nitrogen gas was maintained at 5 bar for nebulisation and 9 L/min at 250 °C for desolvatation, and vaporizer temperature was set at 450 °C. An APPI source was chosen because it allows the detection of non polar or weakly polar organic compounds. The ionization energy was 10 eV. This energy is enough to ionize the organic compounds but too low to ionize the solvent ($CHCl_3$). The high resolution mass spectrometer allows a determination of the molecular formula with less than 5 ppm of error for values of *m*/*z* up to about 500 Da. In addition to better mass resolution and higher mass range capability, this technique also allows the injection of the solvent extract without any further sample treatment.

3. Results.

Mass balance calculations were based on CO_2 measurements in the gas phase and elemental analysis of the $CHCl_3$ organic soluble compounds. The initial reference amount of fluoranthene was thus converted into carbon quantity.

3.1. CO_2 Production.

After 6 months of air oxidation, CO_2 production was greater for clay and calcite than for pure fluoranthene and silica experiments (Figure 12).

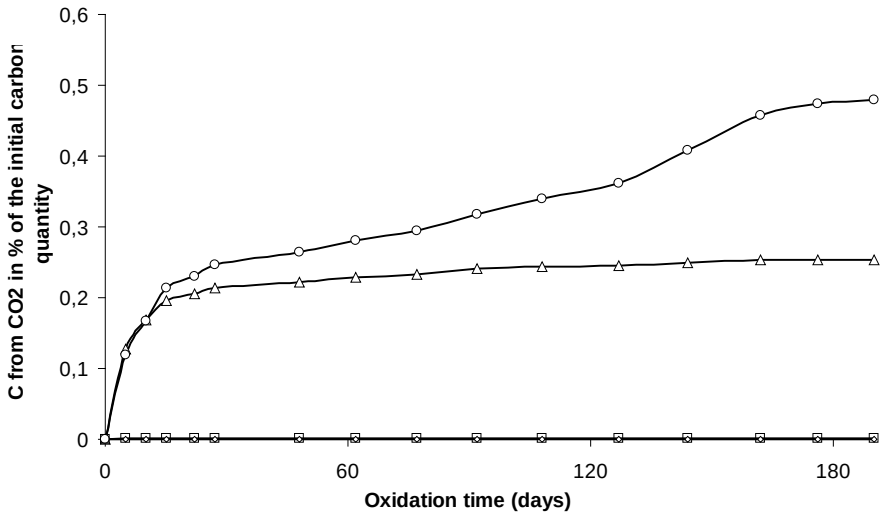

Figure 12: CO_2 production during oxidation experiments at 100°C for pure fluoranthene (◊), for the mixtures fluoranthene/silica (□), fluoranthene/clay (○) and fluoranthene/calcite (Δ).

The carbon quantity released as CO_2 ranges from 0 to 0.6% of the initial carbon introduced as fluoranthene. Limestone degradation was not considered as a source of CO_2 because of the low temperature of the experiments.

3.2. $CHCl_3$ Soluble Organic Matter.

The amount of solvent soluble organic matter (remaining fluoranthene plus reaction products) was compared to the initial fluoranthene quantity (converted in carbon quantity). For the experiments containing pure fluoranthene as well as for mixtures with limestone or quartz sand, more than 83% of the initial weight of organic matter is recovered (Figure 13) after 6 months of oxidation.

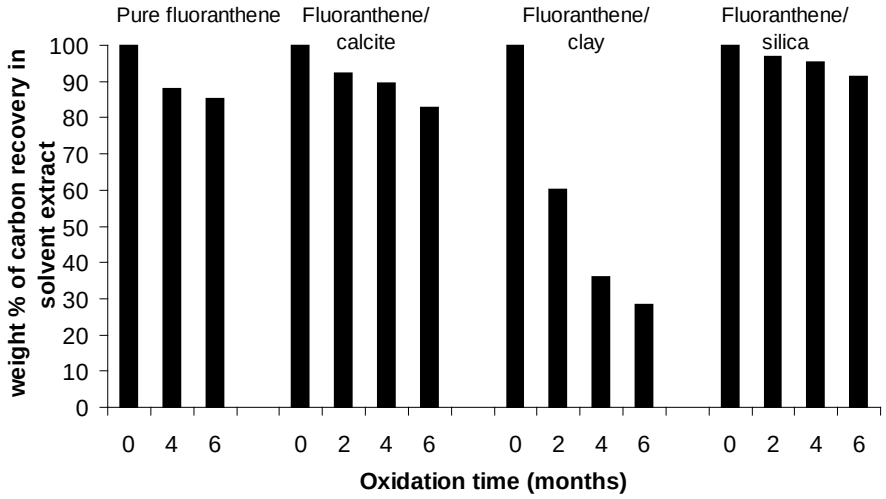

Figure 13: Extractable organic carbon recovery rate in weight % of carbon in initial fluoranthene after air oxidation at 100°C for pure fluoranthene and mixtures with limestone, clay or quartz.

However, for experiments conducted with clay, only 28% of the initial quantity is recovered. Regardless of the occurrence of mineral phases, the organic extract decrease cannot only be explained by the CO_2 production, which represents a very low proportion of the initial carbon form in fluoranthene.

3.3. Fluoranthene Quantification.

After air oxidation, the remaining fluoranthene recovered was quantified for each experiment using GC-MS (Figure 14).

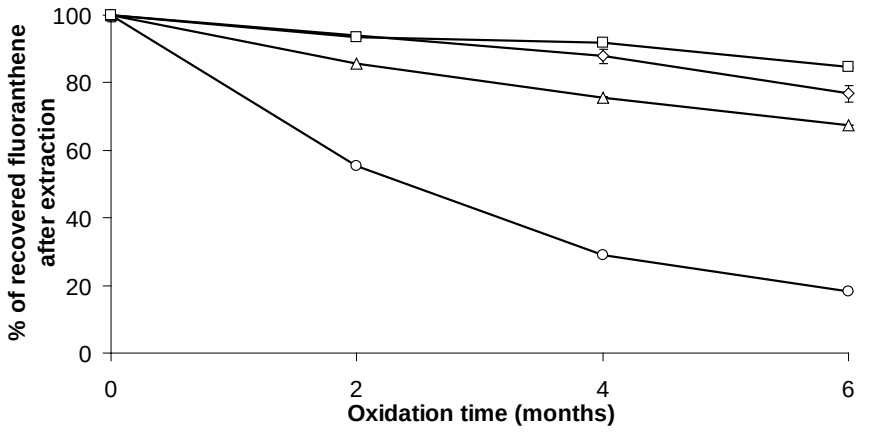

Figure 14: GC-MS quantitation of remaining fluoranthene recovered after $CHCl_3$ extraction as a function of time for pure fluoranthene (◊), for the mixtures fluoranthene/quartz (□), fluoranthene/clay (○) and fluoranthene/limestone (Δ) oxidized at 100°C.

After 6 months of oxidation, fluoranthene recoveries were the following: 76.8% for fluoranthene as sole reactant, 84.5% for the mixture with quartz, 64.7% for the mixture with limestone, and 18.3% for the experiment conducted on clay.

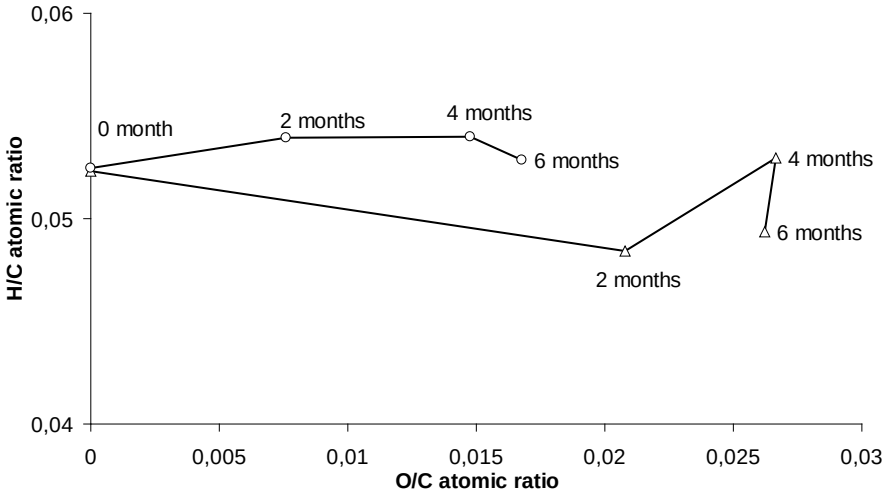

Figure 15: Van Krevelen diagram determined on $CHCL_3$ extracted organic matter for the mixtures fluoranthene/clay (○) and fluoranthene/limestone (Δ).

The evolution of the H/C atomic and O/C atomic ratios calculated after elemental analysis of the extracted compounds is shown in Figure 15. In the case of pure fluoranthene and fluoranthene mixed with quartz, no oxygen was detected while the H/C ratio was constant. In contrast, for clay and limestone, the O/C ratio increases with oxidation time, indicating the formation of oxygen-bearing reaction products. The H/C ratio does not change significantly, values ranging from 0.048 to 0.054.

3.4. Molecular Characterization of $CHCl_3$ Soluble Reaction Products.

No reaction products were detected by GC-MS analysis of the organic extracts obtained from fluoranthene as sole reactant. In contrast, new compounds appear in the organic extract from the oxidation experiments of fluoranthene/quartz, limestone/fluoranthene, and clay/fluoranthene mixtures (Figure 16).

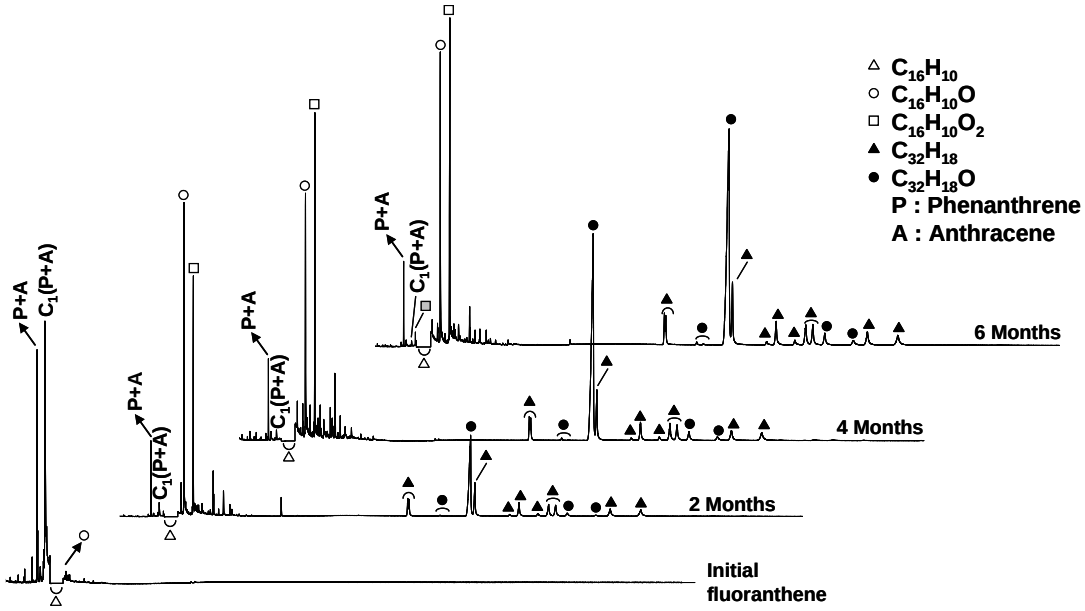

Figure 16: Molecular distribution obtained by GC-MS for the fluoranthene / limestone mixture at different oxidation times at 100 °C showing the increasing contribution of heavier molecular mass compounds from C_{32} series (▲ m/z 402; • m/z 418) .

After two months of oxidation, reaction products of molecular mass higher than that of fluoranthene appear as $C_{32}H_{18}$ (*m*/*z* 402) and $C_{32}H_{18}O$ (*m*/*z* 418). The fragmentation pattern of these reaction products present peaks typical of fluoranthene derivatives (*m*/*z* 200 and *m*/*z* 201). For instance, for every molecular formula, several isomers occur on the chromatograms which correspond to different possible fluoranthene self-addition products, with or without oxygen.

3.5. Gel Permeation Chromatography.

Whereas no significant changes are noticed for fluoranthene as sole reactant or as a mixture with quartz, GPC chromatograms of the fluoranthene/limestone (Figure 17) and fluoranthene/clay (Figure 18) mixtures show high molecular mass compounds.

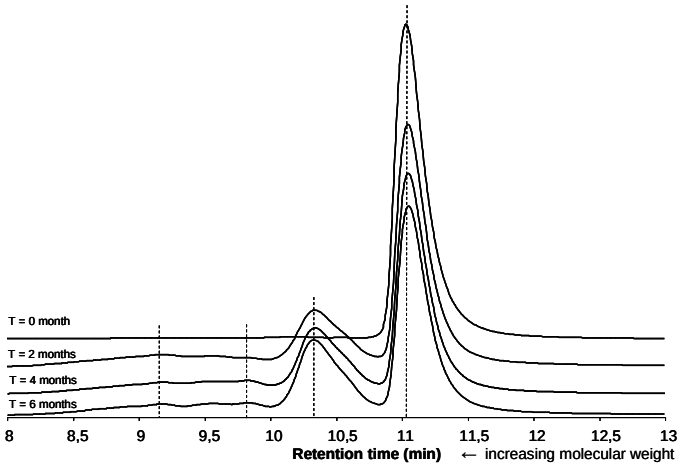

Figure 17: GPC chromatograms for the mixture fluoranthene/limestone for different oxidation times at 100°C (λ=300nm).

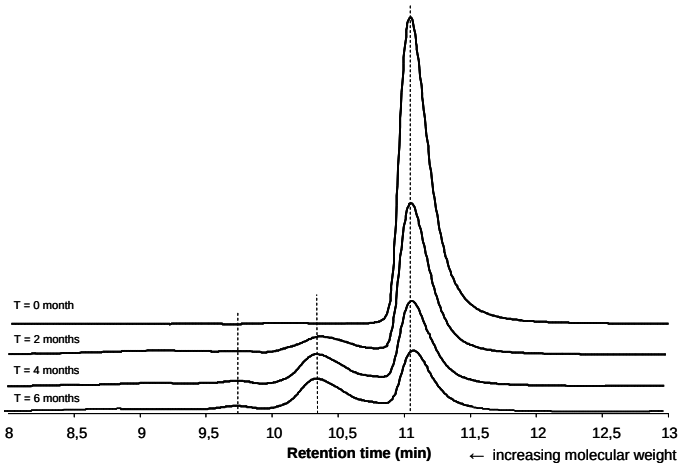

Figure 18: GPC chromatograms for the mixture fluoranthene/clay for different oxidation times at 100°C (λ=300nm).

After two months of oxidation, compounds with molecular masses ranging from 400 Da to more than 1500 Da (relative GPC calibration) are observed and their respective proportions increase with oxidation duration.

3.6. High Resolution Mass Spectrometry

APPI-QTOF analysis of the solvent-soluble reaction products obtained after 6 months of oxidation of fluoranthene mixed with limestone or clay detected several series. The first series (C_{16} series) is based on one fluoranthene unit: $C_{16}H_8$, $C_{16}H_8O$, $C_{16}H_8O_2$, $C_{16}H_8O_3$, $C_{16}H_{10}$, $C_{16}H_{10}O$, $C_{16}H_{10}O_2$, $C_{16}H_8O_3$ (*m/z* 200, 216, 232, 248, 202, 218, 234, 250). A second series (C_{32} series) is obtained by addition of these fluoranthene units on themselves (Table 3).

	$C_{16}H_8$	$C_{16}H_8O$	$C_{16}H_8O_2$	$C_{16}H_8O_3$	$C_{16}H_{10}$	$C_{16}H_{10}O$	$C_{16}H_{10}O_2$	$C_{16}H_{10}O_3$
$C_{16}H_8$	$C_{32}H_{16}$							
200	*400*							
$C_{16}H_8O$	$C_{32}H_{16}O$	$C_{32}H_{16}O_2$						
216	*416*	*432*						
$C_{16}H_8O_2$	$C_{32}H_{16}O_2$	$C_{32}H_{16}O_3$	$C_{32}H_{16}O_4$					
232	*432*	*448*	*464*					
$C_{16}H_8O_3$	$C_{32}H_{16}O_3$	$C_{32}H_{16}O_4$	$C_{32}H_{16}O_5$	$C_{32}H_{16}O_6$				
248	*448*	*464*	*480*	*496*				
$C_{16}H_{10}$	$C_{32}H_{18}$				$C_{32}H_{20}$			
202	*402*				*404*			
$C_{16}H_{10}O$	$C_{32}H_{18}O$	$C_{32}H_{18}O_2$			$C_{32}H_{20}O$	$C_{32}H_{20}O_2$		
218	*418*	*434*			*420*	*436*		
$C_{16}H_{10}O_2$	$C_{32}H_{18}O_2$	$C_{32}H_{18}O_3$	$C_{32}H_{18}O_4$		$C_{32}H_{20}O_2$	$C_{32}H_{20}O_3$	$C_{32}H_{20}O_4$	
234	*434*	*450*	*466*		*436*	*452*	*468*	
$C_{16}H_{10}O_3$	$C_{32}H_{18}O_3$	$C_{32}H_{18}O_4$	$C_{32}H_{18}O_5$	$C_{32}H_{18}O_6$	$C_{32}H_{20}O_3$	$C_{32}H_{20}O_4$	$C_{32}H_{20}O_5$	$C_{32}H_{20}O_6$
250	*450*	*466*	*482*	*498*	*452*	*468*	*484*	*500*

Table 3: Compounds detected by APPI-QTOF for the mixture fluoranthene/limestone oxidized during 6 months at 100°C. Each compound is a combination of the compound at the top and at the left side of the table to give the C32 series.

These fluoranthene-based units can be differently assembled to form new compounds. Compounds detected bear a maximum of four oxygen atoms. Third and fourth series (respectively, C_{48} series and C_{64} series) are based on self-addition of three fluoranthene derivatives within a mass range of 600 to 700 Da, and four fluoranthene derivatives within a mass range of 800 to 900 Da. A fifth series is detected in the range of 1000 to 1100 Da (C_{80} series). In order to follow the evolution of these series with increasing oxidation time, ratios between the most ionisable oxygenated compound in each series and fluoranthene were calculated:

- $C_{32}H_{18}O/C_{16}H_{10}$ ($I_{m/z\ 418}/I_{m/z\ 202}$)
- $C_{48}H_{24}O_2/C_{16}H_{10}$ ($I_{m/z\ 632}/I_{m/z\ 202}$)
- $C_{64}H_{32}O_3/C_{16}H_{10}$ ($I_{m/z\ 848}/I_{m/z\ 202}$)

For the fluoranthene/limestone mixture, an increase in the ratios for C_{32}, C_{48}, and C_{80} series is observed (Figure 19 and Figure 20) with time.

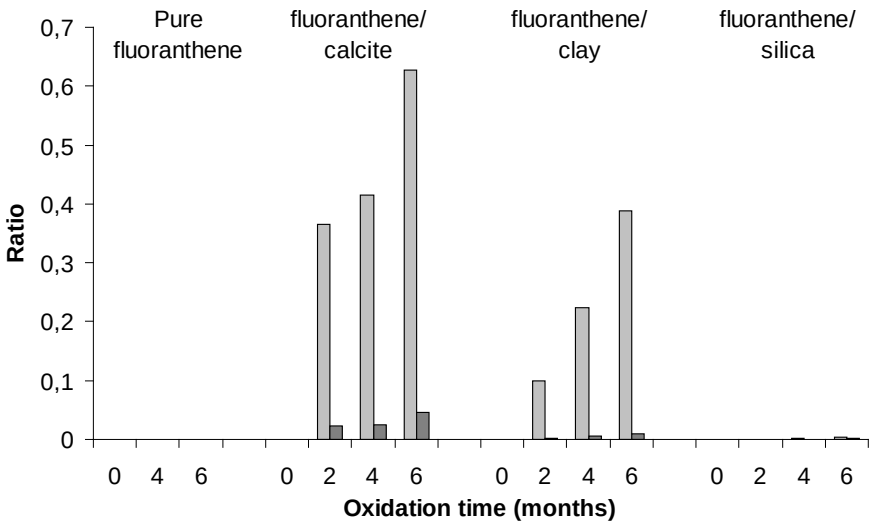

Figure 19: Relative contribution of oxygenated high molecular mass reaction products normalized to unreacted fluoranthene ($I_{m/z\ 416}/I_{m/z\ 202;}$ $I_{m/z\ 632}/I_{m/z\ 202;}$) as determined by APPI-QTOF. The measurements were performed on $CHCl_3$ extracts obtained after oxidation at 100°C of the fluoranthene/limestone and fluoranthene/clay mixtures. Ratios were calculated for the three major series of reaction products identified. No high molecular oxygenated compounds are formed for pure fluoranthene oxidation, while only minor compounds are detected for quartz. For limestone and clay, oxidation leads to the formation of oxygenated products of molecular masses higher than the initial fluoranthene. Ratios are lower for clay than limestone, because polymerization/condensation reactions lead to the increased formation of an insoluble, carbonaceous residue.

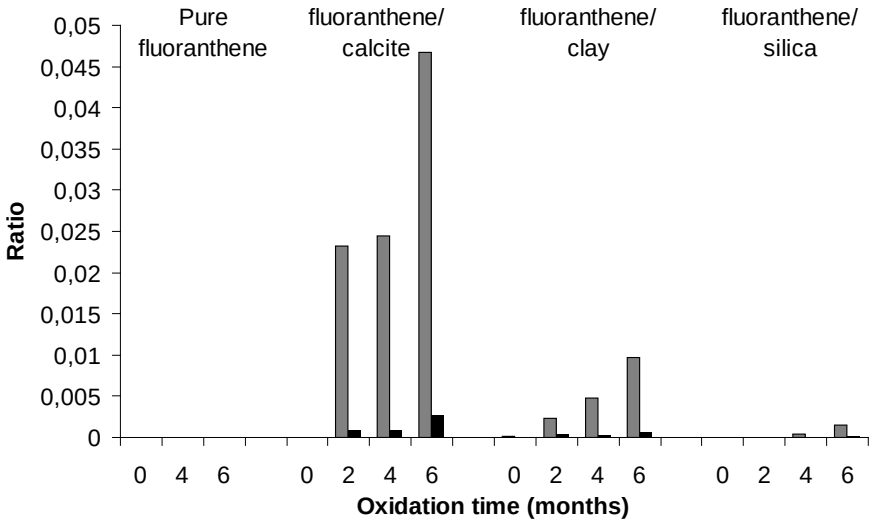

Figure 20: Relative contribution of oxygenated high molecular mass reaction products normalized to unreacted fluoranthene ($I_{m/z\ 632}/I_{m/z\ 202;}$ $I_{m/z\ 848}/I_{m/z\ 202}$) as determined by APPI-QTOF. The measurements were performed on $CHCl_3$ extracts obtained after oxidation at 100°C of the fluoranthene/limestone and fluoranthene/clay mixtures. Ratios were calculated for the three major series of reaction products identified. No high molecular oxygenated compounds are formed for pure fluoranthene oxidation, while only minor compounds are detected for quartz. For limestone and clay, oxidation leads to the formation of oxygenated products of molecular masses higher than the initial fluoranthene. Ratios are lower for clay than limestone, because polymerization/condensation reactions lead to the increased formation of an insoluble, carbonaceous residue.

The same evolution is observed for the fluoranthene/clay mixture. For these two matrixes, the proportion of higher molecular masses increases with oxidation temperature according to GPC analysis. On the contrary, for pure fluoranthene this trend is not observed and is very limited for the fluoranthene/quartz mixture. Other series of high molecular reaction products might exist, but the ionization energy of compounds may increase with the molecular mass and reach values higher than the 10.6 eV energy supplied by the Krypton lamp in the APPI source. However, compounds of higher molecular mass might also not be soluble in $CHCl_3$ and would instead form part of the insoluble carbonaceous residue.

3.7. Scanning Electron Microscopy (SEM)

SEM experiments were performed on the solid residue of the fluoranthene/calcite mixture oxidized for 6 months and then treated with 8.8 M HCl in order to remove carbonates. Observation by SEM allowed the identification of carbonaceous particles of lamellar structure (Figure 21) not detected in the initial carbonate sample.

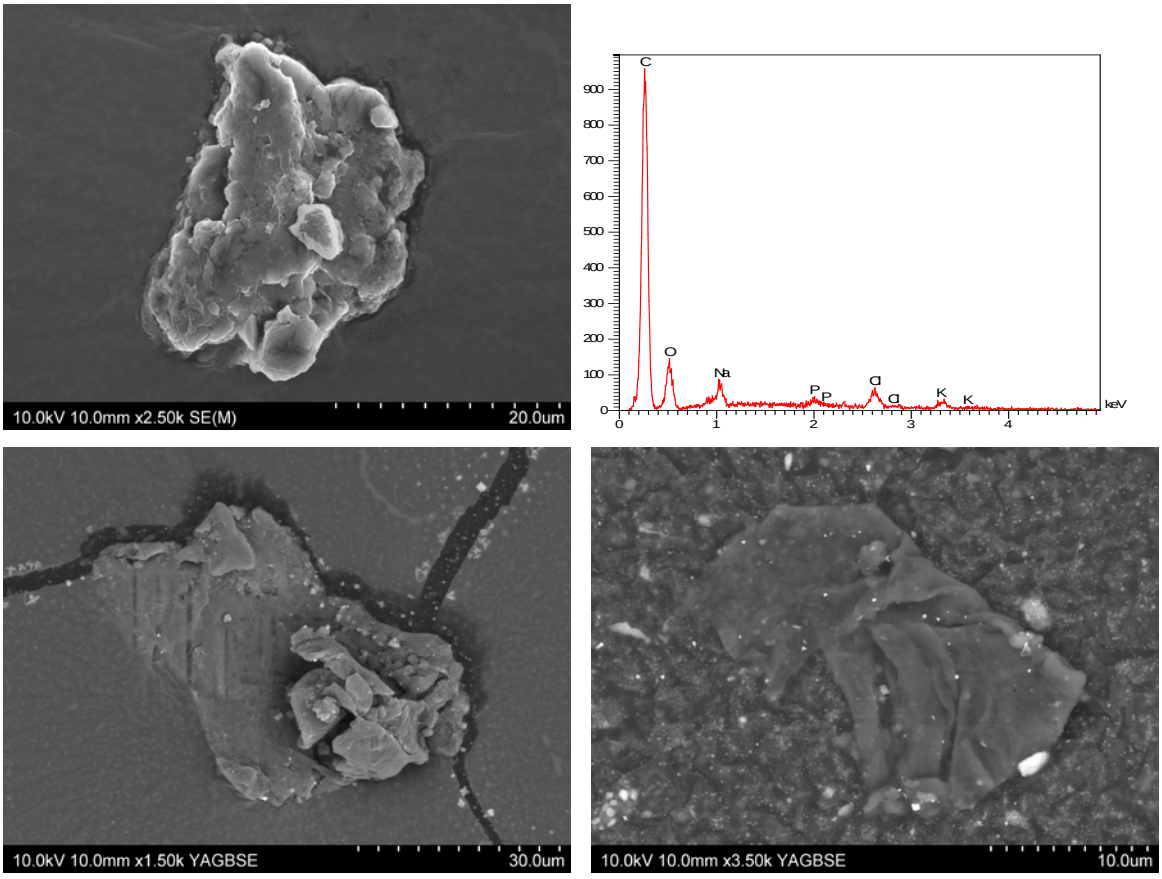

Figure 21: SEM picture and spectrum (Au-Pd metallation) of carbonaceous residue obtained after HCl demineralization of the mixture fluoranthene/limestone oxidized 6 months.

4. Discussion

4.1. Oxidation of Pure Fluoranthene

In the experiments with pure fluoranthene no significant reactivity is detected and the remaining fluoranthene is close to the initial quantity. GC-MS and GPC chromatograms do not show significant modifications; in particular, no compounds heavier than fluoranthene are detected. However, because of the high sensitivity of the technique, APPI-QTOF revealed the presence of reaction products of the C_{32} series after 6 months of oxidation. Because of the experimental temperature (100 °C), O_2 in the singlet state may be a very reactive species to be considered. It may favor the formation of oxygenated compounds (Foote *et al.* 1995) in absence of minerals (although possible influence of the glass bottle walls should not be excluded), leading to the formation of high molecular mass compounds.

4.2. Oxidation of Fluoranthene on Quartz

In the case of the fluoranthene/quartz mixture, GC-MS detected $C_{32}H_{18}$, a product heavier than fluoranthene. APPI-QTOF detected compounds from C_{32} and C_{48} series but at very low intensities. Thus, the oxidation of fluoranthene on quartz is slightly more efficient in the formation of reaction products than for pure fluoranthene.

4.3. Oxidation of Fluoranthene on Limestone

A higher reactivity is observed during the oxidation of the fluoranthene/limestone mixture. GC-MS and GPC chromatograms show the formation of compounds heavier than fluoranthene after 2 months of oxidation. APPI-QTOF allowed detection of compounds up to the C80 series. The mass balance indicates that 17.1% of the initial carbon is not recovered and may participate in the formation of a carbonaceous residue. To explain the origin of these reaction products, O_2 in the singlet state may be involved, as for the case of pure fluoranthene oxidation. A Lewis acid-base reaction between calcium from calcite and fluoranthene was also considered yet rejected because this reaction is only possible in the liquid phase (Jensen 1980; Leach 1999). O_2 can easily chemisorb on carbon even at room temperature, and atomic calcium has been suggested to act as a catalyst for oxygen transfer on coal char (Zhang *et al.*

1988; Zhang *et al.* 1989). While the oxidation of coal char is catalyzed by calcium and $CaCO_3$ (Gopalakrishnan *et al.* 1994), $CaCO_3$ surfaces can also present calcium atoms in ionic form (Ca^{2+}) (Gutmann 1978). In regards to the π-HOMO orbital of fluoranthene, a Lewis acid-base reaction might be possible with the s-LUMO of the Ca^{2+} (Leach 1999). These different hypotheses may explain the catalysis of fluoranthene oxidation by limestone, leading to the formation of higher molecular mass compounds as well as of a carbonaceous residue.

4.4. Oxidation of Fluoranthene on Clay

The oxidation of fluoranthene on clay leads to results similar to those obtained for the oxidation of fluoranthene on limestone. GC-MS and GPC chromatograms are similar for both clay and limestone. In contrast to limestone, 71.4% of the initial carbon was not recovered and may thus contribute to the formation of a carbonaceous residue. From these results we can infer that oxidation of fluoranthene is most efficient in the presence of clay.

As reported in the literature, clays may act as Lewis acid-bases (Bouxin *et al.* ; Trombetta *et al.* 2000). The Brønsted acid-base reaction, also possible for clay, may be ruled out. Indeed, the reaction products for the oxidation of fluoranthene on limestone are similar to those obtained with clay, yet no protons may be provided by limestone ($CaCO_3$). Clays are well-known for their adsorption capabilities of PAHs on account of their Lewis acid properties. This implies a π-HOMO interaction mechanism induced by a radical reaction. Thus, the reaction pathway for fluoranthene oxidation on clay and limestone may be a radical reaction, implying an electron transfer from the mineral matrix to the PAH. For instance, in the case of the insertion of aromatics compounds in clay (Dines 1974), electron transfer may be possible through the different Lewis acid-base functions of both constituents. The present experimental study of fluoranthene oxidation on mineral surfaces demonstrates that the major reaction product is not CO_2 but are high molecular mass compounds, including the formation of a carbonaceous residue insoluble in common organic solvents (e.g., kerogen (Durand 1980; Durand *et al.* 1980)). It was demonstrated elsewhere (Faure and Landais 2000; Faure *et al.* 2006; Faure *et al.* 2006) that the oxidation of organic matter under the conditions described (100 °C) resulted in geochemical results similar to those observed during the oxidation under natural conditions. It is therefore reasonable to believe that these results are relevant to natural conditions existing in soils and sediments in contact with air. Thus, they suggest that low-temperature, mineral-catalyzed air oxidation may be a new pathway to consider for PAHs stabilization is soils and sediments. This mechanism may be relevant for polluted soils during

natural recovery but may also be a more general mechanism for aromatic carbon sequestration in natural soils (e.g., black carbon formation).

Acknowledgments

This research was supported by The Lorraine Region as well as CREGU. The authors thank Regine Mosser Ruck for mineral analysis and the molecular formula of clay.

5. References

Biache, C., Mansuy-Huault, L., Faure, P., Munier-Lamy, C., and Leyval, C., Effects of thermal desorption on the composition of two coking plant soils: Impact on solvent extractable organic compounds and metal bioavailability. *Environ. Pollut.*, **2008**. *156*(3): p. 671-677.

Bouxin, F., Baumberger, S., Pollet, B., Haudrechy, A., Renault, J.H., and Dole, P., Acidolysis of a lignin model: Investigation of heterogeneous catalysis using Montmorillonite clay. *Bioresour. Technol. 101*(2): p. 736-744.

Dabestani, R., Reszka, K.J., and Sigman, M.E., Surface catalyzed electron transfer from polycyclic aromatic hydrocarbons (PAH) to methyl viologen dication: Evidence for ground-state charge transfer complex formation on silica gel. *J. Photochem. Photobiol. A: Chem.*, **1998**. *117*(3): p. 223-233.

Dines, M.B., Intercalation in layered compounds. *J. Chem. Educ.*, **1974**. *51*(4): p. 221-223.

Durand, B., Sedimentary organic matter and kerogen. Definition and quantitative importance of kerogen. *Kerogen: insoluble organic matter from sedimentary rocks*, **1980**: p. 13-34.

Durand, B. and Nicaise, G., Procedures for kerogen isolation. *Kerogen: insoluble organic matter from sedimentary rocks*, **1980**: p. 35-53.

Faure, P., Jeanneau, L., and Lannuzel, F., Analysis of organic matter by flash pyrolysis-gas chromatography-mass spectrometry in the presence of Na-smectite: When clay minerals lead to identical molecular signature. *Org. Geochem.*, **2006**. *37*(12): p. 1900-1912.

Faure, P. and Landais, P., Evidence for clay minerals catalytic effects during low-temperature air oxidation of n-alkanes. *Fuel*, **2000**. *79*(14): p. 1751-1756.

Faure, P., Schlepp, L., Mansuy-Huault, L., Elie, M., Jardé, E., and Pelletier, M., Aromatization of organic matter induced by the presence of clays during flash pyrolysis-gas chromatography-mass spectrometry (PyGC-MS): A major analytical artifact. *J. Anal. Appl. Pyrolysis*, **2006**. *75*(1): p. 1-10.

Foote, C.S., Valentine, J.S., Greenberg, A., Liebman, J.F., and Editors, Active Oxygen in Chemistry. [In: Struct. Energ. React. Chem. Ser., 1995; 2] 1995: Chapman & Hall. 342 pp.

Gopalakrishnan, R., Fullwood, M.J., and Bartholomew, C.H., Catalysis of char oxidation by calcium minerals: Effects of calcium compound chemistry on intrinsic reactivity of doped Spherocarb and Zap chars. *Energy Fuels*, **1994**. *8*(4): p. 984-989.

Granqvist, B., Sandberg, T., and Hotokka, M., Adsorption of organic probes on silica through Lewis interactions: A comparison of experimental results and quantum chemical calculations. *J. Colloid Interface Sci.*, **2007**. *310*(2): p. 369-376.

Gutmann, V., The Donor-Acceptor Approach to Molecular Interactions 1978: Plenum. 279 pp.

Jensen, W.B., The Lewis Acid-Base Concepts: an Overview 1980: Wiley. 364 pp.

Kawahara, S.I., Tsuzuki, S., and Uchimaru, T., Lewis acidity/basicity of π-electron systems: Theoretical study of a molecular interaction between a π system and a Lewis acid/base. *CEJ*, **2005**. *11*(15): p. 4458-4464.

Leach, M.R., Lewis Acid/Base Reaction Chemistry 1999: Meta-Synthesis.Com. 95 pp.

Merino, J., Piña, J., Errazu, A.F., and Bucalá, V., Fundamental study of thermal treatment of soil. *Soil and Sediment Contamination*, **2003**. *12*(3): p. 417-441.

Rivas, F.J., Polycyclic aromatic hydrocarbons sorbed on soils: A short review of chemical oxidation based treatments. *J. Hazard. Mater.*, **2006**. *138*(2): p. 234-251.

Rooney, J.J. and Pink, R.C., Formation and stability of hydrocarbon radical-ions on a silica-alumina surface. *Transactions of the Faraday Society*, **1962**. *58*: p. 1632-1641.

Trombetta, M., Busca, G., Lenarda, M., Storaro, L., Ganzerla, R., Piovesan, L., Lopez, A.J., Alcantara-Rodrìguez, M., and Rodríguez-Castellón, E., Solid acid catalysts from clays Evaluation of surface acidity of mono- and bi-pillared smectites by FT-IR spectroscopy measurements, NH_3-TPD and catalytic tests. *Applied Catalysis A: General*, **2000**. *193*(1-2): p. 55-69.

Zhang, Z.G., Kyotani, T., and Tomita, A., TPD study on coal chars chemisorbed with oxygen-containing gases. *Energy Fuels*, **1988**. *2*(5): p. 679-684.

Zhang, Z.G., Kyotani, T., and Tomita, A., Dynamic behavior of surface oxygen complexes during O_2 chemisorption and subsequent temperature-programmed desorption of calcium-loaded coal chars. *Energy Fuels*, **1989**. *3*(5): p. 566-571.

PART III: SEC-APPI-QTOF and its application to supramolecular systems

Le chapitre précédent a établi les conditions opératoires de la spectrométrie de masse en contexte relativement simple. Cependant les systèmes naturels, comme la matière organique, représentent des systèmes bien plus complexes composés d'un grand nombre de molécules différentes ainsi que de fractions de hautes masses moléculaires qui restent toujours difficile à caractériser.

Lorsque ces systèmes complexes sont analysés par spectrométrie de masse, la très grande quantité d'informations est difficile à interpréter. Dans ce travail de thèse, deux voies différentes ont été étudiées : la simplification pré-analytique et le traitement post-processing. Dans ce chapitre, la simplification pré-analytique a consisté à coupler, pour la première fois, la SEC et la spectrométrie de masse APPI-QTOF rendant possible la caractérisation des composés apolaires des systèmes complexes. Ce couplage a notamment permis de réduire la compétition à l'ionisation rendant possible la caractérisation des composés de hautes masses moléculaires ou ceux faiblement concentrés et ce en s'affranchissant de toute calibration, source de nombreuses erreurs d'interprétation.

Le couplage SEC-APPI-QTOF a été validé par une solution de standards et a ensuite été appliqué avec succès à des systèmes complexes de type asphaltènes.

On-line SEC-APPI-QTOF: a new analytical tool for Complex hydrocarbon mixtures. Application to complex aromatic compounds mixture

Thierry Ghislain, Pierre Faure, Raymond Michels

Submitted to Journal of Chromatography A,

G2R, Nancy-Université, CNRS, B.P. 239, 54506 Vandœuvre-lès-Nancy, France

* Corresponding author. Tel.: +33 3 83 68 47 41; fax: +33 3 83 68 47 01.

E-mail address: Thierry.Ghislain@g2r.uhp-nancy.fr

Abstract

PAHs and oxy-PAHs were analyzed by a new analytical system: SEC-APPI-QTOF. This technique allows to detect hydrocarbons in organic solvents (i.e. chloroform) using an online combination of Size Exclusion Chromatography (SEC), Atmospheric Pressure Photoionization (APPI) and high resolution mass spectrometry (QTOF). A mixture of Polycyclic and Oxy-Polycyclic Aromatic Compound was successfully analyzed to validate the development of this new analytical tool. The choices of analytical parameters as well as necessary compromises are presented. The technique allows the characterization of a large range of polar and non polar molecules. Moreover, this analytical system based on high resolution mass spectrometry, avoids classical problems of SEC calibration (lack of adapted standards) for the determination of the molecular mass distribution of complex organic mixtures.

1. Introduction

LC-MS has become an inevitable technique in analytical chemistry for the characterisation of complex organic mixtures. It has proven its efficiency using electrospray ionization (ESI) and atmospheric pressure chemical ionization (APCI) interfaces. A recent review summarized the extensive abilities of this technique especially for organic compounds analysis in water samples (aquatic environment and water treatment) (Zwiener *et al.* 2004). Among the LC techniques, Size Exclusion Chromatography (SEC) is a widespread method to study complex organic mixtures. Its theoretical principle is to separate the organic constituents of a mixture by molecular size, splitting the initial complex mixture into size classes. The combination of this separation technique with mass spectrometry can be a very interesting solution to gain information on the composition of these different size classes. Indeed, successful SEC-ESI/APCI-MS on-line combination was applied to polymers (Nielen 1996; Prokai *et al.* 2000; Liu *et al.* 2004; Toy *et al.* 2004; Feldermann *et al.* 2005; Desmazières *et al.* 2008; Gruendling *et al.* 2009; Gruendling *et al.* 2010) , to organometallics (Benson *et al.* 2003; Połeć-Pawlak *et al.* 2007; Tastet *et al.* 2008; Schmidt *et al.* 2009), dissolved organic matter (DOM) and humic substances (Klaus *et al.* 2000; Persson *et al.* 2000; Reemtsma *et al.* 2005) in aqueous solution in order to improve interpretation of mass spectra or to determine end-groups for polymers.

A recent review (Herod 2010) points out the need of this type of systems as the analytical conditions described in literature are not adapted to the characterization of non polar complex mixtures such as crude oils, their constituents (i.e. asphaltenes, resins) or those found in polluted soils and sediments. Limitations concern (i) the nature of the mobile phase in the LC application, which must be an organic solvent and (ii) the choice and adaptation of the ionisation source (APPI and APCI) to non polar solutes. In literature, these organic complex mixtures are usually analyzed by ESI or atmospheric pressure photoionization (APPI) without any molecular separation (direct infusion). In the case of organic extracts isolated from soils polluted by PAHs, APPI seems to be the most sensitive ionization source (Moriwaki *et al.* 2004). Thus, analytical requirements adapted to non polar organic complex mixtures imply to develop a new on-line combination of SEC (Size Exclusion Chromatography) and APPI-QTOF. Also, molecular size distributions must be calibrated against standards (usually synthetic polymers like polystyrene). Yet, these standards are often non-adapted to complex organic mixtures contained in natural samples (petroleum, soils and

sediments). The SEC-APPI-QTOF online combination presents interesting potential in the direct determination of mass ranges for complex organic mixtures.

This paper presents development efforts of such SEC-APPI-QTOF combination (Figure 1).

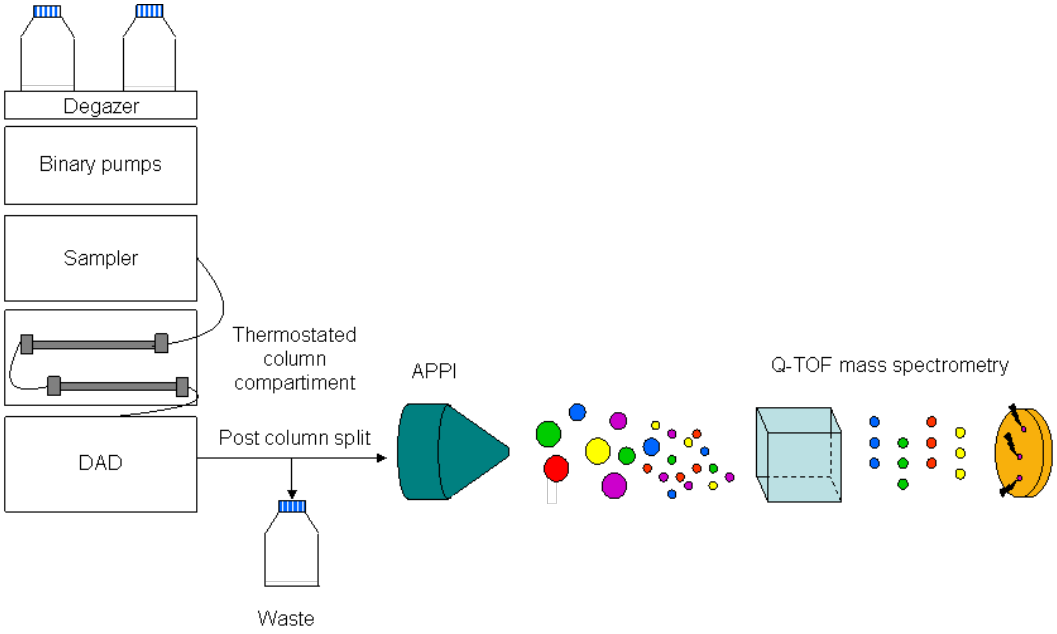

igure 1: Composition of the analytical system involving the SEC and the APPI-Q-TOF mass spectrometry

The major challenge is to be able to find compromises between the contrasted operating conditions of the different analytical tools combined online. Indeed, (i) HPLC-SEC needs high flow rate to be efficient (usually 1 $mL.min^{-1}$) whereas APPI-QTOF hardly works with a flow rate higher than 100 $\mu L.min^{-1}$, (ii) organic solvents adapted to SEC chromatography of non polar compounds are not easily compatible with APPI. This will be illustrated by the analysis of a complex mixture of high molecular mass oxy-PAHs, for which background information is already available (Ghislain *et al.* 2010).

2. Materials and methods

2.1. Sample

The organic complex mixture (named PAH mixture) used in this work, are the reaction products of the air oxidation of fluoranthene in the presence of limestone. These compounds

belong to a mineral catalyzed oxidation pathway leading from fluoranthene to a carbonaceous residue. It was extensively characterized by Ghislain *et al.* (2010) (Ghislain *et al.* 2010) and represents background work to the understanding of the fate of PAHs in polluted soils and sediments (Biache *et al.* 2008; Biache *et al.* 2011). This mixture previously analysed by direct infusion in APPI-QTOF is composed of a PAH and oxy-PAHs (given in Table 1) ranging from fluoranthene ($C_{16}H_{10}$, 202 g.mol^{-1}) to very high molecular mass oxy-PAHs (such as $C_{112}H_{56}O_7$, 1510 g.mol^{-1}).

2.2. Solvents

Tetrahydrofuran, chloroform, *n*-hexane (H.P.L.C. grade) were purchased from V.W.R. and used as received. Benzene and toluene (H.P.L.C. grade) were purchased from Sigma Aldrich. All solvents were used as received.

2.3. SEC

Size Exclusion Chromatography was performed by injecting 50µL of sample into an Agilent HPLC 1100 series chromatograph (Agilent, Waldbronn, Germany) equipped with a Varian PLgel Organic Mixed E column (300 x 7.5mm ID, 5µm for particle size) maintained at 30°C. Detection was ensured by an Agilent Diode Array Detector. Relative molecular mass distributions were calibrated by a polystyrene standard mix (Varian, Les Ulis, France). Tetrahydrofuran was used as mobile phase and maintained at 1 mL.min^{-1}

2.4. SEC-APPI-Mass Spectrometry

Size Exclusion chromatography was performed by injecting 20µL of sample into a Dionex Ulimate 3000 series chromatograph (Dionex, Sunnyvale, CA, USA). Two different GPC columns were tested: a Varian PLgel Organic Mixed E column (300 x 7.5mm ID, 5µm for particle size) called: “Mixed E” for which compounds can be distinguished up to 30 000 g.mol^{-1} and a high resolution GPC column, a Varian PLgel Organic column (250 x 4.6 mm ID, 5µm for particle size and 100Å for pore size) with a mass range until up to 4000 g.mol^{-1} maintained at 30°C called “HR column”. Detection was ensured by a Dionex Diode Array Detector (DAD3000, Dionex, Sunnyvale, CA, USA)

Molecular mass distributions were recorded on a hybrid Quadrupole – Time-Of-Flight mass spectrometer (Bruker Daltonics, Bremen , Germany) equipped with an Atmospheric Pressure Photoionisation (APPI) manufactured by Syagen (Syagen Technology Inc., Tustin, CA, USA), containing a Krypton lamp which produces a 10eV photon beam operating in positive mode. The source parameters were optimized in order to obtain the best signal to noise ratio on m/z 848 (i.e. capillary voltage -4500V, end plate offset -500V). Nitrogen gas was maintained at 5bar for nebulisation and 3 $L.min^{-1}$ at 250°C for desolvatation, vaporizer temperature was set at 450°C.

2.5. Coupling

Solvents, dopants, flow rate, columns, post column division were tested in order to characterize the high molecular mass compounds.

3. Results

Three different analytical tool combinations were tested in order to analyze the oxy-PAHs mixture which composed the initial solution: (i) tuning of the GPC conditions (ii) tuning of the SEC-APPI-QTOF with SEC equipped with the Mixed E column (iii) SEC equipped with a Mixed E column coupled to the HR column.

3.1. Tuning of the SEC only conditions

Chloroform, tetrahydrofuran (THF), *n*-hexane were tested as mobile phases to determine their separation power of the PAH mixture using the Mixed E column. No separation was observed when pure *n*-hexane or mixture of *n*-hexane with THF (50/50 v/v) when used. Only pure chloroform or pure THF lead to obtain resolved chromatograms (Figure 2). Molecular size distribution was determined by using a polystyrene standard mix calibration.

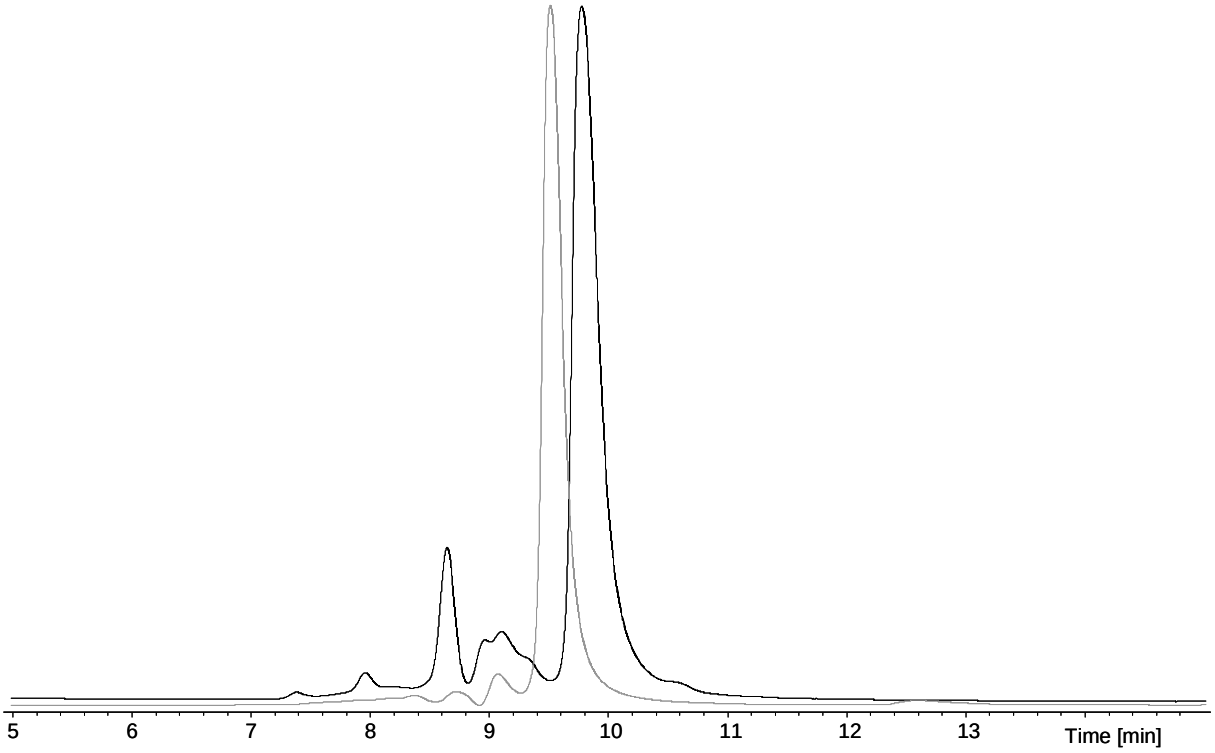

Figure 2: Size Exclusion Chromatograms obtained on Mixed-E column for the oxy-PAH sample using respectively tetrahydrofuran (-) and chloroform (-) as mobile phases. Agilent HPLC 1100 series chromatograph with UV detection (300nm).

Yet, comparison with direct infusion APPI-QTOF mass measurements (Ghislain *et al.* 2010) reveals inaccurate values for our samples; especially for lower molecular mass compounds (Figure 3). Indeed, the main peak should correspond to fluoranthene at m/z 202 however, according to the relative calibration, this peak corresponds to compounds within the mass range 9 to 38 Da. Similar discrepancy is obtained for the second peak, for which polystyrene standards give a mass range within 38-240 while direct infusion APPI-QTOF yields values within mass range 400 to 500 Da (association of two fluoranthene units and/or oxygenated fluoranthene).

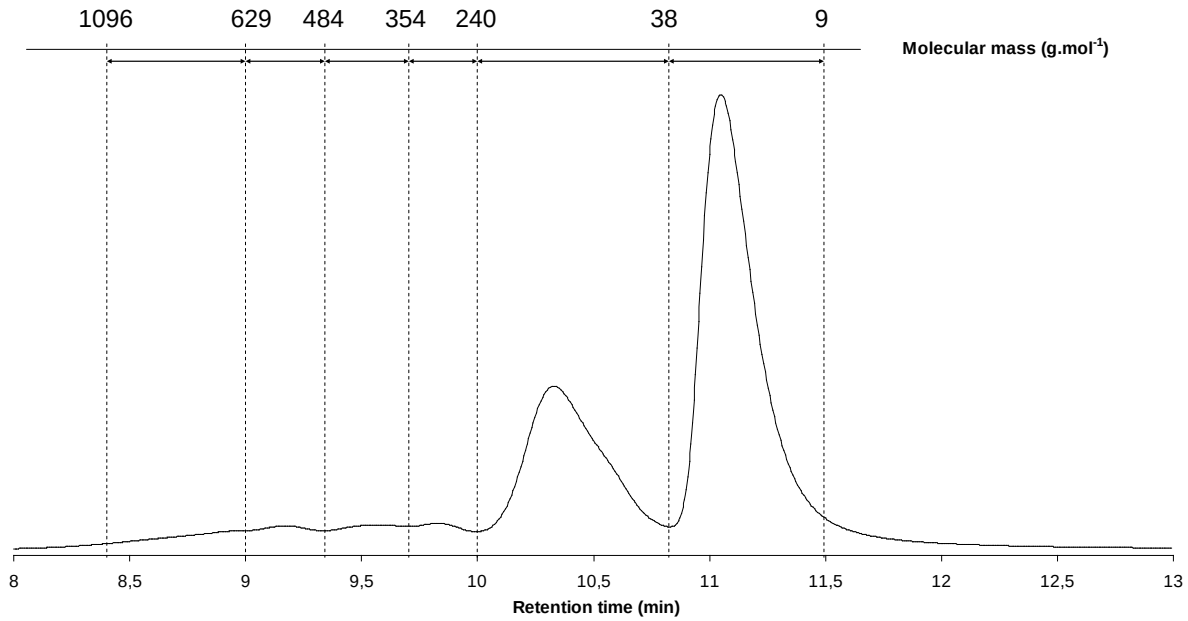

Figure 3: SEC molecular mass distribution of the oxy-PAH mixture (Mixed-E column, THF mobile phase at 1mL.min^{-1}, UV detection at 300nm) according to polystyrene standards calibration. The highest peak corresponds to fluoranthene (m/z 202) and the second highest to PAHs and Oxy-PAHs of m/z ranging from 400 to 500 as determined by direct infusion APPI-QTOF

3.2. APPI-QTOF

Different parameters (nature of the solvent, dopant and flow rate) needed to be adjusted in order to associate SEC and the APPI-QTOF (Figure 1).

Solvent: Chloroform and THF were tested because they were the only solvents to perform satisfactory SEC separation (Figure 2). Because no ionization in the APPI source was observed with THF as mobile phase, with or without dopant, THF was abandoned. On the contrary, chloroform allows to obtain good ionization and a stable spay (i.e. a stable Total Ion Current). This solvent was thus selected for the SEC-APPI-QTOF combination.

Dopant: As efficient dopants (Marchi *et al.* 2009) are generally selected for their low ionization energy or proton affinity (PA) to allow the two main pathways in APPI ionization i.e. charge transfer or proton transfer, benzene (IE=9.24eV; PA=750.4 kJ.mol^{-1}) and toluene (IE=8.83eV; PA=784.0 kJ.mol^{-1}) (NIST) were tested. Thus the mobile phase was composed of a mixture of chloroform and 10% in volume of dopant. Whereas weak ionization was observed for the oxy-PAH mixture (and especially no fluoranthene was detected) when only

chloroform or chloroform with 10% toluene were used, the chloroform with 10% benzene as dopant successfully ionized all compounds. Chloroform with 10% benzene as dopant was then selected for the further experiments.

Flow rate: Flow rate used was 0.5 mL/min. A post-column split needed to be added as to reduce the flow rate in the APPI source. Optimized post-column split was set at 1.8%, i.e. 9µL/min directed to the source and 491µL/min to waste.

3.3. SEC-APPI-QTOF using Mixed E column

Application of the previously described parameters on the SEC-APPI-QTOF online combination using Mixed E column leads to a complete separation of the constituents of the oxy-PAH mixture (Figure 4). C_{16} to C_{80} compounds, were indeed detected with high sensitivity (Figure 5). The heaviest compounds characterized were C_{96} compounds (in the m/z 1200 range) at very low intensity including $C_{96}H_{48}O_5$ and $C_{96}H_{48}O_6$ respectively detected at 47 cps and 78 cps. Yet, no heavier constituent was detected (Table 2) such as C_{112} compounds.

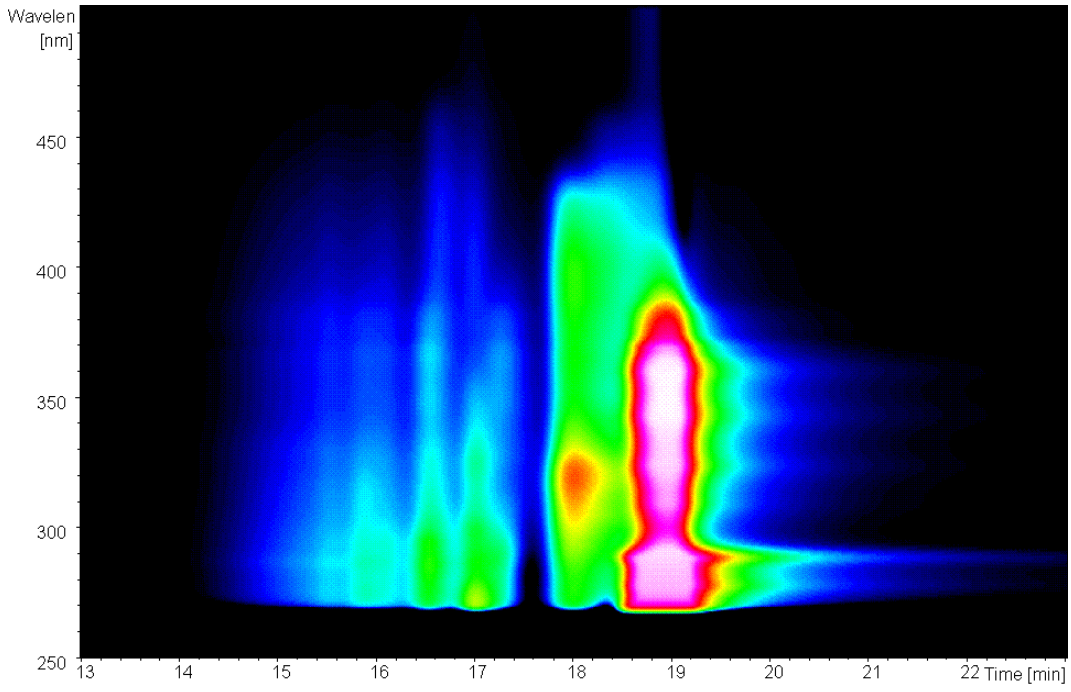

Figure 4: UV chromatogram (250-500 nm) for the oxy-PAH mixture analyzed using GPC Mixed E column. Flow rate at 0.5 mL/min with $CHCl_3/C_6H_6$ 90/10 v/v as mobile phase.

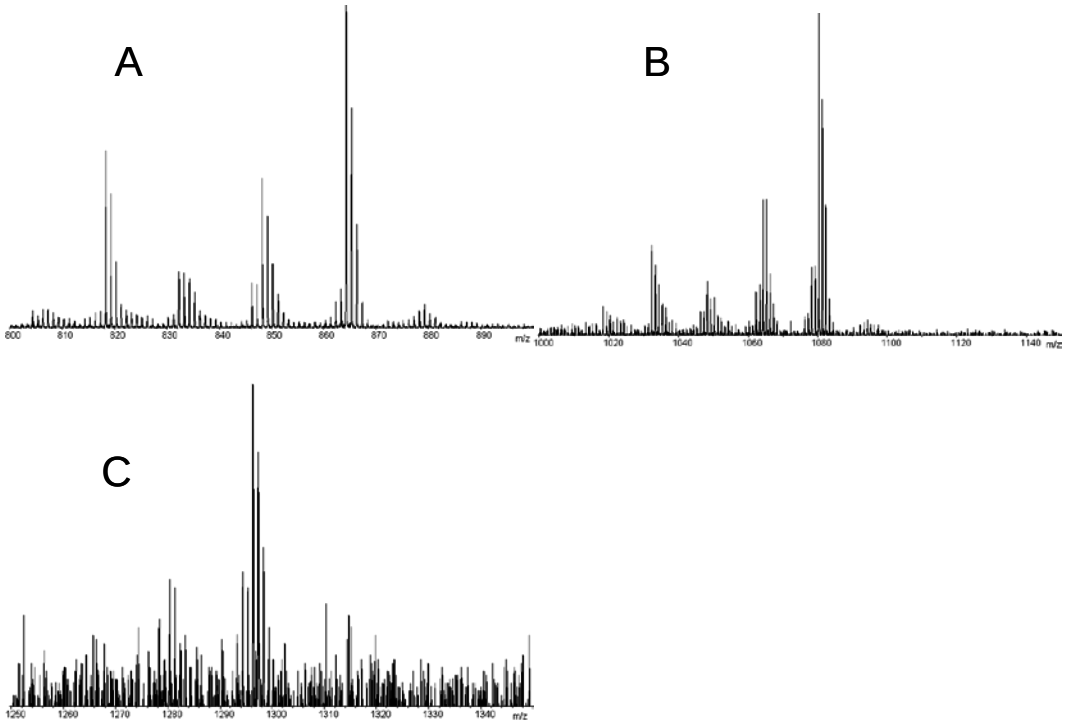

Figure 5: APPI+ mass spectra of the oxy-PAH sample using GPC Mixed E column. Spectrum A: from 800 to 900 Da, spectrum B: from 1000 to 1150 Da, spectrum C: from 1250 to 1300 Da.

Compounds	m/z	Rings + double bonds
$C_{16}H_{10}$	202.078	12
$C_{16}H_{10}O$	218.073	12
$C_{32}H_{16}O$	416.120	25
$C_{32}H_{16}O_2$	432.114	25
$C_{48}H_{24}O_2$	632.177	37
$C_{48}H_{24}O_3$	648.172	37
$C_{64}H_{32}O_3$	848.235	49
$C_{64}H_{32}O_4$	864.230	49
$C_{80}H_{40}O_4$	1064.292	61
$C_{80}H_{40}O_5$	1080.287	61
$C_{96}H_{48}O_5$	1280.350	73
$C_{96}H_{48}O_6$	1296.345	73
$C_{112}H_{56}O_6$	1496.407	85
$C_{112}H_{56}O_7$	1512.402	85

Table 1: List of the constituents of the PAH and oxy-PAH mixture detected in this study. Synthesis and preparation of the mixture is described in Ghislain *et al.* (2010) (18)

3.4. SEC-APPI-QTOF Varian Mixed E and HR columns

An improvement in separation and in detection sensitivity was obtained using both Mixed E and HR columns combined (Figure 6). The SEC chromatogram shows a much better resolution (Figure 8), but the best improvement concerns detection sensitivity, as all compounds are detected (Table 2). For instance the highest molecular mass compounds $C_{112}H_{56}O_6$ and $C_{112}H_{56}O_7$ (m/z 1496 and m/z 1512 respectively) were detected with intensities at 56 and 75 cps, while they were not using only the Mixed-E column. Using only the high resolution column does not allow the detection of these compounds. The mass spectra obtained on these high molecular mass compounds are presented in Figure 7.

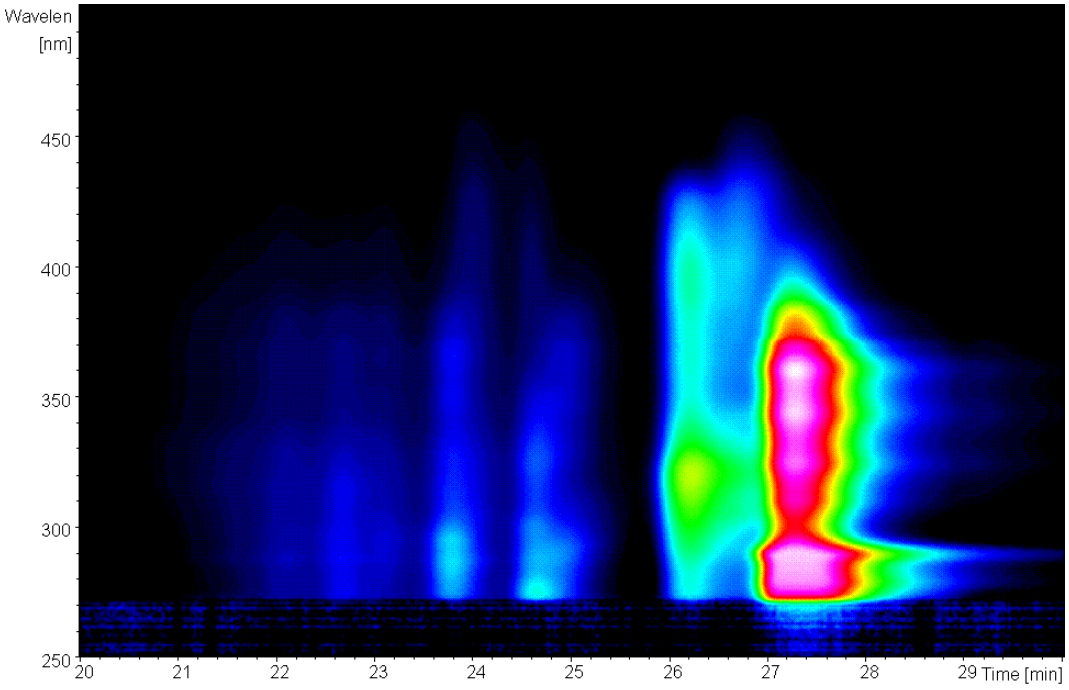

Figure 6: UV chromatogram (250-500 nm) for oxy-PAH mixture using a combination of GPC Mixed E + HR columns. Flow rate at 0.3mL/min with a $CHCl_3/C_6H_6$ 90/10 v/v mobile phase.

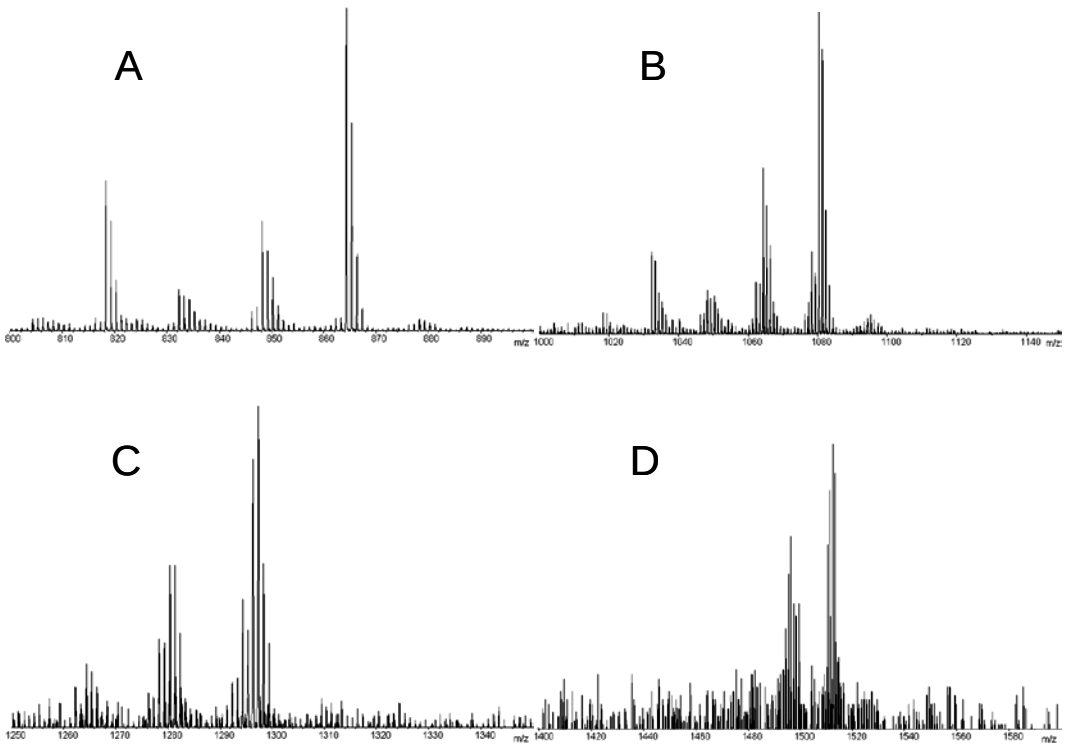

Figure 7: APPI+ mass spectra of the oxy-PAH sample using GPC Mixed E column. Spectrum A: from 800 to 900 Da, spectrum B: from 1000 to 1150 Da, spectrum C: from 1250 to 1300 Da, spectrum D: from 1250 to 1300 Da.

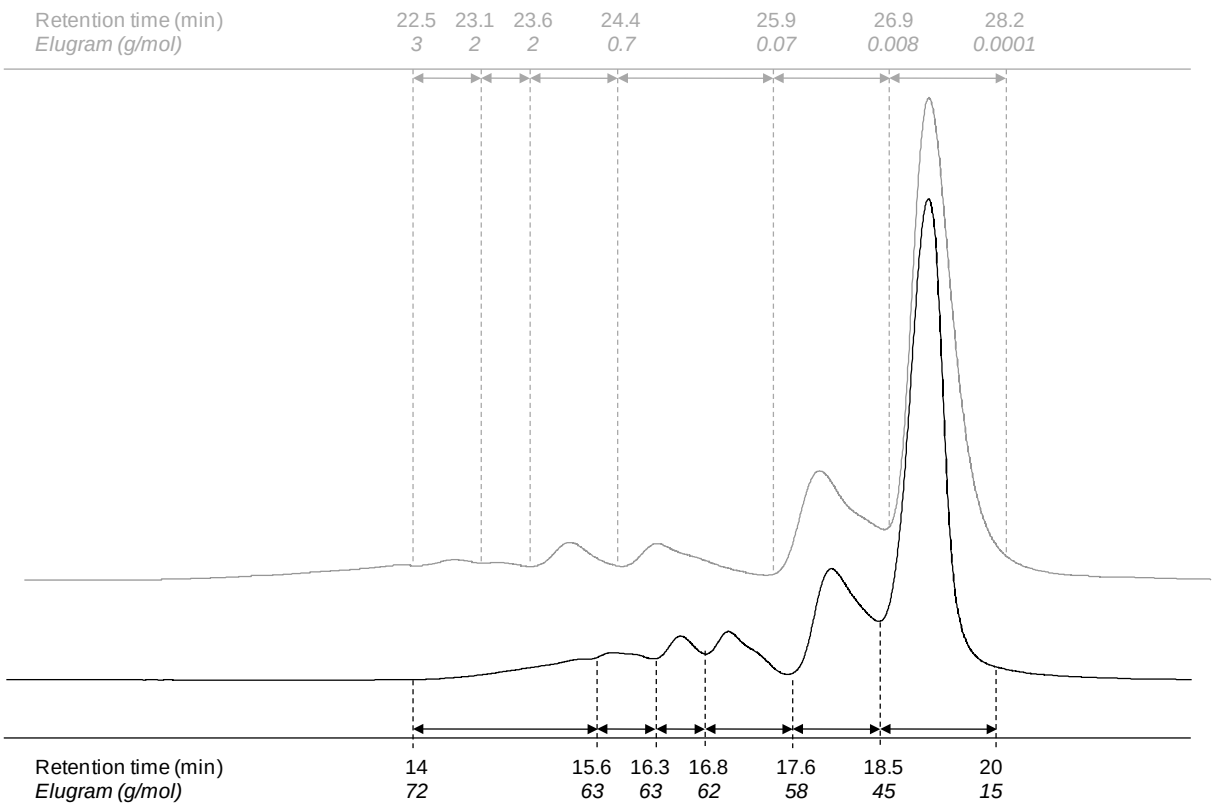

Figure 8: UV chromatograms of the oxy-PAH mixture at 300nm, using GPC Mixed E column (black line); using a combination of GPC Mixed E + HR columns (grey line) with respective molecular mass calibration using polystyrene standards.

Compounds	m/z	Direct infusion I cps	1 column used I cps (RT min)	2 columns used I cps (RT min)
$C_{16}H_{10}$	202	1185556	1826937 (19.4)	1595422 (27.6)
$C_{16}H_{10}O$	218	133321	121514 (19.1)	11538 (27.7)
$C_{32}H_{16}O$	416	322435	120539 (19.1)	185997 (26.6)
$C_{32}H_{16}O_2$	432	10562	1541 (18.4)	1375 (26.1)
$C_{48}H_{24}O_2$	632	10754	8419 (17.1)	18752 (24.3)
$C_{48}H_{24}O_3$	648	1553	1338 (16.9)	3096 (24.1)
$C_{64}H_{32}O_3$	848	268	1954 (16.4)	2174 (23.3)
$C_{64}H_{32}O_4$	864	386	3691 (16.3)	6247 (23.1)
$C_{80}H_{40}O_4$	1064	46	396 (16.0)	456 (22.6)
$C_{80}H_{40}O_5$	1080	51	1005 (15.9)	1301 (22.5)
$C_{96}H_{48}O_5$	1280	Not detected	47 (15.8)	136 (22.0)
$C_{96}H_{48}O_6$	1296	Not detected	78 (15.7)	205 (22.0)
$C_{112}H_{56}O_6$	1496	Not detected	Not detected	56 (21.8)
$C_{112}H_{56}O_7$	1512	Not detected	Not detected	75 (21.7)

Table 2: Measured m/z intensities (counts per second) for the oxy-PAH mixture analyzed by the different analytical configurations: direct infusion APPI-QTOF, on-line SEC-APPI QTOF using Mixed E column and on-line SEC-APPI-QTOF using Mixed E + HR columns.

3.5. Direct infusion mass spectrometry

The oxy-PAH solution was directly injected in the APPI source to compare results with the SEC-APPI-QTOF configurations. The mixture was injected in the same conditions, i.e. concentration, flow rate and solvent composition. Compounds were detected from fluoranthene (m/z 202) to C_{80} compounds (Table 2). No compound of higher molecular mass than C_{80} was detected. The relevant mass spectrum is presented in Figure 9.

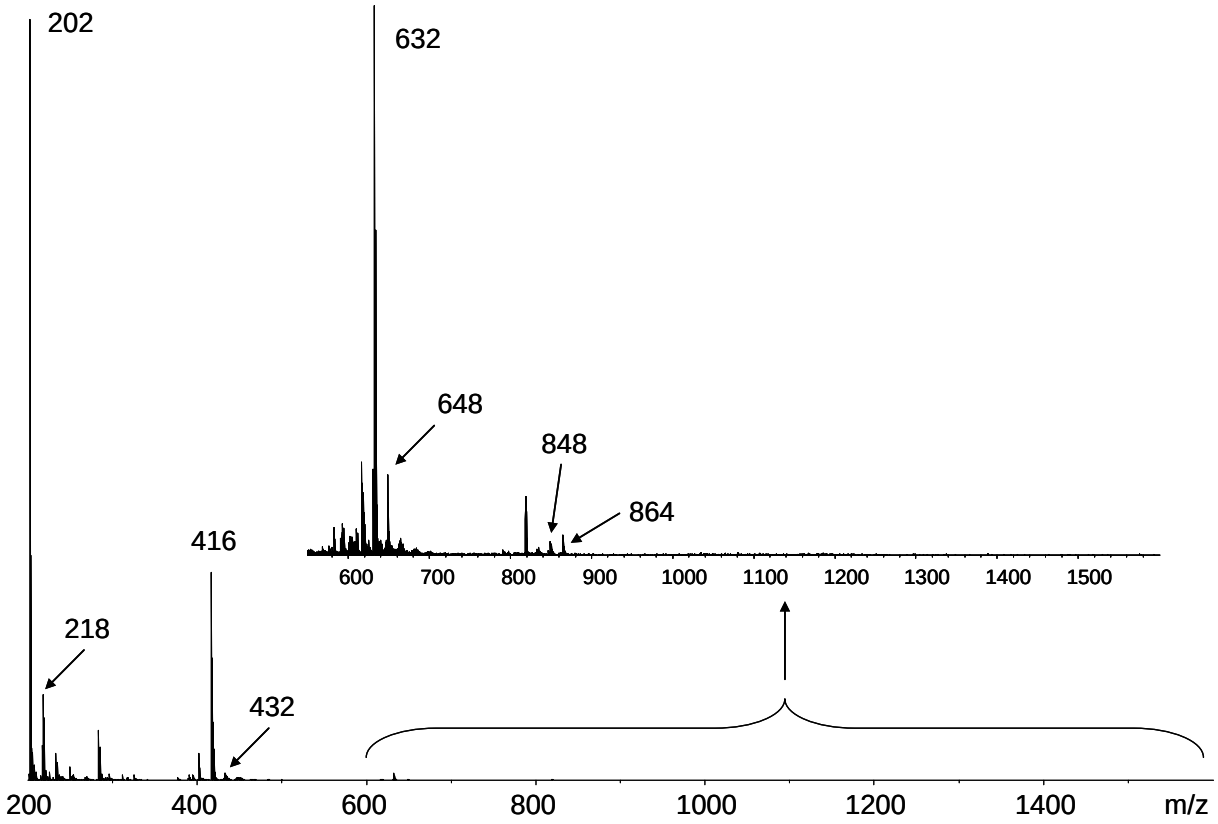

Figure 9: Direct infusion APPI+ mass spectrum of the oxy-PAH sample in chloroform/benzene 90/10 v/v

3.6. Polystyrene injection in SEC-APPI-QTOF using Mixed E column and Mixed E + HR columns

Polystyrene standards were tested on the SEC-APPI-QTOF using Mixed E column (Figure 8). Results gave a mass calibration worst than for THF as mobile phase. Molecular mass determination initially ranging from 200 to 1500 g.mol^{-1} (Figure 3) now indicates a range of 15 to 72 g/mol. When polystyrene standards were injected into the SEC-APPI-QTOF using both E and HR columns combined (Figure 8), results revealed a molecular mass range within 0.0001 to 3 g.mol^{-1} for the same oxy-PAH solution. Increasing chromatography resolving power obviously decreases the quality of the calibration by polystyrene.

4. Discussion

4.1. Improvement of compounds detection

For all different configurations (direct infusion, SEC-APPI-QTOF using one column and SEC-APPI-QTOF using two columns), mass detection intensities obtained for each constituent of the oxy-PAH mixture were measured (Table 2). For fluoranthene, the highest detection intensity was found for the SEC configurations using one or two columns. $C_{16}H_{10}O$ was detected similarly by all configurations. C_{32} compounds were better detected by direct infusion than by using the SEC couplings. C_{48} to C_{80} compounds were all much better detected by coupling SEC and APPI-QTOF using two columns. Intensities were almost 3 times higher for $C_{96}H_{48}O_5$ (m/z 1280) and $C_{96}H_{48}O_6$ (m/z 1296) using two columns than one. For the highest molecular masses, only the coupling of two columns allowed detection of additional compounds overseen with the other analytical configurations. Indeed, the detection of $C_{112}H_{56}O_6$ and $C_{112}H_{56}O_7$ at m/z 1496 and m/z 1512 respectively was only possible when using SEC-APPI-QTOF and two columns coupling.

These experiments reveal that the direct infusion into the APPI-QTOF spectrometer was best configuration for C_{16} and C_{32} compound detection. These compounds are the most concentrated in the solution. It may be possible that competition during the ionization process between the C_{16} - C_{32} compounds and the higher molecular mass products occurred in the APPI source. This leads to significantly reduce the amount of photons or charges available for the ionization of the more diluted higher molecular mass compounds, which did not reach detection limit in the mass spectrometer. The use of a combination of two columns (Mixed E + high resolution) in the SEC-APPI-QTOF coupling allowed detection of the low and higher molecular mass compounds. High resolution chromatography increases the concentration of the individual organic constituents during elution. Competition during ionization in the APPI source was thus strongly reduced, and sufficient ions for each constituent could be obtained to achieve detection.

4.2. APPI-QTOF mass spectrometry and SEC molecular mass calibration.

In order to determine the molecular mass range using SEC, calibration mixtures are run prior to the analysis of the unknown samples, usually using polymer standards (i.e. polystyrenes). Our experiments reveal that for PAHs and oxy-PAHs, this kind of calibration

may not be reliable, especially for low molecular mass compounds. Polystyrenes were also analyzed in SEC-APPI-QTOF with both mixed E and HR columns and results appeared to be inconsistent. This might be explained by the great difference of hydrodynamic radius between polystyrenes and PAHs, as polystyrenes are extended molecules unlike PAHs which are polycondensed, as a consequence retention times of the PAHs mixture do not correspond to those of the polystyrene standards for similar masses. The phenomena has been described by Paul-Dauphin *et al. (2007)* (Paul-Dauphin *et al.* 2007) who demonstrate that the use of pure chloroform for PAH mixtures increases interactions between the stationary phase and solutes. However the authors describe that these interactions lead to a calibration curve having an unusual aspect. This was not the case in our experiments maybe because we used a chloroform-benzene mixture (benzene was added as dopant to enhance the ionization process in the APPI). Thus, the use of a SEC-APPI-QTOF combination allows optimal separation of compounds (based on molecular sizes), direct exact determination of their molecular mass as well as mass spectrometric information (i.e. molecular ion determination).

5. Conclusions

Our experiments successfully coupled Size Exclusion Chromatography to APPI-QTOF mass spectrometry. All compounds in the PAH and oxy-PAH mixture were detected by SEC-APPI-QTOF using two GPC columns while it was not the case for SEC-APPI-QTOF using only one column or for direct infusion APPI-QTOF.

The SEC dual columns-APPI-QTOF combination allowed detection of the compounds present at low concentrations by reducing the ionization competition with the compounds occurring in higher abundances. A consequence is the improvement in the detection of the higher molecular mass compounds in the mixture, revealing the presence of $C_{112}H_{56}O_6$ and $C_{112}H_{56}O_7$ which were not detected in previous work using direct infusion APPI-QTOF (Ghislain *et al.* 2010). In addition, this new analytical tool revealed to be the most suitable detection system for determining the exact molecular masses of the analyzed compounds, avoiding the bias induced by the use of external calibration standards, which are often not adapted, especially when working on unknown complex organic mixtures.

Acknowledgments

This work is included in two regional research projects: ZAM (Zone Atelier Moselle - http://www.ensic.inpl-nancy.fr/Zam) and GISFI (Groupement d'intérêt scientifique sur les friches industrielles – http://www.gisfi.fr) supported by the Regional Council of Lorraine (France) and Ministère de l'Enseignement Supérieur et de la Recherche. The authors thank (i) the Regional Council of Lorraine (France) and CREGU for the doctoral grant accorded to Thierry Ghislain. The HPLC and QTOF instrument were funded by Regional Council of Lorraine (CPER 2004), CNRS and European Funding for Regional Development (FEDER).

6. References

Benson, L.M., Kumar, R., Cavanagh, J., and Naylor, S., Protein-metal ion interactions, stoichiometries and relative affinities determined by on-line size exclusion gel filtration mass spectrometry. *Rapid Commun. Mass Spectrom.*, **2003**. *17*(4): p. 267-271.

Biache, C., Ghislain, T., Faure, P., and Mansuy-Huault, L., Natural oxidation impact on a coking plant soil and its constituents in a natural attenuation context: Experimental air oxidation at low temperature conditions. *Journal of Hazardous Materials*, **2011**. *In press*.

Biache, C., Mansuy-Huault, L., Faure, P., Munier-Lamy, C., and Leyval, C., Effects of thermal desorption on the composition of two coking plant soils: Impact on solvent extractable organic compounds and metal bioavailability. *Environ. Pollut.*, **2008**. *156*(3): p. 671-677.

Desmazières, B., Buchmann, W., Terrier, P., and Tortajada, J., APCI interface for LC- and SEC-MS analysis of synthetic polymers: Advantages and limits. *Anal. Chem.*, **2008**. *80*(3): p. 783-792.

Feldermann, A., Ah Toy, A., Davis, T.P., Stenzel, M.H., and Barner-Kowollik, C., An in-depth analytical approach to the mechanism of the RAFT process in acrylate free radical polymerizations via coupled size exclusion chromatography-electrospray ionization mass spectrometry (SEC-ESI-MS). *Polymer*, **2005**. *46*(19 SPEC. ISS.): p. 8448-8457.

Ghislain, T., Faure, P., Biache, C., and Michels, R., Low-Temperature, Mineral-Catalyzed Air Oxidation: A Possible New Pathway for PAH Stabilization in Sediments and Soils. *Environ. Sci. Technol.*, **2010**. *44*(22): p. 8547-8552.

Gruendling, T., Guilhaus, M., and Barner-Kowollik, C., Design of experiment (DoE) as a tool for the optimization of source conditions in SEC-ESI-MS of functional synthetic polymers synthesized via ATRP. *Macromol. Rapid Commun.*, **2009**. *30*(8): p. 589-597.

Gruendling, T., Voll, D., Guilhaus, M., and Barner-Kowollik, C., A perfect couple: PLP/SEC/ESI-MS for the accurate determination of propagation rate coefficients in free radical polymerization. *Macromol. Chem. Phys.*, **2010**. *211*(1): p. 80-90.

Herod, A.A., Limitations of mass spectrometric methods for the characterization of polydisperse materials. *Rapid Commun. Mass Spectrom.*, **2010**. *24*(17): p. 2507-2519.

Klaus, U., Pfeifer, T., and Spiteller, M., APCI-MS/MS: A powerful tool for the analysis of bound residues resulting from the interaction of pesticides with DOM and humic substances. *Environ. Sci. Technol.*, **2000**. *34*(16): p. 3514-3520.

Liu, X.M., Maziarz, E.P., and Heiler, D.J., Characterization of implant device materials using size-exclusion chromatography with mass spectrometry and with triple detection. *J. Chromatogr. A*, **2004**. *1034*(1-2): p. 125-131.

Marchi, I., Rudaz, S., and Veuthey, J.-L., Atmospheric pressure photoionization for coupling liquid-chromatography to mass spectrometry: A review. *Talanta*, **2009**. *78*(1): p. 1-18.

Moriwaki, H., Ishitake, M., Yoshikawa, S., Miyakoda, H., and Alary, J.F., Determination of polycyclic aromatic hydrocarbons in sediment by liquid chromatography-atmospheric pressure photoionization-mass spectrometry. *Anal Sci*, **2004**. *20*(2): p. 375-7.

Nielen, M.W.F., Characterization of synthetic polymers by size-exclusion chromatography/electrospray ionization mass spectrometry. *Rapid Commun. Mass Spectrom.*, **1996**. *10*(13): p. 1652-1660.

NIST. Available from: http://webbook.nist.gov/chemistry/.

Paul-Dauphin, S., Karaca, F., Morgan, T.J., Millan-Agorio, M., Herod, A.A., and Kandiyoti, R., Probing size exclusion mechanisms of complex hydrocarbon mixtures: The effect of altering eluent compositions. *Energy Fuels*, **2007**. *21*(6): p. 3484-3489.

Persson, L., Alsberg, T., Kiss, G., and Odham, G., On-line size-exclusion chromatography/electrospray ionisation mass spectrometry of aquatic humic and fulvic acids. *Rapid Commun. Mass Spectrom.*, **2000**. *14*(4): p. 286-292.

Połeć-Pawlak, K., Ruzik, R., and Lipiec, E., Investigation of Cd(II), Pb(II) and Cu(I) complexation by glutathione and its component amino acids by ESI-MS and size exclusion chromatography coupled to ICP-MS and ESI-MS. *Talanta*, **2007**. *72*(4): p. 1564-1572.

Prokai, L. and Simonsick Jr, W.J., Coupling size-exclusion chromatography with electrospray ionization mass spectrometry for polymer analysis. *American Chemical Society, Polymer Preprints, Division of Polymer Chemistry*, **2000**. *41*(1): p. 663-664.

Reemtsma, T. and These, A., Comparative investigation of low-molecular-weight fulvic acids of different origin by SEC-Q-TOF-MS: New insights into structure and formation. *Environ. Sci. Technol.*, **2005**. *39*(10): p. 3507-3512.

Schmidt, A.C., Fahlbusch, B., and Otto, M., Size exclusion chromatography coupled to electrospray ionizationmass spectrometry for analysis and quantitative characterization of arsenic interactions with peptides and proteins. *J. Mass Spectrom.*, **2009**. *44*(6): p. 898-910.

Tastet, L., Schaumlöffel, D., Bouyssiere, B., and Lobinski, R., Identification of selenium-containing proteins in selenium-rich yeast aqueous extract by 2D gel electrophoresis, nanoHPLC-ICP MS and nanoHPLC-ESI MS/MS. *Talanta*, **2008**. *75*(4): p. 1140-1145.

Toy, A.A., Vana, P., Davis, T.P., and Barner-Kowollik, C., Reversible Addition Fragmentation chain Transfer (RAFT) polymerization of methyl acrylate: Detailed structural investigation via coupled Size Exclusion Chromatography-Electrospray Ionization Mass Spectrometry (SEC-ESI-MS). *Macromolecules*, **2004**. *37*(3): p. 744-751.

Zwiener, C. and Frimmel, F., LC-MS analysis in the aquatic environment and in water treatment – a critical review. *Anal. Bioanal. Chem.*, **2004**. *378*(4): p. 851-861.

Molecular distribution of Asphaltenes of different origins: Contribution of on-line SEC-APPI-QTOF

Thierry Ghislain*, Coralie Biache, Schumacher Aymeric, Madhaoui Fatima, Pierre Faure, Raymond Michels

Prepared for Energy & Fuel

G2R, Nancy-Université, CNRS, B.P. 239, 54506 Vandœuvre-lès-Nancy, France

* Corresponding author. Tel.: +33 3 83 68 47 41; fax: +33 3 83 68 47 01.

E-mail address: Thierry.Ghislain@g2r.uhp-nancy.fr

1. Introduction

Asphaltenes are known to be the heaviest part and the most polar fraction in crude oils or coal extracts. They are mainly defined as the insoluble fraction obtained after extraction using a light *n*-alkane (*n*-pentane or *n*-heptane usually) (Speight 2004; Speight 2004). It is important to understand their chemical and structural composition as asphaltenes are major constituents of crude oils and have a major control on petroleum properties. These are of key interest from the understanding of the origins and fate of petroleum in sedimentary basins, to reservoir exploitation, petroleum transportation and refining. Thus, over the past years the understanding of the chemical and structural composition of asphaltenes has been of major focus in the research community. In this context, many reviews published reflect the wide variety of analytical methods investigated (Merdrignac *et al.* 2007; Mullins 2007). Among the many aspects of asphaltene analysis, the determination of the molecular size distribution is of special interest. A common analytical method to investigate molecular size distributions of asphaltenes consists in separating and collecting fractions obtained by Size Exclusion Chromatography before analysis by ESI-MS (Karaca *et al.* 2009) or Laser Desorption-MS (Tanaka *et al.* 2004; Morgan *et al.* 2009). Indeed, in literature, several mass spectrometry techniques including different ionization sources and mass analyzers applied to asphaltenes are described.

In the present paper we present an on-line technique coupling Size Exclusion Chromatography (SEC) and APPI-QTOF allowing the continuous mass spectrometric analysis of the full range of size classes of asphaltenes. The main purpose of this method is to (i) reduce the manipulation of the sample between SEC analysis and mass spectrometry (ii) reduce potential influence of chemical or physical modification during analysis (iii) avoid the use of external calibration of the SEC, as this is still in debate (Morgan *et al.* 2009) (iv) to improve compounds detection by reducing ionization competition (or matrix effect). On-line SEC-APPI-QTOF shall thus significantly improve the resolutions of size distribution classes as well as mass spectrometry detection.

2. Materials and methods

2.1. Samples

Coal and coal tar were collected at the site of Homécourt (Lorraine, France). According to the TOC content, 3 to 9g of these samples were submitted to solvent extraction using the automated extractor Dionex ASE 200 and dichloromethane (DCM) at 130°C, 130bar for 5 min) (Li *et al.* 2002; Biache *et al.* 2011)

The crude oil samples used are: a light oil from Kazakhstan (Precaspian basin) and a medium density oil from Pechelbronn (northern Rhine graben, France).

Asphaltenes were extracted from the chloroform extracts or from crude oils by addition of 40 volumes of *n*-pentane heated at 40°C for 15min. The asphaltenes were then filtered on glass microfiber filters (0.7µm pore size) and thoroughly washed by *n*-pentane. Asphaltenes were then dried and diluted in a mixture chloroform/benzene 70/30 v/v to reach the final concentration at 100µg.ml^{-1}.

2.2. Analysis solvents

Chloroform (H.P.L.C. grade) was purchased from V.W.R. and benzene (H.P.L.C. grade) was purchased from Sigma Aldrich were used as received. Chloroform was chosen because it is known to completely dissolve asphaltenes.

2.3. Size Exclusion Chromatography

Gel permeation chromatography was performed by injecting 20µL of sample into a Dionex Ultimate 3000 series chromatograph (Dionex, Sunnyvale, CA, USA). 2 different SEC columns were tested, a Varian PLgel Organic Mixed E column (300 x 7.5mm ID, 5µm for particle size) for which, compounds can be distinguished until 30 000 g.mol^{-1} and a Varian PLgel Organic column (250 x 4.6 mm ID, 5µm for particle size and 100Å for pore size) maintained at 25°C. Detection was ensured by a Dionex Diode Array Detector.

2.4. APPI-QTOF mass spectrometry.

Molecular mass distributions were recorded on a hybrid Quadrupole – Time-Of-Flight mass spectrometer (Bruker Daltonics, Bremen , Germany) equipped with an Atmospheric Pressure PhotoIonisation (APPI) manufactured by Syagen (Syagen Technology Inc., Tustin, CA, USA), containing a Krypton lamp which produces a 10eV photon beam operating in positive mode. The source parameters were optimized and set at: capillary voltage -4500V, end plate offset -500V). Nitrogen gas was maintained at 5bar for nebulisation and 3 $L.min^{-1}$ at 250°C for desolvatation, vaporizer temperature was set at 350°C. Complete description of the system and applications can be found in Ghislain *et al.* 2010.

3. Results

3.1. Molecular distribution of asphaltenes from coal

Analysis by direct infusion APPI-QTOF is presented in Figure 10 and shows a mass distribution profile mainly below 600 Da. Results obtained by on-line SEC-APPI-QTOF reveals a chromatographic time elution range from 15 to 30 min (Figure 11). Five different mass spectra were chosen at noteworthy points of the SEC chromatogram.

For all analysis points (noted from a to e), the mass distribution ranges up to about m/z 600. Yet, maxima of distributions shift: Mass spectrum 2a (20 min) is centred at about 540 Da, mass spectrum 2b (22.5min) at 450 Da, mass spectrum 2c (23.4 min) at 400 Da, mass spectrum 2d (25.3 min) at 320 Da and mass spectrum 2e (27.3 min) shows main peaks below 300 Da. Maxima shift from higher m/z values to lower in accordance to increasing elution times, and thus in relationship to decreasing molecular size classes.

In addition, the comparison of the mass spectrum obtained by direct infusion (Figure 10) and SEC-APPI-QTOF (Figure 11) reveals an improvement of sensitivity in the detection of the higher molecular mass range (between 400 and 600 Da).

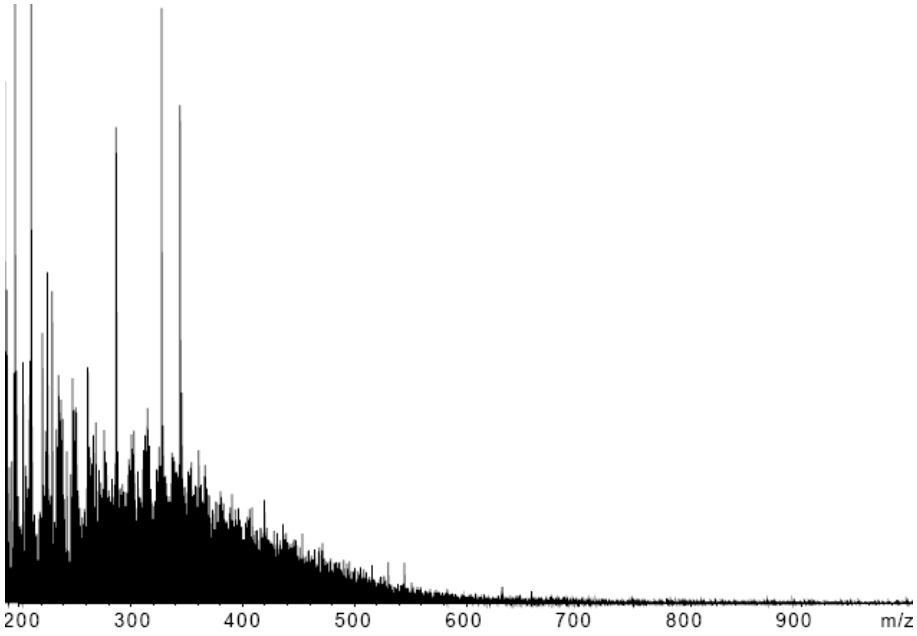

Figure 10: APPI+ mass spectrum of coal asphaltenes in a $CHCl_3/C_6H_6$ (70/30) mixture

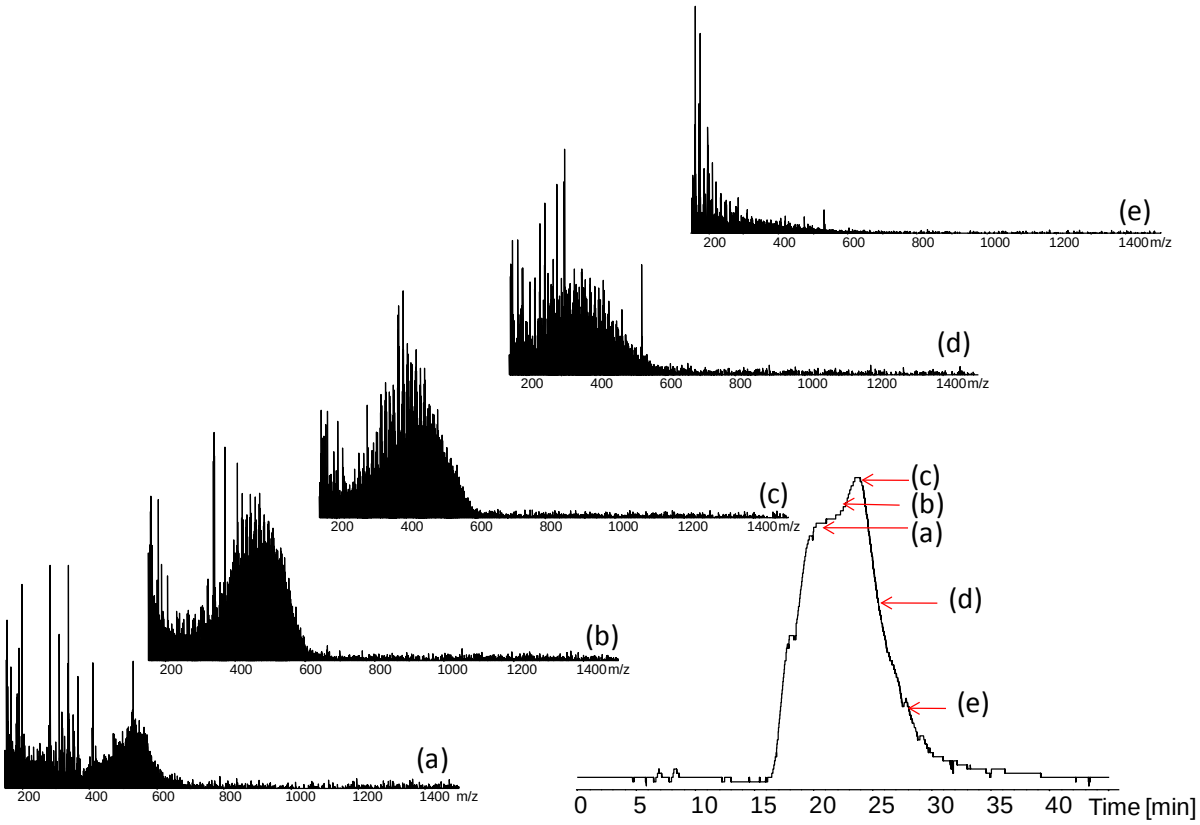

Figure 11: SEC chromatogram at 300 nm of asphaltenes derived from coal with corresponding mass spectra.

3.2. Molecular distribution of asphaltenes from coal tar

Coal tar asphaltenes were analyzed by direct infusion (Figure 3). The mass spectrum shows mass distributions up to about m/z 500, with a specific pattern of mass clusters typical of PAH from coal tar.

SEC-APPI-QTOF (Figure 13) leads to a chromatogram eluting between 15 to 35 minutes. A selection of mass spectra along the elution profile present different distribution profiles centred at about 500 Da on mass spectrum 4a (22.7 min), 320 Da on mass spectrum 4b (25.5 min).

Mass spectra 13c (27.0 min) and 13d (29.0 min) are different from the previous because they reveal a non-asphaltene type mass distribution (compared to those obtained from coal).

by comparing Figure 12 and Figure 13, it can be noticed that the mass distribution profile obtained by direct infusion APPI-QTOF (Figure 12) shows no compounds detection between 500 to 600 Da unlike SEC-APPI-QTOF (Figure 13) for which compounds were detected up to 600 Da.

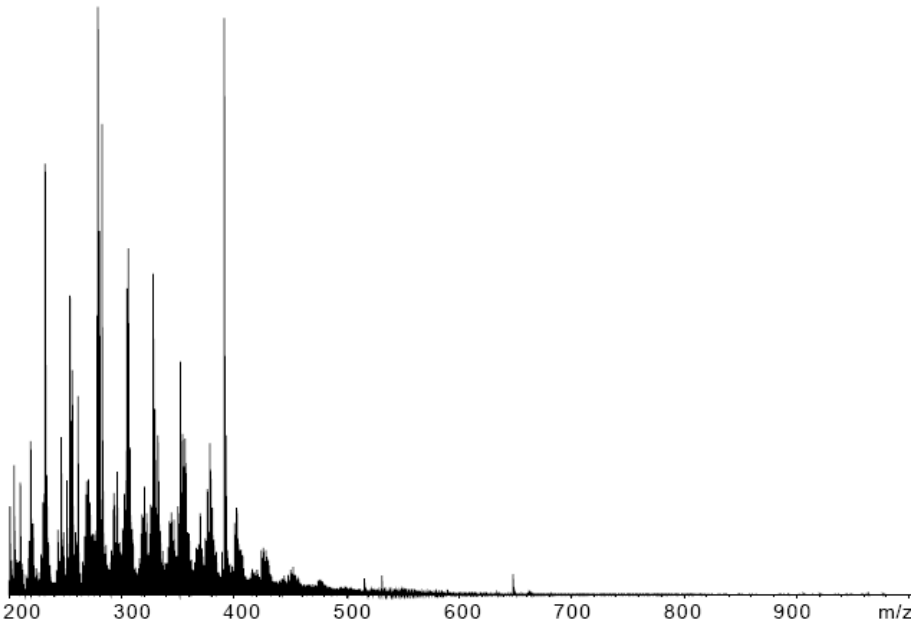

Figure 12: APPI+ mass spectrum of coal tar asphaltenes in a $CHCl_3/C_6H_6$ (70/30) mixture

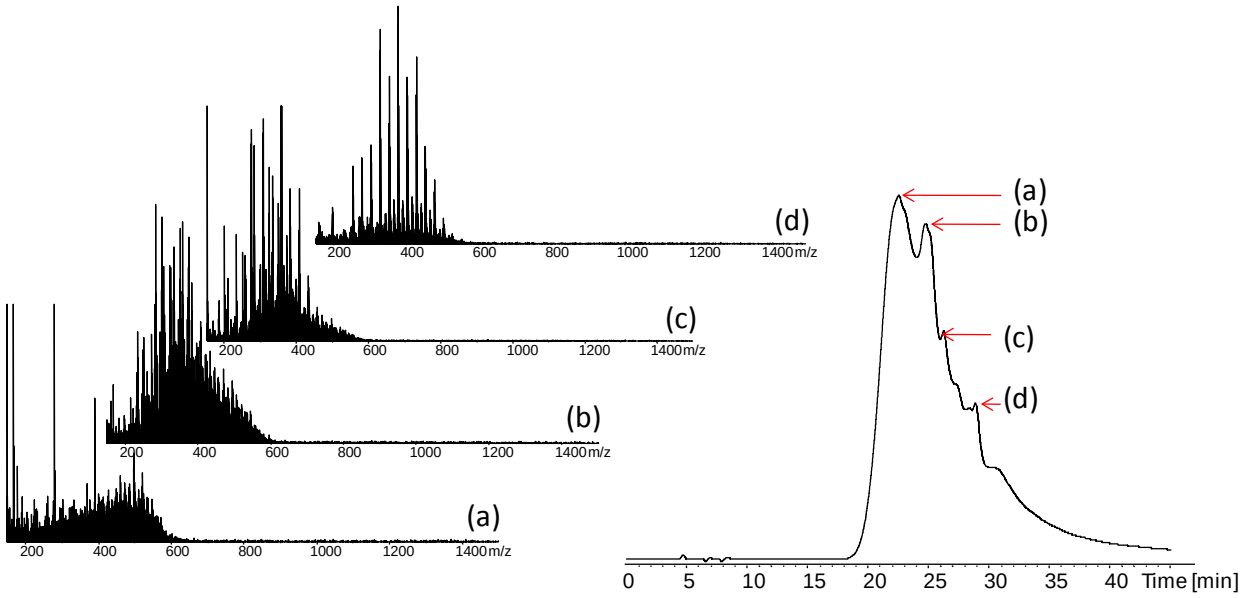

Figure 13: SEC chromatogram at 300 nm of asphaltenes derived from coal tar with corresponding mass spectra.

3.3. Molecular distribution of asphaltenes from crude oil (Pechelbronn)

The direct infusion APPI-QTOF mass distribution profile of the Pechelbronn oil asphaltenes is presented in Figure 14. Compounds are detected to about 700 Da.

SEC chromatogram reveals a distribution within 15 to 36 min (Figure 15). Five different mass spectra were extracted corresponding to interesting point of SEC chromatograms. Mass spectrum 6a (17.0 min) reveals a distribution from 700 to 1200 Da with a maximum at m/z 900 in the higher molecular mass range. Mass spectrum 15b (20.7 min) ranges from 400 to 1000 Da with a maximum at about m/z 550, mass spectrum 15c (22.5 min) from 400 Da to 800 Da with a maximum at about m/z 500, mass spectrum 15d (23.9 min) reveals peaks below 700 Da, mass spectrum 15e (25.9 min) below 350 Da.

Similarly to previous analyses, the extent of the mass distribution profiles as well as the m/z values of the maxima in the higher molecular mass ranges decreases with decreasing molecular sizes. Also, SEC-APPI-QTOF is able to detect compounds up to 1200 Da when APPI-QTOF is limited to 700 Da.

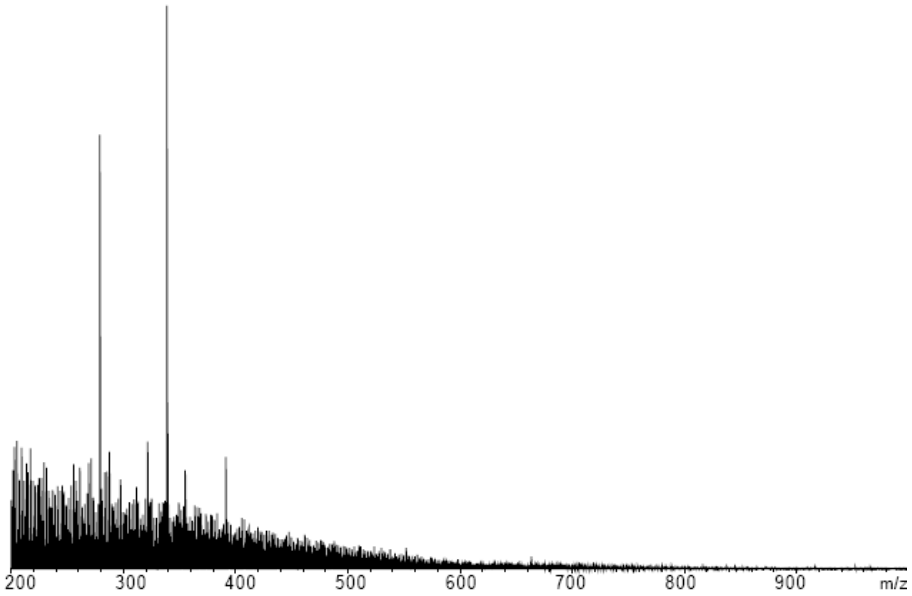

Figure 14: APPI+ mass spectrum of Pechelbronn asphaltenes in a $CHCl_3/C_6H_6$ (70/30) mixture

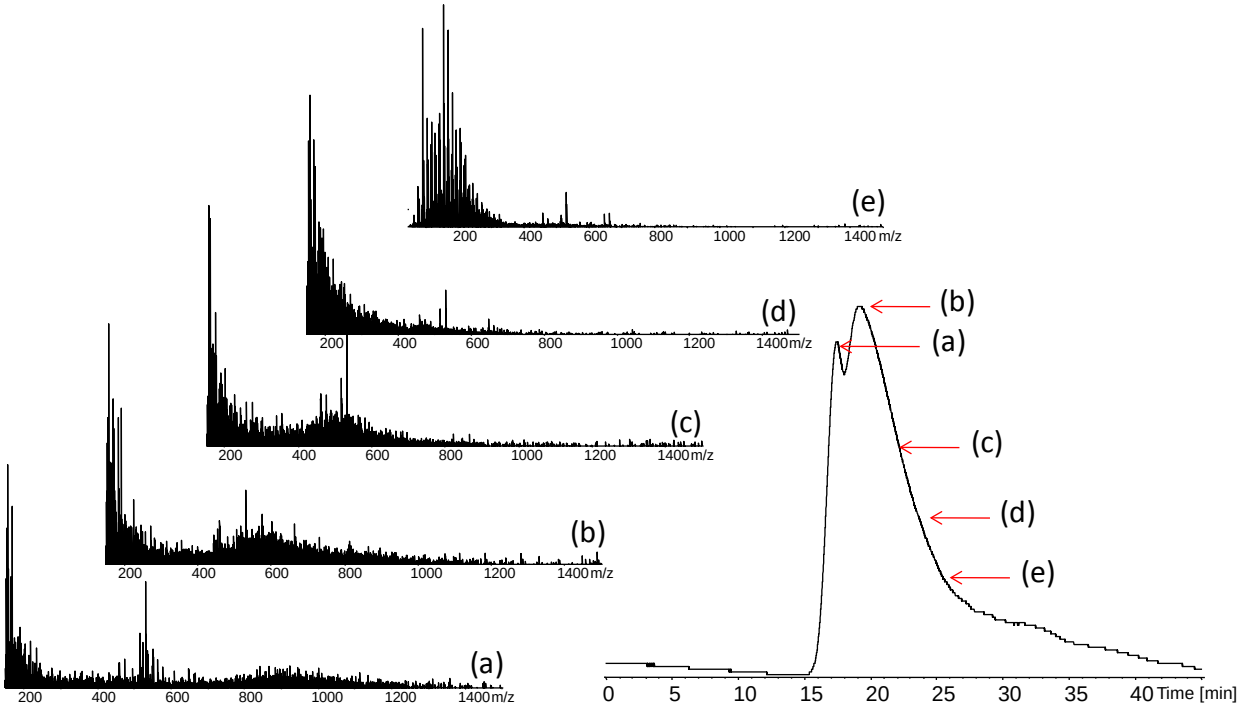

Figure 15: SEC chromatogram at 300 nm of asphaltenes derived from crude oil (Pechelbronn) with corresponding mass spectra.

3.4. Molecular distribution of asphaltenes from crude oil (Kazakhstan)

The direct infusion APPI-QTOF analysis of the asphaltenes from the crude oil of Kazakhstan is presented in Figure 16, with compounds detected to about 800Da.

For SEC-APPI-QTOF, the SEC elution time extents from 15 to 35 min. Mass spectrum 17a (20.6 min) presents a mass distribution within 600 to 1400 Da centred at 900 Da. Mass spectrum 17b (21.6 min) presents a maximum between 400 Da to 1100 Da centred at 600 Da. Mass spectrum 17c (22.7 min) presents a maximum within 300 to 800 Da centred around 500 Da. Final mass spectra give information on peaks below 500 Da for mass spectrum 17d (24.2 min) and 300 Da for mass spectrum 17e (25.6 min). The high molecular mass detection improvement was the most noticeable for these asphaltenes in our study as SEC-APPI-QTOF detects compounds above 1400 Da when direct infusion in APPI-QTOF does not reach roughly 800 Da.

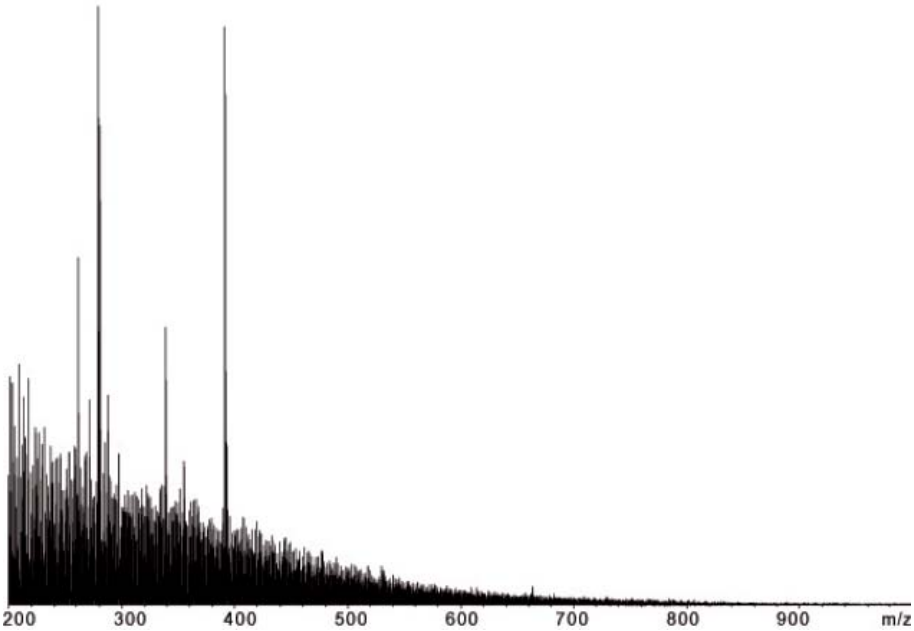

Figure 16: APPI+ mass spectrum of asphaltenes derived from crude oil (Kazakhstan) in a $CHCl_3/C_6H_6$ (70/30) mixture

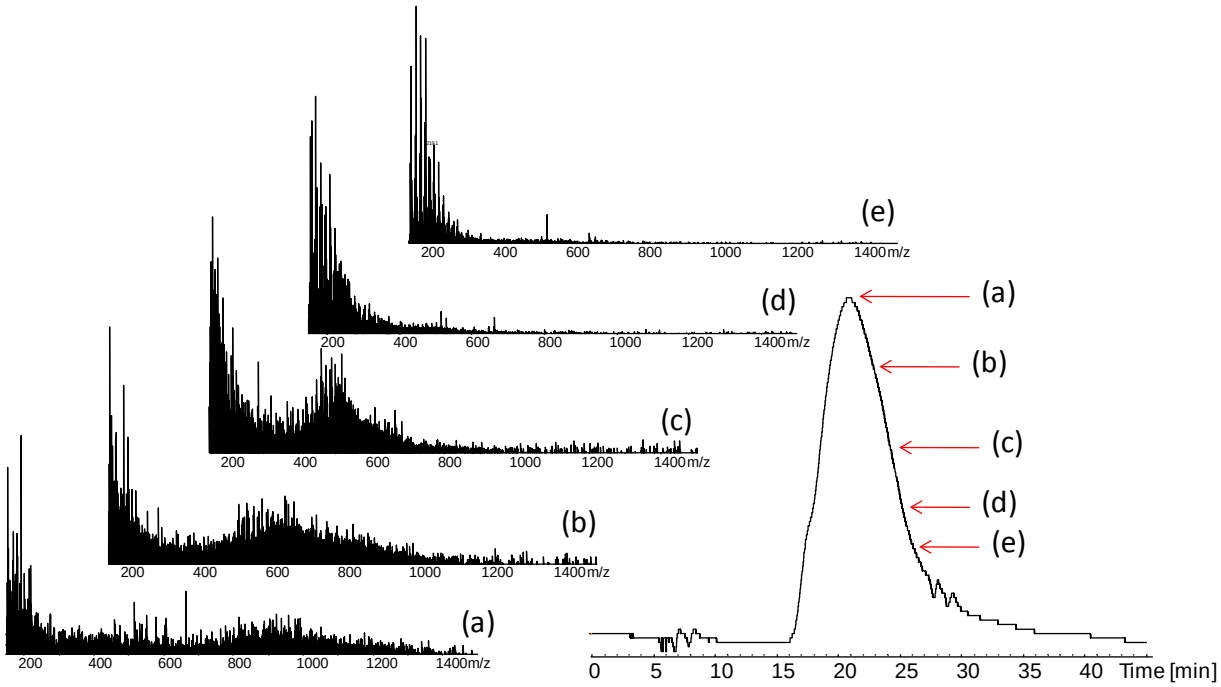

Figure 17: SEC chromatogram at 300 nm of asphaltenes derived from crude oil (Kazakhstan) with corresponding mass spectra.

4. Discussion

4.1. Suitability of SEC

Recent works have pointed out controversial results using SEC (Behrouzi *et al.* 2008; Herod 2010). The debate concerns the inability of SEC to resolve petroleum asphaltenes. However, Herod *(*Herod *2010)* explains that limitations about SEC mainly concern the solvent used and relative calibration when using polystyrene standards. For that purpose we developed on-line SEC-APPI-QTOF (Ghislain *et al.* 2011). Main objectives using this system were the characterization of non polar and weakly polar compounds and to avoid the use of standards for relative calibration, polystyrene standards leading from partially to completely wrong results (Ghislain *et al.* 2011). Paul-Dauphin *et al.* (Paul-Dauphin *et al.* 2007) reveal interactions of aromatic compounds with the column packing material leading to "wrong way calibration curve". This phenomenon was not observed in our experiments (Ghislain *et al.* 2011). This is probably due to the use of benzene as dopant. Benzene interacts readily with the static phase of the SEC column, thus reducing the chemical of physical interactions of this latter with the sample (reducing the enthalpic term). As a consequence, chromatographic separation may be considered as mainly based on hydrodynamic radius (entropic term). Based on this observation we consider that separation which occurred in our experiments is mainly realized in terms of size class resolution.

Wu *et al.* (Wu *et al.* 1995) listed several limitations encountered for asphaltenes (road asphalts) analysis by SEC (i) aliphatic fractions have a tendency to associate, (ii) fractions have a tendency to adsorb on column packing material, (iii) elution order between polar and non polar fractions can be modified and (iv) chemical complexity makes it difficult to find suitable standards. However in our experiments, these inconveniences were taken into account and (i) chloroform was used as it is known to completely dissolved asphaltenes, (ii) the addition of benzene to chloroform considerably reduced adsorption (Ghislain *et al.* 2011), (iii) the order of elution is not a problem as our work was to sort molecules according to their molecular hydrodynamic radius and (iv) standards are not necessary as a high resolution mass spectrometry is used as detector.

4.2. Improvements of high molecular compounds detection and molecular mass determination

SEC separation significantly improves the detection of the higher molecular mass compounds. This may be the consequence of separation between lower and higher molecular size classes thus allowing a relative enrichment of compounds within each size class and probably also a reduction of ionization competition between compounds.

Also, molecular mass range and distribution determination does not need external calibration (use of standards) since the APPI-QTOF was used as detector (Ghislain *et al.* 2011). This shall improve molecular mass interpretation.

4.3. Contribution to the understanding of asphaltenes structures

The comparison of the results obtained by SEC-APPI-QTOF and APPI-QTOF evidences that for each elution time of the SEC chromatograms (i.e. for each size class) a complete range of m/z values is collected. In the higher and intermediate molecular size classes, the m/z ranges are similar to those obtained by APPI-QTOF. Yet, really different are the mass distribution profiles, which show maxima for each size class. These maxima shift from higher to lower molecular mass values as molecular size classes decrease (i.e. elution time increases).

For asphaltenes precipitated from coal tar, two kinds of spectra could be identified along the elution time profile. The shorter elution time size classes (Figure 13a, b) which exhibit a mass spectrometry profile of the "asphaltenes type" and the lower elution time size classes (Figure 13c, d) which exhibit a profile with the repeating of patterns. This can be explained by the composition of coal tar asphaltenes which consist in mixtures of compounds units based on PAHs (Biache *et al.* 2011). Units based on PAHs with low molecular masses (below 400 Da) may be considered as planar molecules (which is the case for the 16 PAHs listed by the US-EPA) for which hydrodynamic radius are thus smaller, authorizing these compounds to penetrate more easily through the pores of the packing material. Consequently, they are detected at later elution times than the oxy-PAHs. The units based on PAHs may thus be separated from oxy-PAHs by SEC and lead to the specific mass distribution patterns (typical mass spectrum of coal tar samples) as shown in spectra 13c and 13d, unlike oxy-PAHs for which hydrodynamic radius are more important and so are eluted faster (spectra 13a, b).

The two different crude oil derived asphaltenes present similar SEC chromatograms; no bimodal distribution was observed as for the coal and coal tar samples. In all cases, it was possible to detect high molecular mass compounds (more than 800 Da) and low molecular mass compounds (below 200 Da). The efficiency of the technique is better for asphaltenes from crude oils as the different mass distributions observed on mass spectra were better resolved than for non petroleum derived asphaltenes.

As described above, distributions of molecular mass profiles for asphaltenes are observed at any SEC elution time. The maximum of distribution in the higher molecular mass ranges is shifting to lower m/z values as molecular size class decreases. The m/z range observed is always lower than 1500 Da. The results are consistent with Mullins *et al.* (Mullins *et al.* 2007) who described asphaltenes as being constituted of small molecular mass units. Results are also consistent with recent works by McKenna *et al.* (McKenna *et al. 2010;* McKenna *et al. 2010)* who studied the validity of Boduszinski model (Boduszynski 1987; Boduszynski 1988; Altgelt *et al.* 1992; Boduszynski *et al.* 1992). Indeed, the Boduszinski model describes asphaltenes as a continuum of compositions, molecular masses, aromaticities and heteroatom contents as a function of boiling point.

5. References

Altgelt, K.H. and Boduszynski, M.M., Composition of heavy petroleums. 3. An improved boiling point-molecular weight relation. *Energy Fuels*, **1992**. *6*(Copyright (C) 2011 American Chemical Society (ACS). All Rights Reserved.): p. 68-72.

Behrouzi, M. and Luckham, P.F., Limitations of size-exclusion chromatography in analyzing petroleum asphaltenes: A proof by atomic force microscopy. *Energy Fuels*, **2008**. *22*(3): p. 1792-1798.

Biache, C., Ghislain, T., Faure, P., and Mansuy-Huault, L., Low temperature oxidation of a coking plant soil organic matter and its major constituents: An experimental approach to simulate a long term evolution. *J. Hazard. Mater.*, 2011. *188*(1-3): p. 221-230.

Boduszynski, M.M., Composition of heavy petroleums. 1. Molecular weight, hydrogen deficiency, and heteroatom concentration as a function of atmospheric equivalent boiling point up to 1400°F (760°C). *Energy Fuels*, **1987**. *1*(Copyright (C) 2011 American Chemical Society (ACS). All Rights Reserved.): p. 2-11.

Boduszynski, M.M., Composition of heavy petroleums. 2. Molecular characterization. *Energy Fuels*, **1988**. *2*(Copyright (C) 2011 American Chemical Society (ACS). All Rights Reserved.): p. 597-613.

Boduszynski, M.M. and Altgelt, K.H., Composition of heavy petroleums. 4. Significance of the extended atmospheric equivalent boiling point (AEBP) scale. *Energy Fuels*, **1992**. *6*(Copyright (C) 2011 American Chemical Society (ACS). All Rights Reserved.): p. 72-6.

Ghislain, T., Faure, P., and Michels, R., On-line SEC-APPI-QTOF: a new analytical tool for complex hydrocarbon mixtures. *J. Chromatogr. A*, **2011**. *submitted*.

Herod, A.A., Limitations of mass spectrometric methods for the characterization of polydisperse materials. *Rapid Commun. Mass Spectrom.*, **2010**. *24*(17): p. 2507-2519.

Karaca, F., Morgan, T.J., George, A., Bull, I.D., Herod, A.A., Millan, M., and Kandiyoti, R., Molecular mass ranges of coal tar pitch fractions by mass spectrometry and size-exclusion chromatography. *Rapid Communications in Mass Spectrometry*, **2009**. *23*(13): p. 2087-2098.

Li, Y., Michels, R., Mansuy, L., Fleck, S., and Faure, P., Comparison of pressurized liquid extraction with classical solvent extraction and microwave-assisted extraction-application to the investigation of the artificial maturation of Mahakam coal. *Fuel*, **2002**. *81*(6): p. 747-755.

McKenna, A.M., Blakney, G.T., Xian, F., Glaser, P.B., Rodgers, R.P., and Marshall, A.G., Heavy petroleum composition. 2. Progression of the boduszynski model to the limit of distillation by ultrahigh-resolution FT-ICR mass spectrometry. *Energy Fuels*, **2010**. *24*(5): p. 2939-2946.

McKenna, A.M., Purcell, J.M., Rodgers, R.P., and Marshall, A.G., Heavy petroleum composition. 1. Exhaustive compositional analysis of athabasca bitumen HVGO distillates by fourier transform ion cyclotron resonance mass spectrometry: A definitive test of the boduszynski model. *Energy Fuels*, **2010**. *24*(5): p. 2929-2938.

Merdrignac, I. and Espinat, D., Physicochemical characterization of petroleum fractions: The state of the art. *Oil and Gas Science and Technology*, **2007**. *62*(1): p. 7-32.

Morgan, T.J., George, A., Alvarez, P., Herod, A.A., Millan, M., and Kandiyoti, R., Isolation of size exclusion chromatography elution-fractions of coal and petroleum-derived samples and analysis by laser desorption mass spectrometry. *Energy Fuels*, **2009**. *23*(12): p. 6003-6014.

Mullins, O.C., Asphaltenes, heavy oils, and petroleomics 2007, New York: Springer. xxi, 669.

Paul-Dauphin, S., Karaca, F., Morgan, T.J., Millan-Agorio, M., Herod, A.A., and Kandiyoti, R., Probing size exclusion mechanisms of complex hydrocarbon mixtures: The effect of altering eluent compositions. *Energy Fuels*, **2007**. *21*(6): p. 3484-3489.

Speight, J.G., Petroleum asphaltenes - Part 1: Asphaltenes, resins and the structure of petroleum. *Oil and Gas Science and Technology*, **2004**. *59*(5): p. 467-477.

Speight, J.G., Petroleum asphaltenes - Part 2: The effect of asphaltenes and resin constituents on recovery and refining processes. *Oil and Gas Science and Technology*, **2004**. *59*(5): p. 479-488.

Tanaka, R., Sato, S., Takanohashi, T., Hunt, J.E., and Winans, R.E., Analysis of the Molecular Weight Distribution of Petroleum Asphaltenes Using Laser Desorption-Mass Spectrometry. *Energy & Fuels*, **2004**. *18*(5): p. 1405-1413.

Wu, C.-s. and Editor, Handbook of Size Exclusion Chromatography. [In: Chromatogr. Sci. Ser., 1995; 69] 1995: Dekker. 463 pp.

PART IV: Post analytical processing for origin and reactivity determination of complex organic matter

La simplification des systèmes complexes par SEC-APPI-QTOF a permis d'obtenir de nombreuses informations complémentaires. Cependant la quantité d'informations obtenue reste très importante et donc difficile à interpréter, d'où la nécessité de développer des outils mathématiques post-processing. Le modèle SNAMS basé sur la combinaison d'une analyse numérique et statistique a permis de pouvoir comparer directement les spectres de masse entre eux et ainsi d'obtenir des informations sur l'origine des échantillons ainsi que sur les traitements physico-chimiques qu'ils ont subi. Ce modèle a, dans un premier temps, été appliqué avec succès aux asphaltènes qui présentent une polydispersité moindre que les échantillons bruts et pour lesquels le profil de distribution semble caractéristique du type d'échantillon. Le modèle a permis de distinguer les échantillons d'origines différentes ainsi que de suivre les processus d'oxydation.

Afin de tester les limites du modèle mathématique, le modèle SNAMS a ensuite été appliqué à des échantillons plus complexes de type matière organique dissoute (DOM). Les résultats ont montré qu'il était possible, avec ce type d'échantillons, de déterminer l'origine des échantillons, de suivre les processus d'altérations (traitements de remédiation), ainsi que de différencier certains protocoles expérimentaux (lixiviation versus percolation).

An easy and fast way to determine the origin of asphaltenes from SNAMS model

Thierry Ghislain[1], Coralie Biache[1], Pierre Faure[1], Julia Mainka[2], Laurence Mansuy-Huault[1], Aymeric Schumacher[1], Fatima Madhaoui[1], Raymond Michels[1]

Prepared for Environmental Science & Technology,

[1]G2R, Nancy-Université, CNRS, B.P. 239, 54506 Vandœuvre-lès-Nancy, France

[2]LEMTA, Nancy-Université, 2, avenue de la Forêt de haye F-54505 Vandœuvre-lès-Nancy

E-mail address: Thierry.Ghislain@g2r.uhp-nancy.fr

Abstract

The model developed in this study (SNAMS model) combines Principal Component Analysis (PCA) and a homemade algorithm. This model, based on APPI-QTOF mass spectrometry of asphaltenes, allows a direct comparison of mass spectra, as asphaltenes represent a lesses polydispersed system than original organic matter. The model developed here was set up in order to follow modifications in complex systems for which mass spectra can be hardly analyzed by a direct comparison. SNAMS model can distinguish asphaltenes from different types (petroleum and non petroleum samples). It can also highlight differences in close origin samples (petroleum samples between each other; ancient coking plant soil and its derivates, e.g. coal and coal tar). Ultimately, this model can follow physical and/or chemical modifications (e.g. oxidation).

1. Introduction

Complex organic matter and crude oils analysis have made an important step forward since ultra high resolution mass spectrometry (FT-ICR) (Marshall *et al.* 1998). This technique allows assignment of molecular formulas with high mass accuracy (Kim *et al.* 2006; Reemtsma 2009). Thus, comparison of samples, using Van Krevelen diagram (Van Krevelen 1950) which sometimes is complemented with C versus mass diagram called Kendrick mass defect diagrams (Kendrick 1963) have been applied to coal (Wu *et al.* 2004), crude oils (Hughey *et al.* 2001) and dissolved organic matter (DOM) (Kim *et al.* 2006).

However, many inconveniences such as background ions and polydispersity of molecules composing organic matter make mass spectra difficult to compare between each others. Moreover, direct comparison can be interesting, for a given sample, to determine the origin (by comparison with known samples or standards) and also to follow chemical or physical alterations such as oxidation (e.g. to follow the fate of organic pollutants or to measure efficiency of other alteration treatments). However, organic matter analyzed by mass spectrometry presents several hundred of peaks (using Q-TOF mass spectrometry) or several thousand of peaks (using FT-ICR mass spectrometry).

Recently, Hur *et al.* (2010) described a method using PCA and FT-ICR to point out similarities or differences between several oil samples (Hur *et al.* 2010). Multivariate statistical approaches have been also recently used on mass spectra obtained with FT-ICR mass spectrometry from DOM. This method used by Sleighter *et al.* (2010) (Sleighter *et al.* 2010) combined PCA and HCA (Hierarchical cluster analysis to underline the relationship in molecular composition of samples from different origins (i.e. DOM from terrestrial to marine along a transect) using average mass spectra parameters or relative magnitude combined to individual formulas. However, they conclude that the use of m/z ratios and corresponding intensities could simplify the statistical analysis.

Based on both observations, a mathematic model named SNAMS (Statistical and Numerical Analysis of Mass Spectra) was developed, based on m/z ratios and corresponding intensities from the direct analysis of samples by APPI-QTOF mass spectrometry. However instead of using original samples including all organic compounds soluble in chloroform, the SNAMS model is based on specific organic fraction (asphaltenes) mass spectra in order to reduce polydispersity of molecules. Thus, this model will explore if asphaltenes mass spectra can be used as fingerprint of a given sample. APPI was chosen according to analyzed samples which correspond to fossil organic matter mostly non functionalized and mostly aromatic and

so better sensitivity is achieved by APPI source (Ghislain *et al.* 2011). Moreover APPI allows the detection of either non polar or weakly polar organic compounds.

Characterization of asphaltenes has been widely described and summarized (Mullins 2007). Usually, ultrahigh resolution mass spectrometry can assign molecular formulas with high precision. However because of the very large number of detected compounds (more than 17 000 (Mullins 2007)), this method can be time-consuming and makes difficult to interpret mass spectra even if Kendrick mass defect plots or Van Krevelen diagram are used.

Based on previous considerations, we develop a mathematic model called SNAMS model, based on statistical and numerical treatments of APPI-QTOF mass spectra applied to asphaltenes. Ultimately, from unknown samples, asphaltenes are isolated by precipitation and then injected in APPI-QTOF. Then, two sub-programs: the NAMS sub-program (Numerical Analysis of Mass Spectrum) and the SAMS sub-program (Statistical Analysis of Mass Spectrum) are successively applied in order to classify asphaltenes by PCA treatments.

The aim of this paper is to evaluate the ability of the SNAMS model to distinguish asphaltenes from different origins (petroleum and coal) and classify samples from the same origin submitted to different alteration degrees.

2. Experimental Details

2.1. Samples

Several crude oil form Pechelbronn (France), Kurzai (Kazakhstan), Ivry (France) were investigated;

A coking plant soil was sampled in the ancient coking plant site from Homécourt (Lorraine, France) (Biache *et al.* 2011). In parallel, a coal (Merlebach, France) and a fresh coal tar from the Pyrolysis Center of Marienneau, France) were also investigated. These samples were then oxidized at 100°C in order to simulate a long term natural oxidation and evaluate the behaviour and fate of organic pollutants, i.e. PAH (Biache *et al.* 2011).

The organic extractions of the samples were carried out on 3 to 9g of samples, according to the TOC concentration, with an automated extractor Dionex ASE (Accelerated Solvent Extractor) 200 (dichloromethane (DCM), 130°C, 130bars). Asphaltenes were isolated by *n*-pentane precipitation during 15 minutes at ebullition temperature (~ 36°C) and recovery

by filtration on a glass microfiber filter (Watman GF/F) following ASTM classical protocol (ASTM D6560 - 00(2005) (Michels *et al.* 1996)).

All samples were diluted in chloroform at 1mg.mL^{-1}, and then diluted 10 times in a mixture of chloroform/benzene 70/30 v/v.

2.2. APPI-QTOF analysis conditions and recordation signal

In order to compare samples, all mass spectra were analyzed in identical conditions. Mass spectra were recorded on a hybrid Quadrupole – Time-Of-Flight mass spectrometer (Bruker Daltonics, Bremen, Germany) equipped with an Atmospheric Pressure PhotoIonisation (APPI) manufactured by Syagen (Syagen Technology Inc., Tustin, CA, USA), containing a Krypton lamp which produces a 10eV photon beam operating in positive mode. The sample was injected through a Hamilton syringe and the flow rate was set at 50µL/min by a syringe pump (Kd Scientific, USA). The source parameters were optimized in order to obtain the best signal to noise ratio (i.e. capillary voltage -4500V, end plate offset -500V). Nitrogen gas was maintained at 5bar for nebulisation and 3L.min^{-1} at 250°C for desolvatation, vaporizer temperature was set at 350°C.

2.3. DOPANS model

2.3.1. Special considerations for mass spectra

Mass spectra were recorded from 70 to 1500 Da for 1 min after Total Ion Current (TIC) stabilization at 1 spectrum/sec rate. Selected points from mass spectrum exclude ranges from 70 to 200 Da to remove many background ions due to the used of chloroform and benzene, and from 1000 to 1500 Da to remove useless points that overload the statistical software for the second range as, in our experiments, asphaltenes were not detected above 1000 Da. For each mass spectrum (200 to 1000 Da domain) background noise was set to 50 cps and below points were removed (Figure 1).

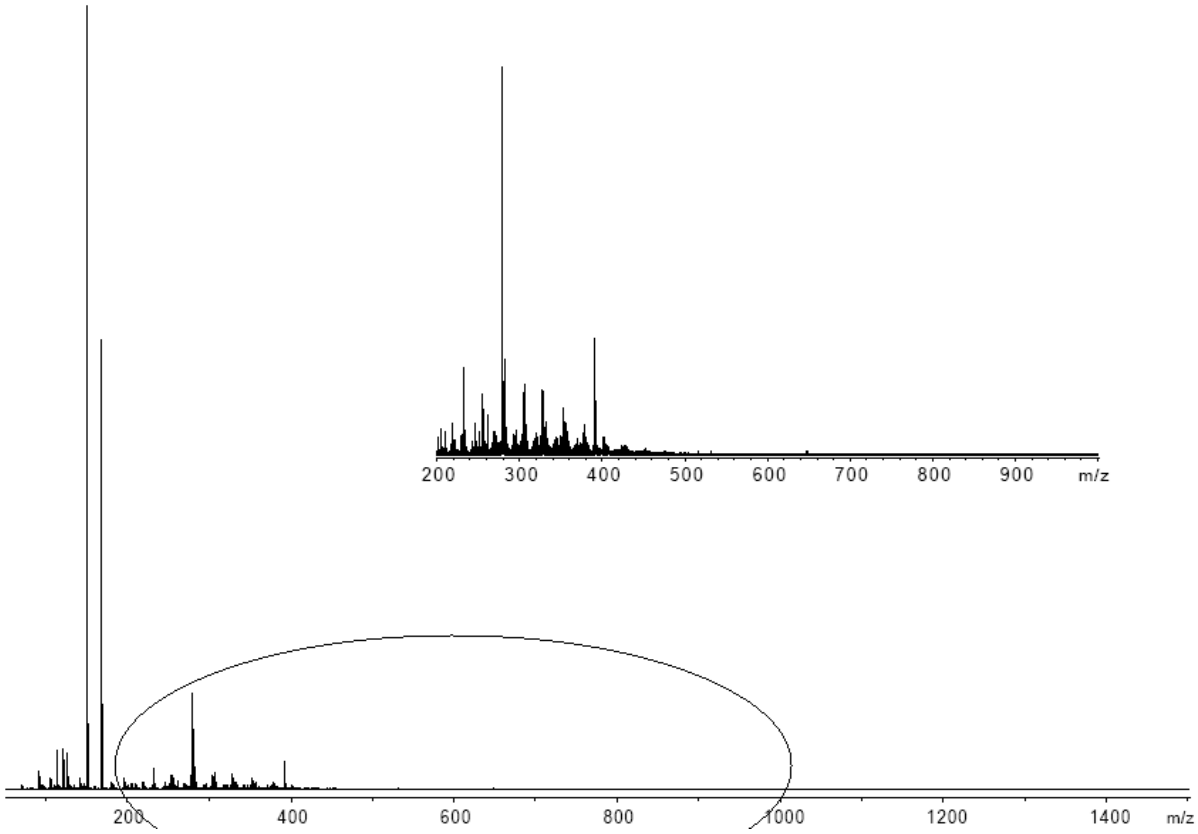

Figure 1: Selected mass spectrum from original mass spectrum acquisition of coal tar asphaltenes by APPI+-QTOF

Mass spectra were then analyzed by a homemade program using MATLAB to give a list of 8000 m/z ratios and corresponding intensities. Only 3 peaks were removed (in addition to isotopic peaks), which correspond to known pollution peaks.

2.3.2. NAMS program

This program is based on an algorithm edited with MATLAB software (Mathworks, Natick, Massachusetts, U.S.A). After APPI-QTOF analysis of asphaltene, the integral mass spectrum is imported to MATLAB (intensity in function of m/z ratio). An homemade algorithm allows (i) to remove perfectly known usual pollution peaks, (ii) to delete out of range points (selected range : 200 to 1000 Da) (Figure 1) and (iii) to select a list of identical m/z ratios for all samples, which is a necessary condition for PCA analysis. The selected list of m/z is obtained by summarizing all points above the background noise (i.e. 50 Da) every 0.1 Da. Tests were also performed using a step of 1 Da and 0.01 Da. To ensure that NAMS sub-program does not change the mass distribution shape, comparison between experimental mass spectrum and calculated mass spectrum are presented in Figure 2.

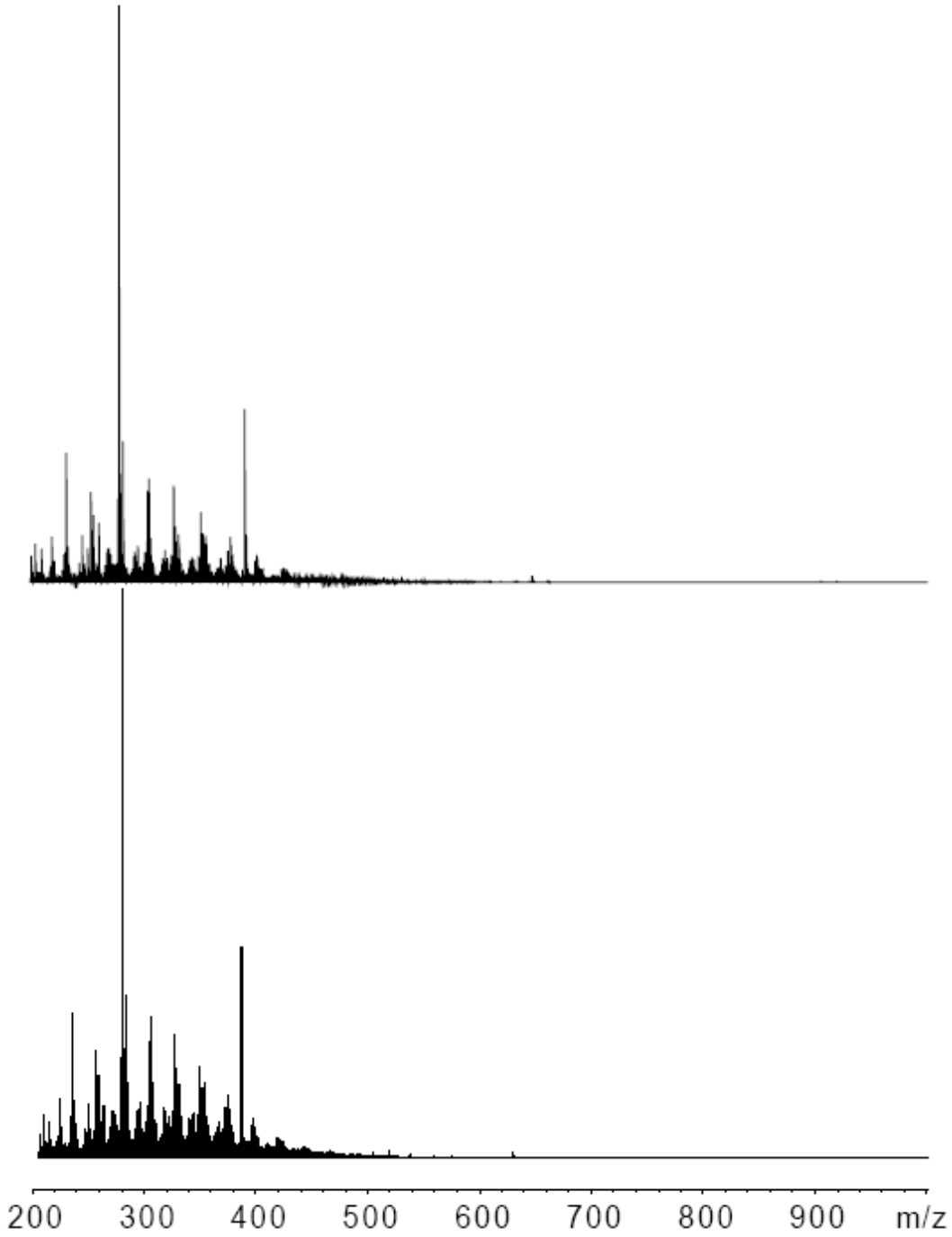

Figure 2: Comparison between experimental mass spectrum for coal tar asphaltenes and numerical mass spectrum obtained by DOPANS model

2.3.3. SAMS program

The new set of data previously obtained is directly analyzed by STATISCTICA software (StatSoft, Inc., Tulsa, Oklahoma, USA). Statistical treatments (Principal Components Analysis or Classification Analysis) were applied to point out the main

differences and similarities between mass spectra. A careful consideration should be made about statictical analysis as a necessary condition for comparison is that m/z ratios for all samples have to be identical.

3. Results and discussion

3.1. Discrimination of asphaltene origin by PCA analysis

The first set of data compares asphaltenes from different origins (Figure 3): crude oil-derived asphaltenes (i.e. Kurzai, Ivry and Pechelbronn) and non petroleum asphaltenes (i.e. from coking plant soil, coal and coal tar).

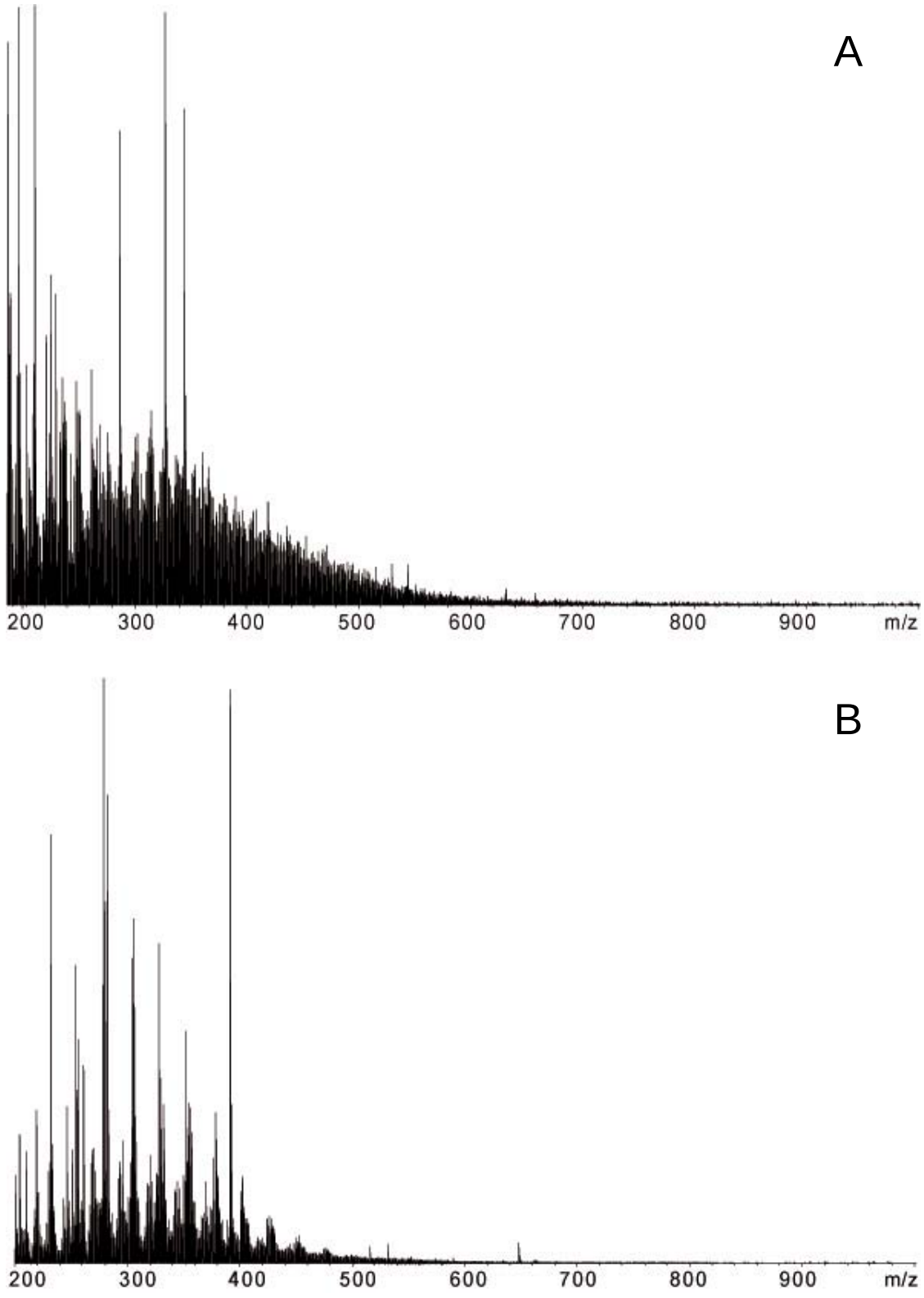
A
200
300
400
500
600
700
800
900
m/z
B
200
300
400
500
600
700
800
900
m/z

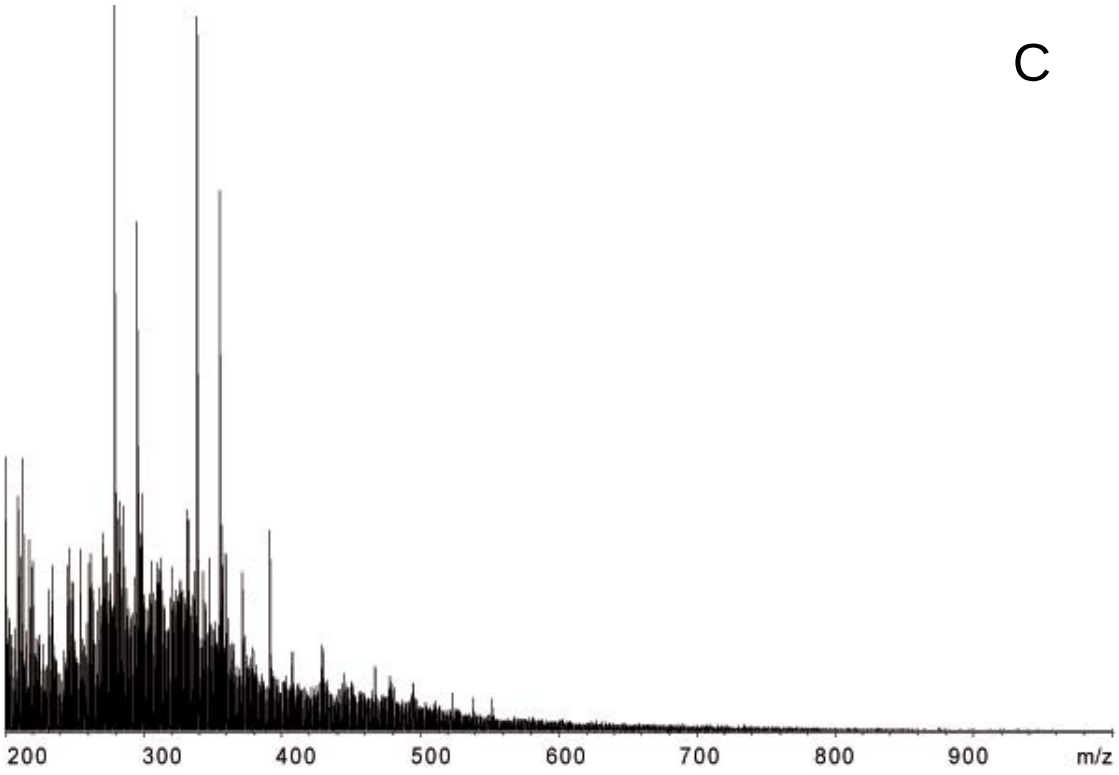
C
200
300
400
500
600
700
800
900
m/z

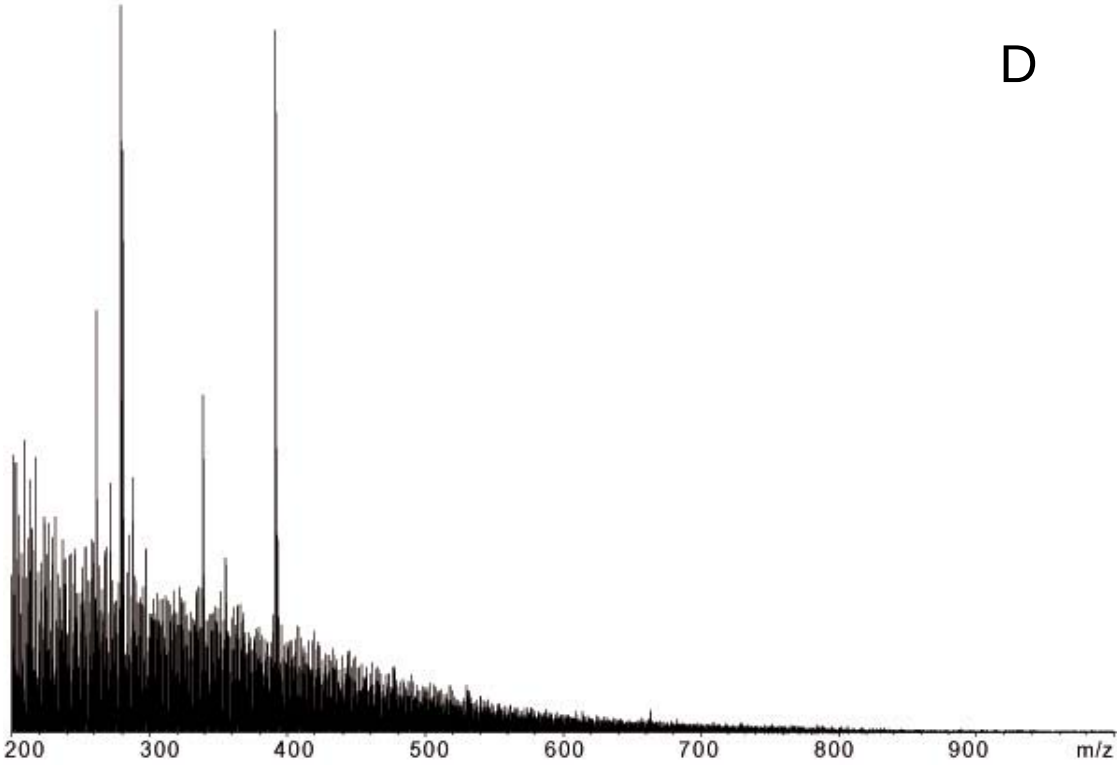
D
200
300
400
500
600
700
800
900
m/z

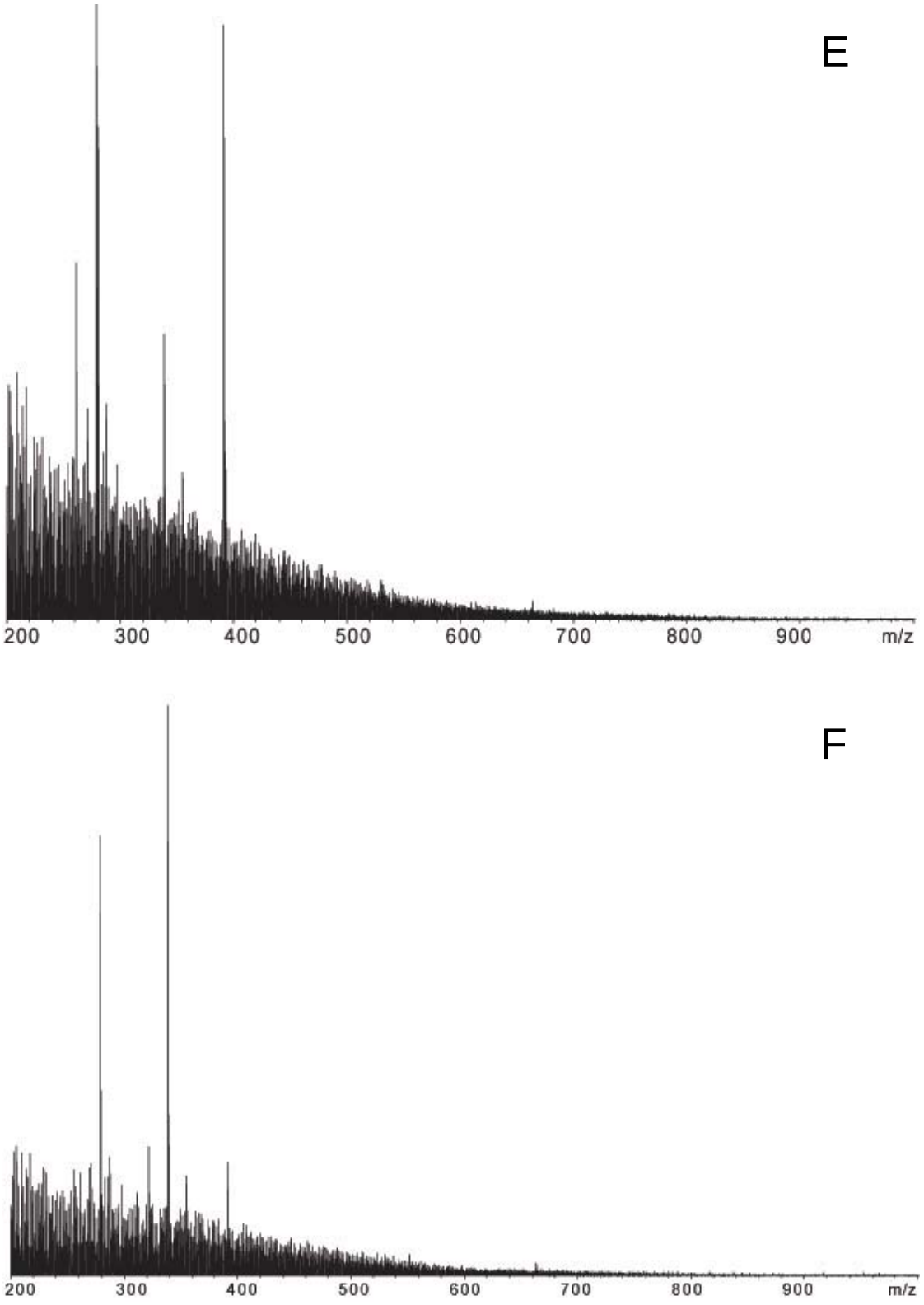

Figure 3: APPI+ mass spectrum of several asphaltenes in chloroform/benzene mixture 70/30 v/v. (A) coal asphaltenes, (B) coal tar asphaltenes, (C) coking plant soil asphaltenes, (D) Kurzai asphaltenes, (E) Ivry asphaltenes, (F) Pechelbronn asphaltenes.

On the correlation circle (Figure 4), axis 1 represents m/z ratios whereas axis 2 represents intensities. In that case, both axes represents 88.65% of the variance (factor 1: 58.36% and factor 2: 30.29%). Correlation is thus explained by both m/z ratios and intensities.

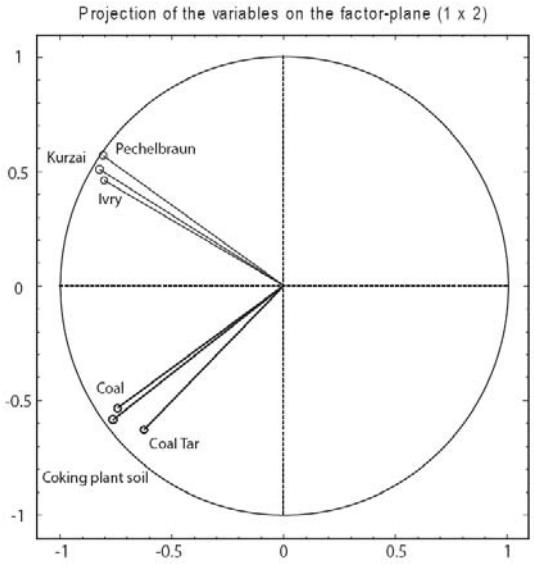

Figure 4: PCA using m/z ratios (1 digit used) determined with NAMS program and intensities for petroleum asphaltenes (Ivry, Pechelbronn, Kurzai) and soil asphaltenes (coal, coal tar, coking plant soil). Factor 1: 58.36%, factor 2: 30.29%; total points explained by PCA: 88.65%.

After analysis by SNAMS model, results revealed that two main groups of variables are distinguished (Figure 4). Asphaltenes from crude oils are highly correlated and located at the top left quarter of the correlation circle whereas those from coal sample derivatives, highly correlated too, are located at the bottom left quarter of the correlation circle. These two groups of parameters symmetrically disposed around factor 1 are then clearly uncorrelated. As m/z ratios were considered as individuals and the different samples considered as parameters, each m/z ratio corresponds to a linear combination of all samples.

Thus differences in these experiments are explained by (i) weaker intensities of low molecular mass compounds (i.e. below 300 Da) for non petroleum asphaltenes versus petroleum-derived asphaltenes (Figure 3) and (ii) by differences in m/z ratios, i.e. asphaltenes from coal derivatives which are strongly aromatic structures and crude oils which are less aromatic and more oxygenated structures; this undergoes to differences in m/z from the first digit which example is presented on Figure 5. As a consequence both groups should be uncorrelated which is shown on correlation circle by an angle between both groups close to 90°.

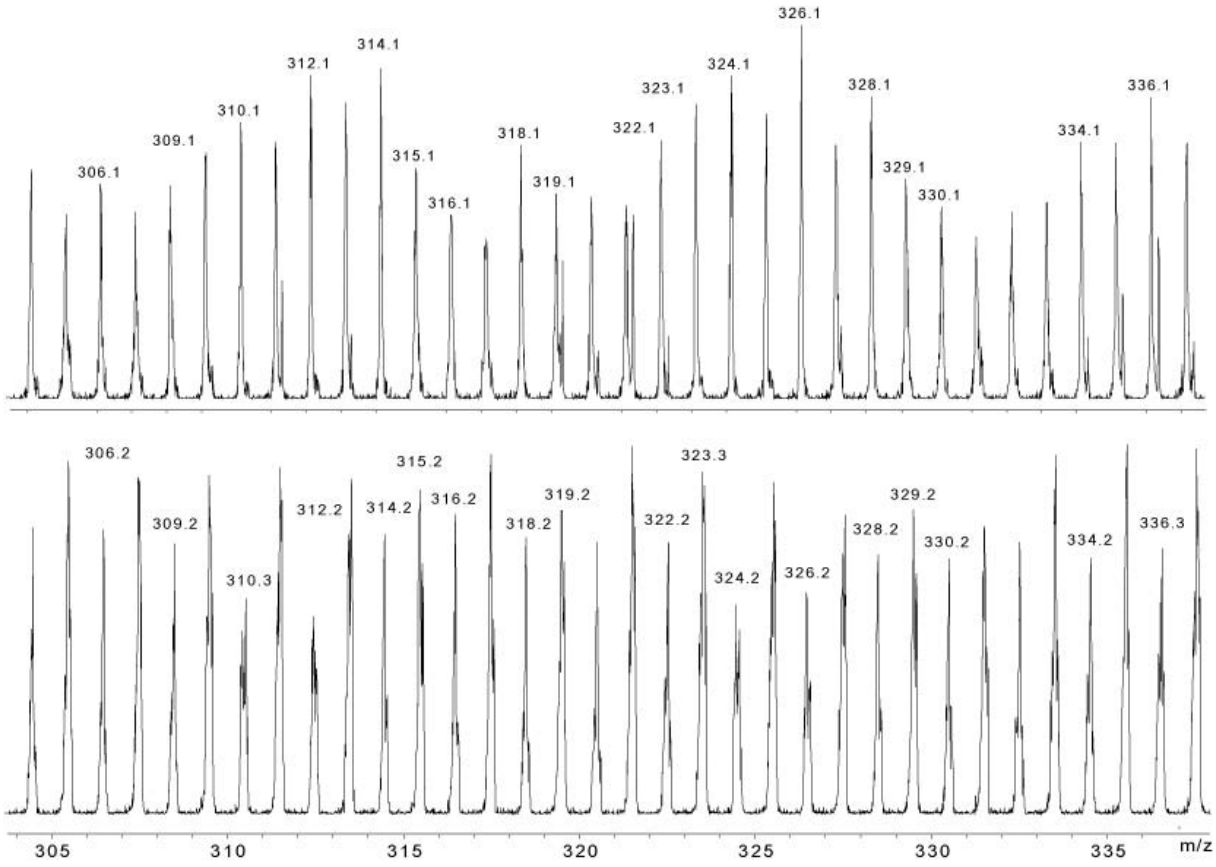

Figure 5: Comparison of APPI+ mass spectra in chloroform/benzene 70/30 solvent mixture of coal asphaltenes (top) and Kurzai petroleum asphaltenes (bottom).

3.2. PCA of asphaltenes from a coking plant soil

The following experiments analyzed samples derived from a coking plant. Asphaltenes from the coking plant soil were precipitated as its two main pollutant contributors, i.e. coal and coal tar (Biache *et al.* 2008; Biache *et al.* 2011). In this experiment, the model was tested in order to verify if the SNAMS model was able to correlate a polluted sample with its main contributors (Figure 6).

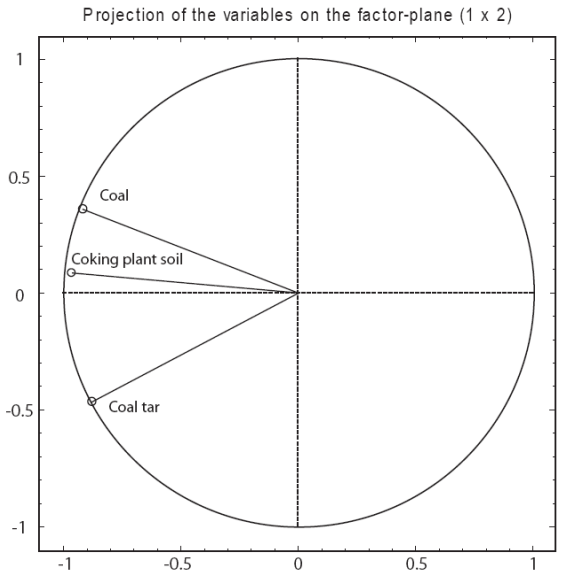

Figure 6: PCA using m/z ratios determined with NAAMS program and intensities for soil asphaltenes (coal, coal tar, coking plant soil). Factor 1: 84.92%, factor 2: 11.65%; total points explained by PCA: 96.57%.

Both axes represent 96.57% of the variance; however, factor 1 explains 84.92% whereas axis 2 represents 11.65%. This is mostly explained by the presence/absence of specific m/z ratios (as axis 1 explains nearly 85% of the variance), and in a lesser extent by differences of intensities for m/z represented in all samples (Figure 3). However, results clearly distinguish these three different samples and ultimately the coking plant soil plot is located between coal and coal tar plots, which confirm that asphaltenes from coking plant soil correspond to a mixture of asphaltenes from coal and coal tar.

3.3. PCA of asphaltenes from crude oils

When only comparing asphaltenes from crude oils (Figure 7) both axes represent almost all original points (i.e. 99.38%). Correlation is mainly explained by factor 1 (factor 1: 91.88%, factor 2: 7.50%). In fact, some m/z presence or absence explain the main differences between samples as direct comparison reveals strong similarities in the mass distribution shape. Ivry asphaltene plot is located is a different quarter of the correlation circle than Kurzai and Pechelbronn asphaltene plots.

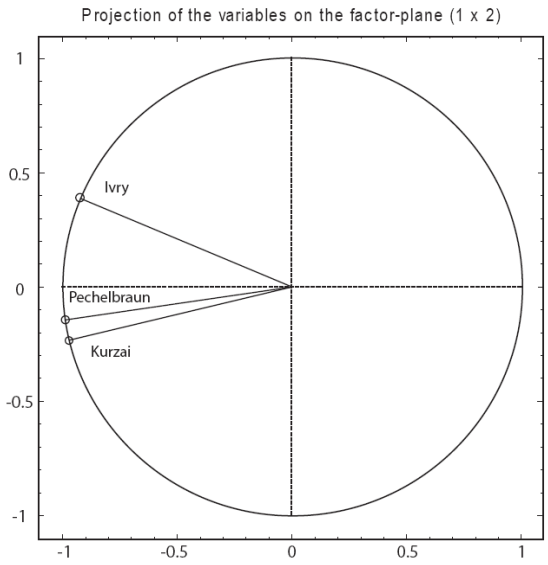

Figure 7: PCA using m/z ratios determined with NAAMS program and intensities for petroleum asphaltenes (Ivry, Pechelbronn, and Kurzai). Factor 1: 91.88%, factor 2: 7.50%; total points explained by PCA: 99.38%.

These results were unexpected as asphaltenes derived from Pechelbronn and Ivry come from the same sedimentary basin but they are not correlated. An explanation may come from the difference in crude oil sampling as Pechelbronn, and Ivry crude oils were sampled at different place and depth. Thus sensitivity of the model seems also to highlight some differences based on crude oil origin and thermal maturation degrees.

3.4. PCA of asphaltenes from coal, coal tar, coking plant soil and corresponding oxidized samples

In order to follow the fate of organic pollutants, coal, coal tar and coking plant soil were oxidized at low temperature for 6 months. Biache *et al.* (2010) (Biache *et al.* 2011) analyzed these samples by usual analytical method such as GC-MS, IR and GPC-HPLC to understand the main alterations processes as low-temperature oxidation is supposed to simulate the long-term fate of fossil organic matter (Faure *et al.* 1999; Elie *et al.* 2000)

The model was thus tested to check its ability to follow these chemical or physical modifications

SNAMS model results located non oxidized and oxidized samples at different parts of the correlation circle. In the case of coal and coal tar, non oxidized sample are located at the top left quarter of the correlation circle whereas oxidized samples are located at the bottom

left quarter of the correlation circle. Similar results were observed for the coking plant soil; however the non oxidized sample is located at the bottom left quarter of the circle and the oxidized samples at the top left quarter. For coal samples (Figure 8), 99.3% of total points are correlated (factor 1: 94.56%, factor 4.74%). The PCA analysis opposed the non oxidized sample in the quarter and oxidized samples in another quarter. Same observations are made for coal tar (Figure 9), with 97.77% of total points are correlated (factor 1: 88.86%, factor 2: 8.91%). For coking plant soil (Figure 10).

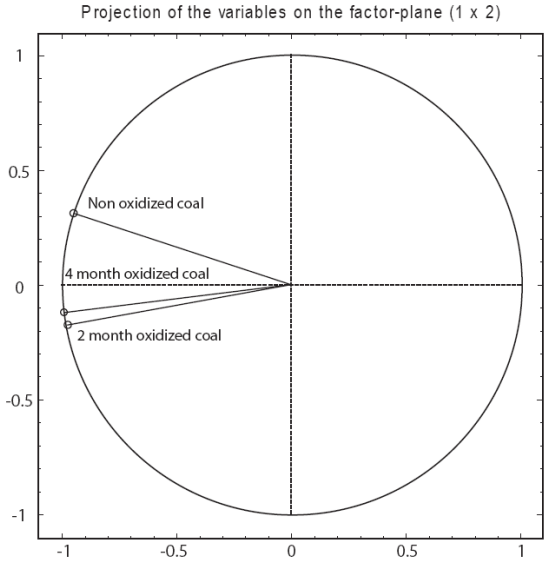

Figure 8: PCA using m/z ratios determined with NAAMS program and intensities for oxidation monitoring of coal asphaltenes. Factor 1: 94.56%, factor 2: 4.74%; total points explained by PCA: 99.3%.

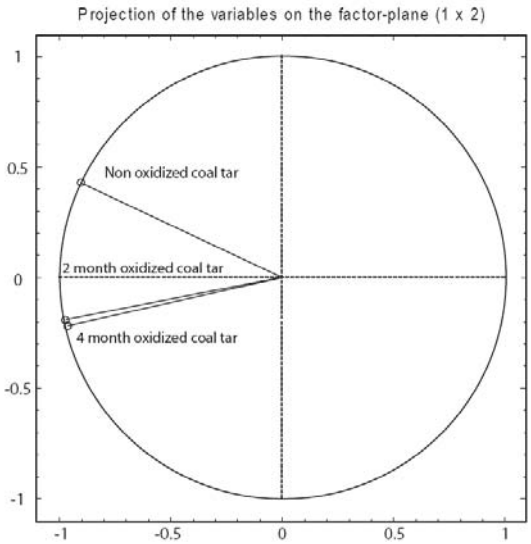

Figure 9: PCA using m/z ratios determined with NAAMS program and intensities for oxidation monitoring of coal tar asphaltenes. Factor 1: 88.86%, factor 2: 8.91%; total points explained by PCA: 97.77%.

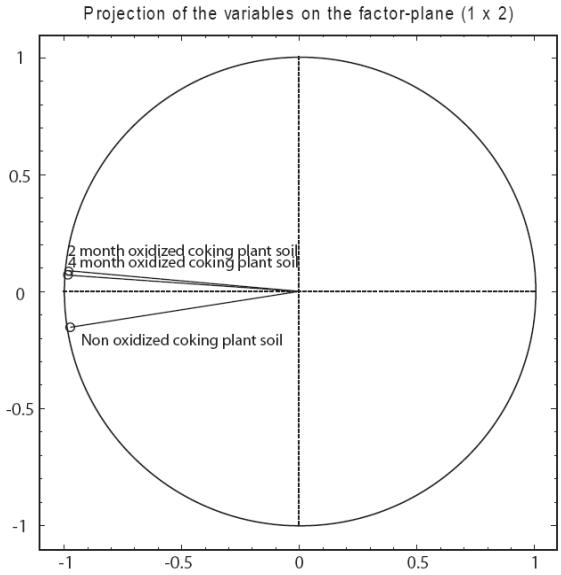

Figure 10: PCA using m/z ratios determined with NAAMS program and intensities for oxidation monitoring of coking plant soil asphaltenes. Factor 1: 98.54%, factor 2: 1.2%; total points explained by PCA: 99.74%.

The model results were then compared to those obtained by Biache *et al*. They noticed that for all samples, no strong differences were highlighted after two months; 2 and 4 months oxidation samples were considered as similar which was confirmed by the model.

3.5. Dendrogram

However in order to test the distinction power of the SNAMS model, all previous samples were analyzed simultaneously. Results were summarized in a dendogram (Figure 11).

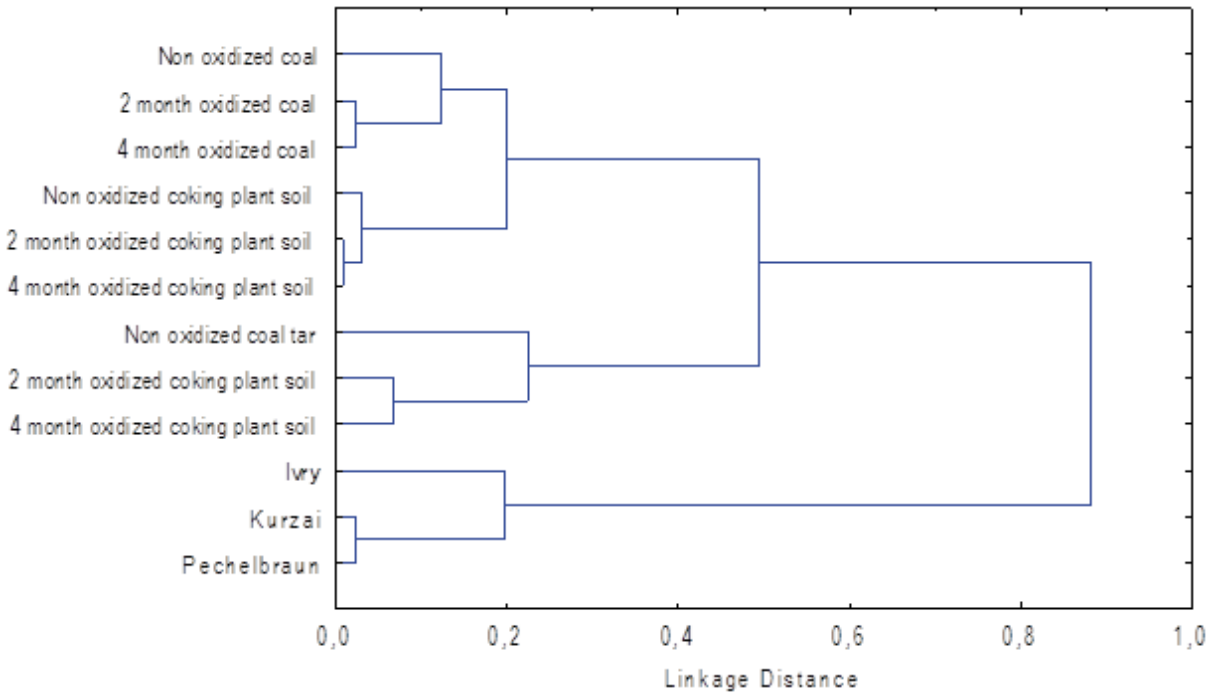

Figure 11: Dendrogram of all analyzed samples, complete linkage, 1-Pearson r

The dendogram reveals a complete distinction of all samples. From the right part of the dendogram to the left, the model resolves first petroleum and non petroleum samples, then a second and third level make the difference between similar samples (i.e. petroleum derived asphaltenes between each other and between coking plant soil, coal and coal asphaltenes. Ultimately the distinction is made between oxidized and non oxidized samples.

This model can thus be used as an easy and fast way to get information from an unknown sample for which asphaltenes can be isolated. The unknown sample can be analyzed with all previous samples which represent a calibration of the model and thus non correlated samples can be removed from the model to get more precise information as unknown sample will differently correlated to remaining known samples. Whereas the model takes into account general (i.e. non petroleum and petroleum derived asphaltenes) or specific samples (i.e. non oxidized and oxidized asphaltenes), the model seems to perfectly fit our samples since at least more than 88% of total points are explained by PCA and most of time this value is close to 99%.

3.6. Outline

Before exploitation of SNAMS model, considerations based on the number of digits to take in account were compared to determine the influence of the mass spectrometry resolution

on the SNAMS model. Experiments were run based only on integer others experiments considered 1 digit then 2 digits. Using integers for m/z ratios i.e. using NAMS sub program with a step of 1 Da and with a better resolution with a step of 0.01 Da are represented on Figure 12 and Figure 13 respectively. Results reveal that considering only integers was not enough to correlate all samples (Figure 12). On the correlation circle, samples are unsorted and no correct distinction was observed. Similar results are observed when considering 2 digits for m/z ratios. Too high resolution can lead to increase the statistical impact of background ions (Figure 13).

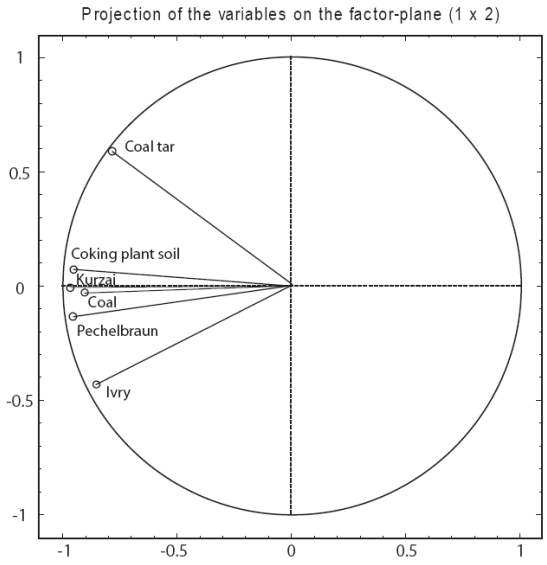

Figure 12: PCA using m/z ratios (0 digit used) determined with NAAMS program and intensities for petroleum asphaltenes (Ivry, Pechelbronn, Kurzai) and soil asphaltenes (coal, coal tar, coking plant soil). Factor 1: 82.75%, factor 2: 9.35%; total points explained by PCA: 92.1%.

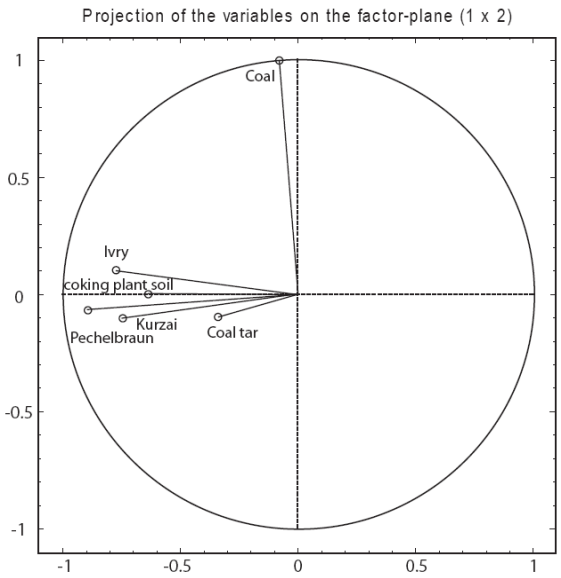

Figure 13: PCA using m/z ratios (2 digits used) determined with NAAMS program and intensities for petroleum asphaltenes (Ivry, Pechelbronn, Kurzai) and soil asphaltenes (coal, coal tar, coking plant soil). Factor 1: 41.02%, factor 2: 16.8%; total points explained by PCA: 57.82%.

4. Conclusion

SNAMS model has been able to distinguish petroleum derived asphaltenes versus non petroleum asphaltenes. The model also allows determining specific organic contributions (coal tar and coal) in a polluted soil (coking plant soil). Ultimately, SMANS model was able to distinguish fresh and altered asphaltenes.

The distinction efficiency of the model was maximum using 1 digit for m/z ratios for all samples, whereas the use of integers (low distinction power) or 2 digits (high influence of background ions) was not adapted.

5. References

Biache, C., Ghislain, T., Faure, P., and Mansuy-Huault, L., Low temperature oxidation of a coking plant soil organic matter and its major constituents: An experimental approach to simulate a long term evolution. *J. Hazard. Mater.*, **2011**. *188*(1-3): p. 221-230.

Biache, C., Mansuy-Huault, L., Faure, P., Munier-Lamy, C., and Leyval, C., Effects of thermal desorption on the composition of two coking plant soils: Impact on solvent extractable organic compounds and metal bioavailability. *Environ. Pollut.*, **2008**. *156*(3): p. 671-677.

Elie, M., Faure, P., Michels, R., Landais, P., and Griffault, L., Natural and laboratory oxidation of low-organic-carbon-content sediments: Comparison of chemical changes in hydrocarbons. *Energy Fuels*, **2000**. *14*(4): p. 854-861.

Faure, P., Landais, P., and Griffault, L., Behavior of organic matter from Callovian shales during low-temperature air oxidation. *Fuel*, **1999**. *78*(13): p. 1515-1525.

Ghislain, T., Faure, P., and Michels, R., Detection and Monitoring of PAH and Oxy-PAHs by High Resolution Mass Spectrometry: Comparison of ESI, APCI and APPI source detection. *Accpeted at Journal of the American Society for Mass Spectrometry*, **2011**.

Hughey, C.A., Hendrickson, C.L., Rodgers, R.P., Marshall, A.G., and Qian, K., Kendrick mass defect spectrum: A compact visual analysis for ultrahigh-resolution broadband mass spectra. *Anal. Chem.*, **2001**. *73*(19): p. 4676-4681.

Hur, M., Yeo, I., Park, E., Kim, Y.H., Yoo, J., Kim, E., No, M.H., Koh, J., and Kim, S., Combination of statistical methods and Fourier transform ion cyclotron resonance mass spectrometry for more comprehensive, molecular-level interpretations of petroleum samples. *Anal. Chem.*, **2010**. *82*(1): p. 211-218.

Kendrick, E., A mass scale based on CH2 = 14.0000 for high resolution mass spectrometry of organic compounds. *Anal. Chem.*, **1963**. *35*(13): p. 2146-2154.

Kim, S., Rodgers, R.P., and Marshall, A.G., Truly "exact" mass: Elemental composition can be determined uniquely from molecular mass measurement at ~0.1 mDa accuracy for molecules up to ~500 Da. *Int. J. Mass spectrom.*, **2006**. *251*(2-3): p. 260-265.

Marshall, A.G., Hendrickson, C.L., and Jackson, G.S., Fourier transform ion cyclotron resonance mass spectrometry: A primer. *Mass Spectrom. Rev.*, **1998**. *17*(1): p. 1-35.

Michels, R., Langlois, E., Ruau, O., Mansuy, L., Elie, M., and Landais, P., Evolution of asphaltenes during artificial maturation: A record of the chemical processes. *Energy Fuels*, **1996**. *10*(1): p. 39-48.

Mullins, O.C., Asphaltenes, heavy oils, and petroleomics 2007, New York: Springer. xxi, 669.

Reemtsma, T., Determination of molecular formulas of natural organic matter molecules by (ultra-) high-resolution mass spectrometry. Status and needs. *J. Chromatogr. A*, **2009**. *1216*(18): p. 3687-3701.

Sleighter, R.L., Liu, Z., Xue, J., and Hatcher, P.G., Multivariate statistical approaches for the characterization of dissolved organic matter analyzed by ultrahigh resolution mass spectrometry. *Environ. Sci. Technol.*, **2010**. *44*(19): p. 7576-7582.

Van Krevelen, D.W., Graphical-statistical method for the study of structure and reaction processes of coal. *Fuel*, **1950**. *29*(Copyright (C) 2011 American Chemical Society (ACS). All Rights Reserved.): p. 269-84.

Wu, Z., Rodgers, R.P., and Marshall, A.G., Two- and Three-Dimensional van Krevelen Diagrams: A Graphical Analysis Complementary to the Kendrick Mass Plot for Sorting Elemental Compositions of Complex Organic Mixtures Based on Ultrahigh-Resolution Broadband Fourier Transform Ion Cyclotron Resonance Mass Measurements. *Anal. Chem.*, **2004**. *76*(9): p. 2511-2516.

Application of SNAMS model to APPI-QTOF mass spectra from dissolved organic matter

Thierry Ghislain, Pierre Faure, Pascale Blanchart, Raymond Michels

Prepared for Environmental Science & Technology,

G2R, Nancy-Université, CNRS, B.P. 239, 54506 Vandœuvre-lès-Nancy, France

* Corresponding author. Tel.: +33 3 83 68 47 41; fax: +33 3 83 68 47 01.

E-mail address: Thierry.Ghislain@g2r.uhp-nancy.fr

Abstract

The aim of this article is to provide an easy and fast way to compare Dissolved Organic Matter (DOM) mass spectra without any pre-treatment except dilution in solvent for mass spectrometry analysis from fossil organic carbon. The SNAMS model which corresponds to an algorithm based on mass to charge ratios (m/z) and corresponding intensities obtained by APPI-QTOF mass spectrometry was evaluated on DOM. Statistical results allow (i) distinguishing different DOM origins and (ii) evaluating effects of alteration (oxidation).

.

1. Introduction

Dissolved organic matter corresponds to the principal ocean carbon sink (Hedges 2002). In a global scheme, molecular composition understanding is one of the key to predict geochemical sub-cycle behaviour (Mopper *et al.* 2007).

However, dissolved organic matter (DOM) is still difficult to analyse due to its very complex composition (chemical constitution and physical structure). Main development on DOM focuses on both extraction methodologies and characterizations mainly operated by mass spectrometry. Main difficulties come from DOM composition which corresponds to a complex polydispersed material containing molecules with different molecular masses, chemical functions and polarities.

Since ultrahigh resolution mass spectrometry (i.e. FT-ICR (Marshall *et al.* 1998)) and regardless of extraction method, many progresses have been done. Coupled to ElectroSpray Ionization (ESI), DOM originated from different aqueous systems have been widely characterized (Kujawinski 2002; Kujawinski *et al.* 2002; Kim *et al.* 2003; Kim *et al.* 2003; Kim *et al.* 2006; Kujawinski *et al.* 2009).

Atmospheric Pressure PhotoIonization (APPI) was also investigated as this source is more sensitive to non polar compounds but also less sensitive to salts, solvents and reduces ionization competition (Robb *et al.* 2000; Hanold *et al.* 2004; D'Andrilli *et al.* 2010).

Another challenge in DOM analysis is data post-processing. Recent works focus on finding mathematical methods for data interpretation (Grinhut *et al.* 2010; Reemtsma 2010) especially when a mass spectrum is obtained from FT-ICR mass spectrometry for which several thousand of compounds are detected due to ultrahigh resolution. Nowadays, Van Krevelen diagrams (Van Krevelen 1950) or Kendrick mass defect diagrams (Kendrick 1963) are usually used to compare mass spectra. Here, we propose an application of the SNAMS model previously described (Ghislain *et al.* 2011). This model was already applied to asphaltenes in order to (i) determine their origins and (ii) to follow physical/chemical alterations. This paper focuses on the application of this model to DOM from fossil organic matter in order to test the ability of the model SNAMS to distinguish DOM origins, and identify mass distribution modifications due to natural or artificial alterations.

2. Experimental Details

2.1. Samples

Polluted soil treatment

Solutions analyzed in this study correspond to gravity-fed water obtained from polluted soil originated from an ancient coking plant soil. Soil was taken and isolated in a lysimeter (LXX) at the GISFI experimental station. Percolation water from three different lysimeter columns (2m of deep and 1m² surface) were collected at several times. These lysimeters contain soil from an ancient coking plant site and exhibit a high contamination by polycyclic aromatic hydrocarbons (~ 1500 µg.g^{-1} of dry soil) inherited from coal tar and coal. Lysimeter column L6 correspond to the reference whereas on L9 and L11 lysimeter column were applied an ISCO (in situ chemical oxidation) treatment corresponding to a Fenton oxidation. This treatment implies a successive injection of hydroperoxyde (H_2O_2) and iron sulphate. The Fenton oxidation was carried out during four days. At the end of the treatment, 380 L of hydrogen peroxide and iron sulphate were injected in the column and 333 L (L09) and 360 L (L11) of percolation solutions were collected. In the reference lysimeter (L06), only water in the same proportion (380 L) was injected and 345 L of percolation solution were recovered.

During this treatment, we collected initial solutions (first solution collected) from the different lysimeters (L06-PI, L09-PI and L11-PI) and after the end of the injection (L09-PF and L11-PF). Evolutions of molecular compositions of water samples were followed by mass spectrometry.

MOL underground laboratory

The samples were divided in two series**:**

A natural series constituted by three samples with different degree of oxidized were collected in the underground laboratory of Mol (Belgium). These samples were air exposed in the gallery during increasing times

An artificial serie: An oxidation experiment was lead in fresh block of Boom clay. This clay was oxidized artificially during 18 months at 80°C in oven. The steps studied in this paper are T0, 6 and 18 months.

Each sample was extracted with leaching of clay in glove boxes without oxygen. 5g of clay were suspended and agitated in 30ml Synthetic Boom Clay Water (SBCW) during 4 days. SBCW is water with a known concentration of ions and pH fixed to 8.4. Each sample was filtered by 0.45µm filters before analyses.

2.2. Samples preparation

Samples were diluted 5 times in a methanol/benzene mixture (1/8.5 v/v) adapted from D'andrilli *et al.* *(D'Andrilli et al. 2010)*. 100µL of the sample was add to 200µL of benzene and 1700µL of methanol and stirred for 1 min.

2.3. Mass Spectrometry

Molecular mass distributions were recorded on a hybrid Quadrupole – Time-Of-Flight mass spectrometer (Bruker Daltonics, Bremen , Germany) equipped with an Atmospheric Pressure Photoionisation (APPI) manufactured by Syagen (Syagen Technology Inc., Tustin, CA, USA), containing a Krypton lamp which produces a 10eV photon beam operating in positive mode. The source parameters were optimized and set at: capillary voltage -4500V, end plate offset -500V. Nitrogen gas was maintained at 5bar for nebulisation and 3L.min^{-1} at 250°C for desolvatation, vaporizer temperature was set at 350°C. Data acquisition was performed for 1 min at 1 spectrum/sec after TIC stabilization.

2.4. SNAMS model

SNAMS model: The model previously describes elsewhere (Ghislain *et al.* 2011) is an algorithm that standardized mass spectrum (i.e. by creating a list identical m/z and corresponding intensities) before a Principal Component Analysis (PCA). Thus a matrix of several samples is obtained allowing correlation of an unknown sample to existing samples in the model.

3. Results and Discussion

3.1. PCA of DOM samples

Different DOM samples were analyzed by APPI-QTOF mass spectrometry (Figure 14 to Figure 19). Due to the presence of many ions, it was difficult and time consumed to directly compare samples

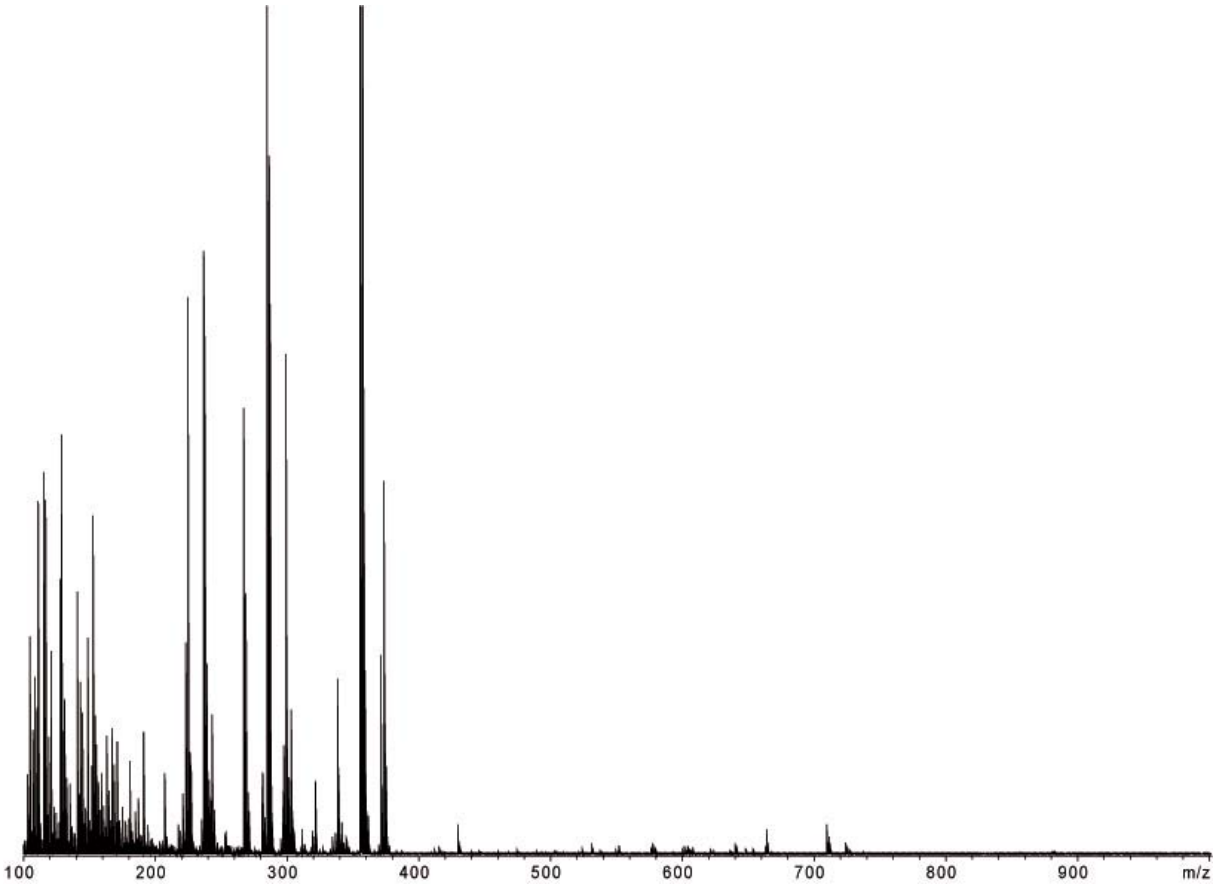

Figure 14: APPI+ mass spectrum of L06-PI recorded in a methanol/benzene mixture 1/8.5 v/v from 100 to 1000Da

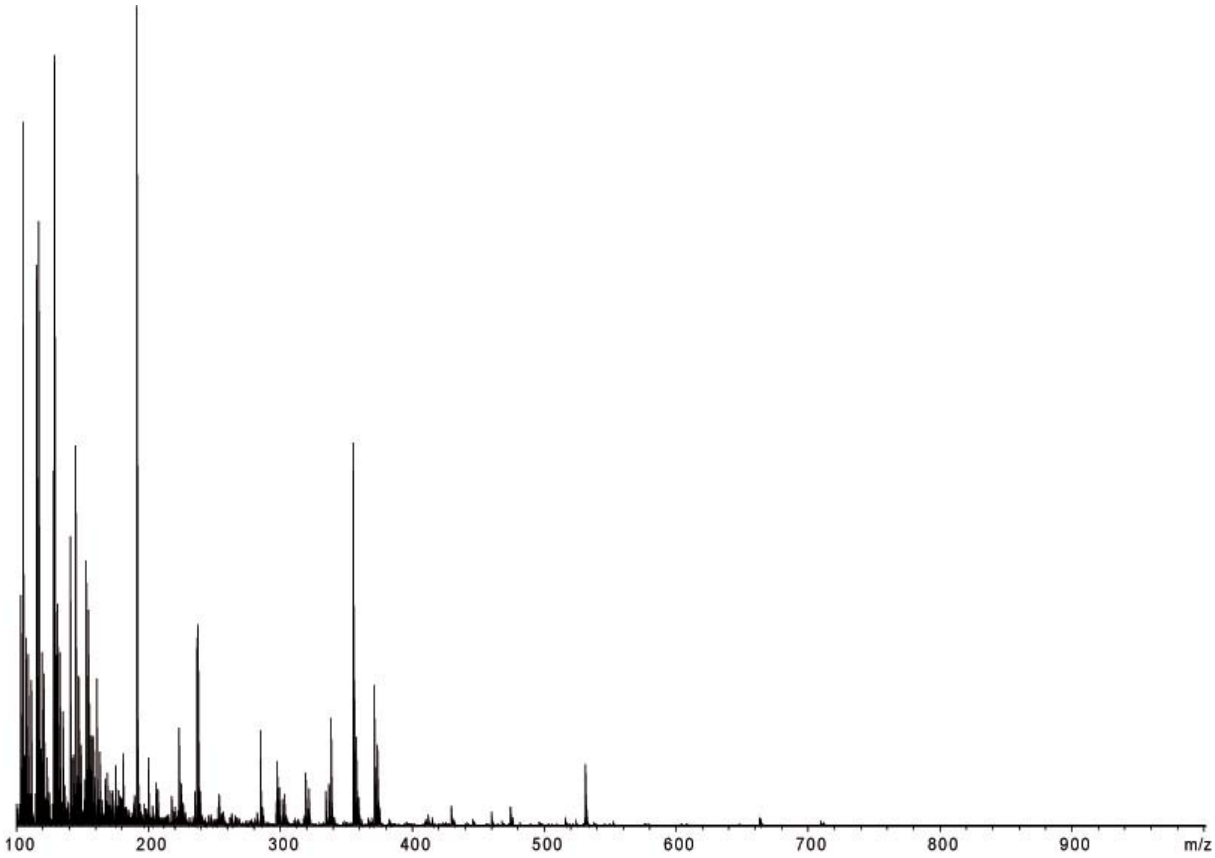

Figure 15: APPI+ mass spectrum of L11-PF recorded in a methanol/benzene mixture 1/8.5 v/v from 100 to 1000Da

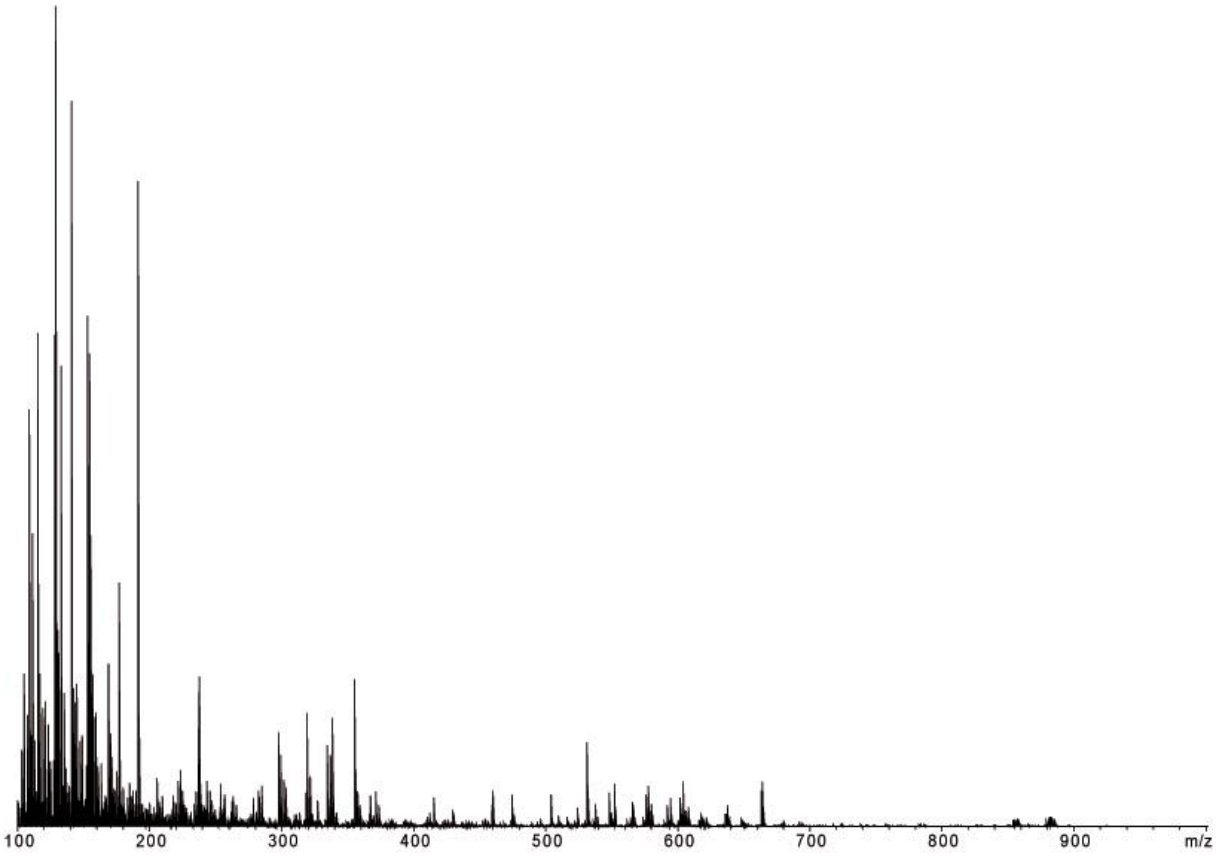

Figure 16: APPI+ mass spectrum of Gal-1 recorded in a methanol/benzene mixture 1/8.5 v/v from 100 to 1000Da.

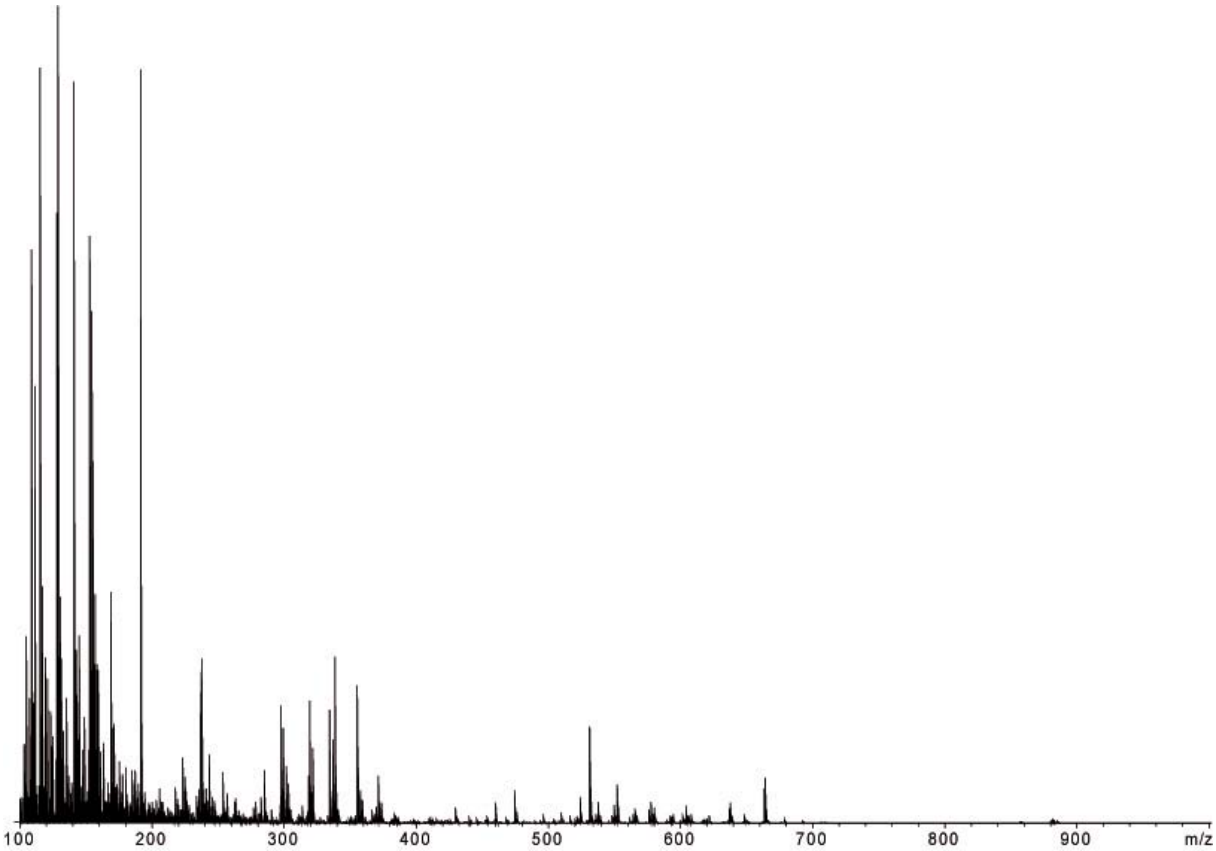

Figure 17: APPI+ mass spectrum of Gal-5 recorded in a methanol/benzene mixture 1/8.5 v/v from 100 to 1000Da

Figure 18: APPI+ mass spectrum of Gal-Ox-0 recorded in a methanol/benzene mixture 1/8.5 v/v from 100 to 1000Da

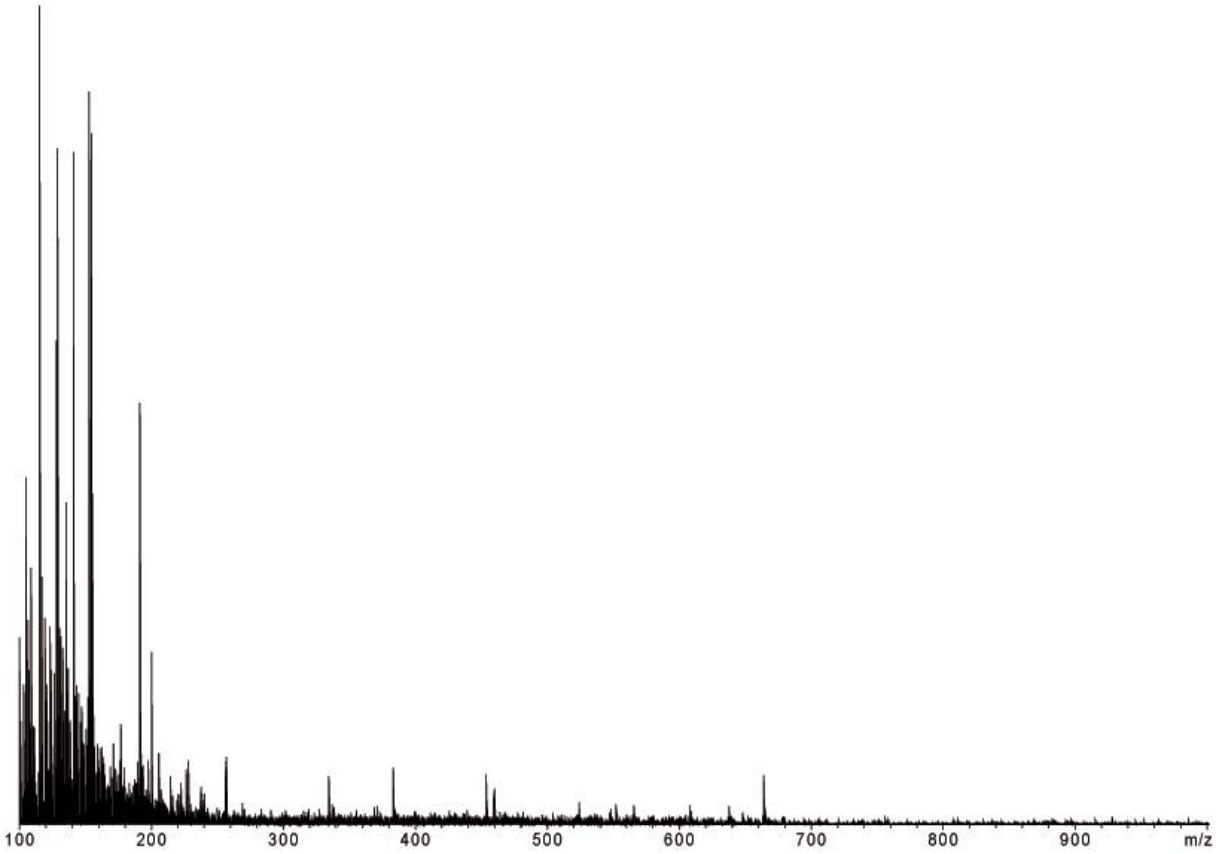

Figure 19: APPI+ mass spectrum of Gal-Ox-18 recorded in a methanol/benzene mixture 1/8.5 v/v from 100 to 1000Da

Thus, mass spectra were analyzed by SNAMS model in order to point out similarities and discrepancies. Results reveal that two main groups are distinguished, located into 2 different quarters in the correlation circle au-dessous. DOM samples originated from the GISFI experimental station are located at the top left quarter whereas DOM samples from the underground laboratory of Mol (Belgium) are located at the left opposite quarter. Correlation factors obtained (factor 1: 61.81%, factor 2: 24.17%) reveal that 85.98% of initial points explain the main differences between these 2 groups. Figure 20 reveals that SNAMS model is able to differentiate DOM obtained by different ways. DOM samples from the experimental station were obtained by percolation whereas DOM samples from experimental underground laboratory were obtained by lixiviation, this is also confirmed by direct comparison of mass spectra as they appear different, however the model highlights how strongly different are the mass spectra. On the contrary to results observed previously for asphaltenes (Ghislain *et al.* 2011), ions which allow distinguishing mass spectrum are mainly within the range of 100 to 300 Da.

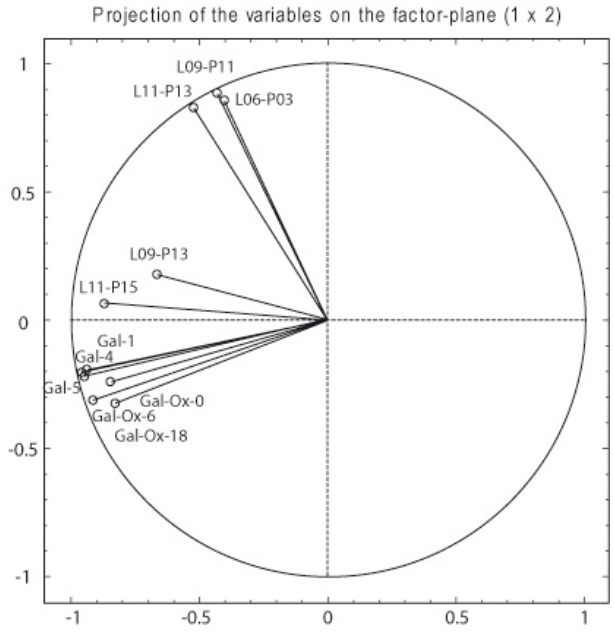

Figure 20: PCA using m/z ratios and corresponding intensities determined by SNAMS model for several DOM samples. Factor 1: 61.81%, factor 2: 24.17%; total points explained by PCA: 85.98%

3.2. PCA of DOM samples from GISFI experimental station

In order to determine the efficiency of the recovery treatments applied to polluted soils at the GISFI experimental station, lixiviates of the different lysimeters were taken at different times and were directly analyzed by APPI-QTOF mass spectrometry then by SNAMS model.

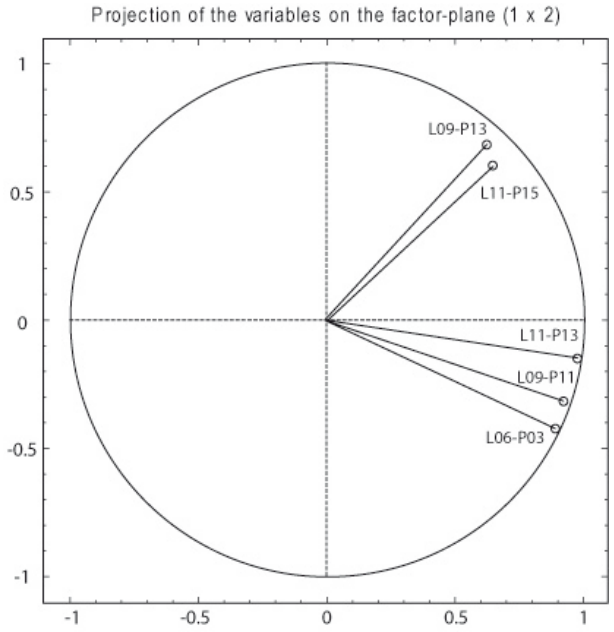

Figure 21: PCA using m/z ratios and corresponding intensities determined by SNAMS model for DOM samples from lysimeters (GISFI experimental station). Factor 1: 68.90%, factor 2: 22.56%; total points explained by PCA: 91.46%

Figure 21 present the SNAMS model results for only DOM from experimental station. The correlation circle reveals a distinction of the 5 different samples (factor 1: 68.90% and factor 2: 22.56%) with a correlation of 91.46%. 2 groups can be highlighted: the 1st group (L06-P03, L09-PI and L11-PI) is located at the right bottom part of the circle and the 2nd group (L09-PF and L11-PF) is locate at the right top quarter of the circle. Results were satisfactory as they follow an evolution starting from L06-PI to L09-PF. SNAMS model applied to GISFI DOM samples confirms an evolution from the untreated reference polluted soil until the late taken (L11-PF and L09-PF). These results allow to follow evolution of the detected organic molecules (with APPI source) and to follow the activity of soil recovery treatment.

3.3. PCA of DOM samples from Mol underground laboratory

Results of SNAMS model for DOM samples from Mol underground laboratory are presented on Figure 22. Correlation circle presents mainly 2 different groups, i.e. 1st group composed of Gal-1, Gal-4, Gal-5 and Gal-Ox-0 located at the top left quarter of the circle. A 2nd group located at the left bottom quarter of the circle is composed of Gal-Ox-6 and Gal-Ox-18. Total points explained by SNAMS model correspond to 94.2% of initial points.

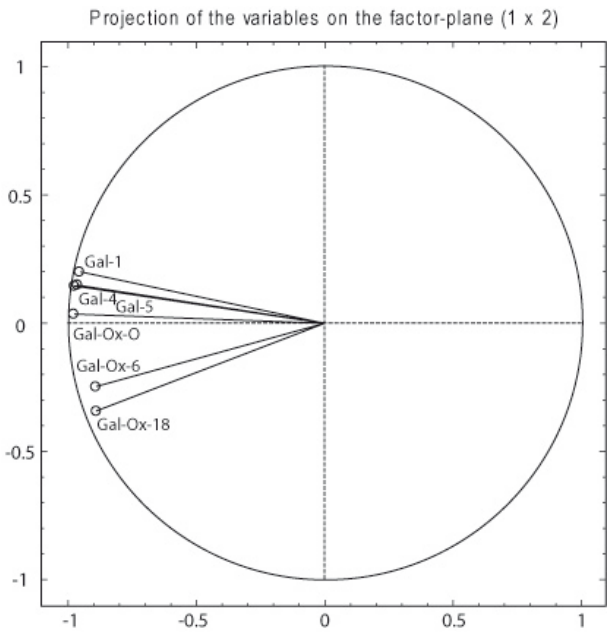

Figure 22: PCA using m/z ratios and corresponding intensities determined by SNAMS model for several DOM samples. Factor 1: 89.85%, factor 2: 4.35%; total points explained by PCA: 94.2%

The first group corresponds to lixiviate obtained from clay taken at different place and depth. According to plot positions on the correlation circle, no strong differences are observed between Gal-1, 4, 5 and Gal-Ox-O These results were confirmed by fluorescence experiments which reveal no strong differences between these DOM samples. A small difference can be seen on the correlation circle between Gal-1, 4, 5 and Gal-Ox-O as clays were taken in different parts of the underground gallery. On the contrary Gal-Ox-O and the group composed of Gal-Ox-6 and 18 are located at different parts on the correlation circle. This is explained as Gal-Ox-O was not oxidized, Gal-Ox-6 and 18 were oxidized for 6 and 18 months. This confirms the ability of SNMAS model to follow oxidation alterations as it has been previously proved for asphaltenes.

3.4. Dendrogram

Dendrogram presented on Figure 23 summarized previous results. The linkage distances versus DOM samples show different are mass spectra. The highest linkage distances (the 3 first stages) allow to separate DOM samples obtained by either lixiviation or percolation. Then following stages make more precised distinctions such as untreated reference polluted soil versus treated polluted soil. It was also possible to highlight the homogeneity of the underground laboratory wall composed mainly of clay as Gal-1, 4, 5 and Gal-Ox-0 are nearly correlated, whereas oxidized samples (Gal-Ox-6 and Gal-Ox-18) where not correlated to non-oxidized sample. The model has proved again its ability to distinguish very different and close type mass spectra.

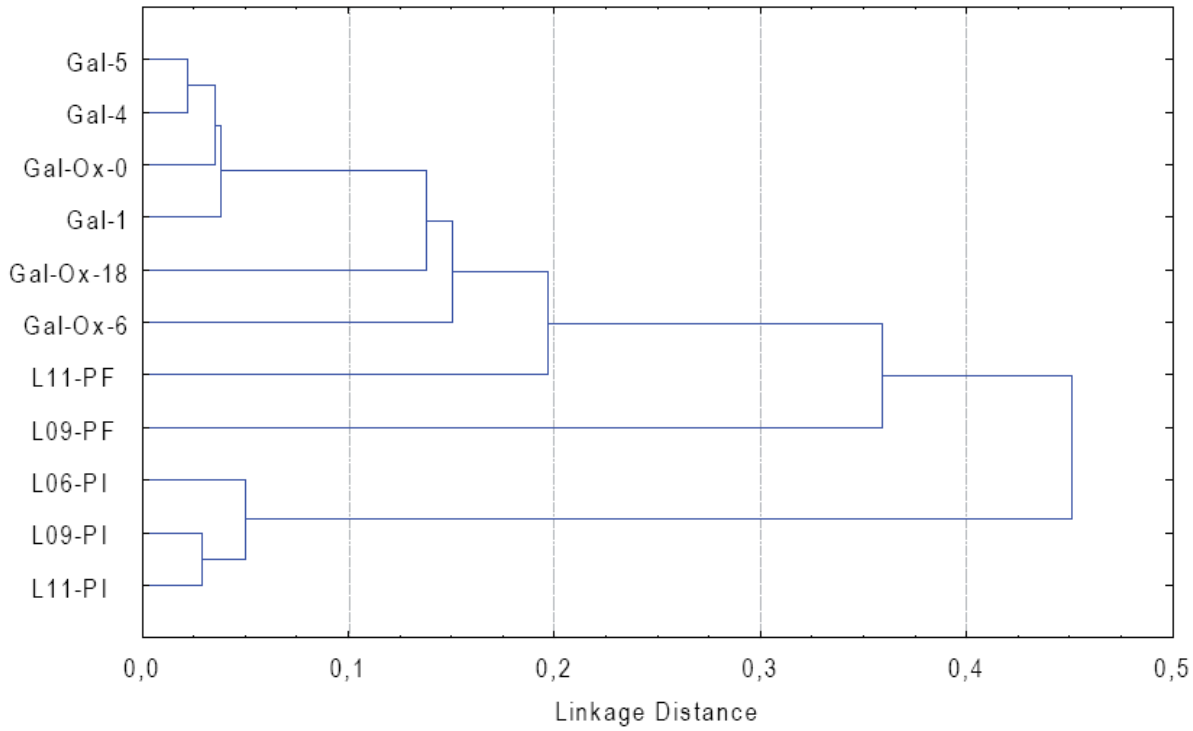

Figure 23: Dendrogram of all previous samples, complete linkage, 1-pearson r

4. References

D'Andrilli, J., Dittmar, T., Koch, B.P., Purcell, J.M., Marshall, A.G., and Cooper, W.T., Comprehensive characterization of marine dissolved organic matter by fourier transform ion cyclotron resonance mass spectrometry with electrospray and atmospheric pressure photoionization. *Rapid Commun. Mass Spectrom.*, **2010**. *24*(5): p. 643-650.

Ghislain, T., Biache, C., Faure, P., Mainka, J., Schumacher, A., Madhaoui, F., and Michels, R., An easy and fast way to determine the origin of asphaltenes from SNAMS model. *Environ. Sci. Technol.*, **2011**. *Submitted*.

Grinhut, T., Lansky, D., Gaspar, A., Hertkorn, N., Schmitt-Kopplin, P., Hadar, Y., and Chen, Y., Novel software for data analysis of Fourier transform ion cyclotron resonance mass spectra applied to natural organic matter. *Rapid Commun. Mass Spectrom.*, **2010**. *24*(19): p. 2831-2837.

Hanold, K.A., Fischer, S.M., Cormia, P.H., Miller, C.E., and Syage, J.A., Atmospheric pressure photoionization. 1. General properties for LC/MS. *Anal. Chem.*, **2004**. *76*(10): p. 2842-2851.

Hedges, J.I., Why Dissolved Organics Matter, in *Biogeochemistry of Marine Dissolved Organic Matter*, A.H. Dennis and A.C. Craig, Editors. 2002, Academic Press: San Diego. p. 1-33.

Kendrick, E., A mass scale based on CH2 = 14.0000 for high resolution mass spectrometry of organic compounds. *Anal. Chem.*, **1963**. *35*(13): p. 2146-2154.

Kim, S., Kaplan, L.A., and Hatcher, P.G., Biodegradable dissolved organic matter in a temperate and a tropical stream determined from ultra-high resolution mass spectrometry. *Limnol. Oceanogr.*, **2006**. *51*(2): p. 1054-1063.

Kim, S., Kramer, R.W., and Hatcher, P.G., Graphical Method for Analysis of Ultrahigh-Resolution Broadband Mass Spectra of Natural Organic Matter, the Van Krevelen Diagram. *Anal. Chem.*, **2003**. *75*(20): p. 5336-5344.

Kim, S., Simpson, A.J., Kujawinski, E.B., Freitas, M.A., and Hatcher, P.G., High resolution electrospray ionization mass spectrometry and 2D solution NMR for the analysis of DOM extracted by C18 solid phase disk. *Org. Geochem.*, **2003**. *34*(9): p. 1325-1335.

Kujawinski, E.B., Electrospray ionization Fourier transform ion cyclotron resonance mass spectrometry (ESI FT-ICR MS): Characterization of complex environmental mixtures. *Environmental Forensics*, **2002**. *3*(3-4): p. 207-216.

Kujawinski, E.B., Hatcher, P.G., and Freitas, M.A., High-resolution fourier transform ion cyclotron resonance mass spectrometry of humic and fulvic acids: Improvements and comparisons. *Anal. Chem.*, **2002**. *74*(2): p. 413-419.

Kujawinski, E.B., Longnecker, K., Blough, N.V., Vecchio, R.D., Finlay, L., Kitner, J.B., and Giovannoni, S.J., Identification of possible source markers in marine dissolved organic matter using ultrahigh resolution mass spectrometry. *Geochim. Cosmochim. Acta*, **2009**. *73*(15): p. 4384-4399.

Marshall, A.G., Hendrickson, C.L., and Jackson, G.S., Fourier transform ion cyclotron resonance mass spectrometry: A primer. *Mass Spectrom. Rev.*, **1998**. *17*(1): p. 1-35.

Mopper, K., Stubbins, A., Ritchie, J.D., Bialk, H.M., and Hatcher, P.G., Advanced instrumental approaches for characterization of marine dissolved organic matter: Extraction techniques, mass spectrometry, and nuclear magnetic resonance spectroscopy. *Chem. Rev.*, **2007**. *107*(2): p. 419-442.

Reemtsma, T., The carbon versus mass diagram to visualize and exploit FTICR-MS data of natural organic matter. *J. Mass Spectrom.*, **2010**. *45*(4): p. 382-390.

Robb, D.B., Covey, T.R., and Bruins, A.P., Atmospheric pressure photoionization: An ionization method for liquid chromatography-mass spectrometry. *Anal. Chem.*, **2000**. *72*(15): p. 3653-3659.

Van Krevelen, D.W., Graphical-statistical method for the study of structure and reaction processes of coal. *Fuel*, **1950**. *29*(Copyright (C) 2011 American Chemical Society (ACS). All Rights Reserved.): p. 269-84.

Conclusions & Perspectives

Conclusions

L'étude de la matière organique complexe en géochimie organique s'est rapidement retrouvée confrontée aux limitations des techniques les plus fréquemment utilisées (GC-MS, HPLC…). En effet, l'utilisation ces techniques ne permet pas de caractériser les composés très polaires et notamment ceux de hautes masses moléculaires. De nos jours, suivre l'anthropisation grandissante des environnements superficiels par le seul suivi des contaminants organiques classiques, issus de la matière organique fossile (généralement dosés par GC-MS ou HPLC) n'est pas satisfaisant. En effet, l'étude du devenir et de la réactivité de la matière organique complexe dans sa globalité (incluant les macromolécules) ne peut être abordée par une telle approche restrictive. Cependant, la matière organique et plus largement les systèmes macromoléculaires sont particulièrement difficiles à caractériser du fait du très grand nombre de molécules, de tailles et de fonctions chimiques différentes. Toutefois des efforts doivent être fait en ce sens car ces systèmes macromoléculaires (i) sont constitués de structures pouvant présenter des effets tout aussi nocifs que les composés généralement suivis tant pour l'environnement que pour les processus de raffinage du pétrole, (ii) présentent des affinité pour certains métaux (par exemple le rhénium et l'osmium pouvant servir de géochronomètre dans un contexte pétrolier, ou des métaux lourds dans le cas de sites contaminés) (iii) sont des intermédiaires réactionnels majeurs aussi bien dans les contextes pétroliers qu'en environnement (incorporation et/ou vecteur de contaminants suivant leur nature et leur degré d'altération).

Ainsi, ce travail de thèse s'est articulé suivant différentes étapes complémentaires pour aborder la matière organique macromoléculaire : adaptation des conditions analytiques à la

matière organique fossile, développement du couplage SEC-APPI-QTOF et traitement post-processing des spectres de masse.

Adaptation des conditions analytiques pour la matière organique fossile

Dans un premier temps, nous avons cherché à déterminer les meilleures conditions analytiques à appliquer au spectromètre de masse (Q-TOF) afin d'étudier les composés peu polaires et de hautes masses moléculaires. La comparaison de l'efficacité des différentes sources d'ionisation à pression atmosphérique pour l'analyse de composés peu polaires (HAPs et oxy-HAPs) nous a permis de sélectionner la photoionisation à pression atmosphérique (APPI) comme source d'ionisation la plus adaptée.

Grâce à cette adaptation des conditions analytiques, il a été possible d'étudier le comportement d'un contaminant organique modèle, le fluoranthène (principal HAP présent dans les sols de cokerie) lors d'expériences d'oxydation à l'air en présence de phases minérales. La source APPI couplée à la spectrométrie de masse Q-TOF a permis de caractériser les produits de réaction du fluoranthène suivant la nature des phases minérales sélectionnées et typiques de celles rencontrées dans les sols (calcite, sable et argile). Nous avons pu montrer qu'un phénomène de polycondensation, basé sur des réactions acide-base de Lewis (transfert d'électrons), transformait le fluoranthène initial (échelle moléculaire) en un résidu carboné de haute masse moléculaire (échelle microscopique).

Développement du couplage SEC-APPI-QTOF

Après cette première étape de développement et d'application, l'étape suivante a consisté à caractériser des systèmes beaucoup complexes (représentatif du milieu naturel), la première étape ciblant un composé modèle. Pour aborder ces systèmes complexes, il nous a paru inévitable de développer un couplage direct entre la chromatographie d'exclusion stérique et la spectrométrie de masse APPI-QTOF. La mise en place de ce couplage a :

- impliqué l'adaptation de la chromatographie d'exclusion stérique (SEC) afin de conserver ces propriétés de séparation tout en permettant une analyse directe par la spectrométrie de masse APPI-QTOF,

- permis d'améliorer sensiblement la sensibilité de la détection des composés par réduction du phénomène de compétition à l'ionisation (ou d'effet matrice),
- permis de s'affranchir d'une calibration de la SEC, qui est généralement peu fiable, aucun standard n'étant représentatif des composés naturels à doser, et est ainsi source d'erreurs majeures pour la détermination de la masse moléculaire.

Ce couplage a donc été développé en utilisant les solutions issues des expériences d'oxydation du fluoranthène, car préalablement caractérisées par injection directe sur l'APPI-QTOF. Une fois ce couplage opérationnel, il convenait de tester son efficacité sur des systèmes plus complexes. Le couplage SEC-APPI-QTOF a donc été appliqué sur des systèmes macromoléculaires de type asphaltènes (d'origine pétrolière et environnementale). La chromatographie d'exclusion stérique a permis de séparer les macromolécules en fonction de leur taille moléculaire (séparation physique), et il a été ainsi démontré que (i) la taille des asphaltènes est limitée (1500 Da) et (ii) les différentes fractions obtenues ont confirmé le modèle de Boduszinski qui défini les asphaltènes comme un continuum de molécules de tailles croissantes.

Traitements Post-processing des spectres de masse

L'amélioration de la détection et de la caractérisation des systèmes moléculaires en spectrométrie de masse par l'utilisation d'une source d'ionisation adaptée (partie I) et du couplage avec la SEC (partie II) a entrainé une nette amélioration de la sensibilité. Par voie de conséquence, cette richesse de signal rend très difficile et consommatrice de temps l'analyse des spectres de masses obtenus. Ainsi, le développement des modèles mathématiques s'est rapidement présenté comme fondamental, ce qui d'ailleurs est de plus en souligné dans les récents articles de synthèse du domaine. Le modèle mathématique SNAMS (Statistical and Numerical Analysis of Mass Spectra) a donc été développé en ce sens. Cet algorithme, constitué de deux sous programmes : une analyse mathématique permettant la numérisation des spectres nommé NAMS (Numerical Analysis of Mass Spectra) et un modèle statistique SAMS (Statistical Analysis of Mass Spectra) a permis de comparer les spectres de masse de différents échantillons entre eux et ainsi d'obtenir des informations non mesurables par exploitation directe des spectres de masse. Le modèle SNAMS a été appliqué dans un premier

temps aux spectres de masse d'asphaltènes de différents pétroles et de sous-produits du charbon, et a permis de :

- distinguer des échantillons d'origines très différentes (i.e. échantillons issus de pétroles versus dérivant de sous produits de l'industrie du charbon),
- classer les asphaltènes de pétrole de diverses origines,
- identifier les contributeurs anthropiques dans un sol de cokerie (charbon et goudron de houille et sol),
- hiérarchiser les échantillons suivant leur degré d'altération, dans notre cas l'oxydation à l'air.

Le résultat positif de ce modèle nous a ensuite conduit à l'appliquer à la matière organique dissoute (MOD), particulièrement complexe à détecter et à caractériser. De la même manière, le modèle SNAMS a permis avec succès de :

- différentier des MOD d'origine différente (eau issue d'une formation géologique et issue d'un sol de cokerie),
- évaluer le degré de transformation de la MOD issue de la percolation de colonne lysimétrique lors d'un traitement de remédiation de sols (oxydation Fenton),
- classer la MOD, issue d'un sédiment provenant d'une barrière géologique et oxydé artificiellement à l'air, suivant la durée d'expérience.

Perspectives

Ce travail de thèse qui couple le développement analytique et la recherche fondamentale portant sur une meilleure compréhension des systèmes organiques macromoléculaires, conduit à proposer plusieurs volets de perspectives complémentaires : un volet technique et un volet de recherche associé.

Poursuite des développements analytiques

Au cours de nos travaux, nous avons abordé essentiellement la matière organique fossile en phase organique. Une application sur de la matière organique dissoute a toutefois été réalisée (article 6) afin de tester l'applicabilité du model SNAMS pour ces matrices. Cette

application a été réalisée avec une source d'ionisation APPI car elle permet de limiter les effets des fortes teneurs en sels (notamment les sulfates) et l'influence de la plupart des solvants. Toutefois, ces eaux devront également être analysées par le biais d'une source ESI particulièrement adaptée à la matière organique très polaire.

Développement du couplage SEC-ESI-QTOF

Nous avons vu que la séparation préalable par la SEC avant analyse en spectrométrie de masse APPI-QTOF permettait une simplification des systèmes macromoléculaires par notamment la réduction de la compétition à l'ionisation. Il parait essentiel de poursuivre ce développement par le biais d'un couplage SEC-ESI-QTOF (i) en l'adaptant aux phases aqueuses et (ii) aux composés organométalliques en phase organique très peu concentrés. Ce couplage devrait permettre d'aborder la structure macromoléculaire de la matière organique dissoute et de mieux comprendre les mécanismes de piégeage des métaux dans la matière organique complexe. En effet, certains métaux présentent des affinités pour les asphaltènes, comme le rhénium et l'osmium (importants pour la datation des réservoirs pétroliers) mais n'ont jamais pu être détectés du fait de leur très faible concentration (de l'ordre du ppt) dans la matière organique. A l'heure actuelle, il est très difficile de savoir sous quelles formes, ils se rencontrent dans la matière organique. Nous avons testé une approche basée sur la réactivité de ces métaux (oxyde de Rhénium (ReO_4^-)) vis-à-vis de composés organiques modèles (alcanes, alcènes, alcynes, composés avec des fonctions oxygénées, azotées et soufrées) en condition de réservoirs (hautes pressions, hautes températures). Les résultats ont montré qu'aucun organométallique n'avait pu se formé dans ce contexte. Une conclusion pourrait être que la matière organique « transporte » les organométalliques par « simple effet de solvatation » (cf. travaux de thèse de Fatima Mahdaoui). Afin de prouver cette théorie, il conviendra d'analyser des huiles à l'aide du couplage, dans le but de diminuer la compétition à l'ionisation et ainsi de permettre à des composés très dilués d'être détectés.

Connaissance des systèmes macromoléculaires

Les minéraux, acteurs de dépollution des sols ?

Nos expériences d'oxydation réalisées à basse température sur un HAP modèle en présence de différentes phases minérales génériques (calcite, silice et argile) ont révélé, dans le cas de l'argile et de la calcite, un mécanisme de polycondensation qui mène à une stabilisation de ce polluant dans le sol en l'excluant du cycle du carbone de surface. Il est essentiel de poursuivre ce travail en ciblant des argiles à propriétés contrastées (structure, degré de substitution, nature des ions interfoliaires…) pour comprendre quels sont les paramètres qui conditionnent les effets catalytiques des argiles et espérer pouvoir définir un procédé de traitement de sols contaminés et l'appliquer dans un premier temps à l'échelle du pilote.

Les asphaltènes – continuum de molécules ?

Les résultats de l'analyse des asphaltènes par couplage SEC-APPI-QTOF a permis de confirmer la composition des asphaltènes sous forme d'un continuum de molécules. Le couplage devrait pouvoir permettre de contribuer à la levée de la polémique sur la taille des asphaltènes souvent originaire des problèmes issus de calibration en SEC.

Il apparait important de continuer les analyses d'asphaltènes, à l'aide d'autres types d'échantillon avec par exemple des degrés de maturation différents et ainsi confirmer la théorie précédente.

Les asphaltènes – classement

De plus, les moyens actuels de classement des asphaltènes ou des huiles pétrolières sont basés sur l'analyse par FT-ICR et la construction de diagrammes (i.e. diagramme de Van Krevelen ou de Kendrick) consommateurs de temps et difficiles à comparer. Il serait donc intéressant de coupler l'analyse des asphaltènes par SEC-APPI-QTOF et le modèle mathématique SNAMS qui permet de comparer les spectres de masse entre eux afin

d’améliorer la précision du modèle et d’être capable de corréler des échantillons très proches par rapport à leur composition moléculaire

Annexe : Liste des figures et des tableaux

Liste des figures

Liste des tableaux